Aston University

Some pages of this thesis may have been removed for copyright restrictions.

If you have discovered material in AURA which is unlawful e.g. breaches copyright, (either yours or that of a third party) or any other law, including but not limited to those relating to patent, trademark, confidentiality, data protection, obscenity, defamation, libel, then please read our Takedown Policy and contact the service immediately

SYNTHESIS, CRYSTALLOGRAPHY AND BIOLOGICAL ACTIVITY OF *MYO*-INOSITOL PHOSPHATES

IAN DAVID SPIERS

Doctor of Philosophy

THE UNIVERSITY OF ASTON IN BIRMINGHAM

MARCH 1996

This copy of the thesis has been supplied on the condition that anyone who consults it is understood to recognise that its copyright rests with its author and that no quotation from the thesis and no information derived from it may be published without proper acknowledgement.

THE UNIVERSITY OF ASTON IN BIRMINGHAM

SYNTHESIS, CRYSTALLOGRAPHY AND BIOLOGICAL ACTIVITY OF *MYO*-INOSITOL PHOSPHATES

A thesis submitted by Ian David Spiers BSc.(Hons) for the degree of Doctor of Philosophy

1996

SUMMARY

The antioxidant property of *myo*-inositol hexakisphosphate is important in the prevention of hydroxyl radical formation which may allow it to act as a 'safe' carrier of iron within the cell. Here, the hypothesis that the recently discovered natural product, *myo*-inositol 1,2,3-trisphosphate represents the simplest structure to mimic phytate's antioxidant activity has been tested. The first synthesis of *myo*-inositol 1,2,3-trisphosphate has been completed, along with its X-ray structure determination and that of key synthetic intermediates. Iron binding studies of *myo*-inositol 1,2,3-trisphosphate demonstrated that phosphate groups with the equatorial-axial-equatorial conformation are required for complete inhibition of hydroxyl radical formation.

myo-Inositol monophosphatase is a key enzyme in recycling myo-inositol from its monophosphates in the brain and its inhibition is implicated in lithium's antimanic properties. Current synthetic strategies require inositol compounds to be protected (often with more than one group), resolved, phosphorylated and deprotected to produce the desired optically active *myo*-inositol phosphates. Here, the synthesis of *myo*-inositol 3-phosphate has been achieved in only 4 steps from *myo*-inositol. The stereoselective addition of the chiral phosphorylating agent (2R,4S,5R)-2-chloro-3,4-dimethyl-5-phenyl-1,3,2-oxazaphospholidin-2-one to a protected inositol intermediate allowed separation of diastereoisomers and easy deprotection to *myo*-inositol 3-phosphate. This strategy also allows the possible introduction of labels of oxygen and sulphur to give a thiophosphate of known stereochemistry at phosphorus which would be useful for the analysis of the stereochemical course of phosphate hydrolysis catalysed by inositol monophosphatase.

Key words: *myo*-Inositol 3-phosphate; *myo*-inositol 1,2,3-trisphosphate; crystallography; *myo*-inositol hexakisphosphate; inositol monophosphatase

TO BARBARA AND MY FAMILY

ACKNOWLEDGEMENTS

I would very much like to thank my supervisors Dr Sally Freeman and Dr Carl Schwalbe for their expert advice, guidance and constant support over the past three years.

Thanks to Dr A. W. Smith, Mr P. H. Hirst (University of Bath) and Dr D. R. Poyner for providing me with the biological data on *myo*-inositol 1,2,3-trisphosphate. I would also like to thank Dr A. J. Blake (University of Nottingham) for collecting the low temperature crystal data, Dr K. R. H. Solomons and Dr J. Barber (University of Manchester) for experimental measurements.

Special thanks for technical assistance and helpful discussions go to Dr's K. C. Ross, J. M. Gardiner, P. A. Lambert, Y.-F. Wang, W. Fraser, B. Denny and Prof. D. C. Billington.

Thanks also to the BBRSC for their financial support for this project.

I would like to thank all my friends in the department for all their help and for making my PhD so enjoyable.

Finally, a special thank-you to Barbara and my family for always being there.

ABBREVIATIONS

2'-AMP	Adenosine 2'-monophosphate
ADP	Adenosine 5'-diphosphate
ATP	Adenosine 5'-triphosphate
CMP	Cytosine 5'-monophosphate
cyclic-AMP	Adenosine 3',5'-cyclic monophosphate
DAG	Diacylglycerol
DMAP	4-Dimethylaminopyridine
DMF	Dimethylformamide
DPPC	Diphenyl phosphorochloridate
EGF	Epidermal growth factor
G protein	Guanosine 5'-triphosphate -binding protein
GDP	Guanosine 5'-diphosphate
GTP	Guanosine 5'-triphosphate
IMPase	Inositol monophosphatase
Ins $(1,2)P_2$	*myo*-Inositol (1,2)-bisphosphate
Ins $(1,2,3)P_3$	*myo*-Inositol (1,2,3)-trisphosphate
Ins $(1,3,4,5)P_4$	*myo*-Inositol (1,3,4,5)-tetrakisphosphate
Ins $(1,3,4,5,6)P_5$	*myo*-Inositol (1,3,4,5,6)-pentakisphosphate
Ins $(1,4,5)P_3$	*myo*-Inositol (1,4,5)-trisphosphate
Ins P_5	*myo*-Inositol pentakisphosphate
Ins P_6	Phytic acid, *myo*-Inositol hexakisphosphate
Ins(1)P	*myo*-Inositol 1-phosphate
*m*CPBA	*meta*-Chloroperoxybenzoic acid
OXDEP	*O*-Xylylene *N,N*-diethylphosphoramidite
PDGF	Platelet-derivedand growth factor
PLC	Phospholipase C
PtdIns $(4,5)P_2$	Phosphatidylinositol (4,5)-bisphosphate
PtdIns	Phosphatidylinositol
TBAF	Tetrabutylammonium fluoride
TBPP	Tetrabenzyl pyrophosphate
THF	Tetrahydrofuran

CONTENTS

LIST OF FIGURES Unless otherwise stated all compounds are racemic, only the D-isomer is shown in the figures

LIST OF TABLES

CHAPTER 1

myo-Inositol phosphates: Biochemistry and chemistry

1.1 The structure of *myo*-inositol

Nine possible isomeric inositols (cyclohexanehexol) exist, with *myo*-inositol **1** being the most abundant naturally occuring isomer (Figure 1.1). The usual numbering of the inositol carbon atoms is in an anticlockwise direction around the ring (D-isomer configuration).

Figure 1.1: The structure of *myo*-inositol

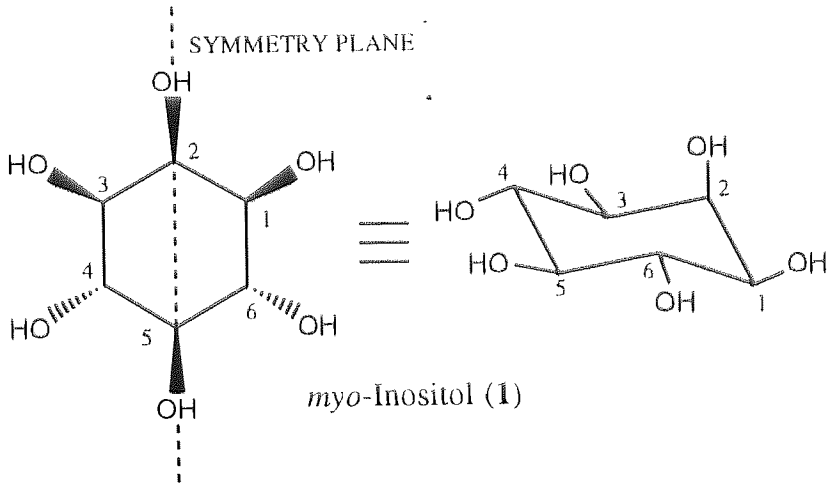

myo-Inositol (**1**)

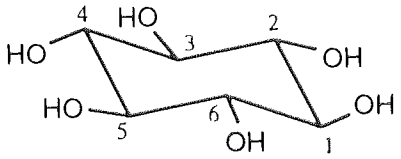

scyllo-Inositol (**2**)

myo-Inositol is a meso compound possessing a plane of symmetry through C-2 and C-5. It has five equatorial hydroxyl groups and one axial hydroxyl group at C-2, whereas *scyllo*-inositol **2** has all equatorial hydroxyl groups. The introduction of functional groups at the symmetry-related pairs C-1, C-3 and C-4, C-6 gives rise to the existence of enantiomers.

1.2 Cell signalling pathways

Phosphoinositide signalling within cells has been extensively reviewed [most recently by Potter & Lampe, 1995] and only a brief outline is given here.

Cells divide their labour within an organism by communicating with one another *via* chemical signals. If the chemical signals are hydrophilic they cannot traverse the cell membrane's lipophilic barrier and so depend on cell surface receptors to translate their information *via* certain signalling pathways to internal responses. Two major signal pathways are known, one involves adenosine 3',5'-cyclic monophosphate (cyclic-AMP) and the other is the phosphoinositide pathway. Common features to both pathways are:-

(1) Receptors are coupled *via* transmembrane mechanisms to an enzyme on the inner face of the membrane which converts precursor molecules into second messengers.

(2) The second messengers act either directly by binding to regulatory sites on cellular proteins or indirectly on protein kinase enzymes which phosphorylate proteins. Both induce conformational changes on the proteins and lead to cellular responses [Berridge, 1985].

The cyclic-AMP pathway has been reviewed by Berridge [Berridge, 1985], and only the phosphoinositide signalling pathway is discussed here.

1.2.1 Phosphoinositide signalling pathway

In 1953, the administration of acetylcholine to secretory cells of the pancreas was shown to increase the incorporation of ^{32}P-labelled phosphate groups into phosphatidylinositol (PtdIns, [Hokin & Hokin, 1953]). This showed that the turnover of PtdIns, a phospholipid in cell membranes, could be affected by an external signal.

Subsequently it was observed that the binding to many receptors could stimulate the hydrolysis of the membrane phospholipid, phosphatidylinositol (4,5)-bisphosphate [PtdIns $(4,5)P_2$], which is catalysed by the enzyme phospholipase C (PLC, [Michell,

1975]). The second messengers, diacylglycerol [DAG] and inositol (1,4,5)-trisphosphate [Ins (1,4,5)P_3] are formed, the latter having an effect on internal calcium signals [Streb *et al.*, 1983]. Two transmembrane mechanisms are involved in this pathway, one in which receptors are linked to G proteins, and the other in which receptors are linked directly or indirectly to tyrosine kinases, each of which will be discussed.

1.2.1.1 G protein-linked receptors

G proteins are guanosine 5'-triphosphate (GTP)-binding proteins linked to receptors which generally have seven membrane-spanning domains connected by extracellular and intracellular loops. The G proteins exist as heterotrimeric structures containing one alpha (G_α), one beta (G_β) and one gamma (G_γ) subunit, designated in order of decreasing mass. The G proteins are associated with the internal surface of the cell membrane as a trimeric complex with guanosine 5'-diphosphate (GDP) bound to the G_α subunit. The receptors are stimulated by agonists, such as hormones and neurotransmitters, which leads to the association of the trimeric-GDP complex to the receptor protein. The G_α subunit exchanges GDP for GTP, causing the GTP-G_α complex to dissociate from the $G_{\beta\gamma}$ subunit and the receptor. The GTP-G_α complex then activates PLC-β1 isozymes and the $G_{\beta\gamma}$ subunits may also activate PLC-β2 isozymes. Inactivation is achieved by the hydrolysis of GTP to GDP by the GTPase activity of the G_α subunit, the G_α subunit can then recombine to form an inactive complex with the $G_{\beta\gamma}$ subunit [Berridge, 1993; Majerus, 1992].

1.2.1.2 Tyrosine kinase-linked receptors

The receptor consists of a single transmembrane protein containing a cytoplasmic tyrosine kinase. Hormones and growth factors, such as platelet derived [PDGF] and epidermal [EGF] growth factors, act by inducing the dimerisation of two receptors. This enables the two kinase domains to phosphorylate each other which provides a site for interaction with a certain domain on PLC-γ1. PLC-γ1 is then phosphorylated

specifically which induces the hydrolysis of PtdIns $(4,5)P_2$. All of the phosphorylation reactions that occur consume ATP which leads to an energy-demanding process [Berridge, 1993; Majerus, 1992].

1.2.2 Second messengers in the phosphoinositide pathway

The two second messengers, Ins $(1,4,5)P_3$ and DAG are metabolised ultimately to inositol and CMP-phosphatidate, which react together to recycle the phospholipid PtdIns (Figure 1.2). PtdIns is then sequentially phosphorylated to PtdIns $(4,5)P_2$ [Majerus, 1992].

Figure 1.2: The phosphoinositide pathway [Majerus, 1992]

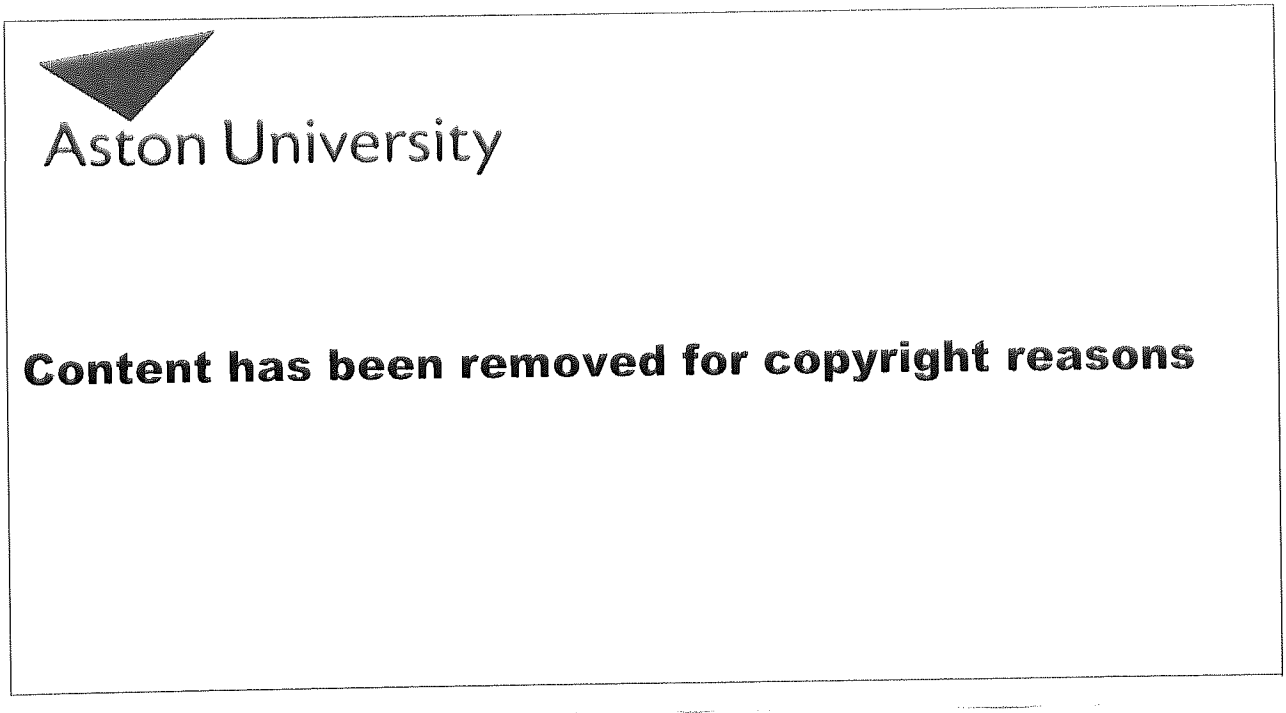

Ins$(1,4,5)P_3$ is phosphorylated by Ins$(1,4,5)P_3$ 3-kinase to inositol (1,3,4,5) tetrakisphosphate [Ins $(1,3,4,5)P_4$] which may also have a role in calcium signalling [Berridge, 1993]. The recycling of inositol from Ins$(1,4,5)P_3$ and Ins $(1,3,4,5)P_4$ is discussed in Chapter 2.

1.2.2.1 Diacylglycerol (DAG)

In the presence of phospholipid and calcium ions DAG activates protein kinase C, which plays an important role in a range of biological processes, presumably through the phosphorylation of specific proteins [Berridge, 1985]. DAG remains in the plane of the membrane and is metabolized by either a kinase or a lipase. Diacylglycerol kinase recycles DAG to phosphatidic acid (Figure 1.2) whereas the lipase hydrolyses DAG to a monoacylglycerol and the eicosanoid precursor arachidonic acid which is used in prostaglandin synthesis [Potter & Lampe, 1995].

1.2.2.1 $Ins(1,4,5)P_3$ and $Ins(1,3,4,5)P_4$: their role in cell signalling

$Ins(1,4,5)P_3$ is thought to control the mobilisation of internal and external calcium. Within the cell there are calcium stores whose locations are uncertain but they have receptors, linked to calcium channels, that seem to be localised on modified portions of the endoplasmic reticulum. There are $Ins(1,4,5)P_3$ sensitive and insensitive calcium stores, the former are proposed to be in the endoplasmic reticulum and the latter have been suggested to have a separate membrane compartment [Berridge, 1993].

When Ins $(1,4.5)P_3$ binds to the receptor (cooperativity may be important), calcium from sensitive stores is released into the cytosol [Berridge, 1993].

External calcium entry into cells can be regulated by a number of calcium channel mechanisms, i.e. channels operated by voltage, by receptors or by second messengers. It has been discussed that $Ins(1,4,5)P_3$ may stimulate calcium entry, either directly by activating specific channels in the plasma membrane, or by an indirect mechanism. The latter is based on calcium flowing into the endoplasmic reticulum before entering the cytosol. It is suggested that when the endoplasmic reticulum is emptied of calcium by $Ins(1,4,5)P_3$, calcium influx starts and when the store is fully charged, calcium entry is prevented [Berridge, 1993].

The role of Ins(1,3,4,5)P_4 in calcium mobilisation may be in regulating calcium entry or in transfer of calcium between intracellular stores, although this is unclear at present [Berridge, 1993].

The small influx in calcium through second messenger-operated channels provides a steady flow of calcium. This can be released to give transient calcium spikes or waves whose frequency is sensitive to agonist concentrations and external calcium levels, but does not cause a marked elevation in intracellular calcium. The calcium waves produced may propagate between stores by a positive feedback mechanism in which calcium amplifies its own release. This could be achieved either by calcium effecting PLC release of Ins (1,4,5)P_3, which could then diffuse from one store to the next, or by calcium itself as a diffusible messenger enhancing its own release. Calcium waves can travel from cell to cell possibly by means of a secreted intermediate such as adenosine triphosphate (ATP) or through gap junctions by diffusion of calcium or Ins (1,4,5)P_3 [Berridge, 1993].

1.2.3 Metabolites of Ins(1,4,5)P_3

Figure 1.3: Metabolism of Ins(1,4,5)P_3 [Potter & Lampe, 1995]

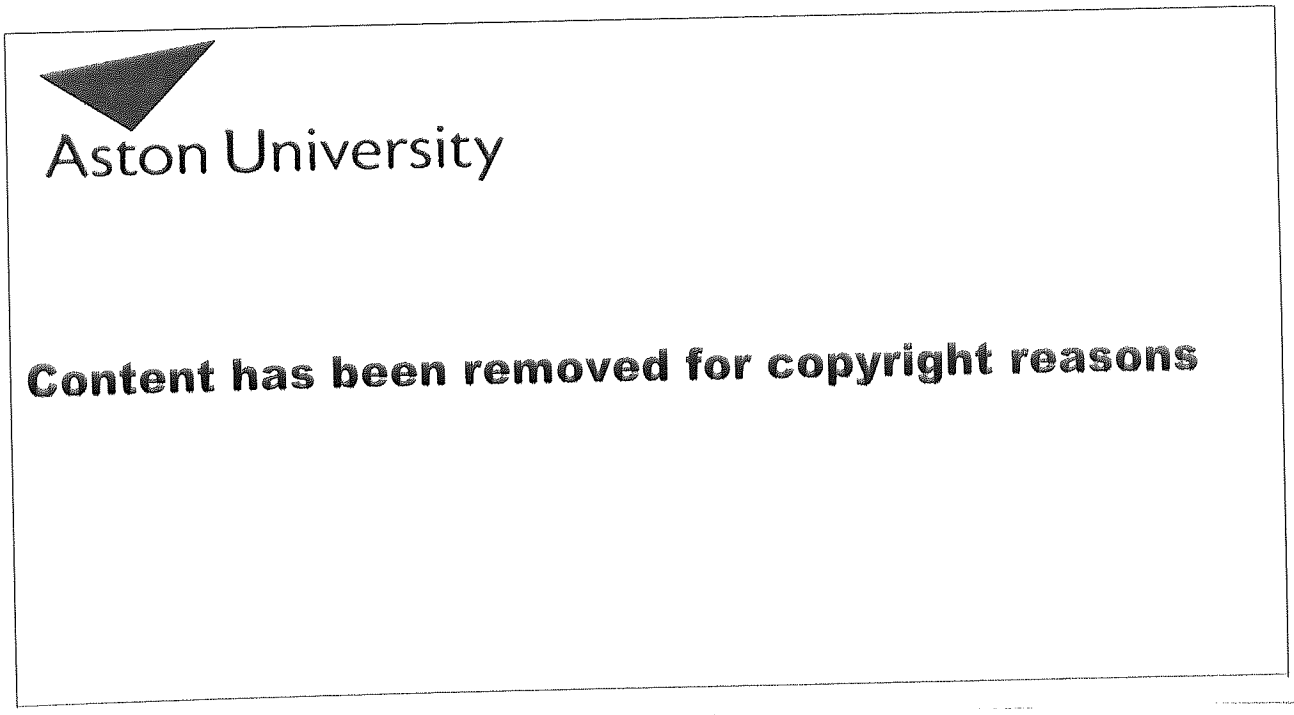

The metabolism of the second messenger Ins(1,4,5)P_3 is complex, generating many inositol phosphates (Figure 1.3), some of which have possible biological roles [Potter & Lampe, 1995].

Two routes have been suggested for the biosynthesis of inositol (1,3,4,5,6) pentakisphosphate [Ins(1,3,4,5,6)P_5] and inositol hexakisphosphate [$InsP_6$, phytic acid], one starting from inositol itself [Stephens & Irvine, 1990] and the other starting from the Ins(1,4,5)P_3 [Figure 1.3; Menniti *et al.*, 1993]. In each case Ins(1,3,4,5,6)P_5 is the *de novo* precursor for $InsP_6$. Both Ins(1,3,4,5,6)P_5 and $InsP_6$ are present in virtually all mammalian cells in higher amounts than any other inositol polyphosphate, and a recent review discusses that their metabolism is more complex and more dynamic than first considered [Menniti *et al.*, 1993]. The possible biological roles of Ins(1,3,4,5,6)P_5 and $InsP_6$ are discussed in Chapter 3.

Other $InsP_5$ isomers are present at lower levels in cells, and as yet their biological activities are not well understood. Stephens and co-workers have suggested that they are involved in $InsP_6$ biosynthesis and degradation [Stephens *et al.*, 1991].

1.3 Strategies for the synthesis of *myo*-inositol phosphates

Many *myo*-inositol phosphates have been synthesized as probes for biological activity, unleashing a vast array of synthetic routes [For good reviews see Billington, 1993; Potter & Lampe, 1995]. A brief account of some strategies used to synthesize inositol phosphates, with illustrations, are given here.

The selective addition of phosphate groups onto specific positions of *myo*-inositol requires the following operations:-

(1) Protection of the hydroxyl groups on the inositol ring which are not to be phosphorylated.

(2) Any enantiomers formed must be resolved (*myo*-inositol phosphates occur naturally in the D configuration) if the optically active inositol phosphate is required.

[Alternatively an optically active precursor could be employed in the synthesis, for example, L-quebrachitol or galactinol, see Chapter 2].

(3) Phosphorylation of the unprotected hydroxyl groups with a suitable phosphorylating agent.

(4) Deprotection of all protecting groups without phosphate migration around the ring.

1.3.1 Protection of the *myo*-inositol ring

Figure 1.4: *myo*-Inositol cyclohexylidene derivatives [Vacca *et al.*, 1989]

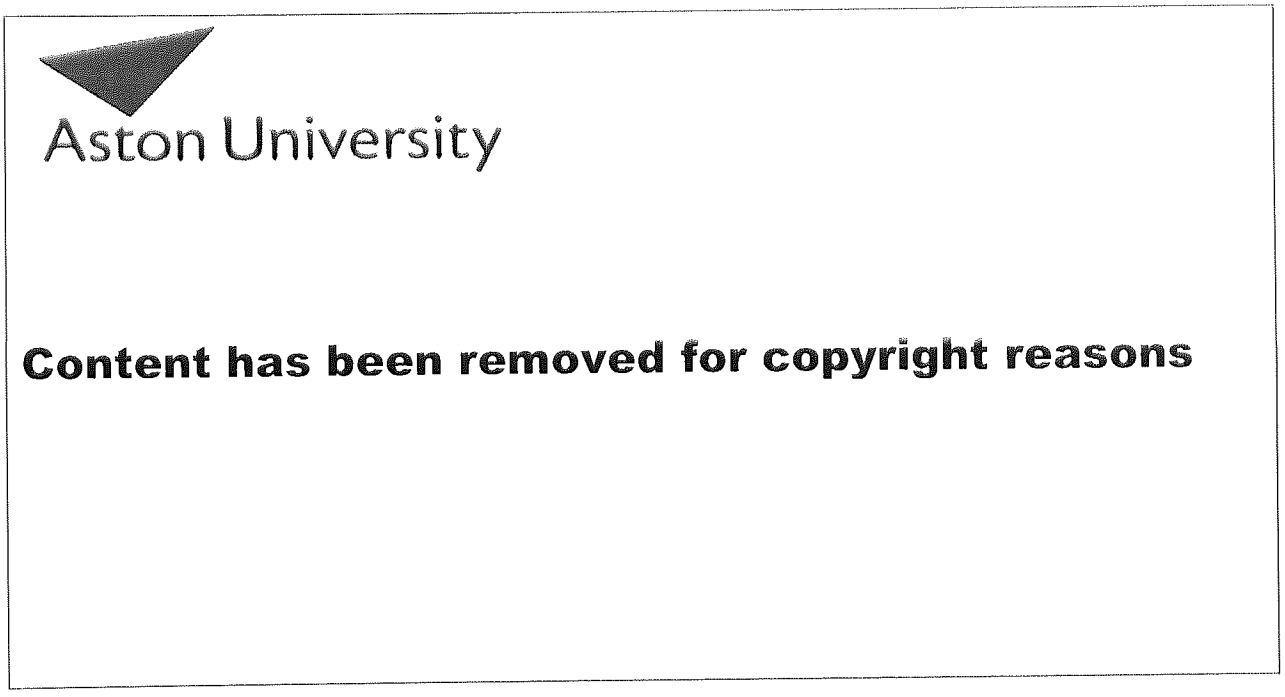

One of the most widely used protecting groups for the *myo*-inositol ring is cyclohexylidene (Figure 1.4). Treating *myo*-inositol with 1,1-diethoxycyclohexane [Dreef *et al.*, 1991] in the presence of an acid catalyst gives the bisacetals of which **3** can be separated by crystallisation, and **4** and **5** by chromatography [Vacca *et al.*, 1989]. Mild acid catalysed hydrolysis of the bisacetals gives rise to **6** by removal of the less stable trans-linked acetal. All of these cyclohexylidene inositol derivatives have conformational constraints imposed on their inositol rings which allows for further protection by selective addition of functional groups such as benzyl [Vacca *et al.*, 1989; Baker *et al.*, 1991], allyl [Vacca *et al.*, 1989; Baker *et al.*, 1991] and *tert*-butyldiphenylsilyl [Bruzik & Tsai, 1992] groups. Other acetals which have been used for protection of the *myo*-inositol ring are isopropylidene [Gigg *et al.*, 1987] and cyclopentylidene [Reese & Ward, 1987].

1.3.2 Resolution of enantiomers of protected *myo*-inositol analogues

Single enantiomers of *myo*-inositol phosphates can be obtained either by starting with a naturally occuring optically active precursor or by resolution of a suitably protected *myo*-inositol intermediate. Resolution can be achieved by introducing another chiral centre into the structure to form a pair of diastereoisomers, which can then be separated by crystallisation or chromatography [Billington, 1993]. Some of the resolving groups that have been used are shown in Figure 1.5. Their efficiency in resolving seems to be structure dependent. The cost and recovery of resolving agents has always been a problem, although recovery has been improved [Desai *et al.*, 1991].

1.3.3 Phosphorylating reagents for *myo*-inositol derivatives and deprotection to *myo*-inositol phosphates

Single enantiomers of suitably protected inositol derivatives have been reacted with both P(III) and P(V) phosphorylating agents (Figure 1.6).

Figure 1.5: Resolving agents that have been used to separate enantiomers of *myo*-inositol derivatives

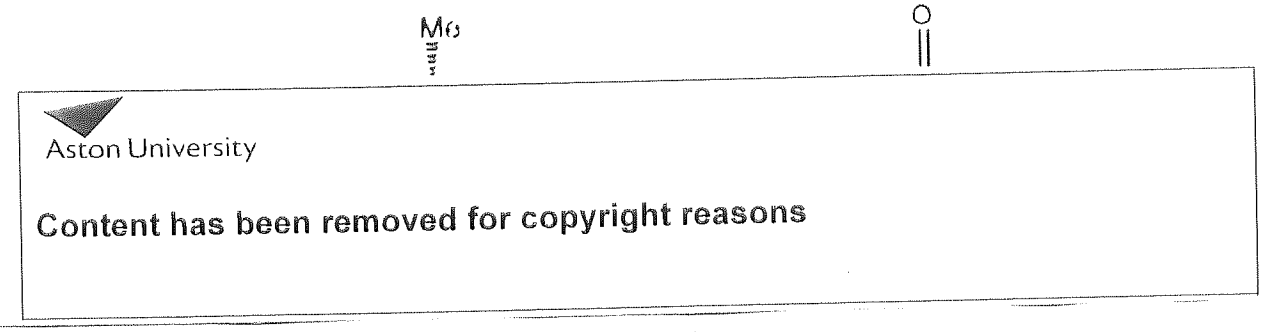

1-*l*-Menthoxyacetyl chloride
[Ozaki & Watanabe, 1991]

Methyl hydrogen 2,3-*O*-cyclohexylidene tartrate
[Ozaki & Watanabe, 1991]

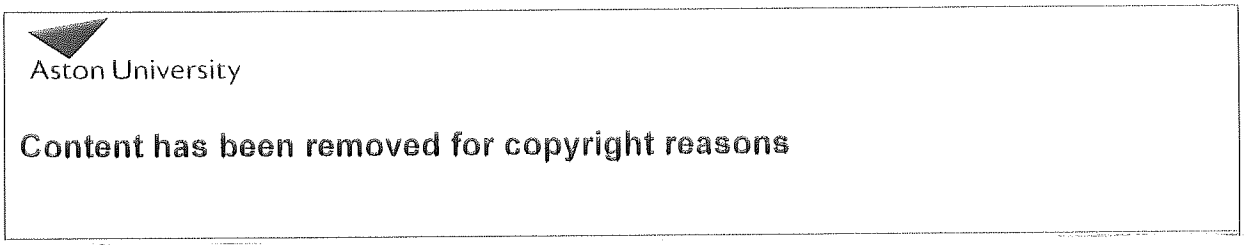

D-glucose orthoacetate
[Shvets *et al.*, 1991]

D-mannose orthoacetate
[Shvets *et al.*, 1991]

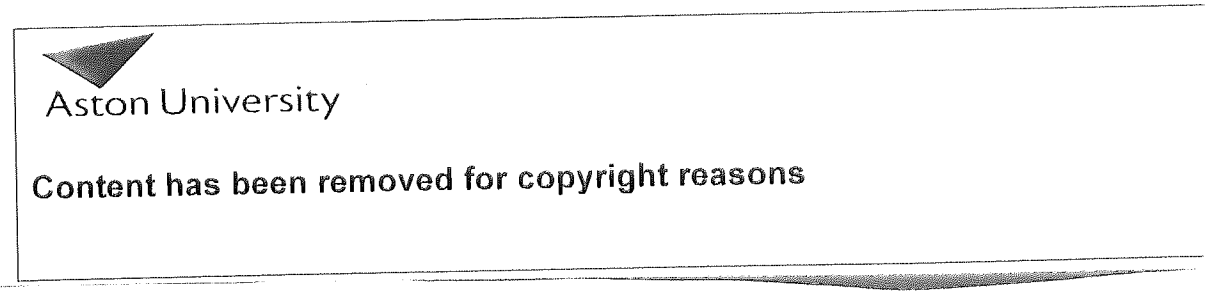

R-(-)-Camphanic acid chloride
[Billington et al., 1987]

Dianilophosphoryl chloride (DAPC, **7**) reacts with protected inositol compounds to give good yields of the phosphorylated product, however, deprotection of the phosphoamide groups was unsuccessful due to the harsh conditions required (AcOH, H_2O, 80°C) [Vacca *et al.*, 1991].

Figure 1.6: P(III) and P(V) reagents used for the phosphorylation of protected *myo*-inositol derivatives

P(V) reagents

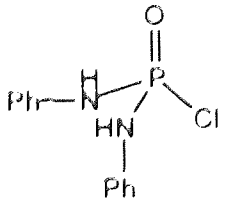

Dianilophosphoryl chloride (DAPC, 7)

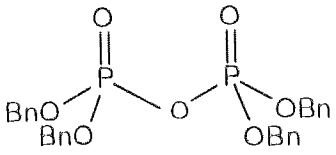

Tetrabenzyl pyrophosphate (TBPP, 9)

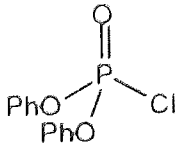

Diphenyl phosphorochloridate (DPPC, 8)

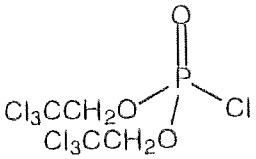

Di(2,2,2-trichloroethyl) phosphorochloridate (**10**)

P(III) reagents

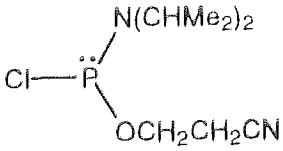

N,*N*-Diisopropylamino (2-cyanoethyl)-chlorophosphine (**11**)

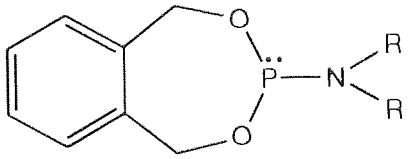

R=Me

O-Xylylene *N*,*N*-dimethylphosphoramidite (**12**)

R=Et

O-Xylylene *N*,*N*-diethylphosphoramidite (OXDEP, **13**)

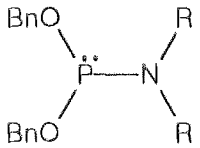

R=CHMe$_2$

Dibenzyl *N*,*N*-diisopropylphosphoramidite (**14**)

R=Et

Dibenzyl *N*,*N*-diethylphosphoramidite (**15**)

Protected *myo*-inositol derivatives have been phosphorylated with diphenyl phosphorochloridate (DPPC, **8**), although the diphenyl phosphate protecting group is unstable during chromatography [Vacca *et al.*, 1991] and phosphate group migration occurs when the phenyl groups are removed by hydrogenolysis. Transesterification of the phenyl esters to benzyl esters has been shown to prevent migration on deprotection [Billington *et al.*, 1987].

Tetrabenzyl pyrophosphate (TBPP, **9**) reacts with a preformed inositol anion, (for example, prepared by the addition of butyl lithium to the protected *myo*-inositol analogue), in good yield [Watanabe *et al.*, 1987]. The benzyl groups of the dibenzyl phosphate triester product can then be removed by hydrogenolysis without migration of the phosphate groups.

Phosphorylation of protected *myo*-inositols with di(2,2,2-trichloroethyl) phosphorochloridate **10** gives rise to the di(2,2,2-trichloroethyl) phosphate triesters, the 2,2,2-trichloroethyl groups from which can be removed using sodium in liquid ammonia [Noble *et al.*, 1992].

Figure 1.7: Reaction of a protected *myo*-inositol (ROH) with a P(III) reagent to give the corresponding phosphite and subsequent oxidation to the phosphate

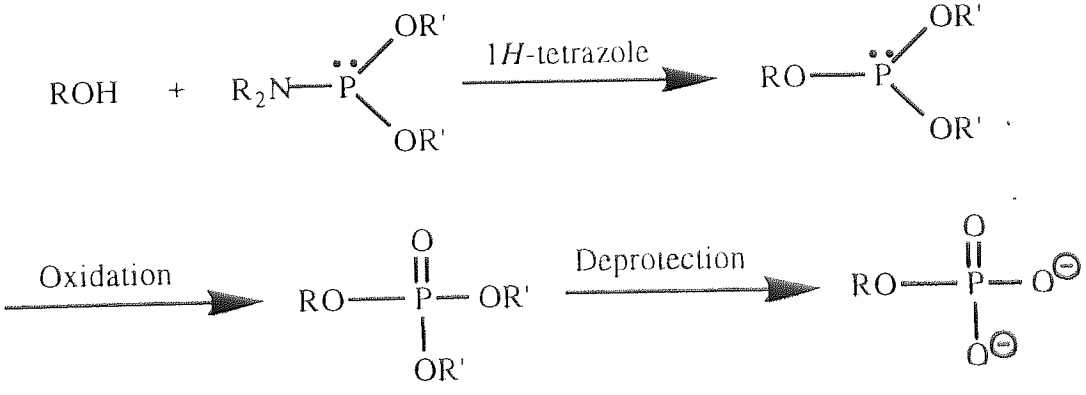

Phosphitylation of protected inositols by P(III) reagents (Figure 1.7), in the presence of the acid catalyst 1*H*-tetrazole, produces the corresponding phosphite, which can be oxidised to give the phosphate triester or treated with sulphur to give the thiophosphate triester.

N,N-Diisopropylamino (2-cyanoethyl)-chlorophosphine **11** (Figure 1.6) is used extensively with nucleosides for the preparation of phosphoramidites for DNA synthesis [Cooke *et al.*, 1987, a]. Reaction of **11** with a *myo*-inositol derivative produces a phosphoramidite by displacement of the chloro group. The phosphoramidite can then be converted to its phosphite triester by treatment with 2-cyanoethanol in the presence of 1*H* tetrazole. The resulting phosphite can then be oxidised with *tert*-butyl hydroperoxide [Cooke *et al.*, 1987, a] or treated with sulphur [Cooke *et al.*, 1987, b] to give the corresponding phosphate or thiophosphate triesters. The cyanoethyl groups can then be removed by treatment with sodium in liquid ammonia, by a β-elimination mechanism, followed by purification using ion-exchange chromatography [Cooke *et al.*, 1987, a & b]

A more direct method to the phosphite triester is to utilise the phosphoramidites (Figure 1.6) *O*-Xylylene *N,N*-dimethylphosphoramidite [**12**; Pietrusiewicz *et al.*, 1992] and its *N,N*-diethylphosphoramidite analogue [OXDEP, **13**; Watanabe *et al.*, 1990]. The resulting phosphites were both oxidised by *meta*-chloroperoxybenzoic acid (*m*CPBA), and deprotection of the *O*-xylylene group was achieved by hydrogenolysis to give the required inositol phosphate. Using OXDEP **13**, the phosphite product was also treated with sulphur, and the *O*-xylylene group was removed with sodium in liquid ammonia, to give rise to the thiophosphate derivative [Watanabe *et al.*, 1990]. This deprotection method avoids the possible poisoning of the catalyst by the thiophosphate during hydrogenolysis.

The two dibenzyl phosphoramidites **14** and **15** (Figure 1.6) were investigated as phosphitylating agents. Dibenzyl *N,N*-diisopropylphosphoramidite **14** was found to be more stable towards chromatographic purification than the *N,N*-diethyl analogue **15**, and was therefore used in more studies for the phosphorylation of *myo*-inositol derivatives. *m*CPBA or *tert*-butyl-hydroperoxide were used to oxidise the corresponding phosphite triesters formed. Overall, treatment of a protected *myo*-inositol derivative with dibenzyl *N,N*-diisopropylphosphoramidite **14**, oxidation of the resulting phosphite with *m*CPBA and removal of the benzyl phosphate esters by hydrogenolysis

gave very high yields of the required inositol phosphates without migration of the phosphate groups [Yu & Fraser-Reid, 1988].

CHAPTER 2

Synthesis of D-*myo*-inositol 3-phosphate using a chiral phosphorylating agent

2.1 INTRODUCTION

2.1.1 Inositol recycling and *de novo* synthesis

Most intake of *myo*-inositol in humans is from plants. However transport of plasma *myo* inositol into the brain is restricted by the blood-brain barrier [Lewin *et al.*, 1976], which has been suggested to be caused by its low affinity for both the transport processes and for the enzyme, phosphatidylinositol synthase [Nahorski *et al.*, 1992].

Figure 2.1: Inositol recycling and *de novo* synthesis [Berridge *et al.*, 1989; Potter, 1990]

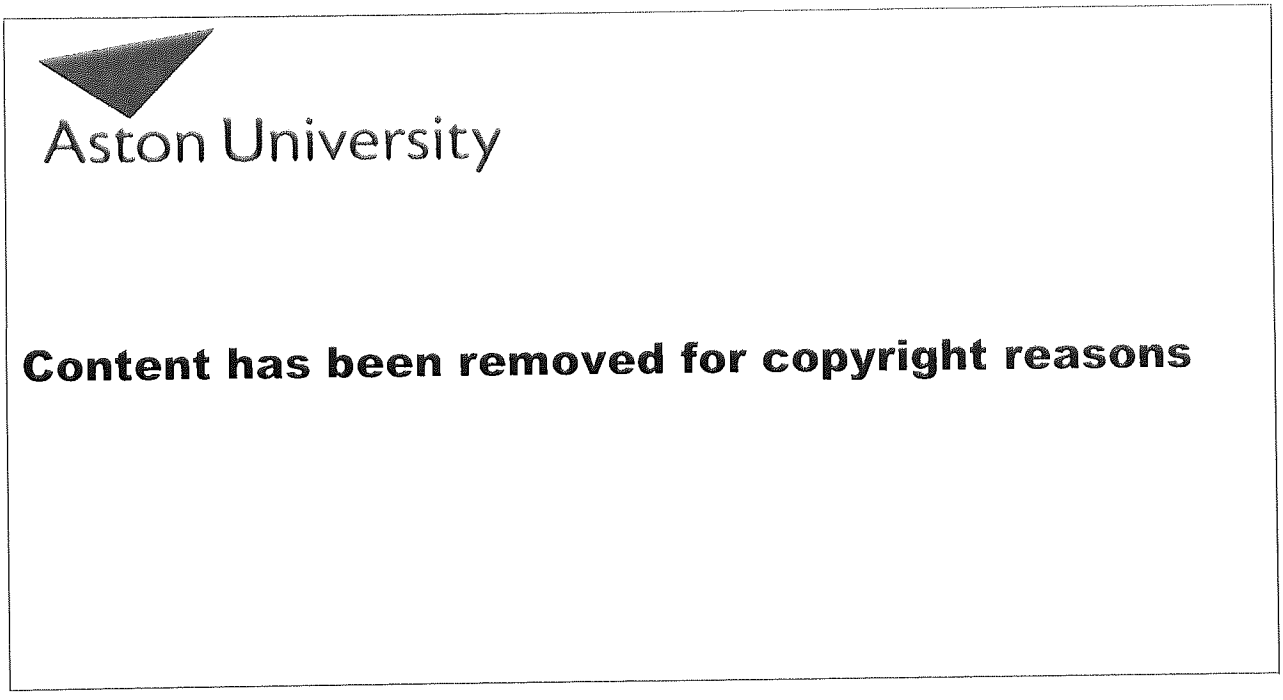

myo-Inositol recycling from the inositide pathway by dephosphorylation of *myo*-inositol phosphates is therefore an important route, as well as *de novo* synthesis (Figure 2.1), to maintain sufficient supplies of inositol in brain cells. The blood-brain barrier may also impose restrictions on inositol supplied by *de novo* synthesis, as the enzyme *myo*-inositol 3-phosphate synthase has been reported to be confined to the cerebral vasculature (blood side) [Wong *et al.*, 1987].

The *myo*-inositol phosphates (Figure 2.1) are metabolised by sequential hydrolysis of phosphate groups catalysed by several different phosphatases, two of which are lithium sensitive [for a good review on these enzymes see Majerus, 1992]. The *de novo* synthesis involves the isomerisation of D-glucose 6-phosphate to D-*myo*-inositol 3-phosphate catalysed by D-*myo*-inositol 3-phosphate synthase [reviewed in Potter, 1990].

2.1.2 Lithium: An uncompetitive inhibitor of inositol monophosphatase

Lithium (Li^+) has antimanic and antidepressive properties, remaining the therapy of choice in the treatment of bipolar disorders, although Li^+ has the disadvantages of a narrow therapeutic window and severe toxicity at elevated levels (which requires plasma concentrations of Li^+ to be monitored). The mechanism by which Li^+ exerts its effects remains unclear [Atack *et al.*, 1995]. Administered Li^+ is distributed widely throughout tissues and fluids in the body, although it has been suggested that Li^+ may have enhanced uptake and concentrate in excitable cells [Gani *et al.*, 1993]. Allison and Stewart first observed that administered Li^+ caused a decrease in inositol levels in rat brain which was accompanied by an increase in inositol 1-phosphate [Ins(1)P] levels [Allison & Stewart, 1971]. Later it was discovered that Li^+ inhibited, in an uncompetitive manner, inositol monophosphatase (IMPase, [Hallcher & Sherman, 1980]), and it was suggested that Li^+ might exert its therapeutic effects in bipolar disorder by depletion of inositol as a consequence of inhibition of IMPase [Berridge *et al.*, 1982]. The main action of Li^+ has also recently been suggested to be the inhibition of IMPase [Nahorski *et al.*, 1992], as this enzyme is responsible for supplying cellular

inositol from both the signalling pathway and the *de novo* synthesis (Figure 2.1). Li^+ also inhibits an additional enzyme (Figure 2.1), inositol polyphosphate 1-phosphatase [Majerus, 1992], although this enzyme does not control recycling of inositol to the extent that IMPase can. Li^+ has a selective action on hyperactive cells with little effect on normal cells, which is ideal when treating conditions involving over-activity in certain brain areas. The increase in concentration of substrate in hyperactive cells provides more enzyme complexes for Li^+ binding and therefore enhanced inhibition [Berridge *et al.*, 1989].

2.1.3 Inositol monophosphatase: Structure and function

Inositol monophosphatase (IMPase) catalyses the hydrolysis of the phosphate group of all *myo*-inositol monophosphates, except *myo*-inositol 2-phosphate [Majerus, 1992], to give inorganic phosphate and *myo*-inositol. IMPase can also catalyse the hydrolysis of adenosine-2'-monophosphate (2'-AMP) [Cole & Gani, 1994]. The structure of IMPase has been determined by X-ray crystallography to a resolution of 2.1Å with lanthanide cation (Gd^{3+}) and sulphate [Bone *et al.*, 1992], to 2.2-2.3Å with Gd^{3+} and D- or L-*myo*-inositol 1-phosphate [Bone *et al.*, 1994, a], to 2.6Å with Mn^{2+}, and to 2.6Å with Mn^{2+} and phosphate [Bone *et al.*, 1994, b]. The enzyme is a dimer with identical subunits, each folded into a five-layered sandwich of three pairs of α-helices and two β-sheets. The active sites are located in large hydrophilic caverns at the base of the two central helices.

2.1.4 The mechanism of inositol monophosphatase and lithium inhibition

Initial studies suggested that the mechanism for IMPase proceeded through a covalent phosphoenzyme intermediate [E-P; Shute *et al.*, 1988]. However, attempts to trap the E-P intermediate have not been successful [Shute *et al.*, 1988, Leech *et al.*, 1993]. Also, IMPase was unable to catalyse the exchange of ^{18}O-label from ^{18}O-water into inorganic phosphate in the absence of inositol [Baker & Gani, 1991]. This result cast further

doubt upon the existence of an E-P intermediate, unless a protein conformational change occurred upon binding of *myo*-inositol. Evidence against a mechanism proceeding *via* a E-P intermediate was obtained when it was shown that inositol phosphothioates were processed by IMPase at only slightly lower rates than the natural substrates [Baker *et al.*, 1991, a & b]: phosphatases that operate *via* E-P intermediates usually process phosphothioate substrates extremely slowly [Gani & Wilkie, 1995]. Also, the crystal structure of IMPase in the presence of substrate [Bone *et al.*, 1994, a] lacked a nucleophilic side chain in the vicinity of the phosphoryl group, which would be required to form a covalently bound E-P intermediate.

An important breakthrough in the elucidation of a mechanism for IMPase was the discovery that there are two magnesium cations in the active site [Ganzhorn & Chanal, 1990; Pollack *et al.*, 1994; Cole & Gani, 1994]. At low concentrations, Mg^{2+} was found to be a noncompetitive activator of IMPase [Hallcher & Sherman, 1980], but at high concentrations, Mg^{2+} was an uncompetitive inhibitor, with a mutually exclusive and similar inhibitory binding site to Li^{+} [Ganzhorn & Chanal, 1990; Leech *et al.*, 1993]. This mode of inhibition together with kinetic studies of Mg^{2+} dependence [Leech *et al.*, 1993] suggested Mg^{2+} binds to IMPase after the substrate. However, direct measurement of Mg^{2+} binding to IMPase [Pollack *et al*, 1993] did not require the presence of substrate, and phosphate was seen to bind only when Mg^{2+} was present [Greasley & Gore, 1993]. These results suggest that Mg^{2+} binds before the substrate to IMPase. It was proposed that two Mg^{2+} cations bind, one before and one after substrate binding, which could explain the two different modes of Mg^{2+} behaviour (noncompetitive activation and uncompetitive inhibition) [Pollack *et al.*, 1994]. This proposal was further supported by activity titration curves and modelling studies based on IMPase X-ray structures [Pollack *et al.*, 1994] and also by IMPase inhibitor studies [Cole & Gani, 1994], all consistent with a two-metal mechanism. Interestingly, fructose-1,6-bisphosphatase, another Li^{+}-sensitive enzyme with sequence homology to IMPase in the metal binding region, has also been shown to use a two-metal mechanism

Figure 2.2 : Proposed kinetic scheme for IMPase catalysis and inhibition by Li^+ or Mg^{2+} [Pollack *et al.*, 1994].

[Zhang *et al.*, 1993]. In the mechanistic model for IMPase [Ganzhorn & Chanal, 1990], it was suggested that one Mg^{2+} site was activating and the other Mg^{2+} site was inhibitory. Pollack and coworkers [Pollack *et al.*, 1994] have recently described both sites to be activating at low Mg^{2+} concentrations, with the second Mg^{2+} site becoming inhibitory if Mg^{2+} remains bound to an enzyme-phosphate complex.

Ganzhorn and Chanal [1990] suggested a preliminary model in which the phosphate ester was attacked directly by a nucleophilic water molecule. Likewise, Leech and co-workers [1993] established by kinetic studies that IMPase operates *via* a direct displacement ternary complex mechanism. Pollack and co-workers [1994] incorporated the latter results with their two metal ion site theory, and their IMPase mutagenesis studies [Pollack *et al.*, 1993], to give the mechanistic scheme shown in Figures 2.2 and 2.3(a). IMPase first binds Mg^{2+} [site 1, in Figure 2.3(a)], then *myo*-inositol monophosphate (I-P), and then a second Mg^{2+} [site 2, in Figure 2.3(a)]. This gives E.Mg.I-P.Mg and the catalytic reaction proceeds (Figure 2.2) to give E.Mg.I.P.Mg

(direct hydrolysis of substrate bound to IMPase by water). *myo*-Inositol and then the second Mg^{2+} [site 2, Figure 2.3(a)] debind, inorganic phosphate is then released, and the enzyme-magnesium complex (E.Mg) is free to bind to another substrate (Figure 2.2).

Li^+ inhibition (and Mg^{2+} at high concentrations) is uncompetitive with respect to *myo*-inositol monophosphates. This form of inhibition implies that the metal cations interact with a complex between the enzyme and substrate, intermediate or product. Inhibition by Li^+ (or Mg^{2+}) has been proposed to be primarily due to binding to the enzyme-phosphate species (E.Mg.P) to give E.Mg.P.Li after hydrolysis and inositol departure, retarding the release of inorganic phosphate (P), though other Li^+-bound species do exist. Enzyme-catalysed hydrolysis in the presence of Li^+ (dotted arrows in Figure 2.2) may proceed too slowly to contribute substantially to the kinetic scheme [Pollack *et al.*, 1994]. At high Li^+ concentrations, Li^+ inhibition becomes noncompetitive [Leech *et al.*, 1993] and this has been attributed to Li^+ binding into the first Mg^{2+} site on the free enzyme [Cole & Gani, 1994].

The functional groups of *myo*-inositol 1-phosphate required for IMPase binding and catalysis have been determined by measuring the activity of inositol phosphate analogues with certain functional groups deleted or replaced [Baker *et al.*, 1989; Baker *et al.*, 1990; Kulagowski *et al.*, 1991]. These studies showed that the phosphate dianion is the primary binding functionality for substrates and inhibitors. The 1-O-atom, 2- and 4-OH groups of Ins(1)P are important in binding whereas the 6-OH group is important for catalysis, with replacement by bulky substituents such as $Me(CH_2)_4$ affording tight binding inhibitors [Baker *et al.*, 1991, c].

Recently two groups [Atack *et al.*, 1995; Wilkie *et al.*, 1995] have both proposed that IMPase mechanism involves the direct hydrolysis of the phosphate by water. Their proposals differ in which of the two metal-ion sites provides activation, through chelation, for the nucleophilic water molecule. Atack and co-workers [1995] suggested the mechanism shown in Figure 2.3(a), from structural and mutagenesis evidence. The water molecule is activated for nucleophilic attack at phosphorus [curly arrow in Figure 2.3(a)] by a combination of Glu-70, one Mg^{2+} ion (site 1) and possibly Thr-95 binding.

Figure 2.3(a): Proposed IMPase enzyme mechanism by Atack *et al.*, 1995.

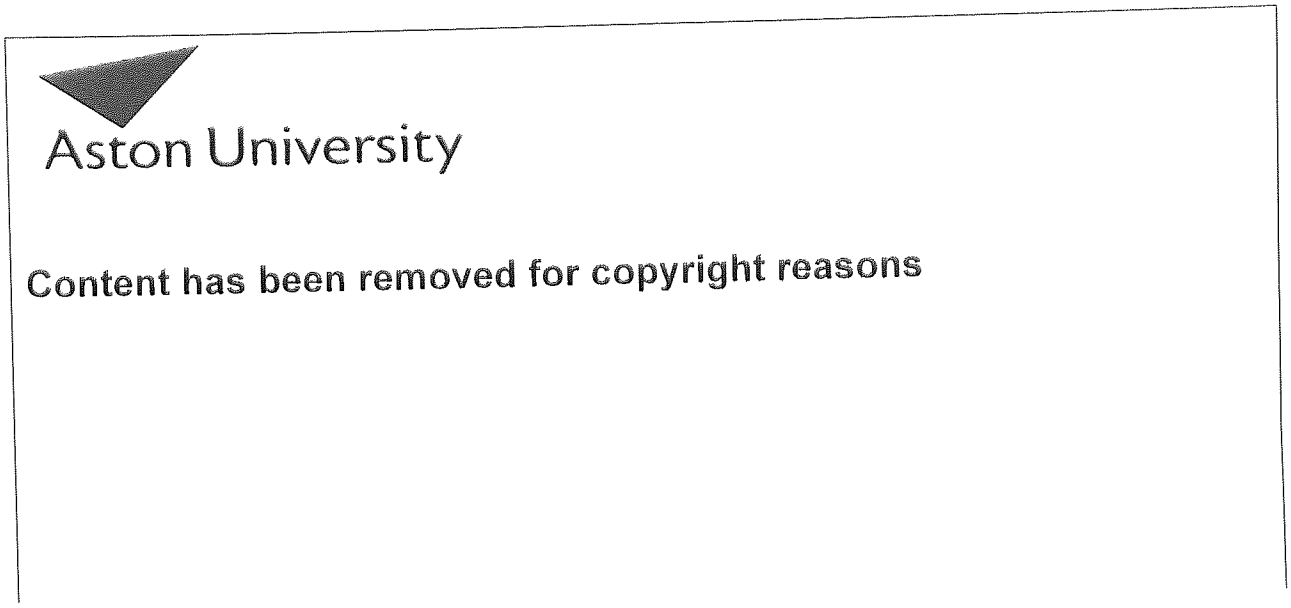

Figure 2.3(b): Proposed IMPase enzyme mechanism by Wilkie *et al.*, 1995.

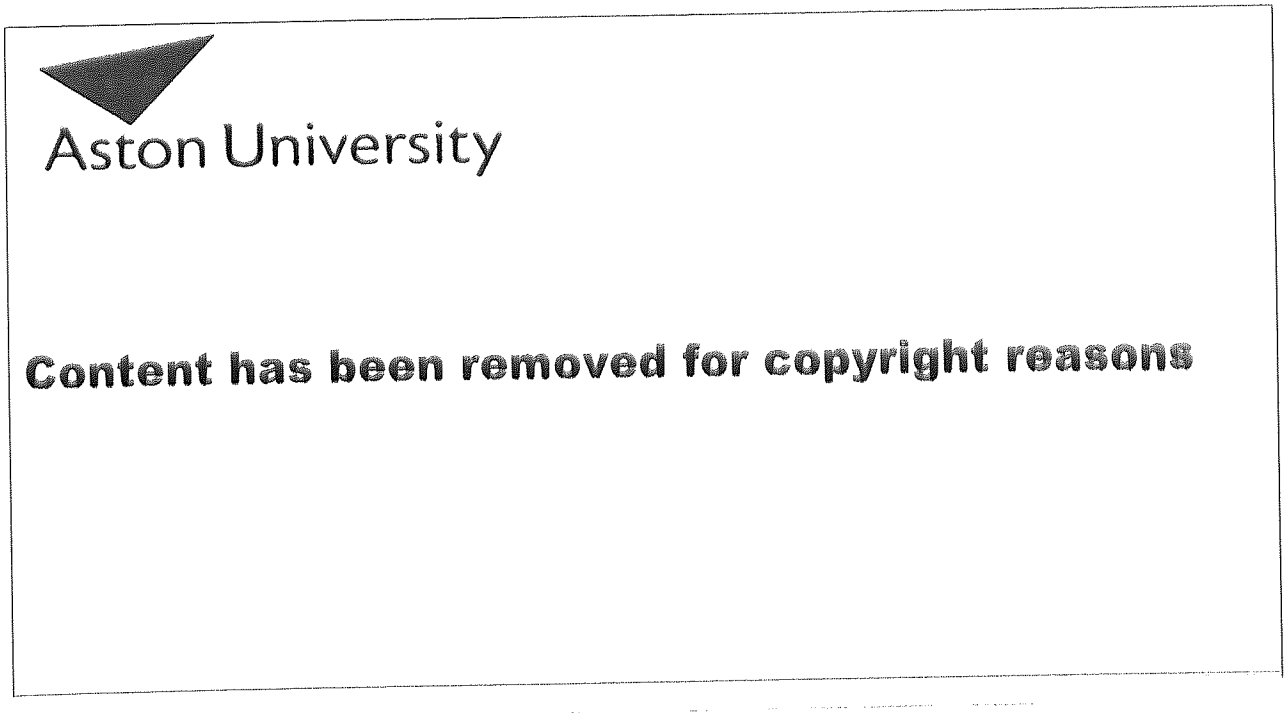

The Mg^{2+} at site 1 co-ordinates also to Asp-90, and to a phosphate oxygen which may help in substrate binding, and stabilising charges of intermediates, as well as enhancing the electrophilicity at phosphorus. A second Mg^{2+} at site 2 is co-ordinated to Asp-90, Asp-93 and Asp-220. This second metal ion is positioned such that it also co-ordinates with both the 6- and 1- O-atoms of Ins(1)P; the latter binding would activate the inositol ester oxygen for departure by acting as a Lewis acid. This model is consistent with the decrease in catalytic rate by removal of the 6-OH group of Ins(1)P [Baker *et al.*, 1989; Baker *et al.*, 1990].

Wilkie and co-workers [1995] suggested the mechanism shown in Figure 2.3(b), from modelling, comparative structural and kinetic studies of IMPase with substrates and inhibitors. The Mg^{2+} at site 1 is co-ordinated to enzyme groups Glu-70, Asp-90, Ile-92, Thr-95 and a water molecule. It is also co-ordinated to two phosphorus oxygen atoms, enhancing the electrophilicity at phosphorus. The Mg^{2+} at site 2 is co-ordinated to Asp-220, Asp-93, Asp-90, the 1-O atom of the Ins(1)P, a phosphate oxygen and a water molecule which is hydrogen bonded to the 6-OH group. This second Mg^{2+} would therefore stabilise the leaving inositol anion and promote nucleophilic attack of water on phosphorus [curly arrow Figure 2.3(b)].

Both research groups propose that Li^+ would occupy metal ion site 2 in their models. The major difference between the models is concerned with which metal position activates the water molecule; the two different sites for the nucleophile would give different stereochemical courses for phosphoryl transfer. If water is co-ordinated to Mg^{2+} at site 1 [Atack *et al.*, 1995], an in-line displacement reaction would occur with inversion of configuration at phosphorus, there being precedence for this proposal from other phospho group transfer mechanisms. If water is co-ordinated to Mg^{2+} at site 2 [Wilkie *et al.*, 1995], retention of configuration at phosphorus would occur *via* an adjacent association and pseudorotation mechanism, which is unknown for enzymatic phosphoryl group transfer reactions.

The exact mechanism by which lithium exerts its inhibition on IMPase is difficult to determine by X-ray crystallography. Apart from the difficulty in achieving an enzyme-phosphate-lithium intermediate as a crystal, Li^+ in enzyme X-ray structures is virtually

invisible because it only has two electrons and the resolution achieved in these large structure determinations is not good enough to see small atoms. Many substrates and inhibitors have been synthesized for IMPase [for a review see Billington, 1993; Potter & Lampe, 1995]. The search for an alternative inhibitor of IMPase (ie. instead of Li^+) may confirm the issue of whether this enzyme is the target of lithium in manic depression therapy.

Stereochemical studies using oxygen isotope labelled chiral thiophosphates as substrates will give a more definite indication of the enzyme mechanism involved for IMPase.

2.1.5 Stereochemical analysis of phosphatase-catalysed phosphate monoester hydrolyses

To study the stereochemical course of a phosphatase enzyme, the generated inorganic phosphate must be made chiral [Cole & Gani, 1995]. Two possible methods are available to create a chiral analogue of phosphate, as there are only three usable isotopes of oxygen (^{16}O, ^{17}O, ^{18}O); Either an alcohol is introduced as an acceptor instead of water (transphorylation) to give a phosphate monoester, or a thiophosphate monoester is used [generating chiral thiophosphate (Psi)]. Although thiophosphate monoesters used as substrates may change the kinetic and possibly the chemical mechanism of the enzyme reactions [Cole & Gani, 1995], the latter method has been used for many stereochemical studies of phosphatases, with the view that thiophosphate substrates do not alter the stereochemical outcome of the enzyme-catalysed process. The study of an enzyme's stereochemical course therefore involves the preparation of the desired chiral analogue of the phosphate substrate with known stereochemistry, reaction of the analogue with the enzyme, analysis of the generated chiral phosphate product, and comparison of its configuration with that of the initial substrate.

The synthesis of chiral phosphorothioates, with ^{16}O replaced by ^{17}O and ^{18}O, has been reviewed by Frey [Frey, 1989].

The first and most widely used methods for the analysis of generated chiral Psi were simultaneously developed by Tsai [1980], and Webb and Trentham [1980]. The

principle behind these methods, is to convert the generated product of unknown chirality (ie. chiral Psi) by enzyme reactions of known stereochemistry to a molecule where ^{18}O is locked into different position(s) dependent on the chirality of the initial product. The different positions can be distinguished by ^{31}P NMR spectroscopy and the distribution of isotopic positional species in the final product determines the chirality of the initial enzymatic product.

Analysis depends on the following observations for isotope effects on ^{31}P NMR spectroscopy :-

a) ^{18}O causes an upfield shift [Cohn & Hu, 1978]

b) the magnitude of the ^{18}O shift is measurably greater for P=O (non-bridged) than for P-O-X (bridged) [Cohn & Hu, 1980]

c) ^{17}O splits and broadens the ^{31}P NMR signals of the ^{31}P nuclei directly bonded to ^{17}O, to the extent that they are not observed [Tsai, 1979].

The enzyme reactions used in the analysis method of Tsai [Tsai, 1980] are shown in Figure 2.4. The chiral Psi enzyme product (generated from a substrate of known stereochemistry) is immediately, without being isolated, converted into ATPγS(B). Firstly, Psi is incorporated into the 1-position of 1,3-bis-P-glyceric acid by glyceraldehyde-3-phosphate dehydrogenase with intact configuration. The 3-phosphoglycerate 1-thiophosphate produced could be one of three possible species, as the reaction could proceed either through the ^{16}O, ^{17}O or ^{18}O. The 3-phosphoglycerate 1-thiophosphate is then converted to ATPγS, catalysed by phosphoglycerate kinase with inversion of configuration at phosphorus. This entails transfer of the thiophosphoryl group, by P-OC cleavage, to ADP. The only species, and its latter products (shown in Figure 2.4), observable by ^{31}P NMR has no ^{17}O isotope position, as the other two species would have broad ^{31}P NMR signals. The thiophosphoryl group is then transferred further, from ATPγS to AMP by myokinase, with inversion of configuration at phosphorus, to give ADPβS. Finally, stereospecific phosphorylation by acetate kinase of ADPβS gives ATPβS(B). On the basis of the stereochemistry involved, two inversions, (R)-[^{16}O, ^{17}O, ^{18}O] Psi would give [β-^{18}O] ATPβ-S(B) [^{18}O at the β

Figure 2.4: Configurational analysis of chiral thiophosphates (Psi)

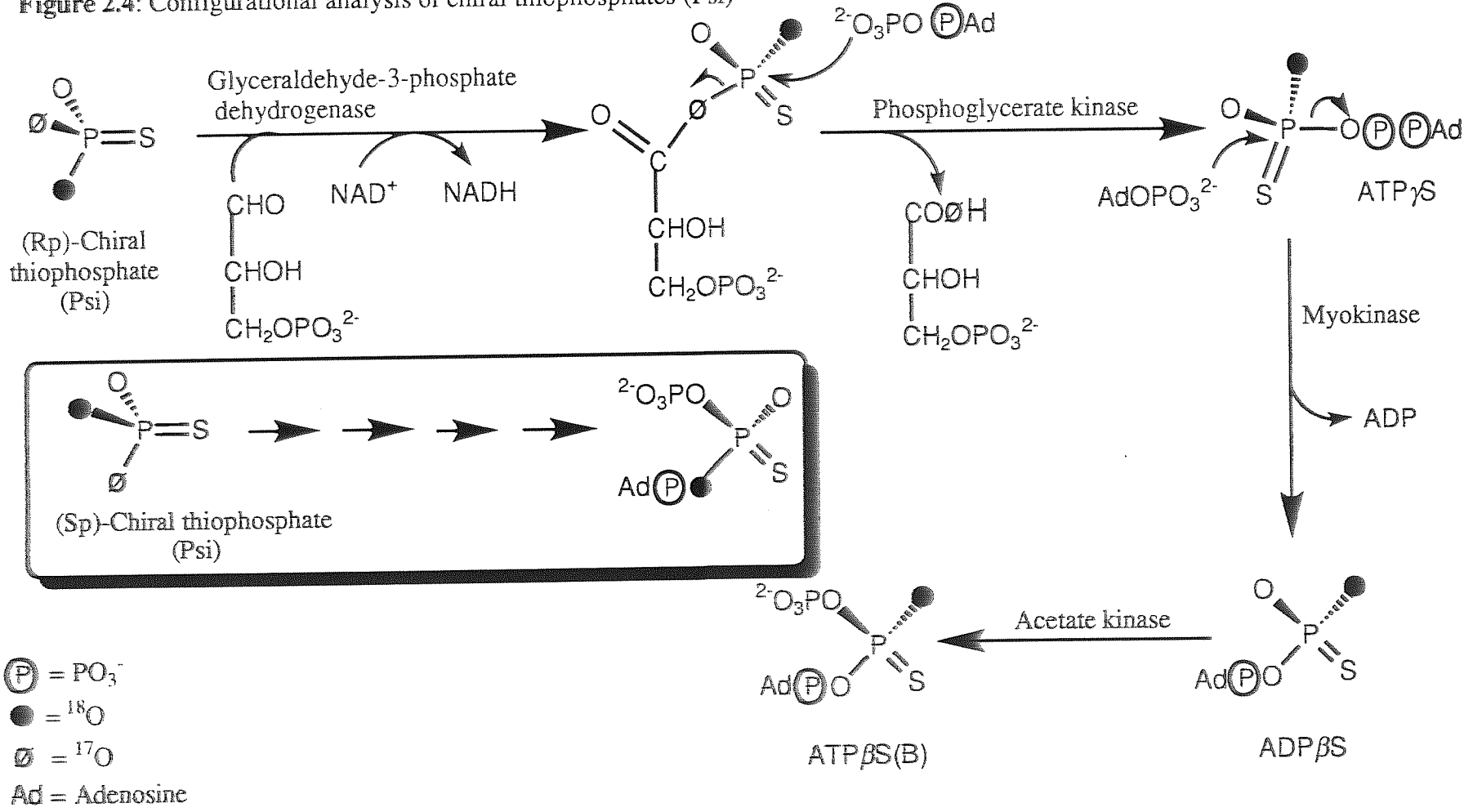

nonbridge position], whereas (S)-[^{16}O, ^{17}O, ^{18}O] Psi would yield [β-$\gamma^{18}O$] ATPβ-S(B) [^{18}O at the β-γ-bridge position]. The two ATPβ-S(B) products could therefore be distinguished by different ^{18}O shifts in ^{31}P NMR signals. In practice, the analysis is complicated by the fact that ^{17}O enrichment in $H_2{}^{17}O$ is less than 60% and so oxygens labelled ^{17}O in Figure 2.4 also have both ^{16}O and ^{18}O. Also ^{18}O contains some ^{16}O and overall this leads to eighteen products. Fortunately many of the products are duplicated and four contain an ^{17}O atom bonded to phosphorus, therefore there are only four unique products [ATPβ S(B)] detectable by ^{31}P NMR (Figure 2.5). Each of these species give a different signal by ^{31}P NMR spectroscopy (A contains no ^{18}O, therefore does not possess a shift, B has a small shift with respect to A, C a larger shift, and D the largest shift) caused by differing amounts and positions of ^{18}O. Rp- and Sp-chiral Psi generate the same product species, but differ in the ratio of B/C species and therefore in the ratio of peak heights B/C (F value) in the ^{31}P NMR spectrum. An Rp-chiral Psi sample should give F < 1 and an Sp-chiral Psi sample should give F > 1.

Figure 2.5: Four product species [ATPβS(B)] detectable by ^{31}P NMR spectroscopy

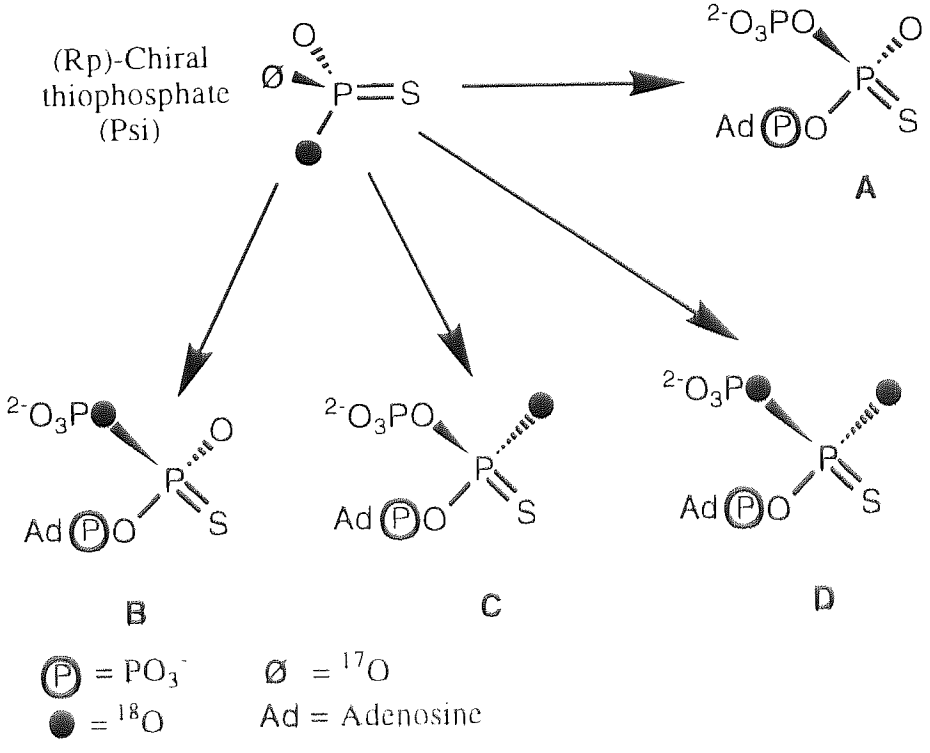

An alternative method for the analysis of chiral Psi involves alkylation and cyclisation, instead of enzymatic derivatisation and stereoselective phosphorylation [Arnold *et al.*, 1987], although the analytical strategy developed in the methods of Tsai (and of Webb and Trentham) is still being reported [Mueller *et al.*, 1993].

2.1.6 Synthesis of *myo*-inositol 1- and 3-phosphates

Figure 2.6: The *myo*-inositol monophosphates

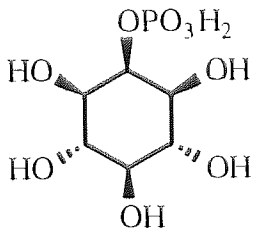

***myo*-inositol 2-phosphate**

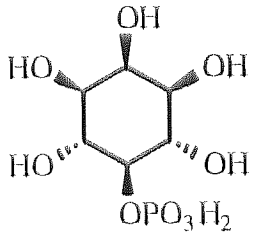

***myo*-inositol 5-phosphate**

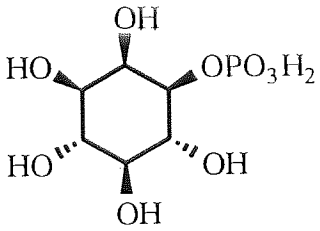

D-*myo*-inositol 1-phosphate (16)

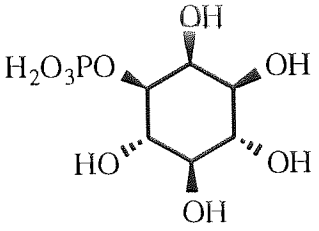

D-*myo*-inositol 3-phosphate (17)

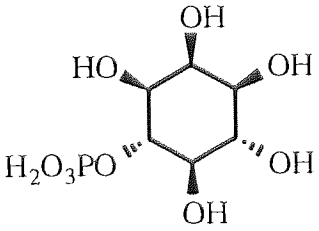

D-*myo*-inositol 4-phosphate

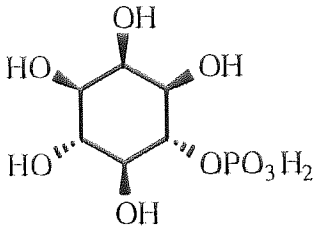

D-*myo*-inositol 6-phosphate

There are six possible *myo*-inositol monophosphates (Figure 2.6): the meso *myo*-inositol 2- and 5-phosphates, and the two enantiomeric pairs, *myo*-inositol 1(3)-phosphate and *myo*-inositol 4(6)-phosphate. They have all been synthesized previously, by a range of synthetic routes (reviewed in Cosgrove, 1980; Billington, 1989; Potter,

1990; Billington, 1993; Potter & Lampe, 1995). A brief outline of some synthetic routes to enantiomerically pure *myo*-inositol 1-phosphate (**16**) and 3-phosphate (**17**) is given here.

D-*myo*-inositol 1-phosphate (**16**) was first synthetically produced from the hydrolysis of natural phospholipids with alkali [Pizer & Ballou, 1959]. Subsequently, D-*myo*-inositol 3-phosphate (**17**) was synthesised from galactinol (Figure 2.7) which aided in elucidating the absolute configuration of the phospholipid product [Ballou & Pizer, 1960]. Benzylation of galactinol (**18**) gave a nonabenzyl derivative (**19**), which was converted to 2,3,4,5,6-penta-*O*-benzyl *myo*-inositol (**20**) on methanolysis of the galactose group. Phosphorylation of the free hydroxyl group with diphenyl phosphorochloridate, followed by hydrogenolysis to remove the protecting groups, gave D-*myo*-inositol 3-phosphate (**17**).

Figure 2.7: Synthesis of D-*myo*-inositol 3-phosphate from galactinol [Ballou & Pizer, 1960]

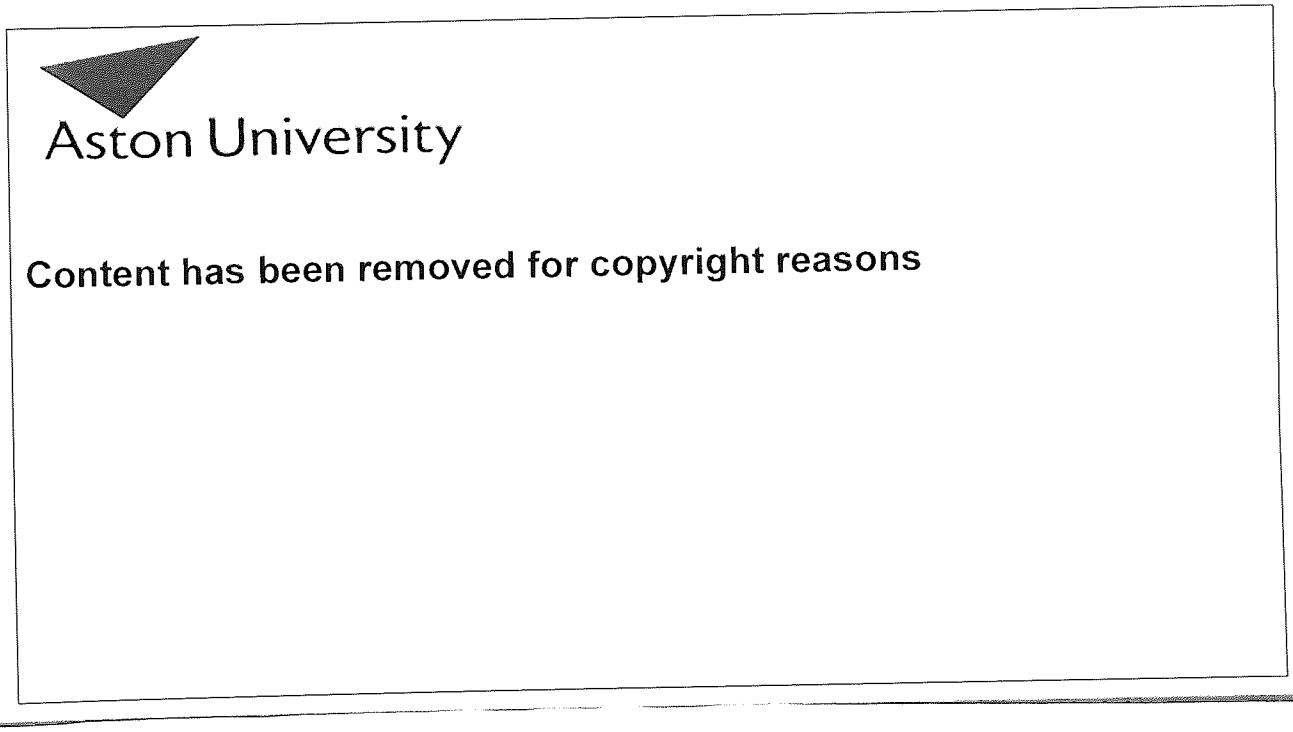

L-quebrachitol (**21**), an optically active natural product, has been used to synthesize both **17** [Mercier *et al.*, 1969; Figure 2.8] and **16** [Akiyama *et al.*, 1990; Figure 2.9]. In each synthesis, L-quebrachitol (**21**) was first converted to a bisacetal with cyclohexanone.

Figure 2.8: Synthesis of D-*myo*-inositol 3-phosphate from L-quebrachitol [Mercier *et al.*, 1969]

Aston University

Content has been removed for copyright reasons

In the synthesis of D-*myo*-inositol 3-phosphate (**17**) [Mercier *et al.*, 1969; Figure 2.8], the bisacetal derivative was tosylated at the 3D-position to give **22**, which was then treated with boron trichloride to cleave both the methyl and acetal groups, generating

Figure 2.9: Synthesis of D-*myo*-inositol 1-phosphate from L-quebrachitol [Akiyama *et al.*, 1990]

3D-*O*-*p*-toluenesulfonyl-*chiro*-inositol. Benzoylation of this pentol gave a fully protected derivative (**23**), which on treatment with NaF in DMF underwent intramolecular benzoyloxy displacement of the tosyl ester, giving the desired D-1,2,4,5,6-penta-*O*-benzoyl *myo*-inositol (**20**) as well as the meso isomer 1,3,4,5,6-penta-*O*-benzoyl *myo*-inositol (**24**). The two products were separated and the free hydroxyl group of D-1,2,4,5,6-penta-*O*-benzoyl *myo*-inositol (**20**) was phosphorylated using diphenyl phosphorochloridate. Subsequent hydrogenolysis of the phenyl groups and hydrolysis of the benzoyl esters gave D-*myo*-inositol 3-phosphate (**17**).

In the synthesis of D-*myo*-inositol 1-phosphate (**16**), the hydroxyl group of the bisacetal derivative was oxidised to a ketone followed by stereoselective reduction with $LiBH_4$ to give an inverted alcohol, which was then benzoylated to give **25** [Akiyama *et al.*, 1990; Figure 2.9]. The fully protected *myo*-inositol (**25**) was treated with $NaI/AlCl_3$, which cleaved the methyl ether and the *trans*-cyclohexylidene acetal to give **26**. Benzoylation and removal of the *cis*-cyclohexylidene acetal by acid-catalysed hydrolysis gave D-3,4,5,6-tetra-*O*-benzoyl *myo*-inositol (**27**). Selective silylation with triethylsilyl chloride at the 1-position gave **28**, benzoylation of the 2-hydroxy group and desilylation with acid generated D-2,3,4,5,6-penta-*O*-benzoyl *myo*-inositol (**29**). Phosphorylation of this alcohol with OXDEP (**13**) followed by hydrogenolysis and base-mediated debenzoylation gave D-*myo*-inositol 1-phosphate (**16**).

Billington and co-workers have devised a synthetic route to both enantiomers **16** and **17** from inositol using (-)-camphanic acid chloride as a resolving agent [Billington *et al.*, 1987; Figure 2.10]. Tetrol **6** was benzylated and the *cis*-cyclohexylidene acetal group was removed by acid-catalysed hydrolysis to give the racemate 1,2-diol (**30**). The diol **30** was selectively allylated at the 1-equatorial hydroxyl position to give **31**, benzylated at the axial 2-hydroxyl position, and then the allyl group was cleaved to give D/L-2,3,4,5,6-penta-*O*-benzyl *myo*-inositol (**32**). Resolution was achieved by conversion of racemate **32** into its diastereoisomeric camphanate esters (**33** and **34**), which were separated by chromatography. The structure of camphanate ester **33** was determined by X-ray crystallography, which allowed the absolute configuration of both esters and any inositol phosphates derived from them to be determined, without

Figure 2.10: Synthesis of D-*myo*-inositol 1- and 3-phosphates from *myo*-inositol using (-)-camphanic acid chloride as a resolving agent [Billington *et al.*, 1987]

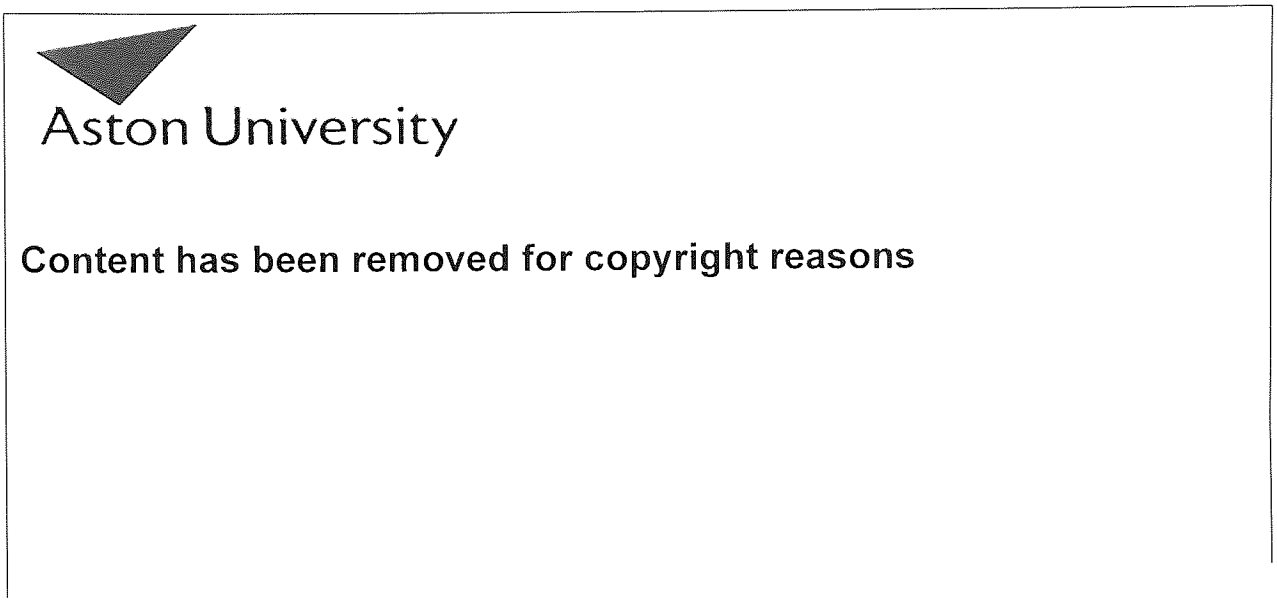

requiring any stereochemical assumptions. Hydrolysis of the individual camphanate esters, phosphorylation with diphenyl phosphorochloridate, followed by transesterification with the anion of benzyl alcohol gave the dibenzyl phosphates, which on hydrogenolysis gave the pure enantiomers **16** and **17**.

Figure 2.11: Synthesis of D-*myo*-inositol 1- and 3-phosphate from *myo*-inositol using D- and L-camphor dimethyl acetals as resolving agents [Pietrusiewicz *et al.*, 1992]

Aston University

Content has been removed for copyright reasons

Recently, Pietrusiewicz and co-workers have reported a short route to D-*myo*-inositol 1- and 3-phosphate from *myo*-inositol using D- and L-camphor dimethyl acetals as both resolving agents and protecting groups [Pietrusiewicz *et al.*, 1992; Figure 2.11]. Inositol was treated with either the D- or L-camphor dimethyl acetal. On partial hydrolysis, four possible monoacetals were generated, one of which precipitated selectively (shown in Figure 2.11). The absolute configurations of the precipitated monoacetals were determined, by X-ray crystallography of a fully protected derivative. The precipitated monoacetals (**35** and **36**) were then selectively phosphorylated at the 1- or 3- hydroxyl positions respectively, with dibenzyl phosphorochloridate. Deprotection by hydrogenolysis of the benzyl phosphate esters and acid-catalysed hydrolysis of the acetals, afforded the desired enantiomers **16** and **17** .

Overall, the number of steps involved in preparing the pure enantiomers **16** and **17** *via* the synthetic routes described above is high except for the method of Pietrusiewicz and co-workers, where resolution and protection was achieved in one step, although their yields were low. None of the methods described above would be capable of introducing a chiral thiophosphate group with known stereochemistry, which would be important to establish the stereochemical mechanism of inositol monophosphatase.

2.1.7 Aims of research

The aim of the project was to investigate the use of a chiral phosphorylating agent for the synthesis of *myo*-inositol monophosphates. Using a chiral phosphorylating agent would enable both the phosphorylation and resolution of a protected *myo*-inositol in one synthetic step. If selective phosphorylation of a partially protected inositol can be achieved with a chiral agent, the diastereoisomers formed could then be separated and deprotected to give pure enantiomers of *myo*-inositol phosphate. This synthetic route should reduce the overall number of steps.

The chiral phosphorylating agent (2R, 4S, 5R)-2-chloro-3,4-dimethyl-5-phenyl-1,3,2-oxazaphospholidin-2-one (major, **37**, Figure 2.12) was chosen for this study for the following reasons. It can be prepared in reasonable yield from (-)-ephedrine [(1R, 2S)-

2-methylamino-1-phenylpropan-1-ol] and phosphorus oxychloride. The major isomer **37** can then be separated from the minor isomer **38** by chromatography [Cooper *et al.*, 1977]. The chloro group of **37** can be substituted by nucleophiles with retention of configuration at phosphorus [Cooper *et al.*, 1977]. The P-N bond can be cleaved by acid-catalysed hydrolysis with inversion of configuration at phosphorus, and the substituted benzyl ester can then be removed by hydrogenolysis. As phosphorylation and deprotection are known to occur with overall inversion of configuration at phosphorus, the major isomer **37** has been successfully used in establishing the stereochemical course of enzyme reactions by the preparation of chiral [^{16}O, ^{17}O, ^{18}O]-phosphates [Blattler & Knowles, 1980].

Figure 2.12: Chiral ephedrine-based phosphorylating agents

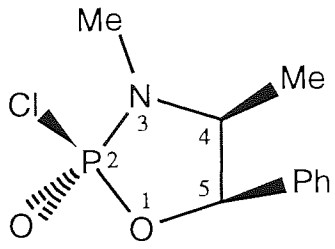

(2R, 4S, 5R)-2-Chloro-3,4-dimethyl-5-phenyl-1,3,2-oxazaphospholidin-2-one
(Major, **37**)

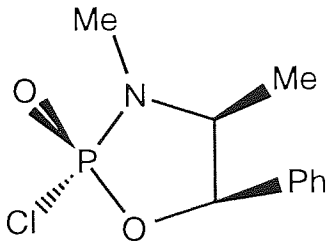

(2S, 4S, 5R)-2-Chloro-3,4-dimethyl-5-phenyl-1,3,2-oxazaphospholidin-2-one
(Minor, **38**)

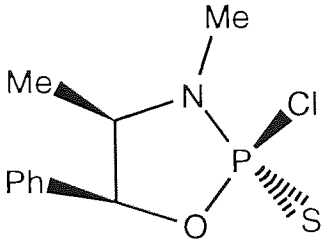

(2R, 4R, 5S)-2-Chloro-3,4-dimethyl-5-phenyl-1,3,2-oxazaphospholidin-2-sulfide
(**39**)

If this methodology is successful, it could be extended to the preparation of a thiophosphate monoester of inositol. The commercially available oxazaphospholidin-2-sulfide (**39**, Figure 2.12) has been used to determine the purity of chiral primary

amines, and primary and secondary alcohols [Johnson et al., 1984]. These two P(V) agents **37** and **39** are therefore ideal candidates for the chiral phosphorylation of protected *myo*-inositols.

2.2 RESULTS AND DISCUSSION

2.2.1 Synthesis of *myo*-inositol 3-phosphate using (2R, 4S, 5R)-2-chloro-3,4-dimethyl-5-phenyl-1,3,2-oxazaphospholidin-2-one (37) as a chiral phosphorylating agent

The general outline of the synthetic strategy is given in Figure 2.13. Each step will now be discussed in detail.

2.2.1.1 Synthesis of D/L-1,2;4,5-di-*O*-cyclohexylidene-*myo*-inositol (3)

The protected *myo*-inositol D/L-1,2;4,5-di-*O*-cyclohexylidene-*myo*-inositol (**3**, Figure 2.13) was chosen for phosphorylation studies, as it can be synthesized by a literature procedure in reasonable yield and purified by crystallisation. It can also react selectively at the 1- / 3- hydroxyl position in preference to the 4- / 6- hydroxyl position [Dreef *et al.*, 1991]. D/L-1,2;4,5-Di-*O*-cyclohexylidene-*myo*-inositol was synthesized using the method described by Dreef and co-workers [1991] from 1,1-diethoxycyclohexane and *myo*-inositol.

1,1-Diethoxycyclohexane (**43**) was first prepared by the reaction of cyclohexanone (**44**) with triethyl orthoformate (**45**) in dry ethanol at room temperature in the presence of *p*-toluenesulfonic acid (Figure 2.14). Distillation of the crude product afforded **43** as a colourless liquid in a yield of 60%, with ^{1}H- and ^{13}C-NMR($CDCl_3$) analysis similar to reported data [Dreef *et al.*, 1991].

Figure 2.13: Synthesis of *myo*-inositol 3-phosphate using **37** as a chiral phosphorylating agent

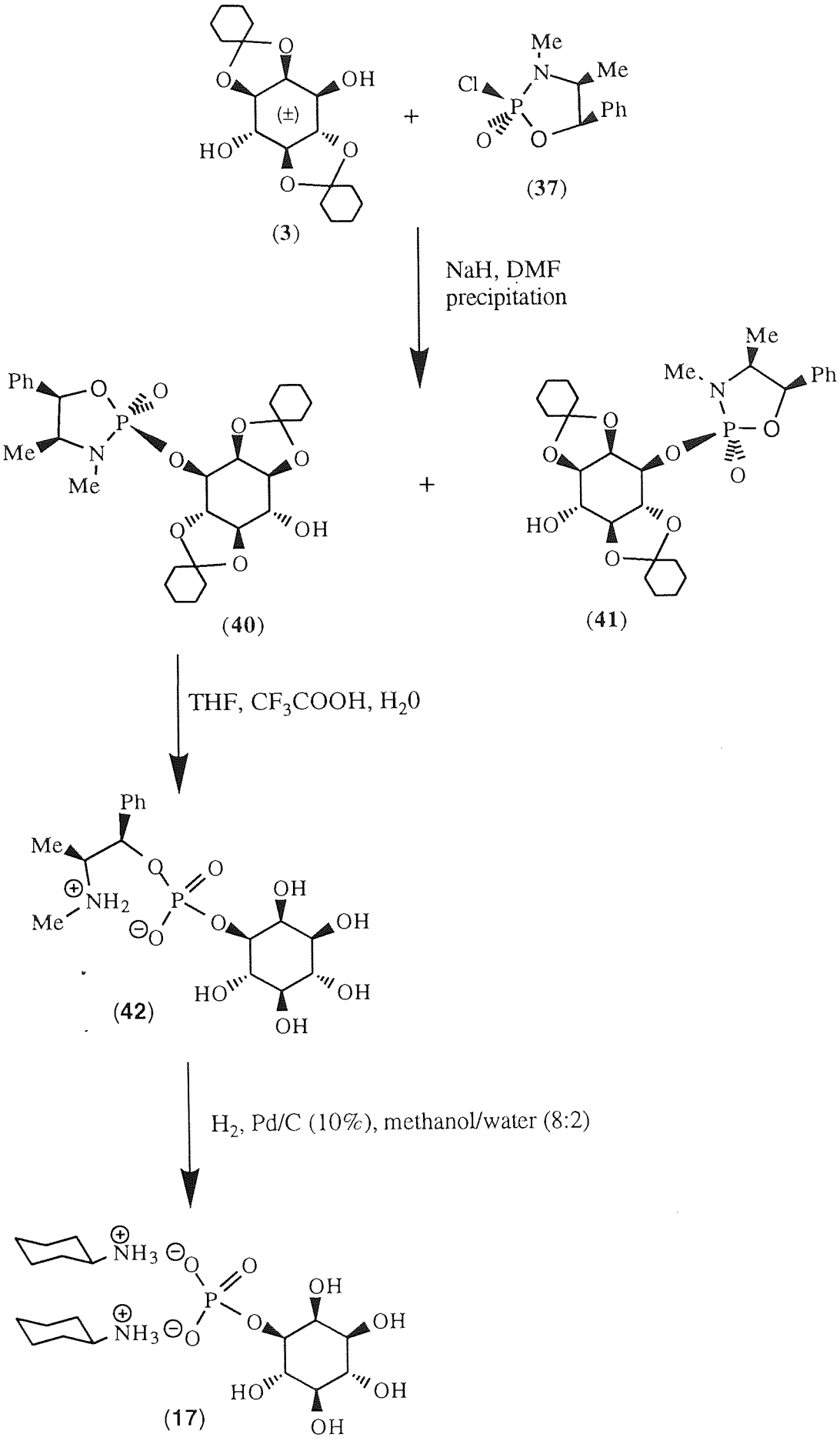

Figure 2.14: Synthesis of 1,1-diethoxycyclohexane (**43**)

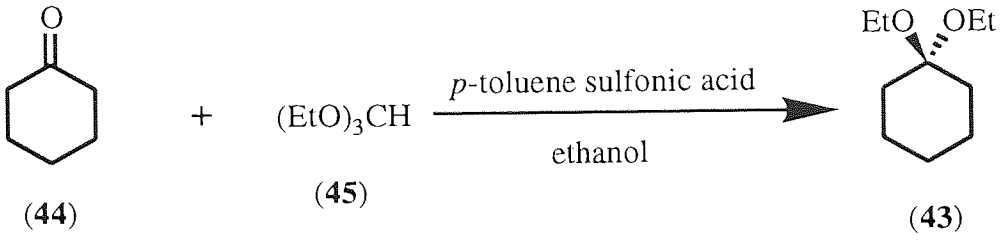

myo-Inositol (**1**) was then reacted with 1,1-diethoxycyclohexane (**43**) and *p*-toluene sulfonic acid in dry dimethylformamide (DMF) at 95°C (Figure 2.15). Three bisacetal products (**3**, **4** and **5**; Figure 2.15) are formed, but the desired derivative **3** crystallises. Crystallization of a small amount of crude product from acetone/hexane afforded compound (**3**) as rectangular plate crystals, one of which was subsequently used for X-ray diffraction structure determination (Section 4.2.1). One crystal was used to seed the remainder of the crude product to give **3** in a yield of 18%. Analysis of **3** by ^{1}H- and ^{13}C-NMR spectroscopy ($CDCl_3$) was similar to reported data [Dreef *et al.*, 1991].

Figure 2.15: Synthesis of D/L-1,2;4,5-di-*O*-cyclohexylidene-*myo*-inositol (**3**)

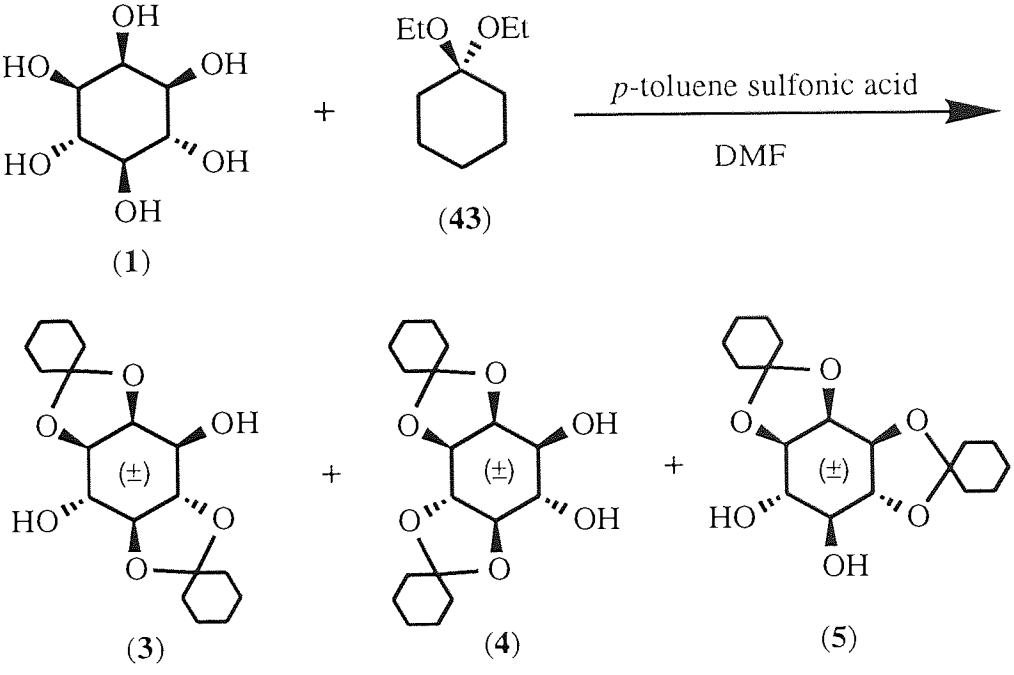

2.2.1.2 Synthesis of (2R, 4S, 5R)-2-chloro-3,4-dimethyl-5-phenyl-1,3,2-oxazaphospholidin-2-one (Major, 37)

Using a method similar to the procedure reported by Cooper and co-workers [Figure 2.16; Cooper *et al.*, 1977], phosphorus oxychloride was allowed to react with a mixture of (-)-ephedrine and triethylamine in CH_2Cl_2. ^{31}P NMR ($CDCl_3$) analysis of the crude product showed the presence of two diastereoisomers : δ 21.3 [s, major, **37**] and δ 25.1 [s, minor, **38**] in a ratio of 17:2.

Figure 2.16: Synthesis of (2R, 4S, 5R)-2-chloro-3,4-dimethyl-5-phenyl-1,3,2 oxazaphospholidin-2-one (major, **37**)

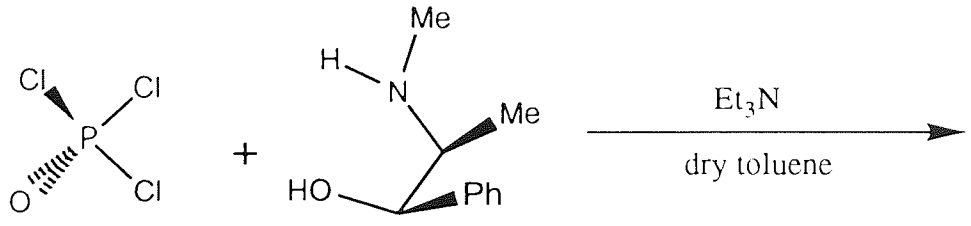

Phosphorus oxychloride

(-)-(1R, 2S)-Ephedrine hydrate

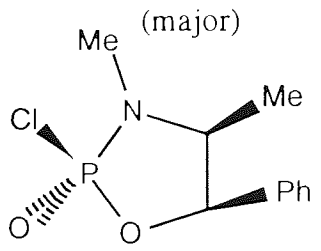

(2R, 4S, 5R)-2-Chloro-3,4-dimethyl-5-phenyl-1,3,2-oxazaphospholidin-2-one (**37**)

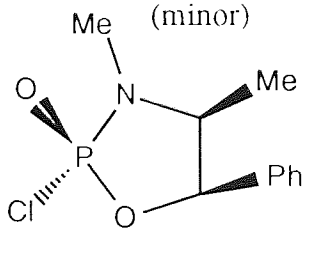

(2S, 4S, 5R)-2-Chloro-3,4-dimethyl-5-phenyl-1,3,2-oxazaphospholidin-2-one (**38**)

The major diastereoisomer **37** was separated from the minor **38** by flash chromatography eluting with ethyl acetate/hexane (2:1), to give a 69% yield of **37**. ^{31}P-, ^{1}H- and ^{13}C-NMR($CDCl_3$) spectral data of **37** were in agreement with that reported by Cooper and co-workers [1977].

2.2.1.3 Selective phosphorylation of D/L-1,2;4,5-di-*O*-cyclohexylidene-*myo*-inositol (3) with (2R, 4S, 5R)-2-chloro-3,4-dimethyl-5-phenyl-1,3,2-oxazaphospholidin-2-one (Major)

A number of small scale experiments were attempted to establish the optimum reaction conditions and the best reagents for selectively phosphorylating the diol (**3**) at the 1-/3-position with (2R, 4S, 5R)-2-chloro-3,4-dimethyl-5-phenyl-1,3,2-oxazaphospholidin-2-one (major, **37**).

1) **Solvent**

Reactions were evaluated in DMF, THF (tetrahydrofuran) or toluene. The use of DMF as the solvent gave the greatest yield and demonstrated the best selectivity, while toluene required heating which caused subsequent breakdown of products (^{31}P NMR spectrum : peaks below 10 ppm). THF as the solvent demonstrated poorer selectivity and gave lower yields than DMF. Pyridine was considered as a solvent, however this was known to cause epimerisation of the P(V) agent which would complicate the reaction [Cullis *et al.*, 1987].

2) **Base**

A 60% dispersion of NaH in oil gave only a poor yield of the required diastereoisomers with evidence of unwanted products below 10 ppm in the ^{31}P spectrum. An improvement was achieved when an excess of NaH dispersion was prewashed in hexane indicating that the dispersion oil hinders the reaction. The presence of traces of water in the reaction will cause the NaH to give sodium hydroxide, which could then catalyze the hydrolysis of the P-N bond and/or cause epimerisation at phosphorus.

t-Butylithium was also investigated and gave a similar result to washed NaH dispersion. *n*-Butyl lithium was not investigated as it can give oxazaphospholidin-2-one ring opening by nucleophilic attack [Seidel *et al.*, 1990]. 95% NaH was found to be the best reagent so long as it was carefully weighed in a glove bag and used under an argon atmosphere, avoiding moisture.

3) **Reaction conditions**

The ideal procedure for the selective phosphorylation was first to preform an anion, by reacting the diol **3** with 95% NaH under argon at 0°C for 1 hour in dry DMF. A solution of the phosphorylating agent **37** in dry DMF was then added dropwise, after which the reaction mixture was stirred for 2 hours and allowed to warm to room temperature. Selectivity was reduced if the reaction was carried out completely at room temperature, although it still went to completion. In the presence of dry DMF and NaH, the phosphorylating agent **37** was analysed by ^{31}P-NMR spectroscopy in $CDCl_3$ to see whether epimerisation and/or breakdown occured. Neither the minor diastereoisomer **38** or any breakdown products were detected, even after 12 hours. On addition of water, epimerisation and breakdown products were present therefore dry reaction conditions were essential.

A large scale reaction was completed using the reactions conditions developed above (Figure 2.17).The reaction between the P(V) agent (**37**) and diol (**3**) proceeds with retention of configuration at phosphorus. This involves apical attack of the nucleophilic anion of the diol on phosphorus, forming a trigonal bipyramidal intermediate which undergoes pseudorotation prior to apical departure of the chloride anion [Figure 2.18; Cooper *et al.*, 1977].

A ^{31}P NMR ($CDCl_3$) spectrum of the crude reaction mixture (Figure 2.19) gave the following peaks :[†]

(1) A peak at δ 19.4 ppm = Diastereoisomer **40** with 3- position phosphorylated (43%).

(2) A peak at δ 19.1 ppm = Diastereoisomer **41** with 1- position phosphorylated (40%).

(3) Two peaks at δ 18.7 and 18.5 ppm = Diastereoisomers (**46/47**) with 4-/6- positions phosphorylated (Total 12%).

(4) Small peak at δ 20.9 ppm = Starting material (5%)

(%) Quantities of each component are estimated from the ^{31}P NMR peak heights.

As anticipated, there was minimal diastereoselectivity observed in this phosphorylation reaction.

Figure 2.17: Chiral phosphorylation of diol (**3**) by oxazophospholidin-2-one (**37**)

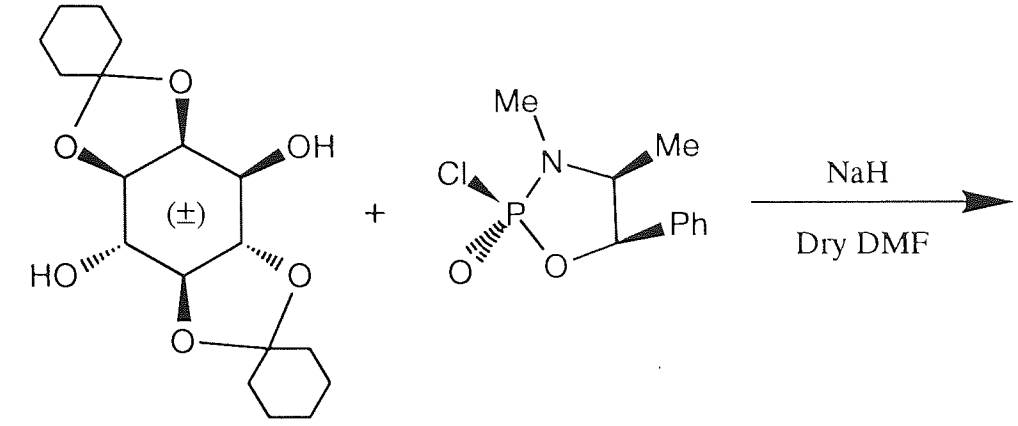

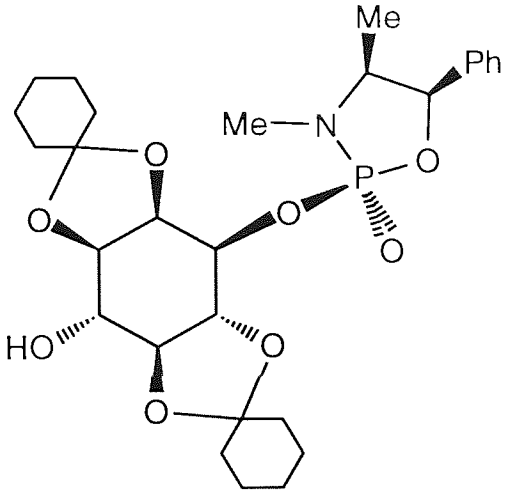

(**41**)

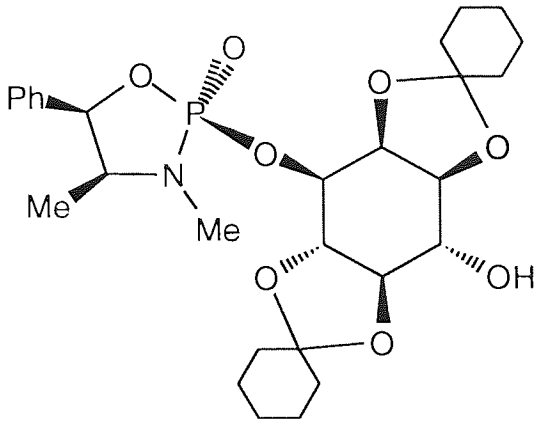

(**40**)

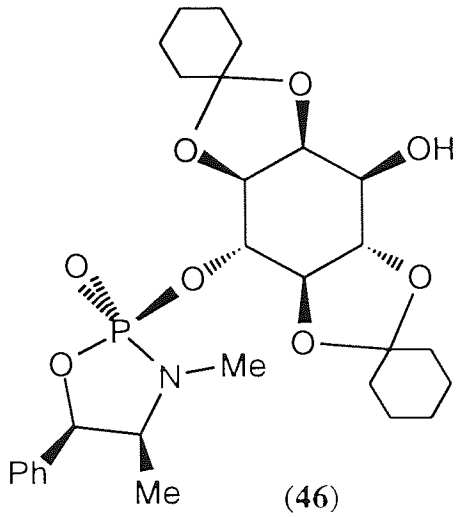

(**46**)

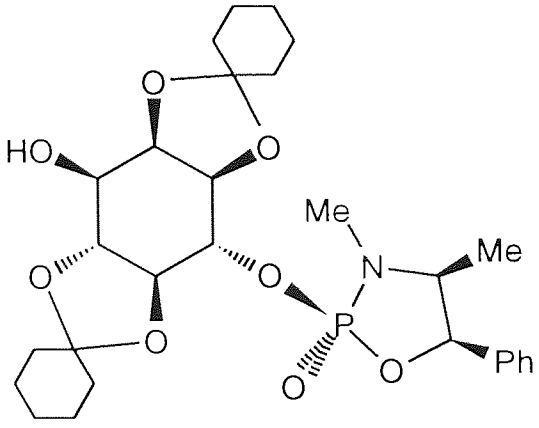

(**47**)

Figure 2.18: Pseudorotation mechanism

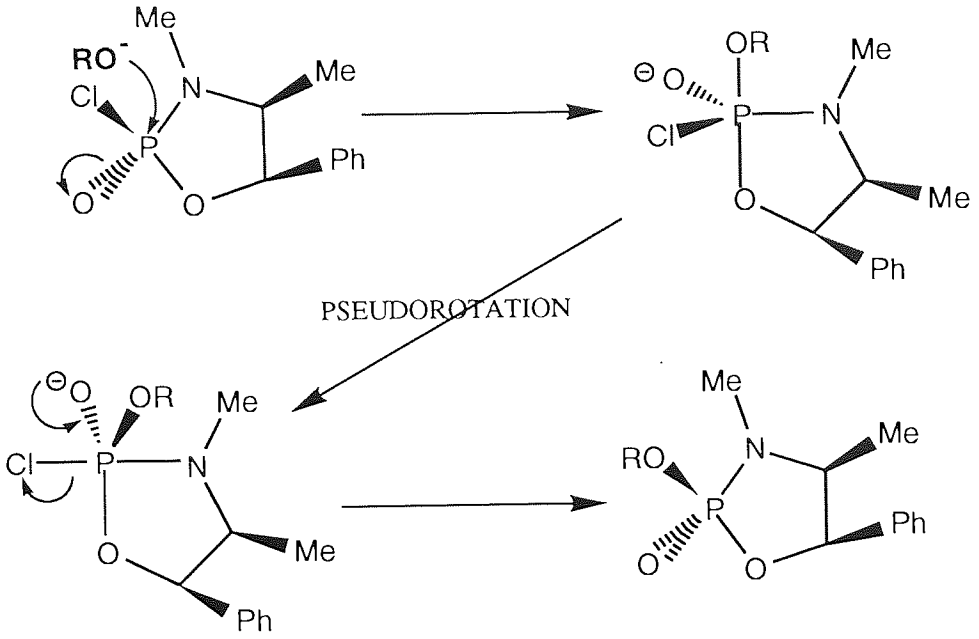

RO$^-$ = Protected inositol anion

Reaction with overall retention of configuration at phosphorus

Attempted separation of the diastereoisomers **40** and **41** by flash chromatography eluting with ethyl acetate/hexane (1:1) was unsuccessful, although it did remove the starting material **37** from the products.

Slow crystallisation from acetone/hexane gave mainly diastereoisomer (**40**, δ 19.9 ppm) with a small amount of diastereoisomer (**41**, δ 19.6 ppm) in a 15:2 ratio, as observed by ^{31}P NMR ($CDCl_3$) spectroscopy (Figure 2.20). Enrichment of the diastereoisomer **40** was therefore observed and subsequent recrystallisations gave >95% pure diastereoisomer **40** in a 17% yield. Isolation of the other diastereoisomer **41** from the filtrate was unsuccessful.

Diastereoisomer **40** was fully characterised by ^{31}P-, ^{1}H- and ^{13}C-NMR spectroscopy, elemental analysis and mass spectrometry. Most notable and informative was the J_{PC} coupling on the three inositol carbons nearest the site of phosphorylation : each was observed as a doublet in the ^{13}C-NMR spectrum.

† At this point in the synthesis, the assignment of peaks 19.4 and 19.1 was uncertain. The configuration of diastereoisomer **40** was established by extrapolating back from the optical rotation measurement of the final *myo*-inositol phosphate. Attempts were made

to assign the configuration of diastereoisomers **40** and **41**, by growing X-ray quality crystals of diastereoisomer **40** and 2D NMR experiments, however both of these approaches failed.

Figure 2.19: ^{31}P NMR ($CDCl_3$) spectrum of the crude reaction mixture from the chiral phosphorylation of diol **3** by oxazaphospholidin-2-one **37**

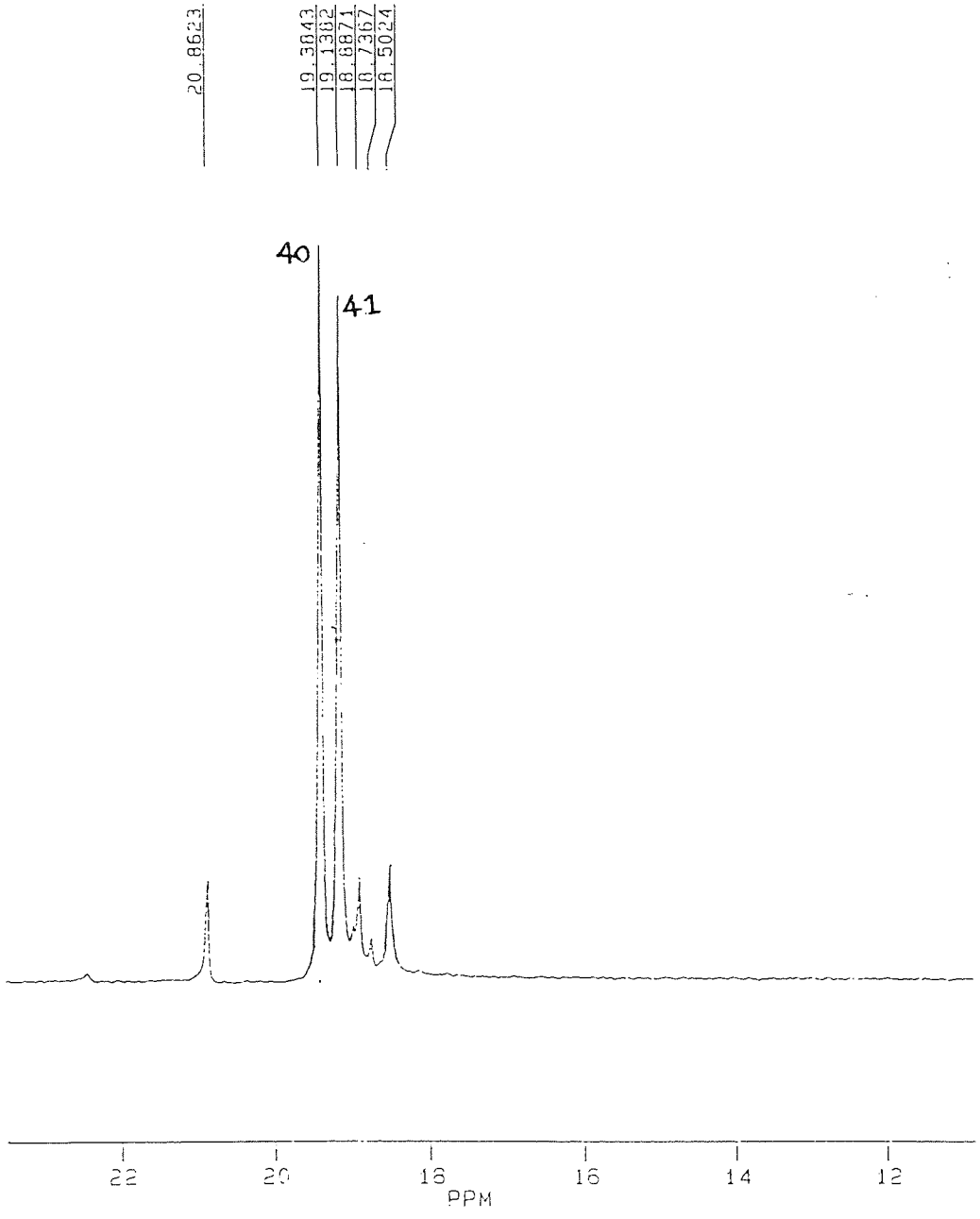

Figure 2.20: ^{31}P NMR ($CDCl_3$) spectrum showing a 15:2 ratio of diastereoisomers (**40**:**41**)

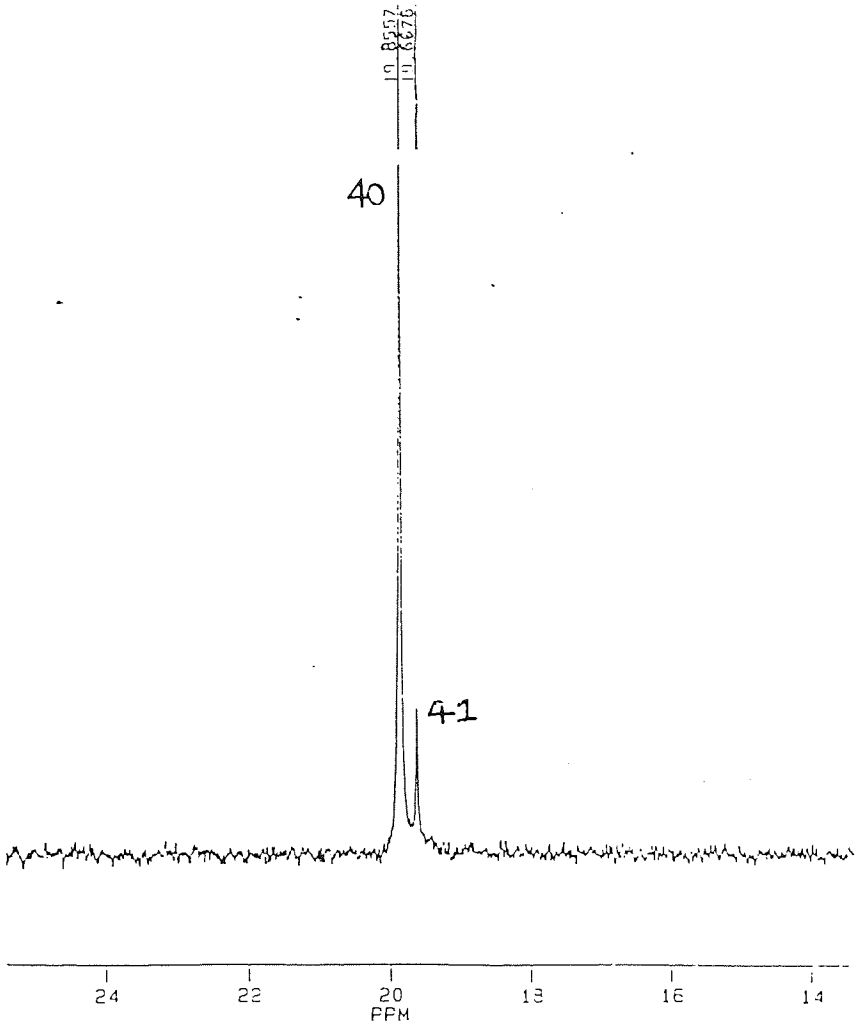

2.2.1.4 P-N bond cleavage of diastereoisomer (40) and removal of the cyclohexylidene acetal protecting groups

Acid catalysed hydrolysis of diastereoisomer (**40**) removes the cyclohexylidene protecting groups and cleaves the P-N bond to form the zwitterion (**42**, Figure 2.21). P-N bond cleavage proceeds with inversion of configuration at phosphorus, by the phosphorus equivalent of the S_N2 displacement reaction [Cooper *et al.*, 1977].

A procedure similar to one previously described [Seidel *et al.*, 1990] for a related compound was employed. A solution of diastereoisomer (**40**) in THF containing aqueous trifluoroacetic acid was stirred at room temperature for 15 minutes. ^{31}P NMR (D_2O) spectroscopy showed a quantitative yield of zwitterion (**42**), with a single peak δ -0.54 ppm. The ^{1}H- and ^{13}C NMR(D_2O) spectra were also consistent with zwitterion (**42**).

Figure 2.21: P-N bond cleavage and removal of acetal protecting groups from diastereoisomer (**40**) by acid-catalysed hydrolysis

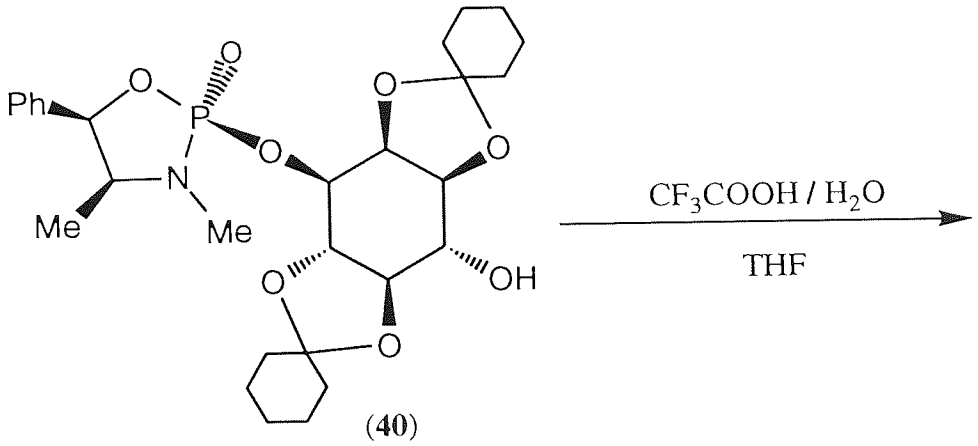

(**40**)

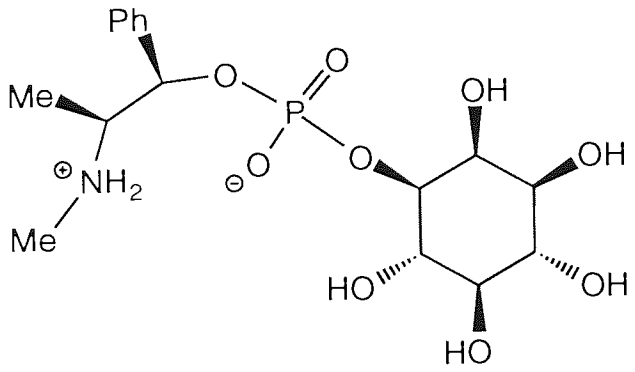

(**42**)

2.2.1.5 Removal of substituted benzyl ester protecting group from zwitterion (42)

Hydrogenolysis of the zwitterion (**42**) using a method reported for benzyl phosphate esters [Berlin *et al.*, 1991] proved successful (Figure 2.22). Zwitterion (**42**) was dissolved in methanol/water (8:2) and treated with palladium-on-carbon under an

Figure 2.22: Removal of the substituted benzyl ester phosphate protecting group from zwitterion (**42**) by hydrogenolysis, to give D-*myo*-inositol 3-phosphate (**17**)

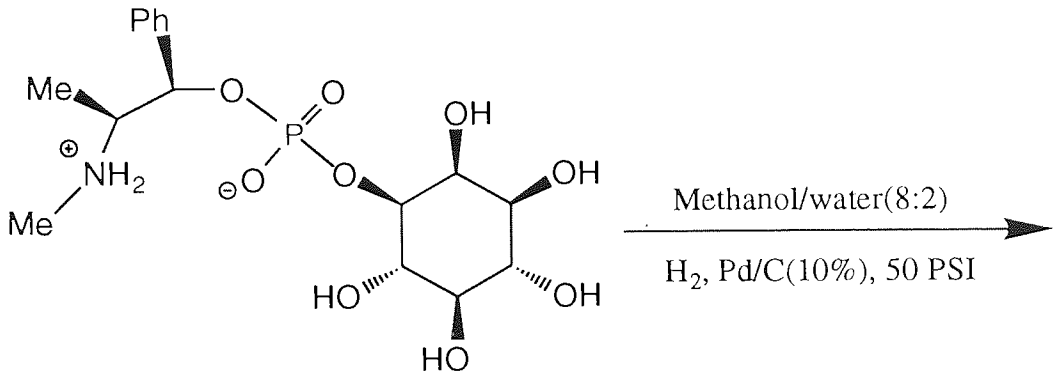

(**42**)

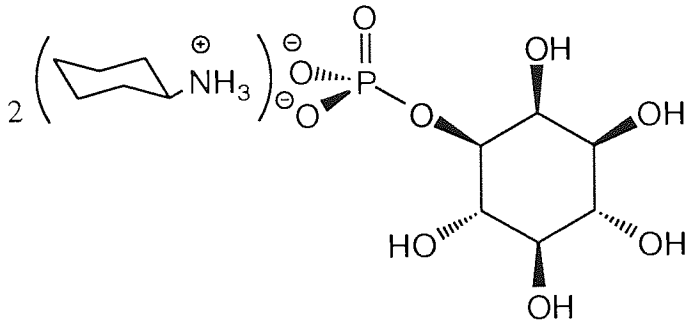

Bis(cyclohexylammonium) salt of D-*myo*-inositol 3-phosphate (17)

atmosphere of hydrogen (50 PSI) for 16 hours. After filtration to remove the catalyst, the cyclohexylammonium salt of **17** was formed by the addition of cyclohexylamine. Recrystallisation from acetone/water afforded the D-*myo*-inositol 3-phosphate salt (**17**, Figure 2.22) in a 95% yield. ^{31}P NMR (D_2O) spectroscopy showed a single peak δ 4.68 ppm with no evidence of any phosphate migration. ^{31}P-, ^{1}H- and ^{13}C-NMR($CDCl_3$) data of **17** were in agreement with reported data [Pietrusiewicz *et al.*, 1992]. Only optical rotation determination can confirm the enantiomeric form (1- or 3-) of the *myo*-inositol phosphate.

In the literature it is reported [Ballou & Pizer, 1960] that the optical rotation of *myo*-inositol 3-phosphate **17** surprisingly changes in sign when the pH is adjusted from

acidic [pH 2, +9.3°] to basic [pH 9, -3.2°]. For *myo*-inositol 3-phosphate **17**, other workers have reported values at pH 9 ranging from -2.8° to -4.9°. Consistent with this, *myo*-inositol 1-phosphate **16**, has been reported to have specific optical rotations of -9.8° at pH 2, and 3.4° to 4.5° at pH 9-9.5. It was therefore considered appropriate to measure the specific optical rotation of the product at low and high pH values. The sample was first converted to the free acid by passage down a DOWEX-50 (H^+ form) column. A sample containing 16.2mg in 2ml of water (pH 1.63) gave a specific optical rotation of +8.9°. The pH of this sample was then adjusted to 11.4 by the addition of cyclohexylamine (4 equiv.) to give the di(cyclohexylammonium) salt, which gave a specific optical rotation of -3.6°. These values are in excellent agreement with those reported in the literature, confirming the synthesis of D-*myo*-inositol 3-phosphate **17**.

2.2.2 Synthesis of *myo*-inositol thiophosphate using 39 as a chiral thiophosphorylating agent

A preliminary investigation was performed with (2R, 4R, 5S)-2-chloro-3,4-dimethyl-5-phenyl-1,3,2-oxazaphospholidin-2-sulfide (**39**, Aldrich) as phosphorylating agent (Figure 2.23). Protected inositol diol **3** was reacted with oxazaphospholidin-2-sulfide **39** under the same conditions as those used for the oxazaphospholidin-2-one reagent (**37**) in section 2.2.1.3.

^{31}P-NMR ($CDCl_3$) spectroscopy of a crude sample (Figure 2.24) showed the following results:

(1) Two peaks at δ 80.8 (s) and 82.4 (s) ppm = (±) Diastereoisomers (**48**) with 1- and 3-position phosphorylated (65%)

(2) Two peaks at δ 82.5 (s) and 83.1 (s) ppm = (±) Diastereoisomers (**49**) with 4- and 6-position phosphorylated (5.5%)

(3) A peak at δ 75.2 ppm = Starting material (**39**) showing that the reaction went to 70% completion.

(%) values are estimated quantities based on ^{31}P-NMR peak heights.

Figure 2.23: Chiral phosphorylation of diol (**3**) by oxazaphospholidin-2-sulfide (**39**)

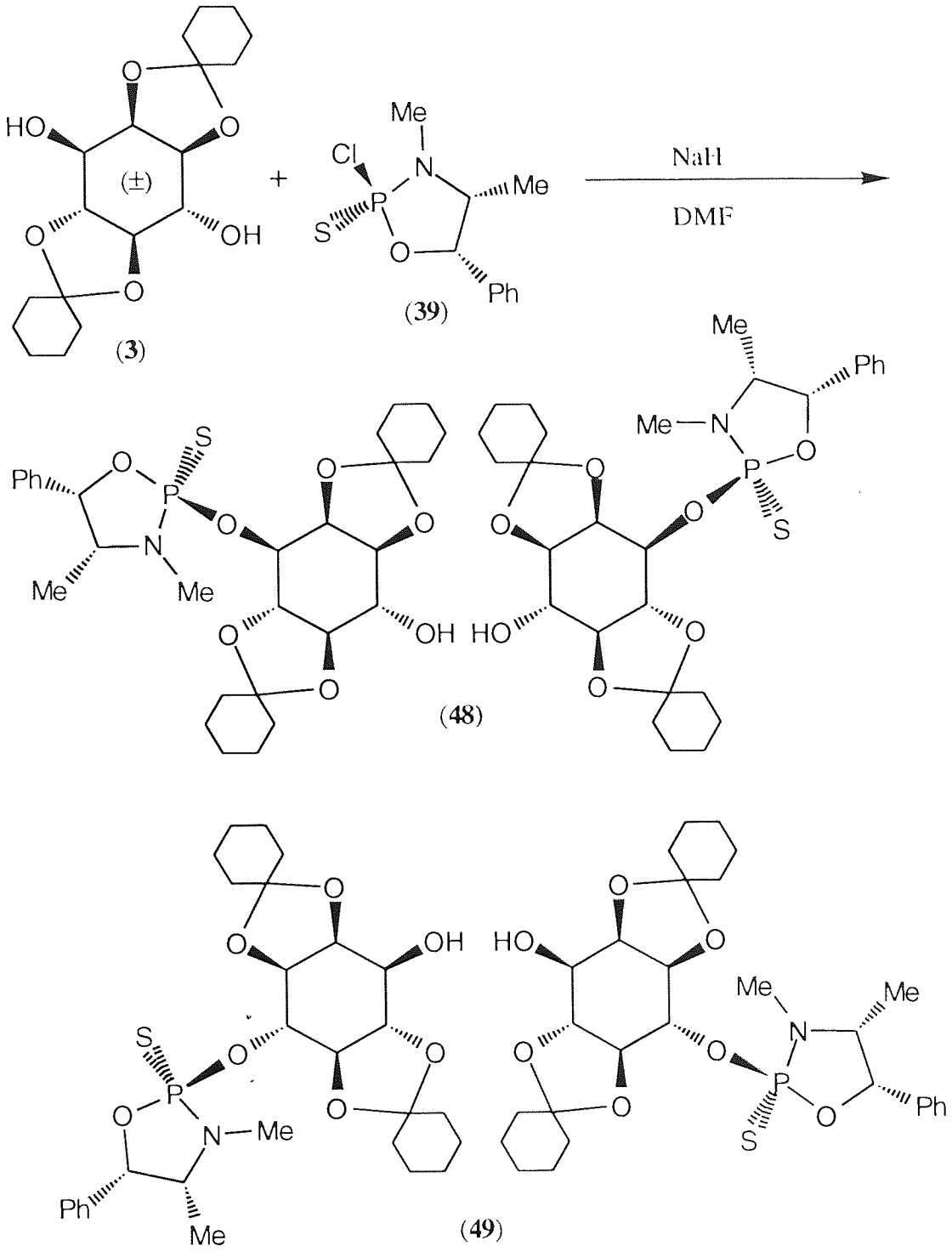

Figure 2.24: ^{31}P NMR ($CDCl_3$) spectrum of the crude reaction mixture from the chiral phosphorylation of diol (**3**) by oxazaphospholidin-2-sulfide (**39**)

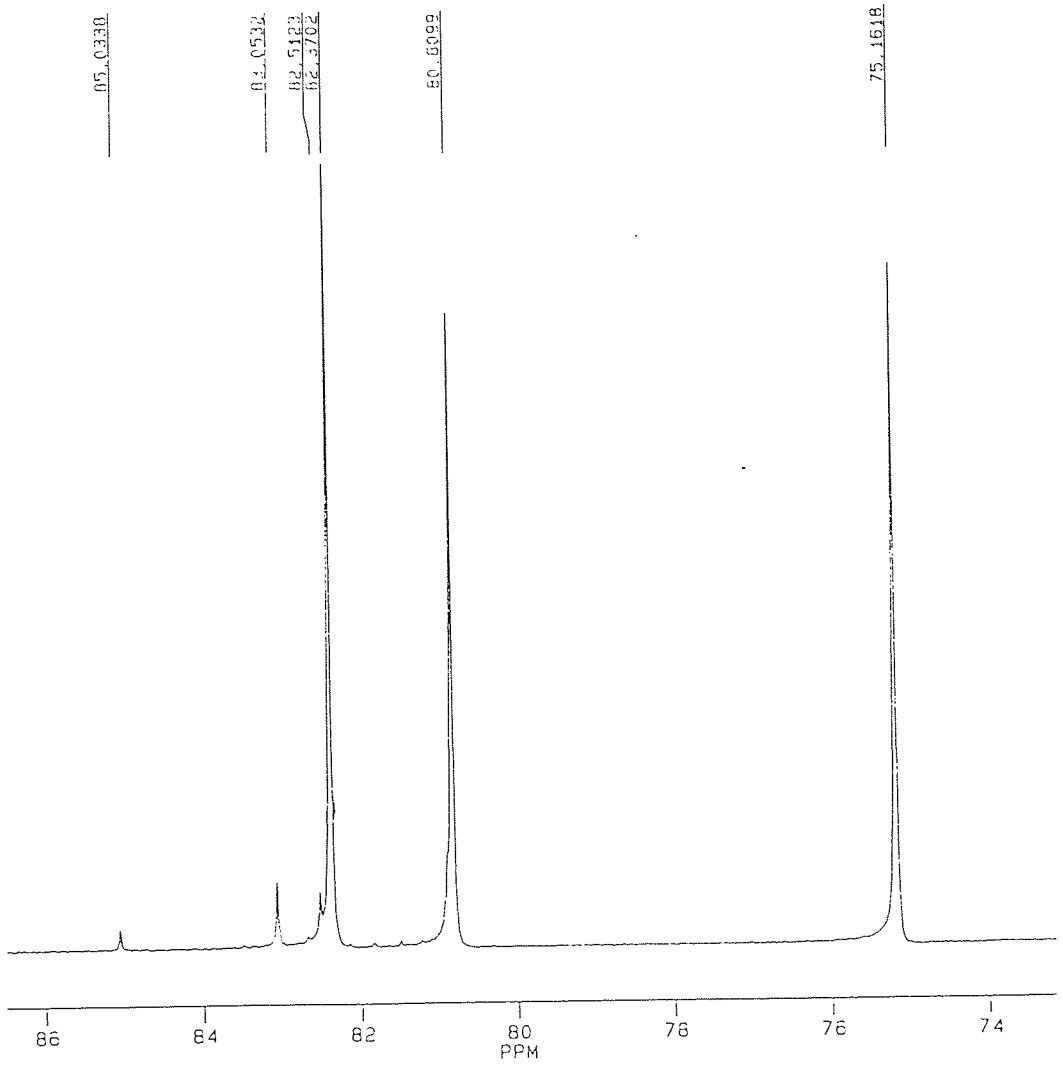

As with the 2-oxo phosphorylating reagent (**37**), little if any diastereoselectivity was observed. Separation of the products was attempted by flash chromatography eluting with ethyl acetate/hexane (1:1). The diastereoisomers **48**, from phosphorylation at positions 1- and 3-, were isolated in 26% yield from **49**, the diastereoisomers from the phosphorylation at positions 4- and 6- and the starting material **39** (Figure 2.25). The pair of diastereoisomers **48** could not be separated, although a small amount of

Figure 2.25: ^{31}P NMR ($CDCl_3$) spectrum showing diastereoisomers **48** isolated from the reaction of the diol **3** with the oxazaphospholidin-2-sulfide **39**

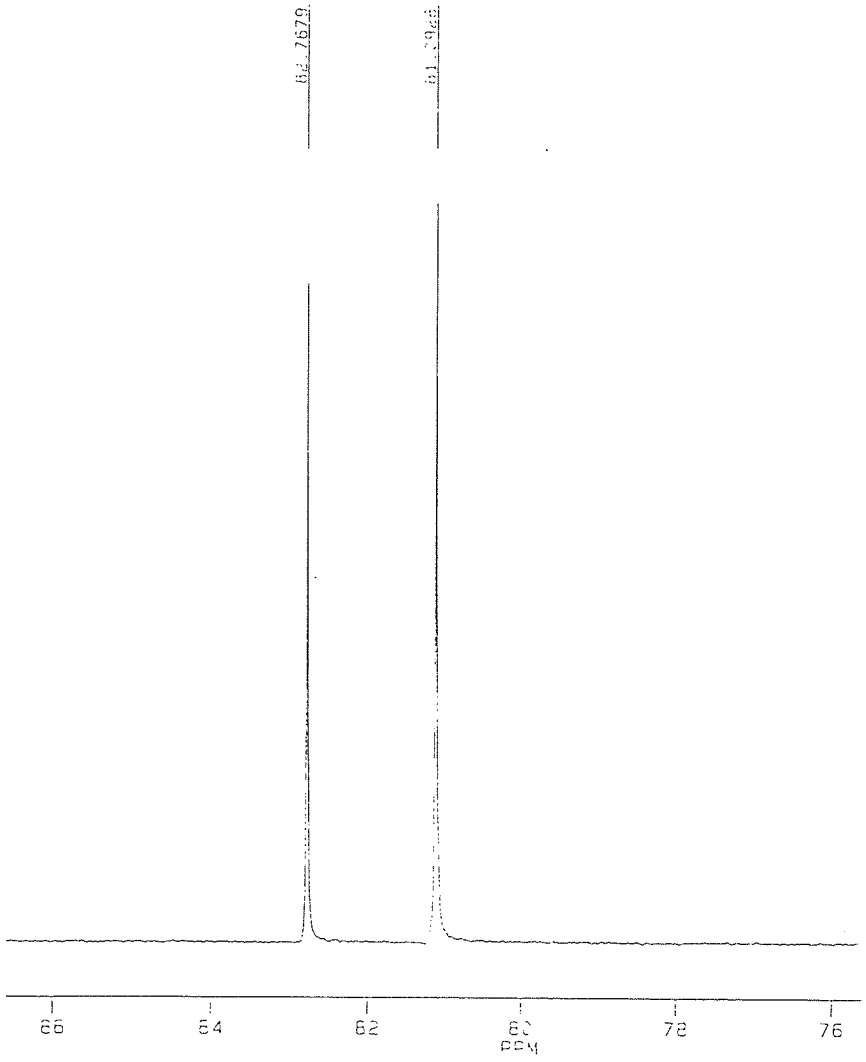

enrichment was observed. Slow crystallisation to separate the diastereoisomers **48** was also unsuccessful. The pair of diastereoisomers **48** (Figure 2.25), with peaks at δp 81.1 and 82.8 ppm in a 1: 0.9 ratio by ^{31}P-NMR ($CDCl_3$) analysis, were subsequently further characterised by ^{1}H- and ^{13}C-NMR spectroscopy, mass spectrometry and elemental analysis.

The enzyme inositol monophosphatase can catalyse the hydrolysis of inositol phosphates with a phosphate at positions 1, 3, 4 or 6. The mixture of diastereoisomers **48** could therefore still be used to produce chiral inositol thiophosphate probes for this enzyme.

Figure 2.26: P-N bond cleavage of diastereoisomers (**48**) by acid-catalysed hydrolysis

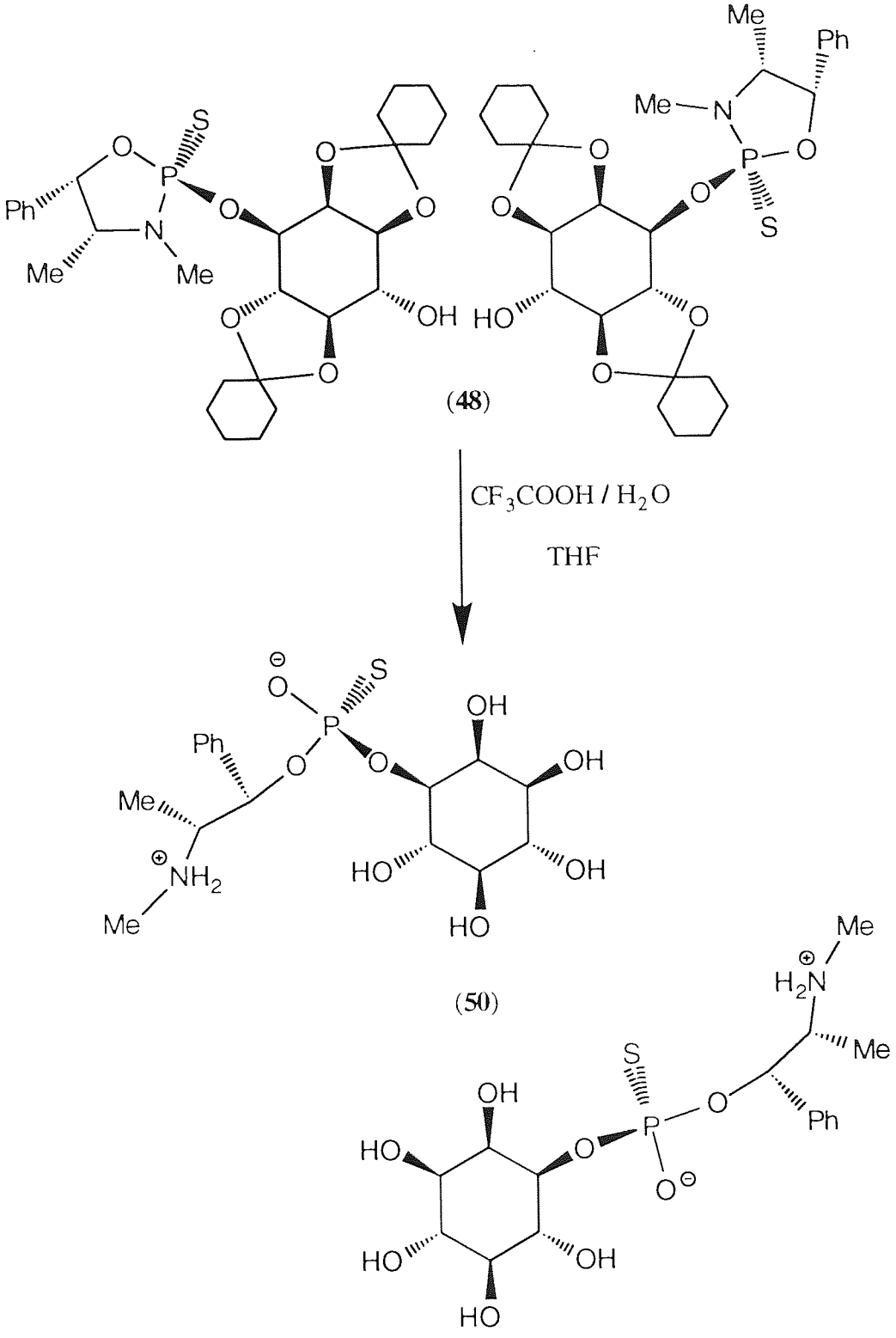

The thiophosphates formed from the pair of diastereoisomers **48** would have the same configuration at phosphorus (if oxygen isotopes were used), and would yield after inositol monophosphatase catalysed hydrolysis, the same labelled [^{17}O, ^{18}O, ^{16}O]-inorganic thiophosphate.

Acid-catalysed hydrolysis of the P-N bond in the pair of diastereoisomers **48** (Figure 2.26) with aqueous trifluoroacetic acid using the same conditions as described for the 2-one analogue **40**, yielded the zwitterions **50** in 69% yield. The zwitterions **50** were analysed by ^{31}P-NMR spectroscopy with 2 peaks at δ 56.5 and 56.9 ppm with a 0.9:1 peak height ratio. The diastereoisomeric mixture of zwitterions **50** was also characterised by ^{1}H- and ^{13}C-NMR spectroscopy.

A different method would be required to remove the benzyl ester protecting groups from zwitterions **50**, as thiol compounds poison palladium catalysts. An alternative approach would be to use sodium in liquid ammonia [Cullis *et al.*, 1986] to generate the racemic *myo*-inositol 1/3-thiophosphates.

2.3 CONCLUSION

Selective phosphorylation of (±)-1,2;4,5-di-*O*-cyclohexylidene *myo*-inositol has been achieved with the chiral P(V) oxazaphospholidin-2-one (**37**) at the 1- and 3-positions. One of the diastereoisomeric products (**40**) was separated by crystallisation, and deprotection afforded pure *myo*-inositol 3-phosphate without phosphate migration. A short synthesis to an optically pure inositol monophosphate has therefore been achieved without the need for extensive protection and separate resolution. It should also be possible to synthesise *myo*-inositol 1-phosphate using a P(V) reagent prepared from the enantiomer, (+)-ephedrine. An ephedrine based chiral phosphorylating reagent has also been used successfully to introduce a thiophosphate group into a protected inositol. Separation of diastereoisomers was achieved on one occasion although this may be improved by using a protected inositol with two different protecting groups present, for example a cyclohexylidene ring protecting positions 1 and 2, and allyl groups

protecting positions 4, 5, and 6. Once phosphorylated, this may lead to a greater difference in the two diastereoisomeric products, which may be separable by flash chromatography.

The synthetic route used should enable the incorporation of stable isotopes of oxygen, required for generating a chiral ^{18}O and ^{17}O labelled thiophosphate derivative of inositol, with known configuration at phosphorus. There is an opportunity to introduce an ^{18}O-label into the thiophosphate at the acid hydrolysis P-N bond cleavage step, by using $H_2{}^{18}O$. If the enzyme (inositol monophosphatase) hydrolysis reaction was then carried out in $H_2{}^{17}O$, a chiral Psi would be generated. Analysis of this chiral Psi would allow determination of the stereochemical course of the enzyme, inositol monophosphatase.

CHAPTER 3

Synthesis of *myo*-inositol 1,2,3-trisphosphate and iron complexation studies of inositol phosphates

3.1 INTRODUCTION

3.1.1 *myo*-Inositol hexakisphosphate and its biological function

myo-Inositol hexakisphosphate ($InsP_6$, phytic acid, phytate, **51**) is the most abundant organic form of phosphate, typically present in soil at concentrations of 10-100 μM [Cosgrove, 1980]. It is found in virtually all mammalian cells in substantial amounts (10μM-1mM) [Szwergold *et al.*, 1987].

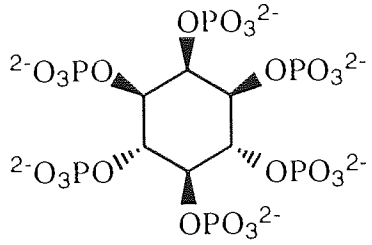

(51)

Figure 3.1 : Chemical structure of $InsP_6$

$InsP_6$ has many possible clinical uses including the prevention and treatment of a range of cancers, recently reviewed by Shamsuddin [Shamsuddin, 1995], although its actual anti-cancer mechanism is at present not fully elucidated.

$InsP_6$'s biological functions in the majority of cells still remains uncertain [Menniti *et al.*, 1993]. Specialised activities for $InsP_6$ have been reported, including its role as a storage compound in seeds [Carpenter *et al.*, 1989] and modulation of the activity of glycolytic enzymes in certain metabolic compartments of skeletal muscle [Koppitz *et al.*, 1986]. $InsP_6$ may also be a neurotransmitter in the mammalian brain along with Ins(1,3,4,5,6)P_5 [Vallejo *et al.*, 1987], with improved binding of $InsP_6$ to neuronal membranes in the presence of trivalent ions, Fe^{3+} and Al^{3+} [Cooke *et al.*, 1991], although chelation of $InsP_6$ to Ca^{2+} has been proposed to be responsible for its extracellular action [Smith & Dürmüller, 1990; Sun *et al.*, 1992]. It has recently been suggested that $InsP_6$ turnover is more rapid than previously thought [Menniti *et al.*, 1993] and that it can be metabolised further to inositol pyrophosphate analogues; possible new forms of phosphate donors in an as yet undescribed set of

phosphotransferase reactions [Stephens *et al.*, 1993], therefore $InsP_6$ may not represent a metabolic end point. Another group of possible functions for $InsP_6$ arises from its anti-oxidant and metal chelation properties [Graf & Eaton, 1990]. In addition, Smith and coworkers [Smith *et al.*, 1994] have described how $InsP_6$ and related compounds can be used as siderophores by *Pseudomonas aeruginosa*, suggesting that $InsP_6$ in the external environment may have a role in supplying Fe^{3+} to free-living organisms.

3.1.2 Iron complexation and antioxidant properties of $InsP_6$

$InsP_6$ has long been of interest to nutritionists, as it is present in high concentrations in wheat bran where it can prevent absorption of trace metals. It has been proposed that one of $InsP_6$'s possible mechanisms for cancer prevention and treatment may be attributed to its ability to bind Fe^{3+} and divalent cations [Shamsuddin, 1995]. Graf and coworkers [Graf *et al.*, 1984] have shown that chelation of Fe^{3+} to $InsP_6$ prevented formation of the highly reactive hydroxyl radical (HO·) from the superoxide radical anion ($O_2^{-}\cdot$) by the iron-catalysed Haber-Weiss redox cycle (Figure 3.2) [Halliwell & Gutteridge, 1989].

$$O_2^{-}\cdot + Fe^{3+} \longrightarrow Fe^{2+} + O_2$$

$$H_2O_2 + Fe^{2+} \longrightarrow Fe^{3+} + HO\cdot + HO^- \qquad \textbf{(Fenton reaction)}$$

$$O_2^{-}\cdot + H_2O_2 \longrightarrow O_2 + HO\cdot + HO^- \qquad \textbf{(Net reaction)}$$

Figure 3.2 : Iron catalysed hydroxyl radical formation

Graf and coworkers [Graf *et al.*, 1984] suggested that the Fenton reaction does not occur with $InsP_6$/monoferric chelates and this was attributed to the unavailability of a coordination site for H_2O_2 in the complex. The presence of a coordination water (free site) in the chelates was determined by competitive displacement of water by an azide molecule and measurement by UV spectroscopy, with replacement giving a new absorption peak at 409 nm. This was further supported by NMR studies, with a

decrease in relaxation rates on addition of an azide molecule to the coordination site of the chelate [Graf *et al.*, 1984]. In $InsP_6$/polyferric chelates hydroxyl radical formation is also inhibited. The low solubility of $InsP_6$/polyferric chelates prevents investigation of the iron coordination chemistry and the existence of a displaceable water, although it was proposed that there would be a free coordination site in $InsP_6$/polyferric chelates (based on the stereochemistry). Inhibition of hydroxyl radical by $InsP_6$/polyferric chelates was explained by the oxidation of Fe^{2+} by molecular oxygen (reverse of first step) catalysed by $InsP_6$ (which also could occur in monoferric chelates), which would give a shift in the redox potential of iron. This rapid removal of Fe^{2+} without generation of HO· would contribute to the anti-oxidant properties of $InsP_6$ [Graf & Empson, 1987]. In contrast, some iron chelates, for example with ADP, do catalyse the formation of hydroxy radicals [Floyd & Lewis, 1983]. This was attributed to the increased solubility of iron on complexation and to the availability of a readily dissociable water ligand in such complexes, which is displaced by H_2O_2 in the Fenton reaction [Graf *et al.*, 1984]. In contrast, Burkitt and Gilbert concluded that $InsP_6$ catalyses the Fenton reaction and they also observed that the first step of the Haber-Weiss cycle is blocked due to a change in the redox potential on complexation of $InsP_6$ with Fe^{3+} [Burkitt & Gilbert, 1990 ; Burkitt & Gilbert, 1991].

3.1.3 $InsP_6$: Low molecular weight chelator of iron

Animal cells possess iron in low molecular weight pools [Pippard *et al.*, 1982] which may transport iron between transferrin (major route of iron entry into cells), ferritin (major iron depot in cells) and proteins which require iron to function [Poyner *et al.*, 1993]. The nature of the ligands which constitute the iron pool is unclear. A number of molecules have been postulated to exert such a role, for example, amino acids [Deighton & Hider, 1989] and ATP [Weaver & Pollack, 1989]. It has recently been proposed that $InsP_6$ may be a more attractive intracellular, low molecular weight, 'safe' chelator of Fe^{3+} [Hawkins *et al.*, 1993] due to its high affinity (in region of 10^{25}-10^{30} [Poyner *et al.*, 1993]), its high cellular concentrations and its antioxidant properties

described above. Cycling of specific phosphate groups on $InsP_6$ [Stephens & Irvine, 1990] could allow directional transport of bound metal ions mediated by controlled and localised phosphorylation and dephosphorylation reactions. Phosphates have also been shown to exchange iron between iron-binding proteins [Morgan, 1977; Cowart *et al.*, 1986].

3.1.4 Siderophore activity of $InsP_6$

Iron is an essential element for the growth of many microorganisms, and in iron depleted conditions, competition for iron is essential for survival. Many pathogens synthesize siderophores, low-molecular-mass high affinity iron chelators and the corresponding cell surface receptors to enable the cellular intake of external iron, reviewed by Neilands [Neilands, 1993]. For example, in *Pseudomonas aeruginosa* , two known siderophores are synthesised under iron-limiting conditions, pyochelin and pyoverdine, discussed by Poole [Poole *et al.*, 1991]. Smith and coworkers [Smith *et al.*, 1994] described that *Escherichia coli* and *Pseudomonas aeruginosa* are two examples of bacteria that can also utilise siderophores produced by other bacterial and fungal species to solubilise and transport environmental iron.

There is a possibility that iron in the environment could be chelated by $InsP_6$ and so its siderophore activity was investigated for the procaryote *Pseudomonas aeruginosa* [Smith *et al.*, 1994] . This study showed that $InsP_6$ can promote radiolabelled ^{55}Fe uptake into cells and allow growth in a mutant strain which is deficient in siderophore production and grown in iron-deficient succinate medium. The transport process was iron repressible: a decrease in the initial transport rate was seen on the addition of iron to the growth medium, although the binding of the $InsP_6/Fe^{3+}$ complex to the cell surface was unaffected by iron concentration. This suggested that some components are regulated by iron, but that the membrane-associated binding proteins are not. It is unclear how iron is released or transported from the $InsP_6/Fe^{3+}$ complex, this study showed intracellular iron accumulation but was unable to determine whether $InsP_6$ enters the cell.

The key to understanding many of the proposed biological properties of $InsP_6$ lies in its physico-chemical properties, particularly the way in which it interacts with metal ions such as Fe^{3+}. Evans and Martin have studied the interactions of Fe^{3+} and Al^{3+} with $InsP_6$ by calorimetry [Evans & Martin, 1988; Evans & Martin, 1991]. Insoluble complexes were mainly formed which were shown to contain 4 equivalents of metal cation for each $InsP_6$.

3.1.5 The structure of $InsP_6$

$InsP_6$, either in the crystalline form as the dodecasodium salt [Blank *et al.*, 1975] or bound to deoxyhemoglobin [Arnone & Perutz, 1974], adopts a chair conformation, with five of the phosphate groups (1-, 3-, 4-, 5- and 6-) surprisingly in axial positions. In the dodecasodium salt, the phosphate groups were stabilised by bridging sodium ions and hydrogen bonded water molecules which could account for its unusual conformation. NMR studies of this salt form in solution support the 5 axial/1 equatorial structure, but in the free acid form, the five phosphate groups are suggested to adopt equatorial positions, with the conformational change occurring at pH 9.4, triggered by a deprotonation [Isbrandt & Oertel, 1980]. However, NMR studies have also suggested conformations of 5-ax/1-eq at low pH (stabilised by hydrogen bonding) and 1-eq/5-ax at high pH (Emsley & Niazi, 1981). Raman studies show that the hexacalcium salt adopts the 1-ax/5-eq conformation [Isbrandt & Oertel, 1980], which is also seen in the crystal structure of hexa(cyclohexylammonium) *myo*-inositol hexasulphate [Blank *et al.*, 1976].

3.1.6 Inositol pentakisphosphates

Further understanding of the iron-binding properties of $InsP_6$ can come from examination of inositol pentakisphosphate isomers ($InsP_5$, Figure 3.3) and lower inositol phosphates. A study of $InsP_5$ isomers is of biological importance because they

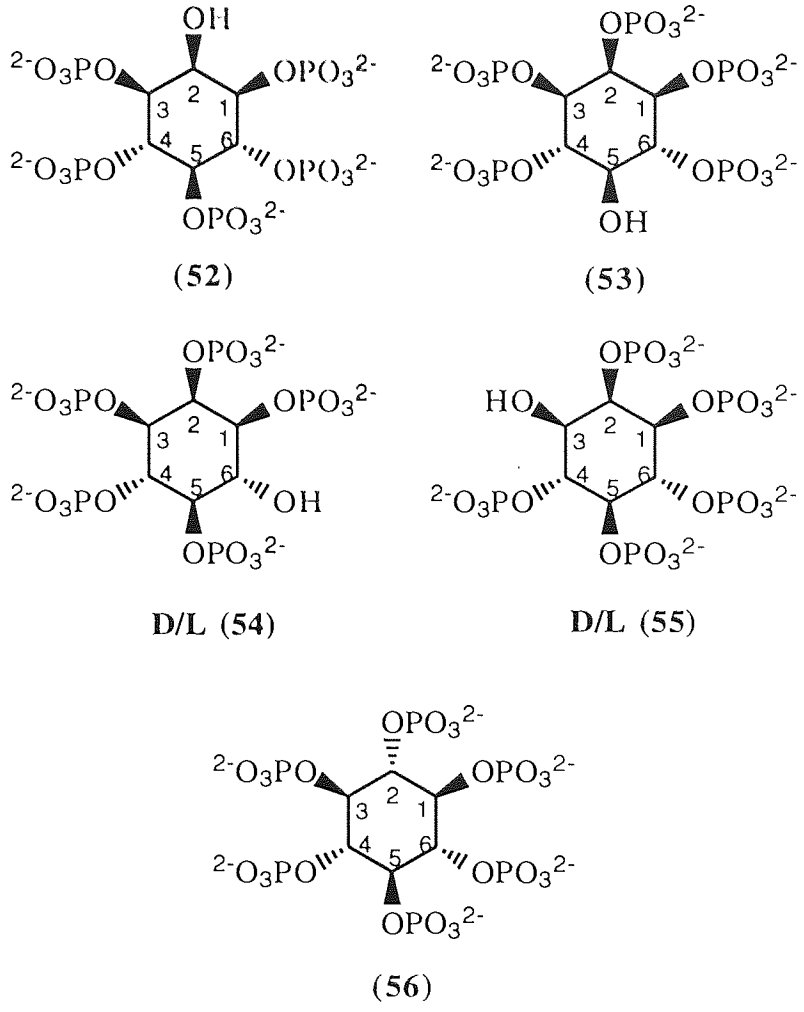

Figure 3.3 : Chemical structures of the $InsP_5$ isomers and *scyllo*-inositol hexakisphosphate

are also present in cells, sometimes at higher concentrations than $InsP_6$. Ins(1,3,4,5,6)P_5 (**52**), which can be formed from or metabolised to $InsP_6$, is a modulator of the oxygen affinity of haemoglobin in amphibians and birds [Isaacks & Harkness, 1980], a function controlled by 1,3-diphosphoglycerate in mammals.

All $InsP_5$ isomers bind Fe^{3+} with high affinity, but only those possessing a *cis* (equatorial-axial-equatorial) 1,2,3-trisphosphate grouping [Ins(1,2,3,4,6)P_5 (**53**) and D/L-Ins(1,2,3,4,5)P_5 (**54**)] are also antioxidant, completely inhibiting hydroxyl radical formation. In contrast Ins(1,3,4,5,6)P_5 (**52**), D/L-Ins(1,2,4,5,6)P_5 (**55**) and *scyllo*-inositol hexakisphosphate (**56**) only caused partial inhibition of hydroxyl radical formation [Hawkins *et al.*, 1993].

3.1.7 *myo*-Inositol 1,2,3-trisphosphate

myo-Inositol 1,2,3-trisphosphate [Ins(1,2,3)P_3, **57**, Figure 3.4] was first noted in 1992 as a minor component in human tonsil B lymphocytes [McConnell *et al.*, 1992].

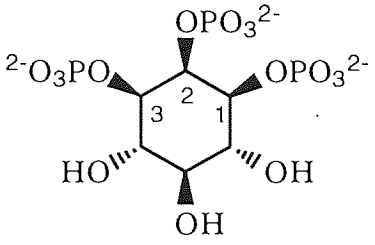

(**57**)

Figure 3.4 : Chemical structure of Ins(1,2,3)P_3

Barker and co-workers have recently found Ins(1,2,3)P_3 to be widespread in mammalian cells at concentrations of 1–10μM, often more abundant than the second messenger Ins(1,4,5)P_3 [Barker, French, 1995; Barker, Wright, 1995].

Ins(1,2,3)P_3 was found to be the first eluting InsP_3 peak by HPLC. It was identified as Ins(1,2,3)P_3 by a combination of periodate oxidation to ribitol, a structurally diagnostic polyol, and ammoniacal hydrolysis to known inositol monophosphates. Ins(1,2,3)P_3 is readily detected in cells labelled for long periods, but not in acutely labelled cells. This slow labelling suggests that Ins(1,2,3)P_3 is probably metabolically related to inositol polyphosphates that also have a slow rate of inositol incorporation such as InsP_6 [Barker, French, 1995; Barker, Wright, 1995]. To test a metabolic link between InsP_6 and Ins(1,2,3)P_3, the dephosphorylation of InsP_6 by cells was investigated. Ins(1,2,3)P_3 was found to be the major product (20% from 70% InsP_6 dephosphorylation) in WRK-1 cells (rat mammary epithelial tumour cells). In HL60 (human promyeloid leukaemia-derived) cells and WRK-1 cells, the concentration of Ins(1,2,3)P_3 changed little either during stimulation through G-protein-coupled receptors that activate phosphoinositidase C or during cell differentiation. However, Ins(1,2,3)P_3 cell concentration was found to double during a single cell cycle along with Ins(1,2)P_2 and

Ins(1,2,3)P_3 containing $InsP_5$ whereas other $InsP_3$ isomers decline in concentration. It was proposed by Barker and coworkers that Ins(1,2,3)P_3 may have a role in iron chelation in the cell. They also suggested that phytase may become activated in the middle of the G1 phase of cell cycle and that this might be related to cell cycle-dependent changes in iron metabolism in which 1,2,3 trisphosphate containing inositol polyphosphates could play some part [Barker, French, 1995; Barker, Wright, 1995]. Although the actual metabolic pathway and role of Ins(1,2,3)P_3 is still unknown, synthesis of Ins(1,2,3)P_3 and study of its physico-chemical properties should help towards elucidating its function in the cell.

3.1.8 Aims of research

The aim of the project was to synthesise for the first time, the natural product *myo*-inositol 1,2,3-trisphosphate, hitherto only available in small quantities from biochemical sources. This compound represents the simplest structure to mimic $InsP_6$'s antioxidant activity, and its iron binding properties were studied to further demonstrate the hypothesis that phosphate groups with the equatorial-axial-equatorial conformation are required for complete inhibition of hydroxyl radical formation. *myo*-Inositol 1,2,3-trisphosphate's ability to facilitate iron uptake into *Pseudomonas aeruginosa* was also tested.

3.2 RESULTS AND DISCUSSION

3.2.1 Synthesis of *myo*-inositol 1,2,3-trisphosphate (57)

The overall scheme for the synthesis of *myo*-inositol 1,2,3-trisphosphate (**57**) is shown in Figure 3.5.

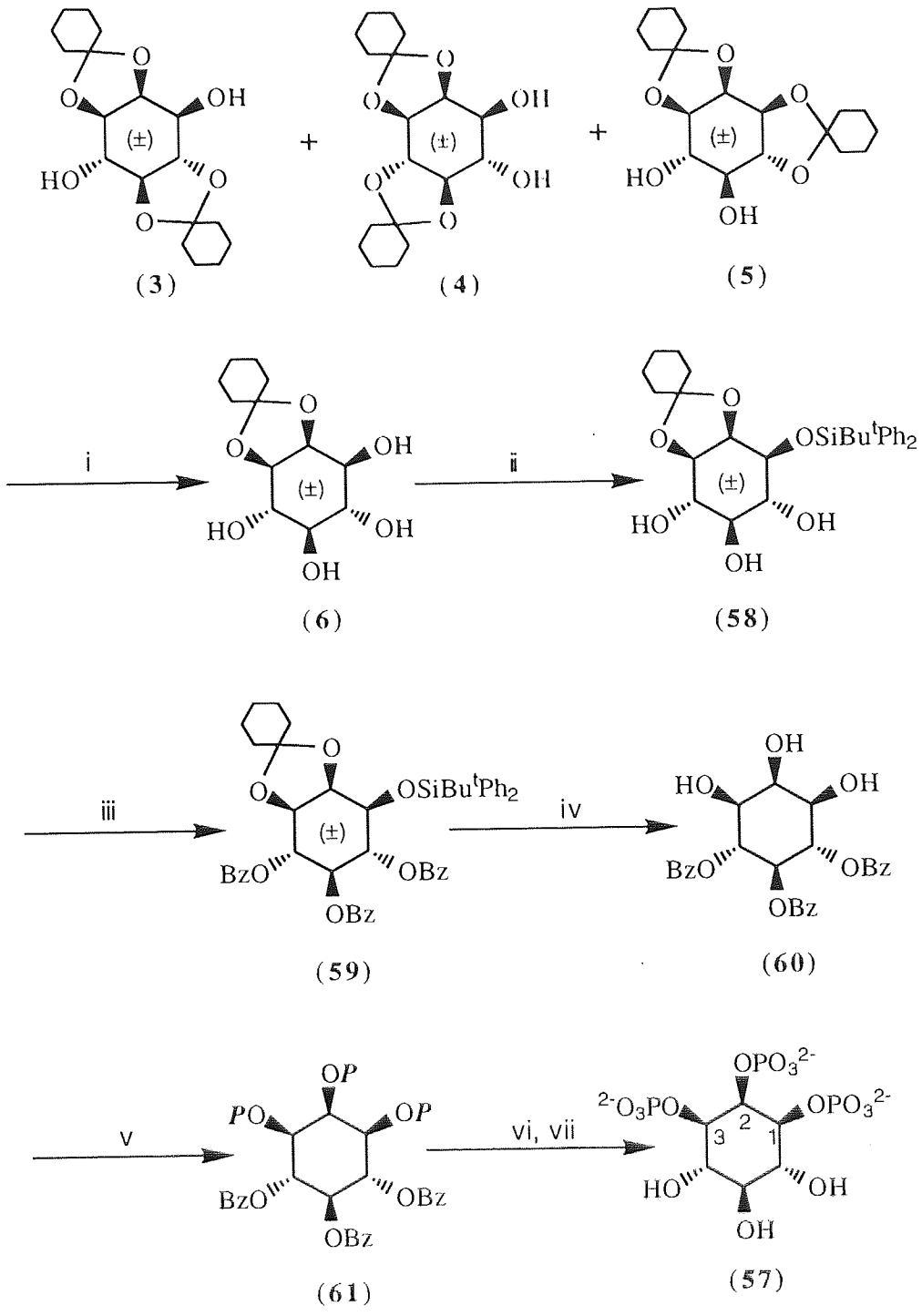

Figure 3.5 : Synthesis of *myo*-inositol 1,2,3-trisphosphate

i. *p*-TsOH, toluene, hexane, EtOH ii. Bu^tPh_2SiCl, imidazole, pyridine
iii. Benzoyl chloride, DMAP, pyridine iv. Aqueous CF_3CO_2H
v. $(BnO)_2PNPr^i_2$, 1*H*-tetrazole, CH_2Cl_2, then *m*CPBA
vi. H_2, Pd/C (10%), EtOH, room temperature, overnight
vii. NaOH (0.5M) Abbreviation: *P* = $(BnO)_2P(O)$; Bn = benzyl; Bz = benzoyl

The main strategy behind the synthesis of (**57**) was to :-

1) Selectively protect the 1-, 2- and 3-position of *myo*-inositol with easily removable protecting agents, allowing deprotection under controlled mild conditions

2) Protect the remaining OH groups at position 4, 5 and 6 with a more stable protecting group

3) Remove the 1-, 2- and 3-position protecting groups without deprotection of 4-, 5-, and 6-position

4) Phosphorylate the (now free) 1-, 2- and 3-position OH groups with a protected P(III) phosphitylating agent and oxidise to give the P(V) compound

5) Remove the remaining protecting groups to give the desired trisphosphate (**57**).

The bis(cyclohexylidene) acetals **3**, **4** and **5** (prepared in Section 2.2.1.1), were used as inositol starting compounds. The subsequent steps to *myo*-inositol 1,2,3-trisphosphate are described below.

3.2.1.1 Synthesis of D/L-*cis*-1,2-*O*-cylohexylidene *myo*-inositol (6)

Tetrol **6** is an ideal intermediate as it protects the 1- and 2-positions of inositol with an acid labile (easy to remove) acetal. The cyclohexylidene acetal also brings about a conformational change in the inositol ring which causes a greater difference in the OH groups' environment and reactivity, allowing more selective reactions to take place.

D/L-*cis*-1,2-*O*-Cylohexylidene *myo*-inositol **6** was prepared by adapting the method described by Baker, Billington and Gani (Figure 3.6, [Baker, Billington & Gani, 1991]). A mixture of the bis(cyclohexylidene) acetals (**3**, **4**, **5**; prepared from the reaction of 1,1-diethoxycyclohexane with inositol (see Section 2.2.1.1, [Dreef *et al.*, 1991])) were dissolved in toluene, hexane and ethanol. Selective removal of the less stable *trans* cyclohexylidene acetal was achieved by adddding a small amount (0.06 equivalent) of *p*-toluenesulphonic acid at 4°C, followed by addition of triethylamine and storage at -20°C. Tetrol **6** formed as a white precipitate in a yield of 53%.

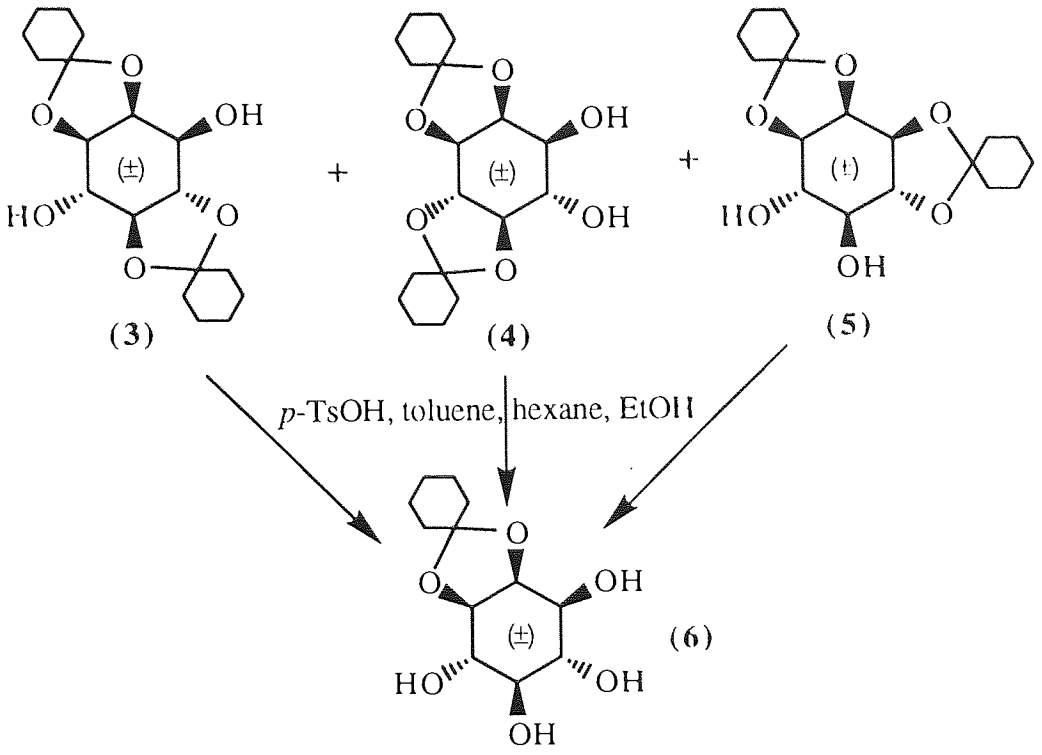

Figure 3.6 : Synthesis of D/L-*cis*-1,2-*O*-cyclohexylidene *myo*-inositol (**6**)

3.2.1.2 Synthesis of D/L-1-*O*-(*tert*-butyldiphenylsilyl)-2,3-*O*-cyclohexylidene *myo*-inositol (58)

Selective protection of tetrol (**6**) at the 1-position with a silyl group gives a compound which can be protected with acid-stable groups at positions 4, 5 and 6. This fully protected intermediate can then be deprotected at positions 1, 2 and 3 by acid hydrolysis or a combination of acid hydrolysis / silyl cleavage by fluoride ion.

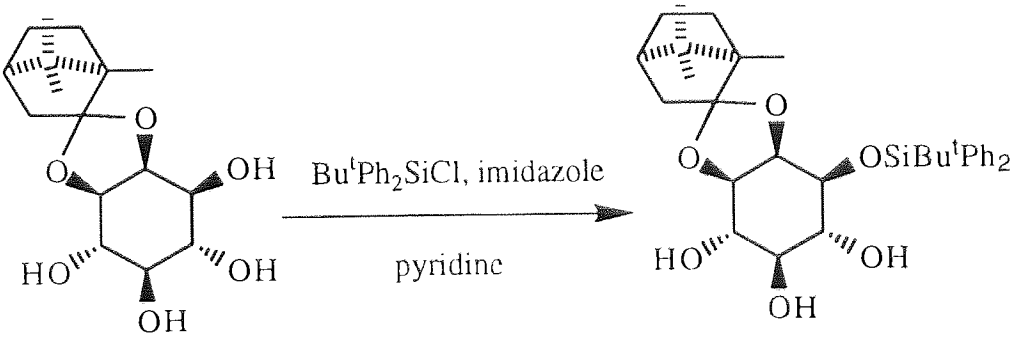

Figure 3.7 : Synthesis of 1D-1-*O*-(*tert*-butyldiphenylsilyl)-2,3-*O*-(D-1',7',7'-trimethyl [2.2.1]bicyclohept-2'-ylidene) *myo*-inositol [Bruzik & Tsai, 1992]

Selective monosilylation at the 1-position of a *myo*-inositol camphor dimethyl acetal derivative has been achieved with the bulky *tert*-butyldiphenylsilyl group (88% yield, [Brusik & Tsai, 1992], Figure 3.7). Triol (**58**, Figure 3.8) was prepared utilising this procedure. *tert*-Butyldiphenylsilyl chloride (1.1 equivalent) was reacted with tetrol (**6**) and imidazole (1.5 equivalents) in pyridine at -10°C. D/L-1-*O*-(*tert*-Butyldiphenylsilyl)-2,3-*O*-cyclohexylidene *myo*-inositol (**58**) was crystallised from DMF / chloroform / hexane to give colourless plate crystals in 58% yield. One of these crystals was used for a X-ray diffraction structure determination (Chapter 4). The ^1H NMR spectrum in $CDCl_3$ included a peak at 1.09 (s, 9 H), for the butyl group.

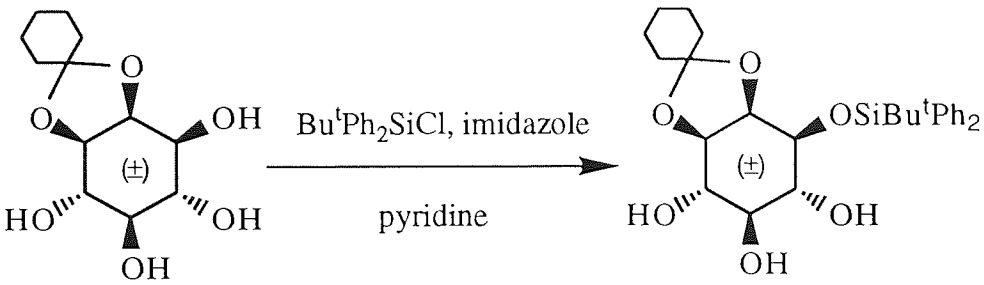

(6) (58)

Figure 3.8 : Synthesis of D/L-1-*O*-(*tert*-butyldiphenylsilyl)-2,3-*O*-cyclohexylidene *myo*-inositol (**58**)

3.2.1.3 Synthesis of D/L-1-*O*-(*tert*-butyldiphenylsilyl)-2,3-*O*-cyclohexylidene-4,5,6-tri-*O*-benzoyl *myo*-inositol (59)

The next step was to protect the hydroxy groups at positions 4, 5 and 6 of D/L-1-*O*-(*tert*-butyldiphenylsilyl)-2,3-*O*-cyclohexylidene *myo*-inositol (**58**). The first protection strategy to be attempted was benzylation. The benzyl group is stable to many conditions and has been used as a protecting group for phosphates as well as alcohols, therefore it would enable the final deprotection to occur in one step. Unfortunately, benzylation of the three free hydroxy groups of triol (**58**) with NaH and benzyl bromide in DMF was unsuccessful, leading to many unidentified compounds, as observed by TLC. This

result may be attributed to alkoxy anion formation leading to silyl migration with the formation of isomers.

In contrast, benzoylation was successful (Figure 3.9). Triol (**58**) was refluxed with benzoyl chloride and the catalyst DMAP in pyridine. The fully protected inositol product (**59**) was purified by flash chromatography and isolated as colourless plate crystals in 73% yield which were suitable for X-ray crystallography (Chapter 4).

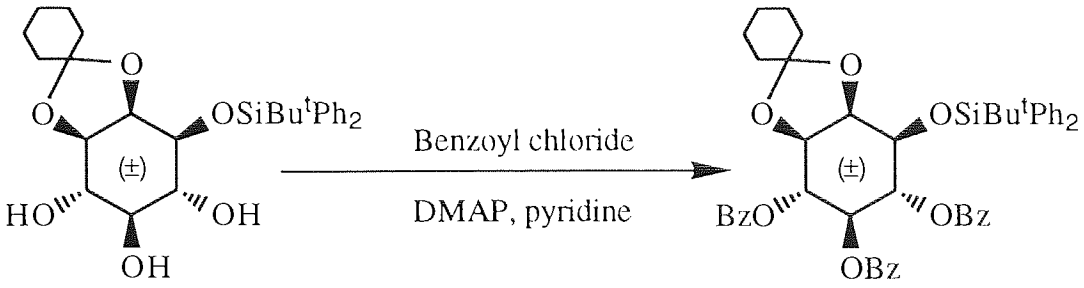

(**58**) (**59**)

Figure 3.9 : Synthesis of D/L-1-*O*-(*tert*-butyldiphenylsilyl)-2,3-*O*-cyclohexylidene-4,5,6-tri-*O*-benzoyl *myo*-inositol (**59**)

3.2.1.4 Synthesis of 4,5,6-tri-*O*-benzoyl *myo*-inositol (60)

To obtain triol (**60**), the silyl and cyclohexylidene groups of the fully protected inositol (**59**) must be removed. Removal of the *tert*-butyldiphenylsilyl group can be achieved either by fluoride ion, for example TBAF or HF, or by acid or base catalysed hydrolysis. Base catalysed hydrolysis is not feasible here as it would also remove the benzoyl protecting groups. The cyclohexylidene acetal protecting group can be removed by acid hydrolysis.

Removal of the silyl group from (**59**) using TBAF in THF was unsuccessful, leading to many unidentified side products. This may be attributed to migration of the benzoyl groups around the inositol ring. Migration of ester groups during desilylation with TBAF has been suggested for similar reactions [Dodd *et al.*, 1975; Hanessian & Lavallee, 1975]. The mechanism behind this migration most likely involves attack of the fluoride anion on silicon with formation of an alkoxide anion. Acyl migration would

then occur by attack of the formed alkoxide on the acyl group. The fluoride ion in THF may also be sufficiently basic to catalyse migration. Base catalysed acyl migration has recently been reported in *myo*-inositols containing benzoates [Chung & Chang, 1995, a] and utilised to synthesize all the possible *myo*-inositol tetrakisphosphates [Chung & Chang, 1995, b].

Removal of the *cis* (cyclohexylidene) ring from (**59**) was achieved by reacting with TFA (20%) in chloroform and D/L-1-*O*-(*tert*-butyldiphenylsilyl)-4,5,6-tri-*O*-benzoyl *myo*-inositol **62** (Figure 3.10) was isolated in 62% yield.

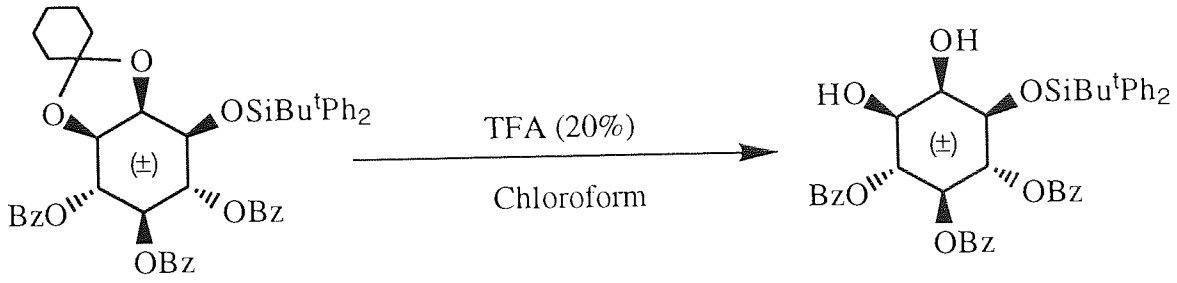

(59) **(62)**

Figure 3.10 : Synthesis of D/L-1-*O*-(*tert*-butyldiphenylsilyl)-4,5,6-tri-*O*-benzoyl *myo*-inositol (**62**)

The desilylation and acetal removal could be achieved in one pot if fully protected inositol **59** was subjected to an acid-catalysed hydrolysis. This strategy would overcome the unsuccessful removal of the silyl group with TBAF and would improve the overall yield, as 62% for removal of the acetal was unexpectedly low.

Brusik and Tsai [Bruzik & Tsai, 1992] have used aqueous HF to remove the *tert*-butyldiphenylsilyl group from an inositol derivative in a 70% yield, in the presence of benzoyl protecting groups. As HF is difficult to work with, **59** was reacted with aqueous TFA (Figure 3.11). After work-up, the crude product was dissolved in diethyl ether and 4,5,6-tri-*O*-benzoyl *myo*-inositol (**60**) precipitated out in a 49% yield (for two steps). The ^{1}H NMR spectrum (Figure 3.12) showed the expected symmetry for triol **60** with a 2:1:1:2 integration pattern for the inositol ring protons, which emphasises equivalent positions at C-1 and C-3, and C-4 and C-6.

The ^{1}H NMR spectrum included ; δ_H (CD_3OD) 4.02 (dd, 2 H, $J_{1/2}$ 2.7 Hz, $J_{1/6}$ 9.7 Hz, H-1/3), 4.19 (t, 1 H, $J_{2/1}$ 2.7 Hz, H-2), 5.67 (t, 1 H, $J_{5/4}$ 9.9 Hz, H-5) and 5.85 (t, 2 H, $J_{4/5} = J_{4/3}$ 9.9 Hz, H-4/6).

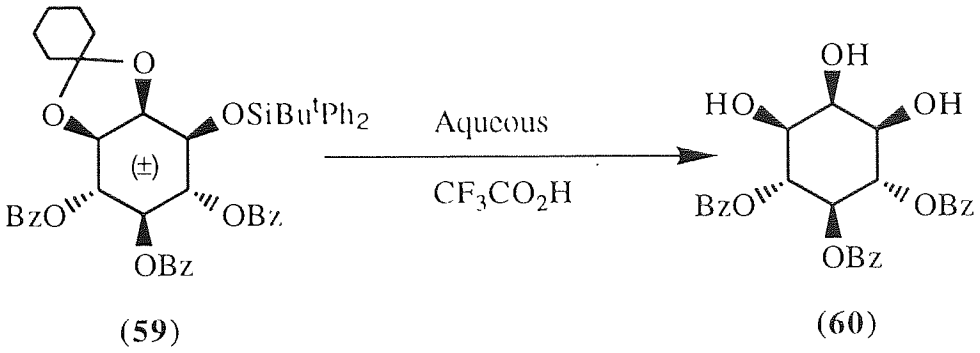

(59) **(60)**

Figure 3.11 : Synthesis of 4,5,6-tri-*O*-benzoyl *myo*-inositol (**60**)

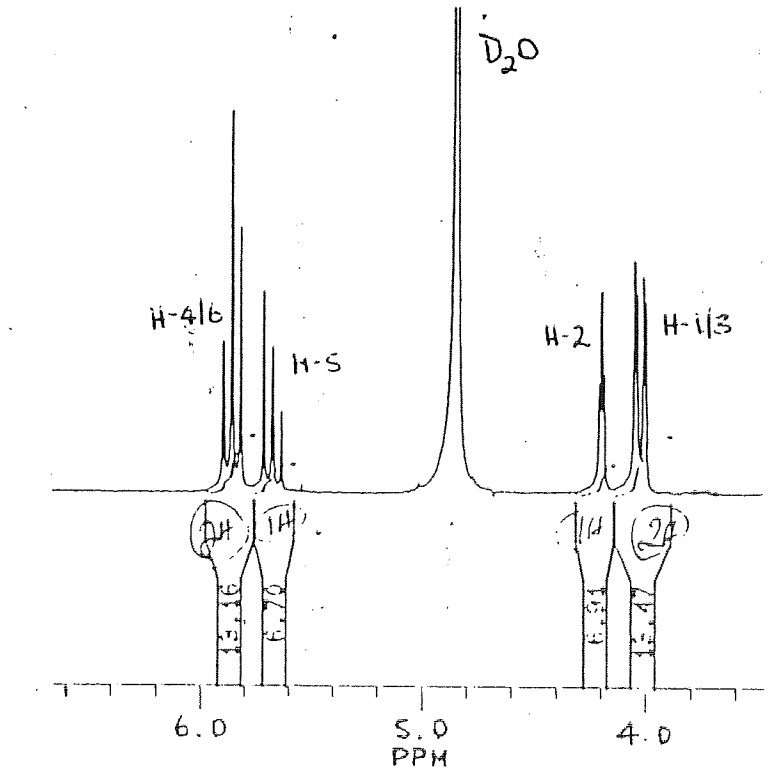

Figure 3.12 : ^{1}H NMR spectrum of inositol ring of 4,5,6-tri-*O*-benzoyl *myo*-inositol

Dibenzyl *N,N*-diisopropylphosphoramidite (**14**) was selected as the P(III) agent to phosphorylate 4,5,6-tri-*O*-benzoyl *myo*-inositol (**60**). This P(III) phosphoramidite has been used successfully to phosphorylate many hindered inositol derivatives [Yu & Reid, 1988] in the presence of 1*H*-tetrazole. Subsequent oxidation of the phosphite intermediate with *m*CPBA to the P(V) derivatives, and hydrogenolysis to remove the benzyl protecting groups gave the desired inositol phosphate in high yields. The dibenzyl *N,N*-diisopropylphosphoramidite (**14**) is prepared from *N,N*-diisopropylphosphorochloridate (**63**).

3.2.1.5 Synthesis of *N,N*-diisopropylphosphorochloridate (63)

Using the procedure described by Tanaka and coworkers [1986], two equivalents of diisopropylamine was addded dropwise to phosphorus trichloride at -78°C to give *N,N*-diisopropylphosphorochloridate (**63**) in 85% yield (Figure 3.13)

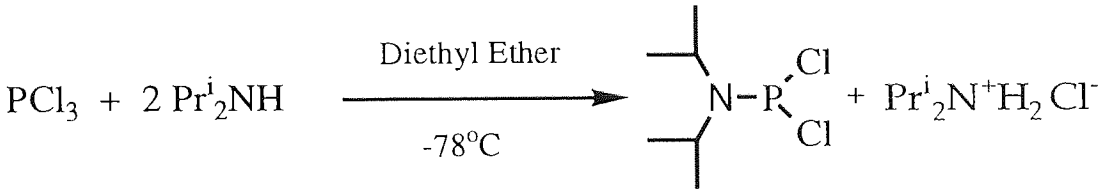

Figure 3.13 : Synthesis of *N,N*-diisopropylphosphorochloridate (**63**)

One of the secondary amine equivalents was needed to neutralise the HCl evolved to give the *N,N*-diisopropylammonium hydrochloride salt, which was removed by filtration. Purification of *N,N*-diisopropylphosphorochloridate (**63**) was accomplished by vacuum distillation.

3.2.1.6 Synthesis of dibenzyl *N,N*-diisopropylphosphoramidite (14)

Using the procedure described by [Yu & Fraser-Reid, 1988], two equivalents of benzyl alcohol and triethylamine was added dropwise to *N,N*-diisopropylphosphorochloridate (**63**) at -78°C (Figure 3.14). The triethylamine was added to neutralise the HCl evolved,

and the triethylamine hydrochloride salt formed was removed by filtration. The crude oil was subjected to flash chromatography to give pure dibenzyl *N,N*-diisopropylphosphoramidite in 50% yield. The product was subjected to ^{1}H and ^{31}P NMR spectroscopy, and the following data were obtained: δ_H ($CDCl_3$) 1.40 (d, 12 H, J_{HH} 6.7 Hz, CH_3), 3.90 (sept, 2 H, J_{HH} 6.7 Hz, CH), 4.9-5.0 (m, 4 H, CH_2) and 7.4-7.6 (m, 10 H, Ph), and δ_P ($CDCl_3$) 148.4(s).

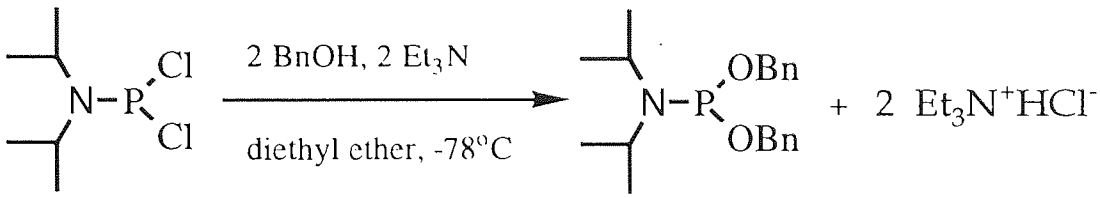

Figure 3.14 : Synthesis of dibenzyl *N,N*-diisopropylphosphoramidite (**14**)

3.2.1.7 Synthesis of 4,5,6-tri-*O*-benzoyl *myo*-inositol 1,2,3-tris(dibenzyl phosphate) (61)

Six equivalents of dibenzyl *N,N*-diisopropylphosphoramidite (**14**) and twelve equivalents of the acid catalyst 1*H*-tetrazole (present to assist cleavage of the P-N bond) were reacted with triol **60**. After 2 hours, the formation of the trisphosphite **64** (Figure 3.15) was detected as shown by ^{31}P NMR spectroscopy, δ_P ($CDCl_3$) 140.9 (s, 2P), 139.9 (s, P). The reaction mixture was cooled to -40°C and eight equivalents of *m*CPBA was then added to oxidise the trisphosphite to the required trisphosphate **61**. Crystallization from diethyl ether/hexane afforded **61** in a 56 % yield as colourless laths. A crystal of **61** was grown from chloroform / hexane and its structure was solved by X-ray diffraction. The structure contained one molecule of water per formula unit (Chapter 4).

The compound was fully assigned by ^{1}H, ^{13}C and ^{31}P NMR spectroscopy. The assignments of the ^{1}H NMR spectrum were confirmed with the aid of a COSY spectrum (Figure 3.16) and data included; δ_H ($CDCl_3$) 4.45 (dd, 2 H, J_{gem} 11.7 Hz, J_{PH} 8.9 Hz, 2 x P-O-CH_AH$_B$Ph), 4.66 (dd, 2 H, J_{gem} 11.8 Hz, J_{PH} 7.5 Hz, 2 x P-O-CH$_A$$H_B$Ph), 4.9-5.05 (m, 6 H, 2 x P-O-CH_2Ph, H-1/3), 5.22 (d, 4 H, J_{PH} 6.1 Hz, 2 x P-

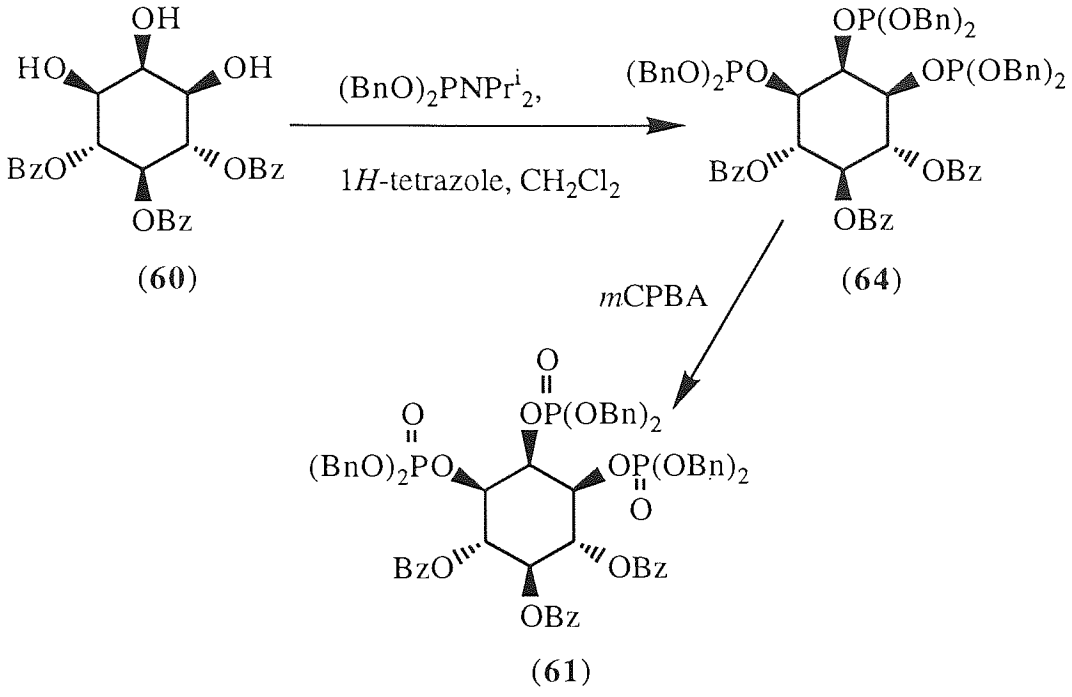

Figure 3.15 : Synthesis of 4,5,6-tri-*O*-benzoyl *myo*-inositol 1,2,3-tris(dibenzyl phosphate) (**61**).

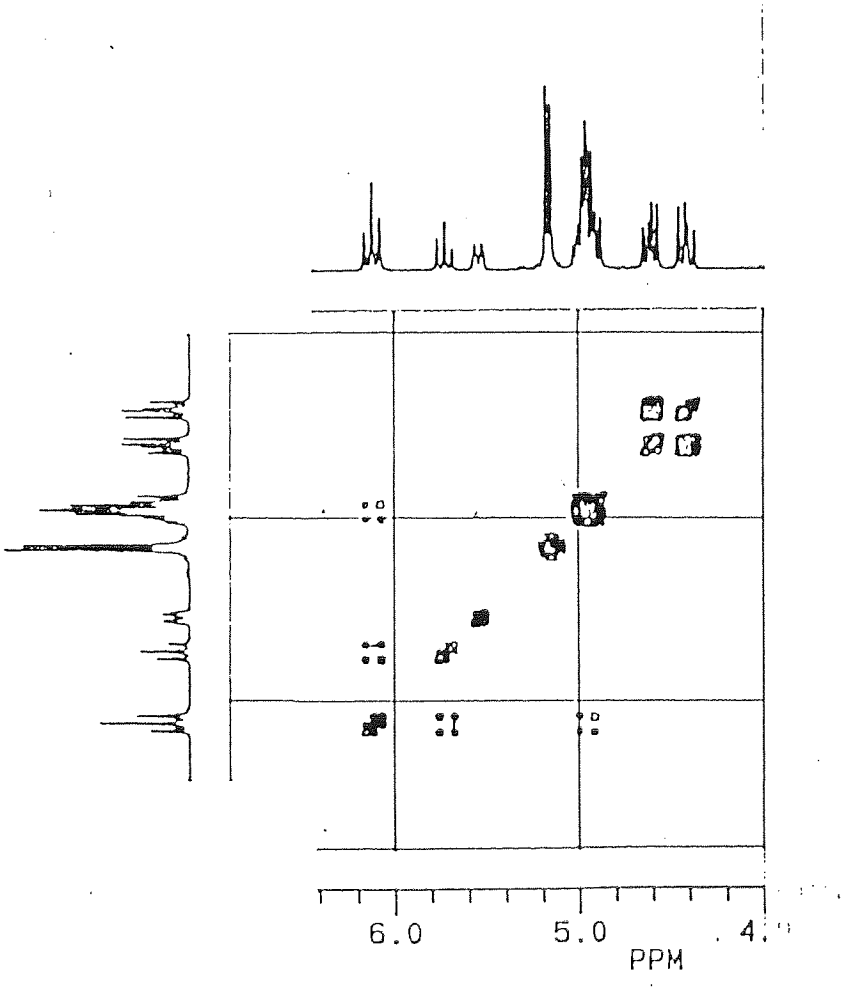

Figure 3.16 : COSY ^{1}H-^{1}H spectrum for 4,5,6-tri-*O*-benzoyl *myo*-inositol 1,2,3-tris(dibenzyl phosphate) (**61**)

O-CH_2Ph), 5.56 (br d, 1 H, J_{PH} 9.3 Hz, H-2), 5.75 (t, 1 H, $J_{5/4}$ 10.0 Hz, H-5) and 6.16 (t, 2 H, $J_{4/3} \sim J_{4/5} \sim$ 10.1 Hz, H-4/6). The ^{31}P NMR showed the presence of two phosphorus environments; δ_P ($CDCl_3$, ^{1}H decoupled) -1.1 (s, 2P, P-1/3), -2.2 (s, 1P, P-2) ; δ_P ($CDCl_3$, ^{1}H coupled) -1.2 (sextet, J_{PH} 8.3 Hz), -2.3 (br sextet, $J_{PH} \sim$ 6.8 Hz).

3.2.1.8 Synthesis of monosodium tetra(cyclohexylammonium) *myo*-inositol 1,2,3-trisphosphate (57)

The final step involves reactions that remove all the protecting groups from **61** to liberate the desired inositol trisphosphate **57**. A similar deprotection of benzyl groups on the phosphate and benzoyl groups on the inositol ring from a fully protected derivative has been reported in one step (two reactions) by Tegge and Ballou [1989] to give D-*myo*-inositol 1,4,5-trisphosphate in 87% yield. Using this methodology, 4,5,6-tri-*O*-benzoyl *myo*-inositol 1,2,3-tris(dibenzyl phosphate) **61** was first hydrogenolysed to remove the benzyl groups to give the free acid (**65**, Figure 3.17) {δ_P (CD_3OD) 1.80 (s, 1P), 1.43 (s, 2P)}. Saponification of the benzoyl groups with sodium hydroxide, elution down a cation exchange column (Dowex-50, H^+ form), and addition of cyclohexylamine gave rise to the desired 1,2,3-trisphosphate (**57**) as a monosodium tetra(cyclohexylammonium) salt which precipitated on the addition of acetone in an 82% yield. Crystallisation of **57** gave a crystal that was suitable for X-ray diffraction (Chapter 4). The X-ray structure determination confirmed the existence of *myo*-inositol 1,2,3-trisphosphate (**57**) as a monosodium tetra(cyclohexylammonium) salt. The monosodium salt of *myo*-inositol 1,2,3-trisphosphate was present before the addition of cyclohexylamine, presumably attributable to the low pKa of the first ionisation: for $InsP_6$ this pKa (at C-2) is 1.1 [Costello *et al.*, 1976]: only five of the sodium cations exchange with H^+ on passage down the Dowex-50 (H^+ form) column. The monosodium tetra(cyclohexylammonium) salt of **57** is formed presumably due to the very high sixth pKa value: for $InsP_6$ the highest pKa value (at C-3) is 12.0 [Costello *et al.*, 1976] and the pKa of cyclohexylamine is 10.64 [James & Lord, 1992]. The highest pKa value for *myo*-inositol 1,2,3-trisphosphate has been measured as 9.56 [Schmitt,

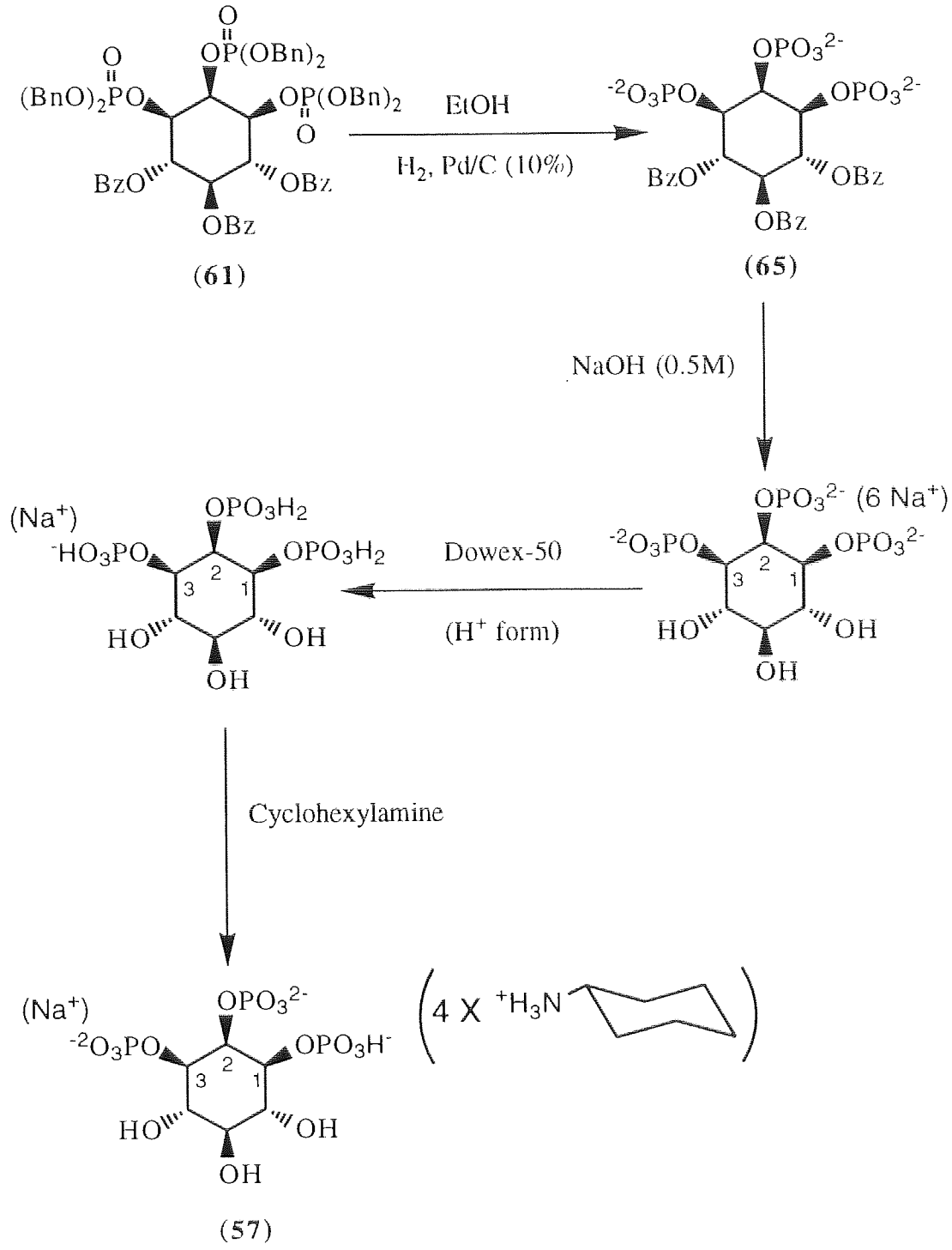

Figure 3.17 : Synthesis of monosodium tetra(cyclohexylammonium) *myo*-inositol 1,2,3-trisphosphate (**57**).

1993]: Only four of the five protons on the phosphates of **57** are ionised by cyclohexylamine. The compound was fully characterised by ^{1}H, ^{13}C and ^{31}P NMR spectroscopy. The ^{1}H NMR of the inositol ring gave δ_H (D_2O) 3.39 (t, 1 H, $J_{4/5}$ 9.2 Hz, H-5), 3.83 (t, 2 H, $J_{4/3} \sim J_{4/5} \sim 9.5$ Hz, H-4/-6), 3.98 (br t, 2 H, $J_{1/6} \sim J_{PH} \sim 8.9$ Hz, H-1/-

3), 4.72 (br d, 1 H, J_{PH} 9.8 Hz, H-2). The ^{31}P NMR spectrum supported the expected symmetry in the molecule, δ_P (D_2O, ^1H decoupled) 1.70 (s, P-2), 3.62 (s, P-1/3) ; δ_P (D_2O, ^1H coupled) 1.70 (d, J_{PH} 8.5 Hz), 3.62 (d, J_{PH} 6.1 Hz).

3.2.2 Inhibition of iron-catalysed hydroxyl radical formation by inositol phosphates

The inhibition of iron-catalysed hydroxyl radical formation by *myo*-inositol 1,2,3-trisphosphate, D/L-*myo*-inositol 1,2-bisphosphate, all *myo*-inositol tetrakisphosphates and $InsP_6$ was studied by Dr D. R. Poyner. D/L-*myo*-Inositol 1,2-bisphosphate was synthesised by Dr S. Freeman and Dr K. R. H. Solomons (described in [Spiers *et al.*, 1995]) and all of the *myo*-inositol tetrakisphosphates were supplied by S-K Chung and Y-T Chang (synthesis described in [Chung & Chang, 1995, b]. The assay for the Haber Weiss reaction was that of Hawkins and co-workers [Hawkins *et al.*, 1993], utilising the hypoxanthine/xanthine oxidase system. Hydroxyl radical was generated and measured in the following assay: in the presence of xanthine oxidase, hypoxanthine was oxidised by molecular oxygen to give xanthine, the superoxide radical anion $O_2^{-\cdot}$ and hydrogen peroxide. The latter two products participated in the iron-catalysed Haber-Weiss process to give $HO\cdot$, which reacted with dimethylsulphoxide (present in assay). The first intermediate formed was the methyl radical, which reacts by at least three routes [Klein *et al.*, 1981]: it can abstract a hydrogen to give methane, dimerise to give ethane or react with molecular oxygen to give Me-O-O·, which reacts to give formaldehyde:

$$2\ Me\text{-}O\text{-}O\cdot \longrightarrow H_2C{=}O + MeOH + O_2$$

The ability of the inositol phosphates to chelate with iron and inhibit or catalyse $HO\cdot$ formation was evaluated by assaying the formaldehyde released by the Hantzsch reaction [Nash, 1953]. This required incubation of the reaction mixture with pentan-2,4-dione (acetylacetone) in the presence of ammonia at 60°C with subsequent measurement of absorbance at 410 nm.

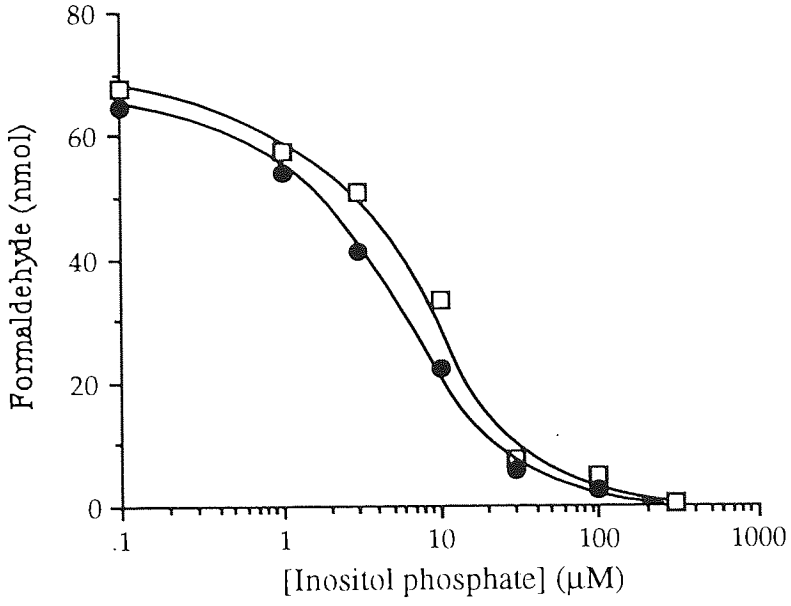

Figure 3.18 : Effects of $InsP_6$ (●) and *myo*-inositol 1,2,3-trisphosphate (**57**, □) on HO· generation. This result is typical of three independent experiments (Dr D R Poyner).

Both Ins(1,2,3)P_3 and $InsP_6$ completely inhibited Fe^{3+}-catalysed hydroxyl radical formation at >100 μM (Figure 3.18), in support of the earlier hypothesis that the *cis* 1,2,3 (equatorial-axial-equatorial) trisphosphate grouping in $InsP_6$ is needed to inhibit Fe^{3+}-catalysed hydroxyl radical formation.

Further confirmation that the 1,2,3-trisphosphate grouping is required for Fe^{3+}-catalysed HO· formation came from studying the family of *myo*-inositol tetrakisphosphates. Only Ins(1,2,3,5)P_4 and D/L-Ins(1,2,3,4)P_4 were able completely or almost completely to inhibit HO· generation when present at 100 μM, thereby resembling $InsP_6$ (Table 3.1).

In contrast, D/L-Ins(1,2)P_2 failed to inhibit HO· production. Unexpectedly however, it substantially potentiated free radical production, thereby resembling other iron chelators such as ATP, ADP or EDTA [Graf *et al.*, 1984; Floyd & Lewis, 1983; Halliwell & Gutteridge, 1978]. An Fe^{3+} - D/L-Ins(1,2)P_2 complex may have less steric constraints than Fe^{3+} - Ins(1,2,3)P_3, so perhaps this allows H_2O or H_2O_2 to enter the co-ordination sphere in the former complex: Graf and coworkers [Graf *et al.*, 1984] have suggested that this would enhance HO· production. However, the difference in

Table 3.1 : Inhibition by *myo*-inositol phosphates of HO•-mediated formaldehyde production. Values represent the amounts of formaldehyde produced, as percentages of control incubations without added inositol phosphates (n=4, Dr D R Poyner).

	Inositol Phosphate Concentration.	
Inositol Phosphate	10 μM	100 μM
D/L-Ins(1,2)P_2	125±4	225±30
Ins(1,2,3)P_3	**51±8**	**7±2**
D/L-Ins(1,2,3,4)P_4	**87±4**	**9±2**
Ins(1,2,3,5)P_4	**67±5**	**2±0.3**
D/L-Ins(1,2,4,5)P_4	86±7	66±3
D/L-Ins(1,2,4,6)P_4	91±5	70±2
D/L-Ins(1,2,5,6)P_4	95±5	77±2
D/L-Ins(1,3,4,5)P_4	95±6	88±7
Ins(1,3,4,6)P_4	101±4	85±8
D/L-Ins(1,4,5,6)P_4	97±6	82±5
Ins(2,4,5,6)P_4	99±5	78±4
InsP_6	**53±5**	**0**

properties may also be attributed to a change in redox-potential between the complexes [Burkitt & Gilbert, 1990; Burkitt & Gilbert, 1991].

Interestingly, it has recently been reported that Ins(1,2,6)P_3, Ins(1,3,5)P_3 and Ins(2,4,6)P_3 each give a range of strong complexes with Fe^{3+} [Mernissi-Arifi, 1994]. The derivative with three vicinal phosphates, Ins(1,2,6)P_3 (equatorial-equatorial-axial), binds Fe^{3+} more strongly than the three alternated phosphates of either Ins(1,3,5)P_3 or Ins(2,4,6)P_3. They have proposed that with Ins(1,2,6)P_3 the arrangement of the phosphates is such that they all participate in binding with Fe^{3+}. In contrast, for Ins(2,4,6)P_3, the axial phosphate on position 2 largely contributes to complex stabilisation.

3.2.3 Siderophore activity of *myo*-inositol 1,2,3-trisphosphate

In view of the similarities between $Ins(1,2,3)P_3$ and $InsP_6$ in their ability to inhibit HO· production, Dr A. W. Smith and P. Hirst examined whether $Ins(1,2,3)P_3$ also had siderophore activity using the reported procedure [Smith *et al.*, 1994]. The iron uptake into cells by the $InsP_6/^{55}Fe$ complex was also measured as a control. *P. aeruginosa* cells (IA1: a siderophore-deficient mutant strain of PAO1 was used) were grown in iron-deficient succinate medium and harvested by centrifugation at 4°C. The cells were suspended to an optical density at 600 nm of 1 (corresponding to 1 x 10^9 cells per ml) and equilibrated at 37°C for 15 mins prior to transport studies. ^{55}Fe-labelled complexes were added to the cell suspension resulting in final concentrations of 100μM $InsP_6$ or $Ins(1,2,3)P_3$, and 200 nM $FeCl_3$ (in a 500:1 molar ratio which makes sure that all iron is bound in a complex). Iron transport was assayed by withdrawing 200μl samples at time intervals and filtering them through 0.2-μm-pore-size cellulose acetate membrane filters. The membrane filters were washed to remove any excess media and allowed to dry. The activity retained on the membrane filters was determined by scintillation counting on the ^3H channel.

As can be seen in Figure 3.19, $Ins(1,2,3)P_3$ promoted iron uptake as a siderophore but with an activity less than that of $InsP_6$. The reason why $Ins(1,2,3)P_3$ activity is less than $InsP_6$ is difficult to determine from just this result. One would expect that $InsP_6$ would have more difficulty in entering the bacterial cells as it has a higher negative charge and is more bulky than $Ins(1,2,3)P_3$, that is if either of the compounds actually enter the cell. If $InsP_6$ just bridges iron to the negatively charged membrane, it may require the phosphates at positions 4, 5 and 6 to achieve this. $InsP_6$ may also have the correct conformation to orientate its bound iron for membrane receptor binding compared to $Ins(1,2,3)P_3$. Alternatively the $InsP_6/Fe^{3+}$ complex may have the required redox potential for reduction to Fe^{2+}. The reduction of ferric to ferrous iron is a possible mechanism which is seen in many bacteria for the release of iron from a siderophore [Neilands, 1993]. Further details of sidephore activity for other inositol phosphates is required before any structural relationship can be determined. Physico-chemical studies

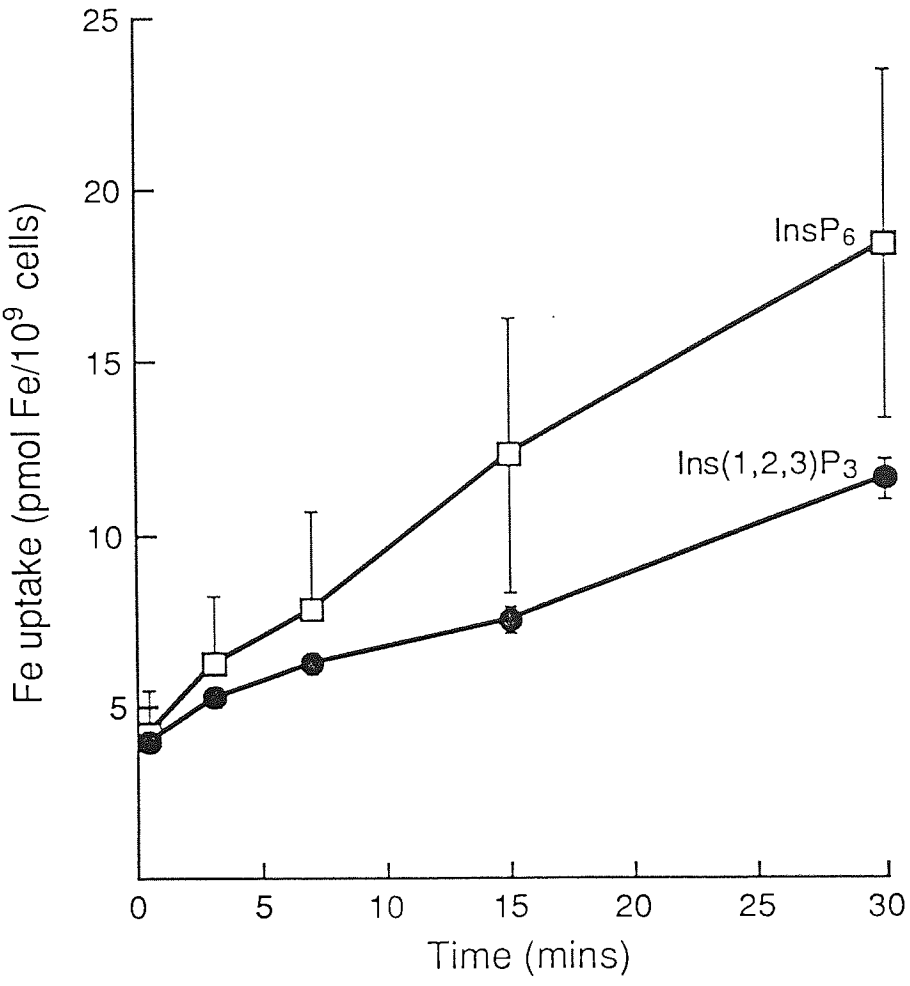

Figure 3.19 : ^{55}Fe transport from inositol phosphates into *Pseudomonas aeruginosa*. A 1:500 complex was formed by addition of 200 nM $^{55}FeCl_3$ to 100μM inositol phosphate (Dr A W Smith & P Hirst).

of other inositol phosphate-iron complexes may also give further insight into the structure required for biological activity. All that can be deduced here is that $Ins(1,2,3)P_3$ and $InsP_6$ iron complexes in the cell environment may be utilised by bacteria for iron uptake.

Thus in two different assays of Fe^{3+} binding, $Ins(1,2,3)P_3$ and $InsP_6$ have similar activity.

3.3 CONCLUSION

The first synthesis of *myo*-inositol 1,2,3-trisphosphate has been completed in seven steps from *myo*-inositol. Suitable crystals of key synthetic intermediates and that of *myo*-inositol 1,2,3-trisphosphate were grown to enable their X-ray structure determination (Chapter 4). These structures and experimental analysis (Chapter 5) allowed full characterisation of the synthesised compounds.

Iron binding studies of *myo*-inositol 1,2,3-trisphosphate demonstrated that phosphate groups with the equatorial-axial-equatorial conformation are required for complete inhibition of hydroxyl radical formation. This was confirmed in the iron binding studies of *myo*-inositol tetrakisphosphates which showed that only Ins(1,2,3,5)P_4 and D/L-Ins(1,2,3,4)P_4 could completely inhibit hydroxyl radical production.

The synthesis of Ins(1,2,3)P_3 should enable further studies to elucidate its function in the cell. A key step would be to determine its metabolic pathway in the cell which should give information as to whether it is a biological end point or an intermediate to the synthesis of other important compounds. It is possible that it is a biological by-product of futile cycling within the cell, which has been suggested for the $InsP_5$ isomers [Stephens, 1991] but this seems wasteful in energy conserved cells.

It was suggested that metal ion-dependent $InsP_6$ binding to membranes was not likely to mediate any physiological response [Poyner *et al.*, 1993] but bearing this in mind, study of $InsP_6$'s chelation properties are important in its possible role as a low molecular weight iron carrier in the cell [Hawkins *et al.*, 1993] and as a sidephore [Smith *et al.*, 1994].

The crystal structure of $InsP_6$ iron complex would give insight into binding and structural conformation, however as yet suitable crystals are not available. If solved, this may not represent what happens in more complicated polyferric systems and may not prove the mechanism by which the hydroxyl radical formation is prevented. Structural and physico-chemical properties of related inositol phosphates give some insight into the conformational requirements for biological activity, which has been shown in our iron binding studies.

It is clear that different Fe^{3+}-inositol phosphate complexes can show a range of properties. Further studies with $InsP_3$ and $InsP_2$ isomers are now needed to see whether some simple structural motif can explain the enhanced HO· generation seen with D/L-$Ins(1,2)P_2$, in contrast to inhibition of this phenomenon by the 1,2,3-trisphosphate grouping. The possible biological consequences of enhanced HO· generation by some inositol phosphates and inhibition by others is intriguing. In the future it will be of interest to determine how $Ins(1,2,3)P_3$ interacts with other inositol phosphates or biologically relevant Fe^{3+} chelators such as ATP.

Overall, this study gives indirect evidence for the possible function of $InsP_6$ and $Ins(1,2,3)P_3$. Direct evidence may come from eliminating $InsP_6$ or $Ins(1,2,3)P_3$ from a cell by genetic means and investigating the effect of the planned deficiency on the cell.

CHAPTER 4

Crystallographic investigation of *myo*-inositol compounds

4.1 INTRODUCTION

4.1.1 The structures of *myo*-inositol compounds

The biological significance of inositol phosphates has been outlined in Chapters 1,2 and 3. The overall structural conformation of inositol compounds is important as it is likely to determine the biological activity in, for example, biochemical enzyme reactions [Majerus, 1992] and metal ion binding [Hawkins *et al.*, 1993]. The overall structural conformation is controlled by many factors such as inositol ring conformation, hydrogen bonding, crystal structure packing forces (in solid state) and ion binding.

The structure of *myo*-inositol [Rabinowitz & Kraut, 1964], the parent compound of this study, and also its dihydrate [Lomer *et al.*, 1963], have previously been analysed by X-ray diffraction. Both structures showed the cyclohexane ring to exist in the chair conformation with one of the six hydroxyl groups axial and the other five equatorial (1a/5e). The distortion of the ring from a perfect chair was small in the two cases, which was also seen in the fully protected derivatives, 1,2,3,4,5,6-hexa-*O*-acetyl-*myo*-inositol [Abboud *et al.*, 1990] and D/L-3,4-di-*O*-acetyl-1,2,5,6-tetra-*O*-benzyl-*myo*-inositol [Steiner *et al.*, 1993]. Ion binding to *myo*-inositol by magnesium chloride [Blank, 1973] and calcium bromide [Cook & Bugg, 1973] as hydrate complexes has been shown to impose more noticeable ring distortion but still retain the expected (1a/5e) conformation.

The structure of two phosphate derivatives of *myo*-inositol have previously been determined by X-ray diffraction. *myo*-Inositol 2-phosphate monohydrate [Yoo *et al.*, 1974] was found to exist in a slightly distorted chair conformation with the phosphate ester axial and the five hydroxyl groups equatorial (1a/5e). On the contrary, the structure of $InsP_6$ (see 3.15) as the dodecasodium salt [Blank *et al.*, 1975] or when bound to deoxyhemoglobin [Arnone & Perutz, 1974] was found to adopt the unusual 5 axial / 1 equatorial conformation .

4.1.2 Aims of research

The aims here were to use X-ray diffraction to determine the structures of synthesised inositol compounds and to fully analyse their conformations. Firstly, this would give further evidence to the assignment of functional groups in their respective positions on the inositol ring, carried out by experimental analysis (Chapter 5). Secondly, it would show the effect substituents have on the conformation of the inositol ring. Finally, it would illustrate the effect hydrogen bonding and counter-ion interactions have on the overall structures.

4.2 EXPERIMENTAL, RESULTS AND DISCUSSION

4.2.1 Crystal structure of D/L-1,2;4,5-di-*O*-cyclohexylidene *myo*-inositol (3) at 293K and 150K

4.2.1.1 Experimental

D/L-1,2;4,5-Di-*O*-cyclohexylidene *myo*-inositol (**3**) slowly crystallised in acetone and hexane to form colourless rectangular plate crystals. A single crystal (0.65 x 0.60 x 0.08 mm) was chosen for X-ray determination at both 293K and 150K. The room temperature data (293K) were collected from an Enraf-Nonius CAD4 diffractometer with monochromated graphite Mo-Kα radiation, λ = 0.71069Å. The low temperature data (150K) were collected from a Stadi-4 diffractometer at Edinburgh University with the help of Dr A. J. Blake, and monochromated graphite Mo-Kα radiation, λ = 0.71069Å was also used.

4.2.1.2 Crystal data

D/L-1,2;4,5-Di-*O*-cyclohexylidene *myo*-inositol (**3**) ($C_{18}H_{28}O_6$) crystallises in the monoclinic space group $P2_1/c$, Z = 4. At 293K, a = 12.445(2), b = 11.050(1), c =

12.652(3)Å, β = 94.03(2)° and V = 1735.6(1)Å^3. At 150K, a = 12.273(2), b = 11.037(5), c = 12.620(4)Å, β = 94.92(2)° and V = 1703.2(10)Å^3. The formula weight is 340.40 (F(000) = 736), the calculated density D_X = 1.303 Mg m^{-3} at 293K and D_X = 1.328 Mg m^{-3} at 150K. The absorption coefficients were μ = 0.058 mm^{-1} (293K) and μ = 0.099 mm^{-1} (150K).

4.2.1.3 Data collection at 293K

Unit cell dimensions were obtained from least squares analysis of setting angles of 25 accurately centred reflections, 9.4 ≤ θ ≤ 13.8°. Intensity data were collected by the ω-2θ scan technique, Bragg angle 2 ≤ θ ≤ 25°. The ω scan angle was calculated from [*M*+*N*(tanθ)]°, where *M* = 0.9, *N* = 0.35 and increased by 25% on each side for background determination. The ω scan speed was varied from 0.4 to 2.8°min^{-1} depending upon intensity. Six different standard reflections were used during data collection: three intensity reflections (measured every two hours) and three orientation reflections (monitored every 200 reflections). No appreciable loss of intensity or crystal movement was detected during collection. The 6381 reflections were measured for -14 ≤ h ≤ 0, -13 ≤ k ≤ 13, -14 ≤ l ≤ 15 and merged to give 3040 independent reflections (R_{int} = 0.0231).

4.2.1.4 Data collection at 150K

Unit cell dimensions were obtained from least squares analysis of setting angles of 32 accurately centred reflections, 28 ≤ θ ≤ 30°. Intensity data were collected by the ω-2θ scan technique, Bragg angle 2.89 ≤ θ ≤ 25.03°. Six different standard reflections were used during data collection: three intensity reflections (measured every hour) and three orientation reflections. No appreciable loss of intensity or crystal movement was detected during collection. The 2169 reflections were measured for -14 ≤ h ≤ 10, 0 ≤ k ≤ 11, 0 ≤ l ≤ 13 and merged to give 2165 independent reflections (R_{int} = 0.0377).

4.2.1.5 Structural determination and refinement for data at 293K

Lorentz, polarisation and intensity corrections (3.5% decay) were applied to the collected data. The space group was determined unambiguously as a result of structure analysis. An initial structure was solved by direct methods using the EEES routine in SHELX-76 [Sheldrick, 1976]. Based on the atomic positions determined from the E-map, the remaining non-hydrogen atoms were located in an electron density map using SHELX-76 [Sheldrick, 1976].

Full-matrix least-squares refinement of atomic positions and anisotropic temperature factors (for non-hydrogen atoms) on F_{obs} was applied using SHELX-76 [Sheldrick, 1976].

All the hydrogen positions were located from difference electron density maps. The hydrogen atoms of the two hydroxy groups were both found to have two possible sites, i.e. they were disordered. To accommodate this disorder, each hydroxy group had the two possible hydrogen sites restrained at a common distance (one free variable was used for all four sites) with an estimated standard deviation of 0.02, their temperature factors were set to a common free variable and the total occupancy for each pair of sites equalled one. Hamilton's test [Hamilton, 1974] was performed to show that the introduction of two more hydrogen atoms (ie. 6 more parameters) into the structure refinement, gave a reduction in the R value that was significantly greater than that expected just from an increase in the degrees of freedom. Comparison of the weighted R values from SHELX-76 [Sheldrick, 1976] for two and four hydrogen atom sites gave a ratio of 1.501:1. The expected ratio from the introduction of 6 more degrees of freedom was 1.005:1 ($\alpha = 0.01$). This shows that the extra two hydrogen atoms make a significant difference in the R value at a 99% probability.

Further refinements of the structure, which included parameters for atomic co-ordinates, temperature factors (anisotropic for non-hydrogen atoms and isotropic for hydrogen atoms) and an overall scale factor, were carried out. In the weighting scheme $1.6014/[\sigma^2(Fo)+gFo^2]$ where g converged to 0.000153, the parameters converged at discrepancy indices R = 0.0289 and Rw = 0.037 for 2136 observed reflections [Fo >

$6\sigma(Fo)]$. The final maximum shift / e.s.d. ratio was 0.002 and the maximum and minimum features on a difference Fourier map were 0.17 and -0.14 e $Å^{-3}$.

4.2.1.6 Structural determination and refinement for data at 150K

Lorentz, polarisation and intensity corrections (1.7% decay) were applied to the collected data. The space group was determined unambiguously as a result of structure analysis. The non-hydrogen atom co-ordinates from the solved structure above (at 293K) were used for an initial structure. Full-matrix least-squares refinement of atomic positions and anisotropic temperature factors (for non-hydrogen atoms) on F_{obs}^2 was applied using SHELXL-93 [Sheldrick, 1993].

All the hydrogen positions were located from difference electron density maps. The hydrogen atoms of the two hydroxy groups were again found to have two possible sites and the disorder was treated as for the data at 293K. Two hydrogen atoms H25 and H30 had fixed temperature factors. Further refinements of the structure, which included parameters for atomic co-ordinates, temperature factors (anisotropic for non-hydrogen atoms and isotropic for hydrogen atoms) and an overall scale factor, were carried out. In the weighting scheme $1/[\sigma^2(Fo^2)+(0.1000P)^2+0.0000P]$ where $P=(Fo^2+2Fc^2)/3$, the parameters converged at discrepancy indices R = 0.0461 and Rw = 0.1143 for 1523 observed reflections [$Fo > 4\sigma(Fo)$]. The final maximum shift / e.s.d. ratio was 0.002 and the maximum and minimum features on a difference Fourier map were 0.26 and -0.34 e $Å^{-3}$.

4.2.1.7 Results and discussion

Full structural data for D/L-1,2;4,5-di-*O*-cyclohexylidene *myo*-inositol (**3**) are given in Tables 4.1 (non-hydrogen atomic co-ordinates), 4.2 (bond lengths and angles), 4.3 (anisotropic displacement parameters) and 4.4 (hydrogen atomic co-ordinates and their isotropic temperature factors), and torsional angles are given in Appendix 1.

Figure 4.1 : ORTEPII diagram [Johnson, 1976] of D/L-1,2;4,5-di-*O*-cyclohexylidene *myo*-inositol at 293K showing the labelling scheme for non-H atoms. Thermal ellipsoids are drawn at the 50% probability level.

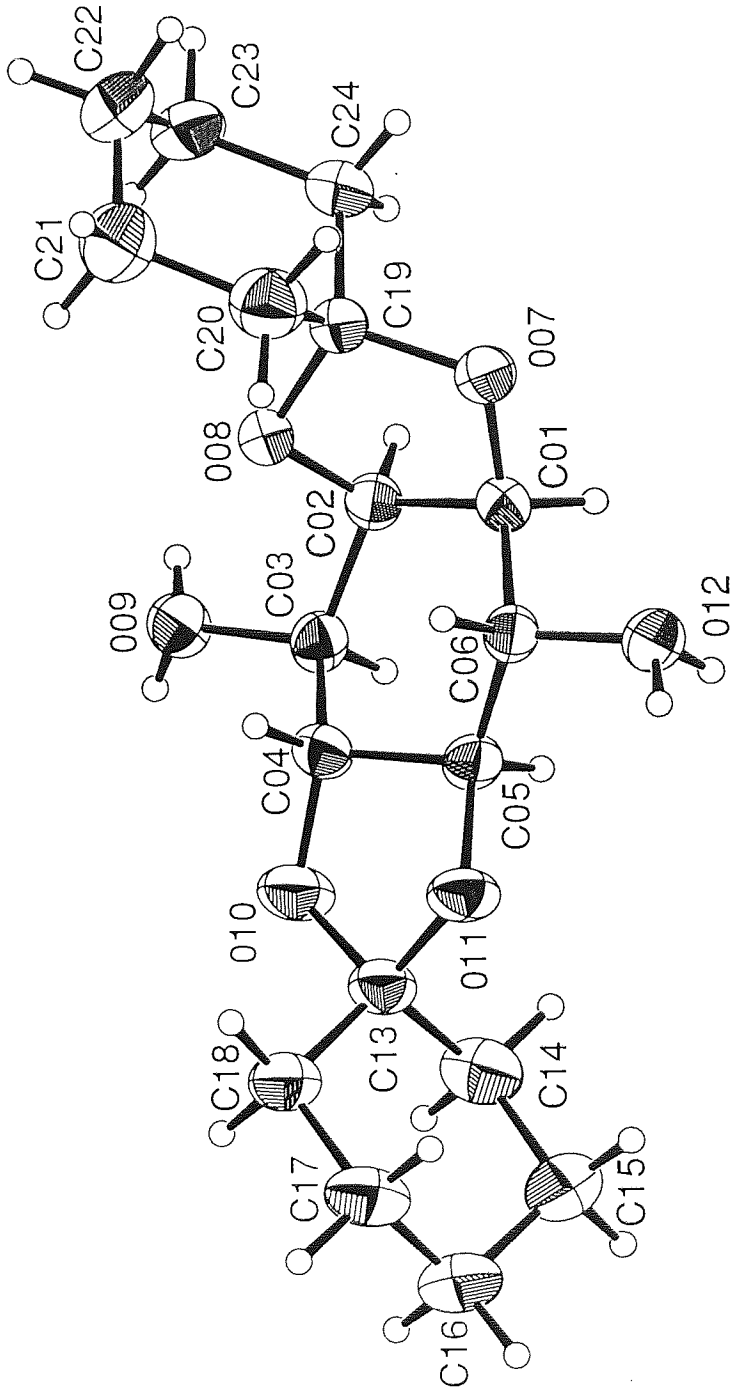

Table 4.1 : Atomic co-ordinates of non-hydrogen atoms (x 10^4) and equivalent isotropic temperature factors (x 10^3) for D/L-1,2;4,5-di-*O*-cyclohexylidene *myo*-inositol (**3**) at 293K and 150K with estimated standard deviations in parentheses. U(eq) is defined as one third of the trace of the orthogonalized U_{ij} tensor.

293K	x	y	z	U(eq)
C(01)	1779(1)	1672(1)	2740(1)	37(1)
C(02)	1535(1)	2673(1)	1917(1)	35(1)
C(03)	432(1)	3271(1)	1868(1)	33(1)
C(04)	121(1)	3460(1)	2978(1)	34(1)
C(05)	144(1)	2275(1)	3559(1)	31(1)
C(06)	1277(1)	1847(1)	3809(1)	31(1)
O(07)	2926(1)	1697(1)	2865(1)	45(1)
O(08)	2358(1)	3529(1)	2217(1)	33(1)
O(09)	452(1)	4377(1)	1302(1)	41(1)
O(10)	964(1)	3839(1)	3048(1)	49(1)
O(11)	-466(1)	2574(1)	4441(1)	39(1)
O(12)	1342(1)	732(1)	4376(1)	38(1)
C(13)	-1344(1)	3305(2)	3996(1)	39(1)
C(14)	-2323(2)	2543(2)	3692(2)	51(1)
C(15)	-2866(2)	2082(2)	4654(2)	61(1)
C(16)	-3124(2)	3106(2)	5391(2)	59(1)
C(17)	-2121(2)	3819(2)	5727(2)	52(1)
C(18)	-1582(2)	4294(2)	4772(2)	47(1)
C(19)	3303(1)	2824(1)	2456(1)	38(1)
C(20)	4013(2)	3471(2)	3282(2)	55(1)
C(21)	4478(2)	4626(2)	2853(2)	64(1)
C(22)	5055(2)	4393(2)	1851(2)	69(1)
C(23)	4332(2)	3751(2)	1026(2)	57(1)
C(24)	3888(2)	2585(2)	1460(2)	47(1)

Table 4.1 continued

150K	x	y	z	U(eq)
C(01)	1770(2)	1681(3)	2757(2)	17(1)
C(02)	1512(2)	2677(3)	1924(2)	18(1)
C(03)	392(2)	3273(3)	1870(2)	18(1)
C(04)	86(2)	3472(3)	2971(2)	18(1)
C(05)	122(2)	2299(3)	3574(2)	18(1)
C(06)	1282(2)	1875(3)	3829(2)	18(1)
O(07)	2941(2)	1699(2)	2878(2)	24(1)
O(08)	2353(2)	3539(2)	2227(2)	19(1)
O(09)	410(2)	4379(2)	1291(2)	22(1)
O(10)	-1029(2)	3837(2)	3031(2)	25(1)
O(11)	-479(2)	2610(2)	4459(1)	20(1)
O(12)	1369(2)	768(2)	4417(2)	21(1)
C(13)	-1389(2)	3319(3)	3999(2)	21(1)
C(14)	-2375(3)	2527(3)	3718(3)	24(1)
C(15)	-2897(3)	2079(3)	4702(3)	30(1)
C(16)	-3155(3)	3135(3)	5429(3)	29(1)
C(17)	-2148(3)	3883(3)	5734(3)	26(1)
C(18)	-1632(3)	4331(3)	4752(3)	25(1)
C(19)	3320(2)	2829(2)	2459(2)	20(1)
C(20)	4066(3)	3477(3)	3280(3)	26(1)
C(21)	4530(3)	4642(3)	2839(3)	32(1)
C(22)	5070(3)	4421(3)	1816(3)	33(1)
C(23)	4306(3)	3759(3)	997(3)	28(1)
C(24)	3881(3)	2587(3)	1449(3)	24(1)

Table 4.2 : Bond lengths (Å) and bond angles (°) for D/L-1,2;4,5-di-*O*-cyclohexylidene *myo*-inositol (**3**) at 293K and 150K with estimated standard deviations in parentheses

Bond	293K Distance (Å)	150K Distance (Å)
C(01)-C(02)	1.535(2)	1.535(4)
C(01)-O(07)	1.426(2)	1.433(3)
C(02)-C(03)	1.521(2)	1.520(4)
C(02)-O(08)	1.426(2)	1.432(3)
C(03)-O(09)	1.417(2)	1.424(4)
C(04)-C(03)	1.498(2)	1.487(4)
C(04)-C(05)	1.500(2)	1.500(4)
C(04)-O(10)	1.423(2)	1.435(3)
C(05)-C(06)	1.500(2)	1.506(4)
C(05)-O(11)	1.431(2)	1.432(3)
C(06)-C(01)	1.541(2)	1.541(4)
C(06)-O(12)	1.425(2)	1.429(3)
C(13)-C(14)	1.509(3)	1.510(4)
C(13)-C(18)	1.511(2)	1.513(4)
C(14)-C(15)	1.520(3)	1.527(4)
C(15)-C(16)	1.514(3)	1.533(5)
C(16)-C(17)	1.511(3)	1.509(5)
C(17)-C(18)	1.518(2)	1.522(4)
C(19)-C(20)	1.501(3)	1.504(4)
C(19)-C(24)	1.523(3)	1.524(4)
C(20)-C(21)	1.518(3)	1.530(5)
C(21)-C(22)	1.521(3)	1.520(5)
C(22)-C(23)	1.507(3)	1.522(5)
C(23)-C(24)	1.520(3)	1.524(4)
O(07)-C(19)	1.439(2)	1.447(3)
O(08)-C(19)	1.425(2)	1.432(4)
O(10)-C(13)	1.446(2)	1.451(3)
O(11)-C(13)	1.442(2)	1.444(3)

Table 4.2 continued

Bonds	293K Angles (°)	150K Angles (°)
C(01)-C(02)-C(03)	118.4(1)	118.2(2)
C(01)-C(02)-O(08)	101.1(1)	101.0(2)
C(01)-C(06)-O(12)	108.7(1)	108.7(2)
C(01)-O(07)-C(19)	109.0(1)	108.9(2)
C(02)-C(01)-O(07)	102.1(1)	102.1(2)
C(02)-C(03)-O(09)	110.3(1)	109.9(2)
C(02)-O(08)-C(19)	105.1(1)	104.9(2)
C(03)-C(02)-O(08)	110.6(1)	110.6(2)
C(03)-C(04)-O(10)	114.1(1)	114.1(2)
C(04)-C(03)-C(02)	108.3(1)	108.8(2)
C(04)-C(03)-O(09)	111.6(1)	111.7(2)
C(04)-C(05)-C(06)	111.3(1)	111.3(2)
C(04)-C(05)-O(11)	100.8(1)	101.2(2)
C(04)-O(10)-C(13)	107.4(1)	107.1(2)
C(05)-C(04)-C(03)	109.9(1)	110.3(2)
C(05)-C(04)-O(10)	102.2(1)	101.7(2)
C(05)-C(06)-C(01)	106.7(1)	106.7(2)
C(05)-C(06)-O(12)	113.4(1)	113.8(2)
C(05)-O(11)-C(13)	104.7(1)	104.4(2)
C(06)-C(01)-C(02)	115.6(1)	115.4(2)
C(06)-C(01)-O(07)	111.4(1)	111.5(2)
C(06)-C(05)-O(11)	116.8(1)	116.6(2)
O(07)-C(19)-C(20)	110.7(1)	110.7(2)
O(07)-C(19)-C(24)	109.5(1)	109.7(2)
O(07)-C(19)-O(08)	105.4(1)	105.0(2)
O(08)-C(19)-C(20)	108.9(1)	109.0(2)
O(08)-C(19)-C(24)	110.8(1)	110.6(2)
O(10)-C(13)-C(14)	108.8(1)	109.0(2)
O(10)-C(13)-C(18)	109.5(1)	109.1(2)
O(10)-C(13)-O(11)	105.6(1)	105.7(2)
O(11)-C(13)-C(14)	111.3(1)	110.9(2)
O(11)-C(13)-C(18)	109.2(1)	109.6(2)
C(13)-C(14)-C(15)	112.3(2)	112.3(3)
C(13)-C(18)-C(17)	112.6(2)	112.9(3)
C(14)-C(13)-C(18)	112.2(1)	112.2(2)
C(14)-C(15)-C(16)	111.6(2)	111.3(3)

Table 4.2 continued

Bonds	293K Angles (°)	150K Angles (°)
C(15)-C(16)-C(17)	110.9(2)	111.2(3)
C(16)-C(17)-(C18)	111.0(2)	111.1(3)
C(19)-C(20)-C(21)	111.8(2)	111.9(3)
C(19)-C(24)-C(23)	111.1(2)	111.0(3)
C(20)-C(19)-C(24)	111.5(1)	111.6(3)
C(20)-C(21)-C(22)	111.7(2)	112.2(3)
C(21)-C(22)-C(23)	111.3(2)	111.4(3)
C(22)-C(23)-C(24)	111.3(2)	111.4(3)

Table 4.3 : Anisotropic displacement parameters (x 10^3) for D/L-1,2:4,5-di-*O*-cyclohexylidene *myo*-inositol (**3**) at 293K and 150K with estimated standard deviations in parentheses

293K	U11	U22	U33	U23	U13	U12
C(01)	37(1)	26(1)	37(1)	2(1)	11(1)	-2(1)
C(02)	40(1)	29(1)	29(1)	-1(1)	12(1)	-3(1)
C(03)	40(1)	31(1)	28(1)	-1(1)	5(1)	2(1)
C(04)	35(1)	33(1)	33(1)	4(1)	8(1)	-1(1)
C(05)	37(1)	33(1)	26(1)	-2(1)	9(1)	-1(1)
C(06)	36(1)	28(1)	30(1)	-2(1)	6(1)	-1(1)
O(07)	37(1)	36(1)	64(1)	8(1)	16(1)	3(1)
O(08)	35(1)	28(1)	45(1)	2(1)	11(1)	3(1)
O(09)	50(1)	39(1)	34(1)	8(1)	11(1)	10(1)
O(10)	46(1)	57(1)	47(1)	20(1)	21(1)	18(1)
O(11)	38(1)	49(1)	32(1)	8(1)	14(1)	6(1)
O(12)	43(1)	38(1)	33(1)	2(1)	7(1)	9(1)
C(13)	38(1)	43(1)	36(1)	8(1)	12(1)	6(1)
C(14)	43(1)	58(1)	50(1)	4(1)	5(1)	-9(1)
C(15)	48(1)	55(1)	82(2)	-8(1)	21(1)	-1(1)
C(16)	48(1)	65(1)	65(1)	1(1)	26(1)	2(1)
C(17)	46(1)	66(1)	46(1)	9(1)	16(1)	-4(1)
C(18)	40(1)	47(1)	55(1)	-1(1)	16(1)	-7(1)
C(19)	35(1)	32(1)	47(1)	4(1)	13(1)	7(1)
C(20)	46(1)	55(1)	55(1)	3(1)	4(1)	1(1)
C(21)	54(1)	53(1)	86(2)	-10(1)	7(1)	-8(1)
C(22)	48(1)	54(1)	107(1)	-8(1)	25(1)	10(1)
C(23)	51(1)	56(1)	68(1)	4(1)	30(1)	14(1)
C(24)	44(1)	41(1)	58(1)	7(1)	21(1)	1(1)

Table 4.3 continued

150K	U11	U22	U33	U23	U13	U12
C(01)	16(2)	15(2)	21(2)	-2(1)	5(1)	-1(1)
C(02)	20(2)	19(2)	15(2)	-4(1)	4(1)	-2(1)
C(03)	21(2)	16(2)	17(2)	1(1)	0(1)	0(1)
C(04)	15(2)	17(2)	21(2)	1(1)	3(1)	-1(1)
C(05)	22(2)	18(2)	15(2)	-3(1)	6(1)	-4(1)
C(06)	20(2)	13(2)	19(2)	-1(1)	1(1)	1(1)
O(07)	18(1)	21(1)	34(1)	9(1)	8(1)	4(1)
O(08)	16(1)	18(1)	24(1)	0(1)	5(1)	0(1)
O(09)	26(1)	22(1)	19(1)	5(1)	6(1)	3(1)
O(10)	21(1)	32(1)	23(1)	11(1)	10(1)	8(1)
O(11)	18(1)	27(1)	16(1)	5(1)	6(1)	5(1)
O(12)	22(1)	22(1)	20(1)	4(1)	4(1)	2(1)
C(13)	20(2)	27(2)	17(2)	4(1)	5(1)	3(1)
C(14)	22(2)	24(2)	26(2)	-6(2)	4(1)	2(1)
C(15)	26(2)	27(2)	39(2)	0(2)	12(2)	-2(2)
C(16)	26(2)	31(2)	33(2)	4(2)	12(2)	1(2)
C(17)	20(2)	33(2)	27(2)	-3(2)	6(1)	7(2)
C(18)	18(2)	29(2)	30(2)	-3(2)	6(1)	4(2)
C(19)	21(2)	12(2)	27(2)	6(1)	5(1)	2(1)
C(20)	23(2)	24(2)	31(2)	3(1)	4(2)	3(2)
C(21)	25(2)	25(2)	45(2)	0(2)	1(2)	-2(2)
C(22)	22(2)	26(2)	52(2)	7(2)	10(2)	-1(2)
C(23)	25(2)	27(2)	33(2)	7(2)	12(2)	1(2)
C(24)	21(2)	21(2)	31(2)	0(2)	7(1)	3(2)

Table 4.4 : Hydrogen atomic co-ordinates (x 10^3) and isotropic temperature factors (x 10^3) for D/L-1,2;4,5-di-*O*-cyclohexylidene *myo*-inositol (**3**) at 293K and 150K with estimated standard deviations in parentheses

293K	x	y	z	U(iso)
H(25)	611(1)	403(1)	334(1)	30(4)
H(26)	-22(1)	168(1)	313(1)	29(4)
H(27)	170(1)	243(1)	422(1)	30(4)
H(28)	155(1)	89(1)	247(1)	27(4)
H(29)	166(1)	235(1)	122(1)	28(4)
H(30)	-9(1)	272(1)	149(1)	25(4)
H(31)	-211(2)	485(2)	440(1)	59(6)
H(32)	-91(2)	470(2)	499(1)	58(5)
H(33)	-160(2)	328(2)	613(2)	65(6)
H(34)	-230(2)	450(2)	623(2)	69(6)
H(35)	-363(2)	365(2)	500(1)	55(6)
H(36)	-345(2)	278(2)	603(2)	75(6)
H(37)	-236(2)	151(2)	504(2)	68(6)
H(38)	-354(2)	163(2)	441(2)	87(7)
H(39)	-285(2)	303(2)	328(1)	55(5)
H(40)	-212(2)	186(2)	326(2)	58(6)
H(41)	360(1)	368(2)	390(1)	50(5)
H(42)	458(2)	293(2)	352(2)	59(6)
H(43)	387(2)	520(2)	269(2)	69(6)
H(44)	496(2)	496(2)	340(2)	82(7)
H(45)	571(2)	389(2)	202(2)	79(7)
H(46)	530(2)	514(2)	154(2)	87(7)
H(47)	374(2)	426(2)	78(1)	59(6)
H(48)	473(2)	356(2)	39(2)	66(6)
H(49)	338(2)	216(2)	91(2)	59(6)
H(50)	446(2)	205(2)	165(1)	55(5)
H(51)	-15(2)	462(3)	109(3)	45(5)
H(52)	113(3)	81(3)	496(2)	45(5)
H(53)	71(3)	427(3)	73(2)	45(5)
H(54)	88(3)	26(3)	412(3)	45(5)

Table 4.4 continued

150K	x	y	z	U(iso)
H(25)	58(2)	407(3)	334(2)	17
H(26)	-27(2)	165(2)	316(2)	5(6)
H(27)	170(2)	248(3)	423(2)	16(7)
H(28)	150(2)	90(2)	249(2)	7(6)
H(29)	166(2)	237(2)	124(2)	13(7)
H(30)	-11(2)	267(3)	150(2)	18
H(31)	-214(2)	490(3)	434(2)	20(7)
H(32)	-90(3)	481(3)	496(3)	41(10)
H(33)	-161(2)	335(3)	611(2)	20(8)
H(34)	-233(3)	458(3)	621(3)	35(9)
H(35)	-369(3)	361(3)	506(2)	21(8)
H(36)	-355(3)	281(3)	610(3)	37(9)
H(37)	-238(3)	152(3)	512(2)	22(8)
H(38)	-359(3)	158(3)	449(3)	41(9)
H(39)	-290(2)	301(3)	329(2)	18(8)
H(40)	-217(2)	187(3)	330(3)	28(8)
H(41)	366(2)	362(3)	392(3)	25(8)
H(42)	467(3)	291(3)	347(2)	22(8)
H(43)	394(3)	519(3)	268(2)	22(8)
H(44)	509(3)	499(4)	333(3)	57(12)
H(45)	574(3)	402(3)	194(3)	38(10)
H(46)	528(3)	524(3)	149(3)	43(10)
H(47)	365(3)	425(3)	78(2)	24(8)
H(48)	471(3)	358(3)	33(3)	33(9)
H(49)	336(3)	210(3)	91(3)	29(9)
H(50)	450(3)	206(3)	162(2)	19(8)
H(51)	-25(3)	461(5)	113(4)	7(8)
H(52)	95(4)	77(5)	493(3)	7(8)
H(53)	72(4)	430(4)	70(3)	7(8)
H(54)	95(4)	26(4)	408(4)	7(8)

The inositol ring is in a distorted chair conformation with the oxygen at C02 (Figure 4.1) in an expected axial position and the other five oxygen atoms in equatorial positions. All the C-C and C-O bond lengths (Table 4.2) were comparable with those of *myo* inositol [Rabinowitz & Kraut, 1964]. However, the ring angles (Table 4.2) largely deviate from that of *myo*-inositol itself which has a mean angle of 110.7° [Rabinowitz & Kraut, 1964], and 111° expected for the undistorted chair [Bucourt, 1974]. The torsion angles of O07-C01-C02-O08 [-35.9(1)° at 293K and -36.6(2) at 150K] and O10-C04-C05-O11 [-41.9(1)° at 293K and -42.7(3) at 150K], which would normally be closer to 60°, show the extent to which the ring has been twisted to accommodate both five-membered ring acetal linkages, although a small distortion could be due to crystal packing.

Aston University

Content has been removed for copyright reasons

Figure 4.2 : Equations for asymmetry parameters [Duax & Norton, 1975].

The asymmetry parameters (Figure 4.2) of the inositol ring were calculated [Duax & Norton, 1975] and are shown in Table 4.5. A perfect chair form has a parameter of zero and deviation from this is calculated by comparison of symmetry related torsion angles. The calculated parameters indicate the ring is twisted, as one good rotation axis is retained [$\Delta C_2(1\text{-}2)$ = 3.70 at 293K and 4.03 at 150K] and is orthogonal to a poor plane

of mirror symmetry [$\Delta C_s(3)$ = 25.20 at 293K and 24.30 at 150K]. Twisting of the ring is also indicated by one torsional angle becoming much smaller than normal and its opposite torsional angle becoming much larger than normal. This is observed in the torsion angles C03-C04-C05-C06 [72.0(2) at 293K, 71.2(3) at 150K] and C06-C01-C02-C03 [-35.7(2) at 293K, -36.2(4) at 150K].

Table 4.5 : Asymmetry parameters for inositol ring of D/L-1,2;4,5-di-*O*-cyclohexylidene *myo*-inositol (**3**) at 293K and 150K

293K		150K	
$\Delta C_s(1)$ = 15.45	$\Delta C_2(1\text{-}2)$ = 3.70	$\Delta C_s(1)$ = 15.25	$\Delta C_2(1\text{-}2)$ = 4.03
$\Delta C_s(2)$ = 10.42	$\Delta C_2(2\text{-}3)$ = 25.29	$\Delta C_s(2)$ = 9.70	$\Delta C_2(2\text{-}3)$ = 24.12
$\Delta C_s(3)$ = 25.20	$\Delta C_2(3\text{-}4)$ = 28.60	$\Delta C_s(3)$ = 24.30	$\Delta C_2(3\text{-}4)$ = 27.85

ΔC_s = Mirror related asymmetry parameter

ΔC_2 = Two fold related asymmetry parameter

Table 4.6 : Distances of C atoms from best fit planes for data at 293K [Davies, 1986]

Aston University

Content has been removed for copyright reasons

Table 4.7 : Distances of C atoms from least squares plane for data at 150K (SHELXL-93 [Sheldrick, 1993]).

Aston University

Content has been removed for copyright reasons

The distances of atoms from best fit and least squares planes (Tables 4.6 and 4.7) show that atoms C01 and C02 have been pulled in closer to the ring system. It also shows that atoms C04 and C05 have been distorted further away from the ring.

The two cyclohexylidene rings are in chair conformations with their ring and torsion angles slightly deviating from that of the ideal chair [Bucourt, 1974]. The slight distortion is expected as compensation for the acetal linkages.

The two acetal five-membered rings have different conformations. The axial/equatorial linked ring adopts a distorted half-chair with atoms C02 above and O08 below the plane of C01, O07, C19 with $\Delta C_2(2\text{-}8)$ 7.76 at 293K and 7.63 at 150K. The equatorial/equatorial linked ring adopts an envelope in which C05 is below a plane through O11, C13, O10, C04 with $\Delta C_s(5)$ 1.59 at 293K and 1.95 at 150K.

The C01-C02 and C04-C05 ring junctions are shown in Figure 4.3 for data at 293K (the angles shown are similar to those of the data at 150K). The C01-C02 ring junction is a *cis* junction, as the endocyclic torsion angles involving this bond have the same sign and have a similar value. The endocyclic torsion angles for the C04-C05 ring junction are unequal and of opposite signs, which shows that it is a *trans* junction.

Cis junctions are known to be flexible, whereas *trans* junctions are rigid [Bucourt, 1974]. If the less stable *trans* acetal linkage is cleaved by acid, the *cis* acetal remaining

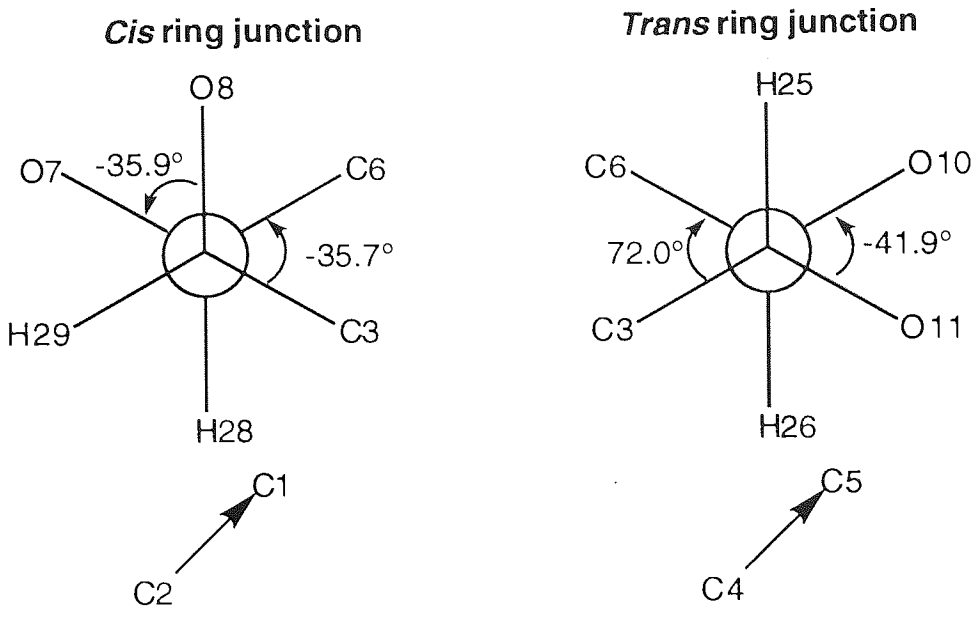

Figure 4.3 : *Cis* and *trans* ring junctions of D/L-1,2;4,5-di-*O*-cyclohexylidene *myo*-inositol (**3**) at 293K drawn as Newman projections

could exist as two possible conformers (flexible). However, if the *cis* acetal linkage is cleaved, the*trans* acetal being rigid would only exist as one conformer. Therefore, cleavage of the *trans* rather than the *cis* acetal linkage should lead to a greater entropy increase, which may explain why the *trans* linkage is preferentially cleaved by acid hydrolysis.

The structure showed the unusual existence of two half-occupied hydrogen atom sites on both the 3- and 6- hydroxyl groups at both temperatures. All four sites are a covalent bond distance from one oxygen atom and a hydrogen bond distance from an oxygen in a symmetry-related molecule, with O····O contact distances of 2.74-2.77 Å. The dimensions of these intermolecular hydrogen bonds are shown in Table 4.8. This hydrogen bond disorder leads to apparent interactions of the type O-H···H-O, where the two hydrogen atoms are only 1.14-1.24 Å apart from each other and therefore are mutually exclusive. These results are comparable with a dynamic phenomenon, seen in the β–cyclodextrin carbohydrates from neutron diffraction studies, called flip-flop hydrogen bonding [Saenger *et al.*, 1982].

Table 4.8 : Geometry of flip-flop hydrogen bonding in D/L-1,2;4,5-di-*O*-cyclohexylidene *myo*-inositol (**3**) at 293K and 150K with estimated standard deviations in parentheses

For data at 293K

	$d_{O\text{-}H.....O}$ (Å)	$\alpha_{O\text{-}H.....O}$ (°)	Symmetry acceptor [a]
O09-H51...O12	1.98(2)	163(1)	(-X, 0.5+Y, 0.5-Z)
O09-H53...O12	1.94(2)	170(1)	(X, 0.5-Y, -0.5+Z)
O12-H52...O09	1.96(2)	165(1)	(X, 0.5-Y, 0.5+Z)
O12-H54...O09	1.97(2)	166(1)	(-X, 0.5-Y, 0.5-Z)

For data at 150K

	$d_{O\text{-}H.....O}$ (Å)	$\alpha_{O\text{-}H.....O}$ (°)	Symmetry acceptor [a]
O09-H51...O12	1.96(4)	154(5)	(-X, 0.5+Y, 0.5-Z)
O09-H53...O12	1.87(3)	177(5)	(X, 0.5-Y, -0.5+Z)
O12-H52...O09	1.90(3)	163(5)	(X, 0.5-Y, 0.5+Z)
O12-H54...O09	1.95(3)	157(5)	(-X, 0.5-Y, 0.5-Z)

[a]Symmetry transformation to be applied to acceptor atom .

The two half occupied hydrogen sites and the mutually exclusive hydrogen positions are indicative of the flip-flop hydrogen bonding dynamic disorder (Figure 4.4) of which only a time averaged equilibrium is observed. The hydrogen atoms flip from one position to the other in a concerted mechanism which is favoured due to the entropic contribution of two equivalent or near equivalent states [Jeffrey & Saenger, 1991].

Figure 4.4 : Flip-flop hydrogen bonding (conformational mechanism) [Jeffrey & Saenger, 1991]

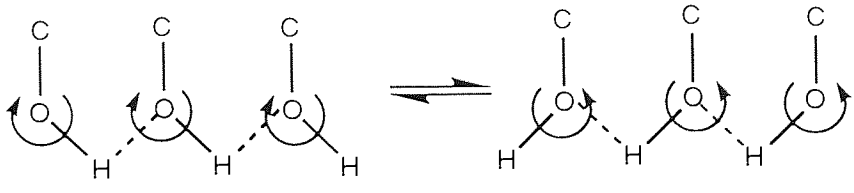

Figure 4.5 : Crystal packing diagram [Davies, 1986] of **3** showing flip-flop hydrogen bonding in a ring system involving symmetry related molecules through a single plane

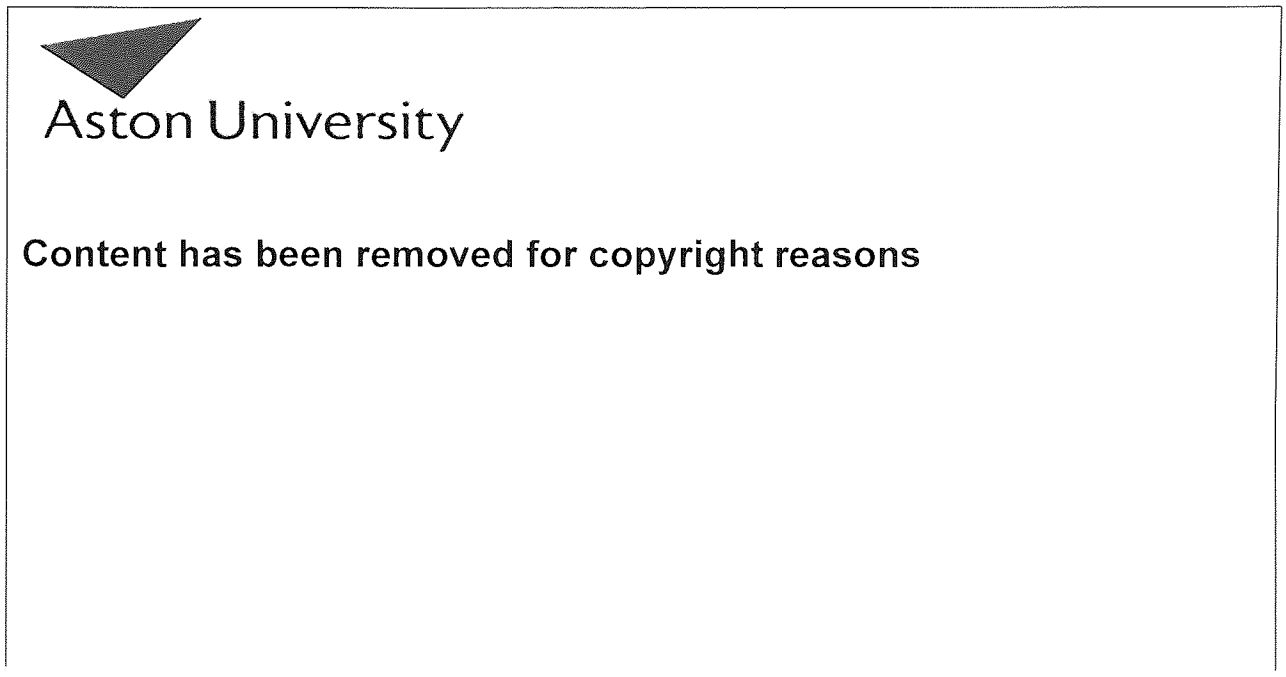

Figure 4.5 is a crystal packing diagram of **3** [Davies, 1986] which shows that the flip-flop hydrogen bonding produces a tetramer about the centres of symmetry at 0, 0.5, 0 and 0, 0, 0.5, involving four symmetry related molecules through a single plane.

Room temperature(293K) crystallography is unable to distinguish between static and dynamic disorder because it observes the space and time average of a statistical distribution of hydrogen bonds. Statistical disorders are seen when the hydrogen bonds are ordered one way in one unit cell in the crystal and in the opposite way in another.

In studies of β-cyclodextrin, confirmation of a dynamic disorder has been shown using low temperature experiments. At low temperature the flip-flop system should become ordered in one of the two possible directions. Calorimetric measurements indicated an exothermic reaction at -46°C (227K) which corresponds to ordering of hydrogen bonds. Neutron diffraction studies at -100°C (173K) also confirmed the disorder was dynamic by the disappearance of flip-flop hydrogen bonds [Saenger *et al.*, 1983].

The low temperature data (150K) for D/L-1,2;4,5-di-*O*-cyclohexylidene *myo*-inositol (**3**) showed that the structure still had the disordered hydrogen bonding seen at room temperature. This could be because the ordering of the flip-flop hydrogen bonds occurs one way in one unit cell and in the other way in another, or that the disorder is statistical.

A differential scanning calorimetry (DSC) study of a crystalline powder of D/L-1,2;4,5-di-*O*-cyclohexylidene *myo*-inositol (**3**) was carried out from room temperature to -40°C (233K). No exothermic reaction was recorded at low temperature, although this was limited to -40°C (233K). The only conclusion drawn from this result was that if ordering occurs, it must take place below -40°C (233K).

A comparison of spatial distances [Davies, 1986] of O9 and O12 from nearby atoms was evaluated to see if reaction selectivity at the 1-/3- position, when compared with the lack of reactivity at the 4-/6- position, is caused by steric hindrance of surrounding groups (Figure 4.6).

The two oxygen are positioned in similar environments and no conclusive evidence can be obtained from the spatial distances for reaction selectivity.

Figure 4.6 : Spatial distances (Å) of O9 and O12 from nearby atoms

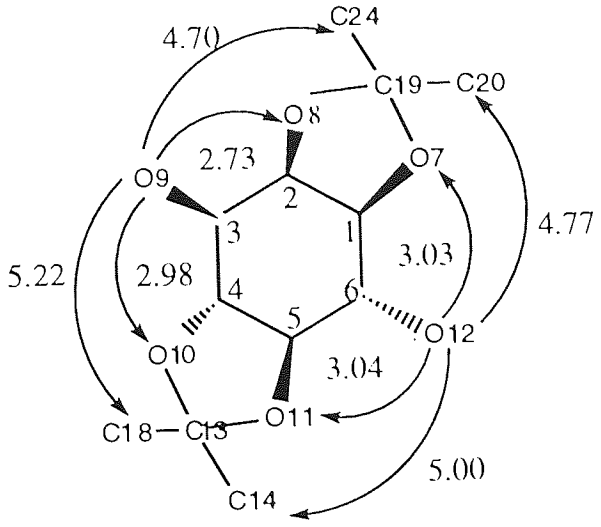

4.2.2 Crystal structure of D/L-1-*O*-(*tert*-butyldiphenylsilyl)-2,3-*O*-cyclohexylidene *myo*-inositol (58)

4.2.2.1 Experimental

D/L-1-*O*-(*tert*-Butyldiphenylsilyl)-2,3-*O*-cyclohexylidene *myo*-inositol (**58**) slowly crystallised in DMF, chloroform and hexane to form colourless plate crystals. A single crystal (0.35 x 0.25 x 0.10 mm) was chosen for X-ray determination. The data were collected from an Enraf-Nonius CAD4 diffractometer with monochromated graphite Mo-Kα radiation, λ = 0.71069Å at 293 K.

4.2.2.2 Crystal data

D/L-1-*O*-(*tert*-Butyldiphenylsilyl)-2,3-*O*-cyclohexylidene *myo*-inositol (2 x $C_{28}H_{38}O_6Si.DMF.0.5$ x $CHCl_3$) crystallises in the triclinic space group $P\bar{1}$ with a = 9.556(3), b = 16.834(3), c = 20.186(4)Å, α = 80.45(2), β = 77.74(2), γ = 89.02(2)°, Z =

2 and V 3128.6(13)Å^3. The formula weight is 1130.13 (F(000) = 1210) and the calculated density D_X = 1.200 Mg m^{-3}. The absorption coefficient μ = 0.180 mm^{-1}.

4.2.2.3 Data collection

Unit cell dimensions were obtained from least squares analysis of setting angles of 25 accurately centred reflections, $8.52 \leq \theta \leq 15.55°$. Intensity data were collected by the ω-2θ scan technique, Bragg angle $2.12 \leq \theta \leq 25.04°$. The ω scan angle was calculated from $[M+N(\tan\theta)]°$, where M = 0.9, N = 0.35 and increased by 25% on each side for background determination. The ω scan speed was varied from 0.6 to 2.1°min^{-1} depending upon intensity. Six different standard reflections were used during data collection: three intensity reflections (measured every three hours) and three orientation reflections (monitored every 200 reflections). No appreciable loss of intensity or crystal movement was detected during collection. The 11746 reflections were measured for $-1 \leq h \leq 10$, $-19 \leq k \leq 19$, $-22 \leq l \leq 23$ and merged to give 9744 independent reflections (R_{int} = 0.0267).

4.2.2.4 Structural determination and refinement

Lorentz, polarisation and intensity corrections (4.2% decay) were applied to the collected data. The space group was determined unambiguously as a result of structure analysis. An initial structure was solved by direct methods using the EEES routine in SHELX-76 [Sheldrick, 1976]. Based on the atomic positions determined from the E-map, the remaining non-hydrogen atoms were located in an electron density map using SHELXL-93 [Sheldrick, 1993].

Full-matrix least-squares refinement of atomic positions and anisotropic temperature factors (for non-hydrogen atoms) on F_{obs}^2 using SHELXL-93 showed that in each asymmetric unit there are two molecules of triol **58**, one molecule of DMF and one molecule of chloroform (with half occupancy).

From difference electron density maps, hydrogen positions were found for each of the three inositol OH groups and for the inositol rings. The other hydrogen atoms were assumed to ride on attached atoms and were placed in calculated positions, their common temperature factors were set as free variables in chemical groups of similar kind. Further refinement of the structure which included parameters for atomic co-ordinates, temperature factors (anisotropic for non-hydrogen atoms and isotropic for hydrogen atoms), overall scale factor and an extinction parameter were carried out. In the weighting scheme $1/[\sigma^2(Fo^2)+(0.1000P)^2+0.0000P]$ where $P=(Fo^2+2Fc^2)/3$, the parameters converged at discrepancy indices R = 0.0604 and R_W = 0.1597 for 4463 observed reflections [$Fo > 4\sigma(Fo)$]. The final maximum shift / e.s.d. ratio was 0.001 and the maximum and minimum features on a difference Fourier map were 0.394 and -0.244 e $Å^{-3}$.

4.2.2.5 Results and discussion

Full structural data for the crystal structure of D/L-1-*O*-(*tert*-butyldiphenylsilyl)-2,3-*O*-cyclohexylidene *myo*-inositol are given in Tables 4.9 (non-hydrogen atomic co-ordinates), 4.10 (bond lengths and angles), 4.11 (anisotropic displacement parameters) and 4.12 (hydrogen atomic co-ordinates and their isotropic temperature factors), and the torsional angles are given in Appendix 1.

The inositol rings for both inositol molecules (in one asymmetric unit) are in a distorted chair conformation with the oxygen at C2 and C74 (Figures 4.7 and 4.8) in the expected axial position and the other five oxygen atoms in equatorial positions for each molecule. The two inositol structures in the asymmetric unit are enantiomers (Figure 4.9). Molecule one is D-1-*O*-(*tert*-butyldiphenylsilyl)-2,3-*O*-cyclohexylidene *myo*-inositol (by convention) and molecule two is L-1-*O*-(*tert*-butyldiphenylsilyl)-2,3-*O*-cyclohexylidene *myo*-inositol. All the C-C and C-O bond lengths (Table 4.10) were comparable with those of *myo*-inositol [Rabinowitz & Kraut, 1964]. However, the inositol ring angles (Table 4.10) deviate from expected values (*myo*-inositol has a mean angle of 110.7° [Rabinowitz & Kraut, 1964] and the perfect chair an angle of 111°

[Bucourt, 1974]) at the positions where the silyl and the cyclohexylidene groups are attached to the inositol ring. The torsion angles O8-C2-C3-O9 = 30.6(5) and O81-C75-C76-O82 = 37.4(4), which would normally approach 60°, show that the inositol oxygen atoms at the *cis* ring junctions have moved closer together to accommodate the acetal linkage. The *cis* junctions show expected endocyclic torsion angles which have the same sign and similar values [C1-C2-C3-C4 = 35.1(6), O8-C2-C3-O9 = 30.6(5) and C74-C75-C76-C77 = 36.9(6), O81-C75-C76-O82 = 37.4(4)]. The asymmetry parameters of the inositol rings were calculated [Duax & Norton, 1975] and are shown in Table 4.13. The inositol rings of the two molecules are distorted but in different ways. The ring of molecule one is twisted with a good two-fold axis retained [ΔC_2(2-3) = 2.28], whereas molecule two has a ring that is flattened at one end (C75) and puckered at the opposite end (C78), retaining a good mirror plane [ΔC_S(75) = 2.85]. These differences in ring distortion (Figure 4.9) for the enantiomers of the same chemical structure show how crystal packing and hydrogen bonding must play an important part in determining the conformation of flexible rings and that care must be taken when trying to extrapolate precise structural detail from crystal structures. The distances of ring atoms from least squares planes (Table 4.14) confirm the ring distortions, showing that the inositol carbon atoms C02, C03 (twisted) and C75 (flattened) are pulled in much closer to the plane, and C05, C06 (twisted) and C78 (puckered) are pushed further away from the plane.

The cyclohexylidene rings in both molecules are in chair conformations with their ring and torsion angles slightly deviating from that of a perfect chair [Bucourt, 1974]. The slight distortion is expected as compensation for the acetal linkages.

The acetal five-membered rings for both molecules have different conformations (Figure 4.20). Molecule one adopts a distorted half-chair with atoms C02 below and O08 above a C03-O09-C30 plane with ΔC_2(2-8) = 1.98. Molecule two adopts a distorted envelope with atom C75 below a C76-O81-O82-C103 plane with ΔC_S(75) = 4.40. These conformational differences in the five-membered rings are caused by the different distortions within the inositol ring.

Table 4.9 : Atomic co-ordinates of non-hydrogen atoms (x 10^4) and equivalent isotropic temperature factors (x 10^3) for D/L-1-*O*-(*tert*-butyldiphenylsilyl)-2,3-*O*-cyclohexylidene *myo*-inositol (**58**) and solvents, DMF and chloroform with estimated standard deviations in parentheses. U(eq) is defined as one third of the trace of the orthogonalized U_{ij} tensor.

	x	y	z	U(eq)
C(01)	3250(5)	3288(3)	2964(2)	50(1)
C(02)	1891(6)	3687(3)	2819(2)	54(1)
C(03)	1096(6)	4162(3)	3361(2)	58(1)
C(04)	2042(6)	4594(3)	3708(2)	56(1)
C(05)	3251(5)	4076(3)	3890(2)	47(1)
C(06)	4154(5)	3812(3)	3255(2)	49(1)
O(07)	4063(3)	3028(2)	2366(1)	52(1)
O(08)	2145(3)	4275(2)	2210(1)	54(1)
O(09)	340(4)	4752(2)	2969(2)	78(1)
O(10)	1240(5)	4810(2)	4329(2)	78(1)
O(11)	4163(4)	4496(2)	4197(2)	57(1)
O(12)	5358(4)	3372(2)	3416(2)	67(1)
Si(13)	4412(2)	2115(1)	2190(1)	51(1)
C(14)	3197(5)	1866(3)	1638(2)	53(1)
C(15)	3241(6)	1127(3)	1399(2)	70(2)
C(16)	2358(7)	939(3)	999(3)	80(2)
C(17)	1386(7)	1491(4)	809(3)	78(2)
C(18)	1300(6)	2219(3)	1032(2)	71(2)
C(19)	2201(5)	2402(3)	1437(2)	58(1)
C(20)	4080(6)	1350(3)	2993(2)	63(1)
C(21)	4700(6)	1439(3)	3548(3)	76(2)
C(22)	4451(8)	879(4)	4151(3)	93(2)
C(23)	3607(9)	223(4)	4210(3)	116(3)
C(24)	3001(10)	116(4)	3674(4)	137(3)
C(25)	3223(8)	669(3)	3088(3)	106(2)
C(26)	6336(6)	2174(3)	1692(2)	65(1)
C(27)	6447(8)	2798(4)	1034(3)	99(2)
C(28)	6840(7)	1355(3)	1494(3)	93(2)
C(29)	7332(6)	2430(4)	2126(3)	94(2)

Table 4.9 continued

	x	y	z	U(eq)
C(30)	895(6)	4757(3)	2254(2)	62(1)
C(31)	1350(6)	5598(3)	1889(3)	75(2)
C(32)	1767(7)	5650(3)	1121(3)	88(2)
C(33)	587(8)	5335(3)	827(3)	92(2)
C(34)	176(7)	4485(3)	1174(3)	80(2)
C(35)	-242(6)	4417(3)	1945(3)	76(2)
C(74)	2669(5)	3216(2)	7250(2)	45(1)
C(75)	1500(5)	2663(2)	7168(2)	44(1)
C(76)	597(5)	2984(3)	6651(2)	49(1)
C(77)	1418(5)	3504(2)	6010(2)	46(1)
C(78)	2368(6)	4122(3)	6178(2)	48(1)
C(79)	3425(5)	3700(3)	6577(2)	50(1)
O(80)	3684(3)	2768(2)	7576(1)	46(1)
O(81)	2109(3)	1973(2)	6904(2)	53(1)
O(82)	61(4)	2260(2)	6502(2)	64(1)
O(83)	412(4)	3869(2)	5625(2)	59(1)
O(84)	3110(4)	4594(2)	5568(2)	61(1)
O(85)	4357(4)	4251(2)	6733(2)	76(1)
Si(86)	3645(1)	2496(1)	8398(1)	46(1)
C(87)	3746(5)	3415(2)	8797(2)	49(1)
C(88)	4130(6)	4160(3)	8407(2)	59(1)
C(89)	4214(6)	4838(3)	8700(3)	71(2)
C(90)	3938(6)	4772(3)	9403(3)	77(2)
C(91)	3582(6)	4037(3)	9803(2)	75(2)
C(92)	3478(6)	3372(3)	9508(2)	69(2)
C(93)	1915(5)	1951(3)	8844(2)	49(1)
C(94)	1720(6)	1122(3)	8901(2)	66(1)
C(95)	411(8)	749(4)	9205(3)	79(2)
C(96)	-727(7)	1174(4)	9444(3)	79(2)
C(97)	-595(7)	1998(4)	9395(3)	79(2)
C(98)	720(6)	2371(3)	9099(2)	62(1)
C(99)	5273(6)	1860(3)	8411(3)	64(1)
C(100)	5378(7)	1218(3)	7944(3)	85(2)
C(101)	5319(7)	1457(4)	9155(3)	97(2)

Table 4.9 continued

	x	y	z	U(eq)
C(102)	6606(6)	2429(3)	8145(3)	84(2)
C(103)	988(5)	1610(3)	6677(2)	57(1)
C(104)	1630(7)	1249(3)	6057(3)	78(2)
C(105)	2523(9)	529(4)	6241(3)	111(2)
C(106)	1644(9)	-99(3)	6799(4)	128(3)
C(107)	1023(8)	266(3)	7420(3)	96(2)
C(108)	135(6)	992(3)	7248(3)	75(2)
C(147)	9957(19)	1707(7)	4233(6)	122(6)
L(148)	10291(5)	2399(2)	4696(2)	123(1)
L(149)	9195(7)	2056(3)	3590(3)	200(3)
L(150)	9309(7)	829(3)	4724(2)	167(2)
N(152)	6637(7)	2838(3)	5430(3)	103(2)
C(153)	7154(8)	3543(4)	5054(4)	112(2)
O(154)	7077(6)	3804(2)	4441(3)	116(2)
C(155)	6902(10)	2554(6)	6087(4)	153(3)
C(156)	5648(15)	2401(6)	5155(6)	213(5)

Note : L = Chloride atom

Table 4.10 : Bond lengths (Å) and bond angles (°) for D/L-1-*O*-(*tert*-butyldiphenylsilyl)-2,3-*O*-cyclohexylidene *myo*-inositol (**58**) and solvents, DMF and chloroform with estimated standard deviations in parentheses

Bond	Distance (Å)	Bond	Distance (Å)
C(01)-O(07)	1.422(5)	C(26)-C(28)	1.539(7)
C(01)-C(06)	1.512(6)	C(26)-C(27)	1.537(7)
C(01)-C(02)	1.514(6)	C(30)-C(31)	1.508(7)
C(02)-O(08)	1.422(5)	C(30)-C(35)	1.524(7)
C(02)-C(03)	1.526(6)	C(31)-C(32)	1.505(7)
C(03)-O(09)	1.447(5)	C(32)-C(33)	1.520(8)
C(03)-C(04)	1.516(7)	C(33)-C(34)	1.504(7)
C(04)-O(10)	1.422(5)	C(34)-C(35)	1.508(7)
C(04)-C(05)	1.506(6)	C(74)-O(80)	1.422(5)
C(05)-O(11)	1.428(5)	C(74)-C(79)	1.506(6)
C(05)-C(06)	1.513(6)	C(74)-C(75)	1.519(6)
C(06)-O(12)	1.424(5)	C(75)-O(81)	1.423(5)
O(07)-Si(13)	1.646(3)	C(75)-C(76)	1.519(6)
O(08)-C(30)	1.428(5)	C(76)-O(82)	1.430(5)
O(09)-C(30)	1.427(5)	C(76)-C(77)	1.507(6)
Si(13)-C(14)	1.866(4)	C(77)-O(83)	1.429(5)
Si(13)-C(20)	1.868(5)	C(77)-C(78)	1.517(6)
Si(13)-C(26)	1.895(6)	C(78)-O(84)	1.406(5)
C(14)-C(19)	1.377(6)	C(78)-C(79)	1.517(6)
C(14)-C(15)	1.403(6)	C(79)-O(85)	1.412(5)
C(15)-C(16)	1.359(7)	O(80)-Si(86)	1.637(3)
C(16)-C(17)	1.370(7)	O(81)-C(103)	1.433(5)
C(17)-C(18)	1.368(7)	O(82)-C(103)	1.442(5)
C(18)-C(19)	1.379(6)	Si(86)-C(87)	1.873(4)
C(20)-C(25)	1.384(7)	Si(86)-C(93)	1.879(5)
C(20)-C(21)	1.403(6)	Si(86)-C(99)	1.876(5)
C(21)-C(22)	1.388(7)	C(87)-C(88)	1.376(6)
C(22)-C(23)	1.354(8)	C(87)-C(92)	1.393(6)
C(23)-C(24)	1.369(8)	C(88)-C(89)	1.379(6)
C(24)-C(25)	1.359(8)	C(89)-C(90)	1.372(6)
C(26)-C(29)	1.533(7)	C(90)-C(91)	1.366(7)

Table 4.10 continued

Bond	Distance (Å)	Bond	Distance (Å)
C(91)-C(92)	1.367(6)	C(104)-C(105)	1.512(8)
C(93)-C(98)	1.383(6)	C(105)-C(106)	1.525(9)
C(93)-C(94)	1.393(6)	C(106)-C(107)	1.492(8)
C(94)-C(95)	1.382(7)	C(107)-C(108)	1.510(8)
C(95)-C(96)	1.340(8)	C(147)-L(149)	1.641(13)
C(96)-C(97)	1.381(8)	C(147)-L(148)	1.683(11)
C(97)-C(98)	1.383(7)	C(147)-L(150)	1.684(11)
C(99)-C(100)	1.537(7)	N(152)-C(153)	1.338(8)
C(99)-C(101)	1.550(7)	N(152)-C(155)	1.405(8)
C(99)-C(102)	1.552(7)	N(152)-C(156)	1.458(12)
C(103)-C(104)	1.492(6)	C(153)-O(154)	1.259(8)
C(103)-C(108)	1.520(7)		

Bonds	Angles (°)	Bonds	Angles (°)
O(07)-C(01)-C(06)	110.8(4)	C(02)-O(08)-C(30)	105.8(3)
O(07)-C(01)-C(02)	110.7(3)	C(30)-O(09)-C(03)	108.9(3)
C(06)-C(01)-C(02)	113.3(4)	O(07)-Si(13)-C(14)	109.0(2)
O(08)-C(02)-C(01)	112.6(4)	O(07)-Si(13)-C(20)	110.9(2)
O(08)-C(02)-C(03)	102.7(4)	C(14)-Si(13)-C(20)	107.9(2)
C(01)-C(02)-C(03)	115.8(4)	O(07)-Si(13)-C(26)	105.1(2)
O(09)-C(03)-C(04)	109.1(4)	C(14)-Si(13)-C(26)	110.0(2)
O(09)-C(03)-C(02)	102.8(4)	C(20)-Si(13)-C(26)	113.9(2)
C(04)-C(03)-C(02)	115.3(4)	C(19)-C(14)-C(15)	115.8(4)
O(10)-C(04)-C(05)	107.3(4)	C(19)-C(14)-Si(13)	121.7(3)
O(10)-C(04)-C(03)	110.8(5)	C(15)-C(14)-Si(13)	122.5(4)
C(05)-C(04)-C(03)	112.0(4)	C(16)-C(15)-C(14)	123.0(5)
O(11)-C(05)-C(04)	111.6(3)	C(15)-C(16)-C(17)	119.4(5)
O(11)-C(05)-C(06)	108.1(4)	C(16)-C(17)-C(18)	119.8(5)
C(04)-C(05)-C(06)	110.6(4)	C(17)-C(18)-C(19)	120.3(5)
O(12)-C(06)-C(01)	109.4(4)	C(18)-C(19)-C(14)	121.9(4)
O(12)-C(06)-C(05)	110.9(4)	C(25)-C(20)-C(21)	115.4(5)
C(01)-C(06)-C(05)	109.2(4)	C(25)-C(20)-Si(13)	123.5(4)
C(01)-O(07)-Si(13)	130.7(3)	C(21)-C(20)-Si(13)	121.1(4)

Note : L = Chloride atom

Table 4.10 continued

Bonds	Angles (°)	Bonds	Angles (°)
C(22)-C(21)-C(20)	121.7(5)	O(84)-C(78)-C(77)	109.8(3)
C(23)-C(22)-C(21)	120.0(5)	O(84)-C(78)-C(79)	110.0(4)
C(22)-C(23)-C(24)	119.6(6)	C(77)-C(78)-C(79)	110.0(3)
C(25)-C(24)-C(23)	120.5(6)	O(85)-C(79)-C(74)	107.0(3)
C(24)-C(25)-C(20)	122.7(6)	O(85)-C(79)-C(78)	112.1(4)
C(29)-C(26)-C(28)	107.9(5)	C(74)-C(79)-C(78)	111.5(4)
C(29)-C(26)-C(27)	109.4(5)	C(74)-O(80)-Si(86)	129.2(3)
C(28)-C(26)-C(27)	109.1(4)	C(75)-O(81)-C(103)	105.7(3)
C(29)-C(26)-Si(13)	110.3(3)	C(76)-O(82)-C(103)	108.5(3)
C(28)-C(26)-Si(13)	111.6(4)	O(80)-Si(86)-C(87)	109.4(2)
C(27)-C(26)-Si(13)	108.6(4)	O(80)-Si(86)-C(93)	110.5(2)
O(09)-C(30)-O(08)	106.0(3)	C(87)-Si(86)-C(93)	107.4(2)
O(09)-C(30)-C(31)	110.7(4)	O(80)-Si(86)-C(99)	103.5(2)
O(08)-C(30)-C(31)	107.8(4)	C(87)-Si(86)-C(99)	112.0(2)
O(09)-C(30)-C(35)	109.1(4)	C(93)-Si(86)-C(99)	114.0(2)
O(08)-C(30)-C(35)	112.1(4)	C(88)-C(87)-C(92)	116.6(4)
C(31)-C(30)-C(35)	110.9(4)	C(88)-C(87)-Si(86)	122.0(3)
C(32)-C(31)-C(30)	112.5(4)	C(92)-C(87)-Si(86)	121.4(3)
C(31)-C(32)-C(33)	112.3(5)	C(87)-C(88)-C(89)	122.1(4)
C(34)-C(33)-C(32)	109.9(4)	C(90)-C(89)-C(88)	119.6(5)
C(33)-C(34)-C(35)	112.0(4)	C(91)-C(90)-C(89)	119.5(4)
C(34)-C(35)-C(30)	113.2(5)	C(90)-C(91)-C(92)	120.5(4)
O(80)-C(74)-C(79)	109.8(4)	C(91)-C(92)-C(87)	121.6(4)
O(80)-C(74)-C(75)	110.7(3)	C(98)-C(93)-C(94)	115.9(5)
C(79)-C(74)-C(75)	112.7(4)	C(98)-C(93)-Si(86)	120.8(3)
O(81)-C(75)-C(74)	110.4(4)	C(94)-C(93)-Si(86)	123.2(4)
O(81)-C(75)-C(76)	101.4(3)	C(95)-C(94)-C(93)	121.5(5)
C(74)-C(75)-C(76)	117.4(4)	C(96)-C(95)-C(94)	121.0(5)
O(82)-C(76)-C(77)	111.7(4)	C(95)-C(96)-C(97)	119.8(6)
O(82)-C(76)-C(75)	102.3(3)	C(98)-C(97)-C(96)	119.1(6)
C(77)-C(76)-C(75)	114.2(4)	C(97)-C(98)-C(93)	122.6(5)
O(83)-C(77)-C(76)	108.2(4)	C(100)-C(99)-C(101)	110.1(4)
O(83)-C(77)-C(78)	112.3(3)	C(100)-C(99)-C(102)	108.1(5)
C(76)-C(77)-C(78)	111.6(3)	C(101)-C(99)-C(102)	107.3(5)

Table 4.10 continued

Bonds	Angles (°)	Bonds	Angles (°)
C(100)-C(99)-Si(86)	112.6(4)	C(107)-C(106)-C(105)	110.3(5)
C(101)-C(99)-Si(86)	111.0(4)	C(106)-C(107)-C(108)	111.8(5)
C(102)-C(99)-Si(86)	107.4(3)	C(107)-C(108)-C(103)	111.3(5)
O(81)-C(103)-O(82)	105.5(3)	L(149)-C(147)-L(148)	114.9(8)
O(81)-C(103)-C(104)	108.8(4)	L(149)-C(147)-L(150)	117.1(8)
O(82)-C(103)-C(104)	110.4(4)	L(148)-C(147)-L(150)	113.0(6)
O(81)-C(103)-C(108)	111.2(4)	C(153)-N(152)-C(155)	123.2(7)
O(82)-C(103)-C(108)	108.9(4)	C(153)-N(152)-C(156)	116.3(7)
C(104)-C(103)-C(108)	111.9(4)	C(155)-N(152)-C(156)	120.2(7)
C(103)-C(104)-C(105)	111.0(4)	O(154)-C(153)-N(152)	126.9(7)
C(104)-C(105)-C(106)	111.2(6)		

Note : L = Chloride atom

Table 4.11 : Anisotropic displacement parameters (x 10^3, for non-hydrogen atoms) for D/L-1-*O*-(*tert*-butyldiphenylsilyl)-2,3-*O*-cyclohexylidene *myo*-inositol (**58**) and solvents, DMF and chloroform with estimated standard deviations in parentheses

	U11	U22	U33	U23	U13	U12
C(01)	70(4)	47(3)	38(2)	-13(2)	-17(2)	8(3)
C(02)	58(4)	59(3)	49(3)	-22(2)	-11(3)	7(3)
C(03)	62(4)	67(3)	50(3)	-16(3)	-15(3)	13(3)
C(04)	81(4)	50(3)	37(3)	-12(2)	-15(3)	15(3)
C(05)	67(3)	38(2)	39(2)	-8(2)	-17(2)	-1(2)
C(06)	58(3)	50(3)	45(3)	-21(2)	-16(2)	6(3)
O(07)	70(2)	47(2)	46(2)	-21(1)	-18(2)	12(2)
O(08)	66(2)	56(2)	46(2)	-17(2)	-17(2)	14(2)
O(09)	78(3)	108(3)	58(2)	-33(2)	-25(2)	42(2)
O(10)	118(3)	85(3)	40(2)	-25(2)	-28(2)	60(3)
O(11)	80(2)	52(2)	45(2)	-19(1)	-17(2)	-5(2)
O(12)	66(3)	75(2)	76(2)	-42(2)	-32(2)	21(2)
Si(13)	67(1)	45(1)	50(1)	-19(1)	-23(1)	11(1)
C(14)	68(4)	50(3)	47(3)	-16(2)	-23(3)	10(3)
C(15)	101(5)	56(3)	70(3)	-26(3)	-42(3)	8(3)
C(16)	116(5)	61(3)	80(4)	-31(3)	-47(4)	2(3)
C(17)	93(5)	92(4)	57(3)	-14(3)	-30(3)	-31(4)
C(18)	74(4)	85(4)	59(3)	-9(3)	-28(3)	7(3)
C(19)	70(4)	62(3)	46(3)	-16(2)	-20(3)	6(3)
C(20)	94(4)	51(3)	52(3)	-16(2)	-31(3)	17(3)
C(21)	100(5)	65(3)	72(4)	-18(3)	-38(3)	6(3)
C(22)	140(6)	88(4)	66(4)	-3(3)	-60(4)	9(4)
C(23)	196(8)	71(4)	82(4)	13(3)	-49(5)	-19(5)
C(24)	225(10)	96(5)	97(5)	27(4)	-76(6)	-73(6)
C(25)	175(7)	77(4)	77(4)	13(3)	-65(4)	-40(4)
C(26)	75(4)	59(3)	66(3)	-23(3)	-17(3)	10(3)
C(27)	106(5)	94(4)	79(4)	-3(3)	10(4)	11(4)
C(28)	82(5)	88(4)	115(5)	-49(4)	-16(4)	30(4)
C(29)	63(4)	120(5)	109(5)	-53(4)	-13(4)	-3(4)
C(30)	70(4)	68(3)	59(3)	-27(3)	-29(3)	21(3)
C(31)	91(4)	59(3)	89(4)	-26(3)	-40(3)	17(3)
C(32)	127(6)	62(3)	77(4)	-4(3)	-34(4)	14(4)

Table 4.11 continued

	U11	U22	U33	U23	U13	U12
C(33)	146(6)	73(4)	68(4)	-13(3)	-46(4)	32(4)
C(34)	102(5)	84(4)	72(4)	-29(3)	-51(3)	21(3)
C(35)	77(4)	80(4)	82(4)	-23(3)	-37(3)	15(3)
C(74)	58(3)	40(2)	38(2)	-11(2)	-12(2)	7(2)
C(75)	55(3)	41(2)	37(3)	-4(2)	-13(2)	3(2)
C(76)	49(3)	50(3)	55(3)	-14(2)	-20(3)	11(3)
C(77)	54(3)	44(2)	46(3)	-17(2)	-19(2)	20(2)
C(78)	74(4)	41(2)	32(2)	-9(2)	-15(2)	9(3)
C(79)	66(3)	47(2)	42(2)	-10(2)	-22(2)	-1(3)
O(80)	52(2)	49(2)	41(2)	-3(1)	-22(2)	5(2)
O(81)	59(2)	44(2)	63(2)	-12(1)	-30(2)	7(2)
O(82)	69(2)	57(2)	78(2)	-9(2)	-44(2)	1(2)
O(83)	73(3)	61(2)	49(2)	-9(2)	-30(2)	23(2)
O(84)	105(3)	44(2)	37(2)	-4(2)	-23(2)	2(2)
O(85)	104(3)	76(2)	50(2)	10(2)	-35(2)	-40(2)
Si(86)	55(1)	42(1)	43(1)	-4(1)	-21(1)	1(1)
C(87)	58(3)	46(2)	46(3)	-4(2)	-18(2)	-6(2)
C(88)	89(4)	50(3)	42(3)	-5(2)	-21(3)	-3(3)
C(89)	104(5)	48(3)	68(3)	-15(2)	-24(3)	-4(3)
C(90)	108(5)	68(3)	61(3)	-29(3)	-19(3)	-8(3)
C(91)	107(5)	81(4)	38(3)	-19(3)	-9(3)	-14(3)
C(92)	98(5)	57(3)	49(3)	-7(2)	-10(3)	-12(3)
C(93)	62(3)	49(3)	38(2)	3(2)	-25(2)	1(3)
C(94)	76(4)	59(3)	62(3)	-7(2)	-15(3)	-10(3)
C(95)	94(5)	71(4)	76(4)	-3(3)	-28(4)	-27(4)
C(96)	61(4)	102(5)	72(4)	9(3)	-27(3)	-23(4)
C(97)	58(4)	99(5)	78(4)	-3(3)	-22(3)	15(4)
C(98)	58(4)	61(3)	66(3)	3(3)	-21(3)	2(3)
C(99)	61(4)	57(3)	75(3)	-6(2)	-24(3)	9(3)
C(100)	88(5)	58(3)	108(5)	-24(3)	-12(4)	25(3)
C(101)	92(5)	103(5)	98(5)	14(4)	-52(4)	22(4)
C(102)	56(4)	93(4)	106(5)	-15(3)	-26(3)	6(3)
C(103)	62(3)	53(3)	63(3)	-6(2)	-30(3)	3(3)
C(104)	113(5)	68(3)	63(3)	-21(3)	-34(3)	7(3)
C(105)	176(8)	87(4)	93(5)	-50(4)	-55(5)	50(5)

Table 4.11 continued

	U11	U22	U33	U23	U13	U12
C(106)	223(10)	52(4)	126(6)	-15(4)	-79(6)	27(5)
C(107)	144(6)	62(3)	86(4)	-4(3)	-39(4)	-3(4)
C(108)	90(4)	60(3)	81(4)	-2(3)	-34(3)	-17(3)
C(147)	215(17)	87(8)	60(7)	15(6)	-35(9)	-79(10)
L(148)	164(4)	100(2)	109(3)	-6(2)	-47(3)	-10(2)
L(149)	329(8)	145(4)	150(4)	33(3)	-142(5)	-121(5)
L(150)	239(6)	138(3)	124(3)	-4(3)	-45(4)	-82(4)
N(152)	135(5)	75(3)	109(4)	-8(3)	-54(4)	2(3)
C(153)	123(6)	79(5)	141(7)	-3(5)	-60(5)	1(4)
O(154)	169(5)	74(3)	118(4)	-1(3)	-71(4)	7(3)
C(155)	137(7)	218(9)	94(5)	39(6)	-53(5)	33(6)
C(156)	268(14)	177(10)	207(11)	-41(9)	-61(10)	-93(11)

Note L = Chloride atom

Table 4.12 : Hydrogen atomic co-ordinates (x 10^4) and isotropic temperature factors (x 10^3) for D/L-1-*O*-(*tert*-butyldiphenylsilyl)-2,3-*O*-cyclohexylidene *myo*-inositol (**58**) and solvents, DMF and chloroform with estimated standard deviations in parentheses

	x	y	z	U(iso)
H(68)	2970(38)	2841(21)	3311(18)	34(10)
H(69)	1282(45)	3288(24)	2759(20)	49(13)
H(70)	318(53)	3842(27)	3767(24)	77(15)
H(71)	2493(39)	5050(21)	3424(18)	31(10)
H(72)	2831(37)	3600(21)	4194(17)	31(10)
H(73)	4448(45)	4300(25)	2911(21)	56(13)
H(10)	690(62)	5200(33)	4303(27)	92(20)
H(11)	3484(86)	4531(45)	4703(41)	184(32)
H(12)	5850(73)	3551(38)	3664(33)	129(27)
H(39)	3904(6)	750(3)	1519(2)	83(7)
H(40)	2413(7)	440(3)	855(3)	83(7)
H(41)	786(7)	1372(4)	530(3)	83(7)
H(42)	630(6)	2591(3)	909(2)	83(7)
H(43)	2135(5)	2902(3)	1580(2)	83(7)
H(44)	5293(6)	1883(3)	3511(3)	102(9)
H(45)	4865(8)	956(4)	4514(3)	102(9)
H(46)	3440(9)	-154(4)	4613(3)	102(9)
H(47)	2432(10)	-339(4)	3711(4)	102(9)
H(48)	2780(8)	587(3)	2736(3)	102(9)
H(49)	5665(35)	2649(30)	757(23)	148(8)
H(50)	7504(21)	2814(29)	708(22)	148(8)
H(51)	6216(46)	3381(15)	1185(26)	148(8)
H(52)	6262(44)	1170(29)	1138(18)	148(8)
H(53)	6701(49)	902(23)	1951(15)	148(8)
H(54)	7965(13)	1426(32)	1256(21)	148(8)
H(55)	7007(50)	3000(13)	2282(22)	148(8)
H(56)	8389(25)	2495(26)	1798(22)	148(8)
H(57)	7349(53)	1984(21)	2575(14)	148(8)
H(58)	569(6)	5962(3)	2000(3)	78(5)
H(59)	2157(6)	5773(3)	2054(3)	78(5)
H(60)	2624(7)	5340(3)	1006(3)	78(5)

Table 4.12 continued

	x	y	z	U(iso)
H(61)	1989(7)	6207(3)	910(3)	78(5)
H(62)	-242(8)	5676(3)	898(3)	78(5)
H(63)	917(8)	5350(3)	337(3)	78(5)
H(64)	977(7)	4136(3)	1055(3)	78(5)
H(65)	-620(7)	4303(3)	1005(3)	78(5)
H(66)	-419(6)	3854(3)	2147(3)	78(5)
H(67)	-1128(6)	4701(3)	2064(3)	78(5)
H(141)	2202(40)	3558(21)	7546(18)	37(10)
H(142)	922(43)	2515(22)	7569(20)	41(12)
H(143)	-189(40)	3263(20)	6836(17)	28(10)
H(144)	2060(38)	3185(20)	5744(17)	27(9)
H(145)	1716(44)	4429(23)	6417(19)	44(12)
H(146)	4014(44)	3268(24)	6280(20)	58(12)
H(83)	743(56)	4121(29)	5238(25)	73(18)
H(84)	2969(59)	5068(32)	5563(26)	84(20)
H(85)	4747(50)	4533(26)	6385(23)	56(15)
H(112)	4341(6)	4209(3)	7931(2)	69(6)
H(113)	4456(6)	5336(3)	8423(3)	69(6)
H(114)	3993(6)	5225(3)	9605(3)	69(6)
H(115)	3409(6)	3989(3)	10279(2)	69(6)
H(116)	3223(6)	2878(3)	9789(2)	69(6)
H(117)	2488(6)	814(3)	8732(2)	84(8)
H(118)	319(8)	193(4)	9243(3)	84(8)
H(119)	-1604(7)	915(4)	9643(3)	84(8)
H(120)	-1379(7)	2299(4)	9559(3)	84(8)
H(121)	804(6)	2926(3)	9070(2)	84(8)
H(122)	4536(29)	776(19)	8176(20)	121(7)
H(123)	6406(19)	935(23)	7922(21)	121(7)
H(124)	5264(40)	1468(25)	7430(9)	121(7)
H(125)	4388(26)	1083(19)	9406(21)	121(7)
H(126)	5394(40)	1938(18)	9439(20)	121(7)
H(127)	6269(24)	1098(20)	9135(24)	121(7)
H(128)	6660(47)	2881(17)	8461(17)	121(7)
H(129)	6527(49)	2719(21)	7635(8)	121(7)

Table 4.12 continued

	x	y	z	U(iso)
H(130)	7560(30)	2072(23)	8113(20)	121(7)
H(131)	2226(7)	1650(3)	5719(3)	107(6)
H(132)	872(7)	1083(3)	5854(3)	107(6)
H(133)	3335(9)	705(4)	6402(3)	107(6)
H(134)	2888(9)	289(4)	5835(3)	107(6)
H(135)	879(9)	-309(3)	6626(4)	107(6)
H(136)	2250(9)	-543(3)	6923(4)	107(6)
H(137)	1793(8)	426(3)	7618(3)	107(6)
H(138)	429(8)	-133(3)	7760(3)	107(6)
H(139)	-188(6)	1237(3)	7655(3)	107(6)
H(140)	-704(6)	821(3)	7106(3)	107(6)
H(151)	10917(19)	1568(7)	4002(6)	100
H(157)	7619(8)	3875(4)	5267(4)	326(27)
H(158)	5936(63)	2294(56)	6431(49)	326(27)
H(159)	7025(108)	3172(21)	6151(58)	326(27)
H(160)	7813(69)	2215(53)	6203(57)	326(27)
H(161)	5521(110)	2033(65)	5657(26)	326(27)
H(162)	6693(50)	2306(75)	4851(44)	326(27)
H(163)	4831(83)	2237(75)	4903(49)	326(27)

Figure 4.7 : ORTEPII drawing [Johnson, 1976] of molecule one of D/L-1-*O*-(*tert*-butyldiphenylsilyl)-2,3-*O*-cyclohexylidene *myo*-inositol (**58**) with the $CHCl_3$ site and the molecule of DMF, showing the labelling scheme for non-H atoms (L = Cl). Thermal ellipsoids are drawn at the 50% probability level.

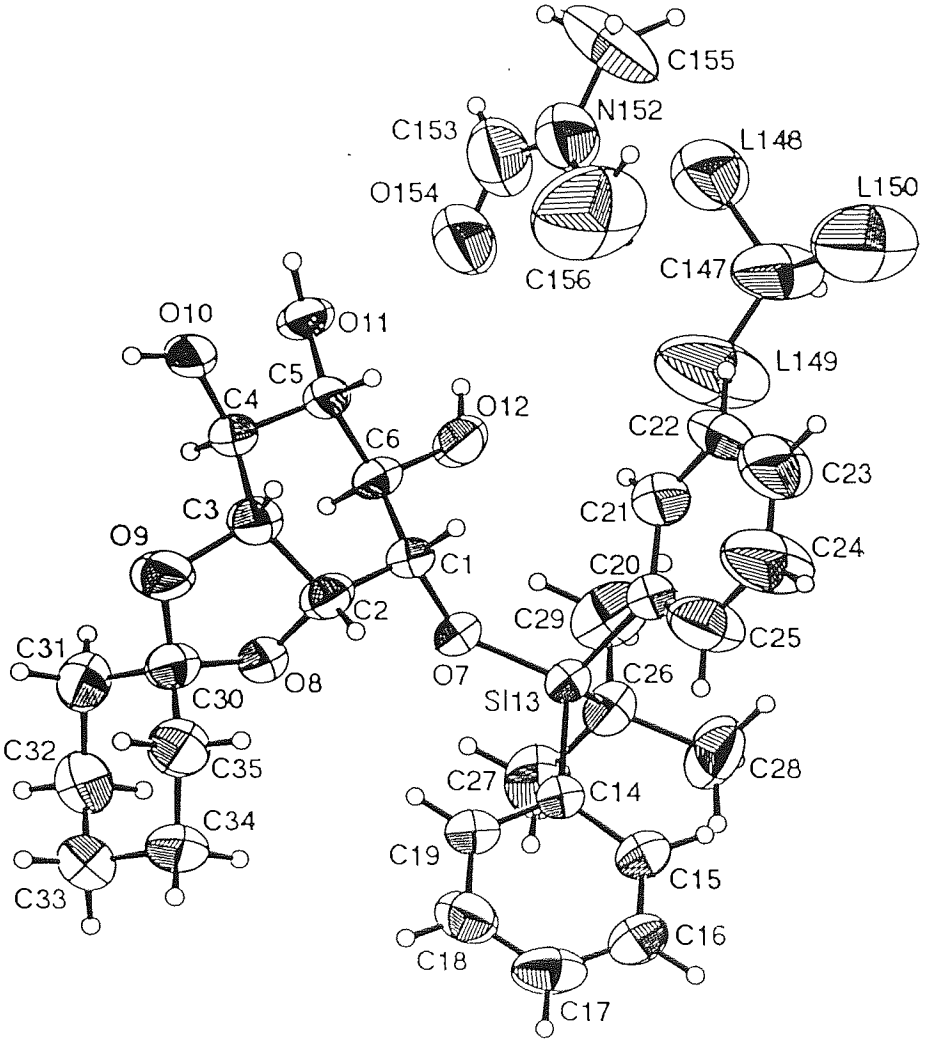

Figure 4.8 : ORTEPII drawing [Johnson, 1976] of molecule two of D/L-1-*O*-(*tert*-butyldiphenylsilyl)-2,3-*O*-cyclohexylidene *myo*-inositol (**58**) with the $CHCl_3$ site showing the labelling scheme for non-H atoms (L = Cl). Thermal ellipsoids are drawn at the 50% probability level.

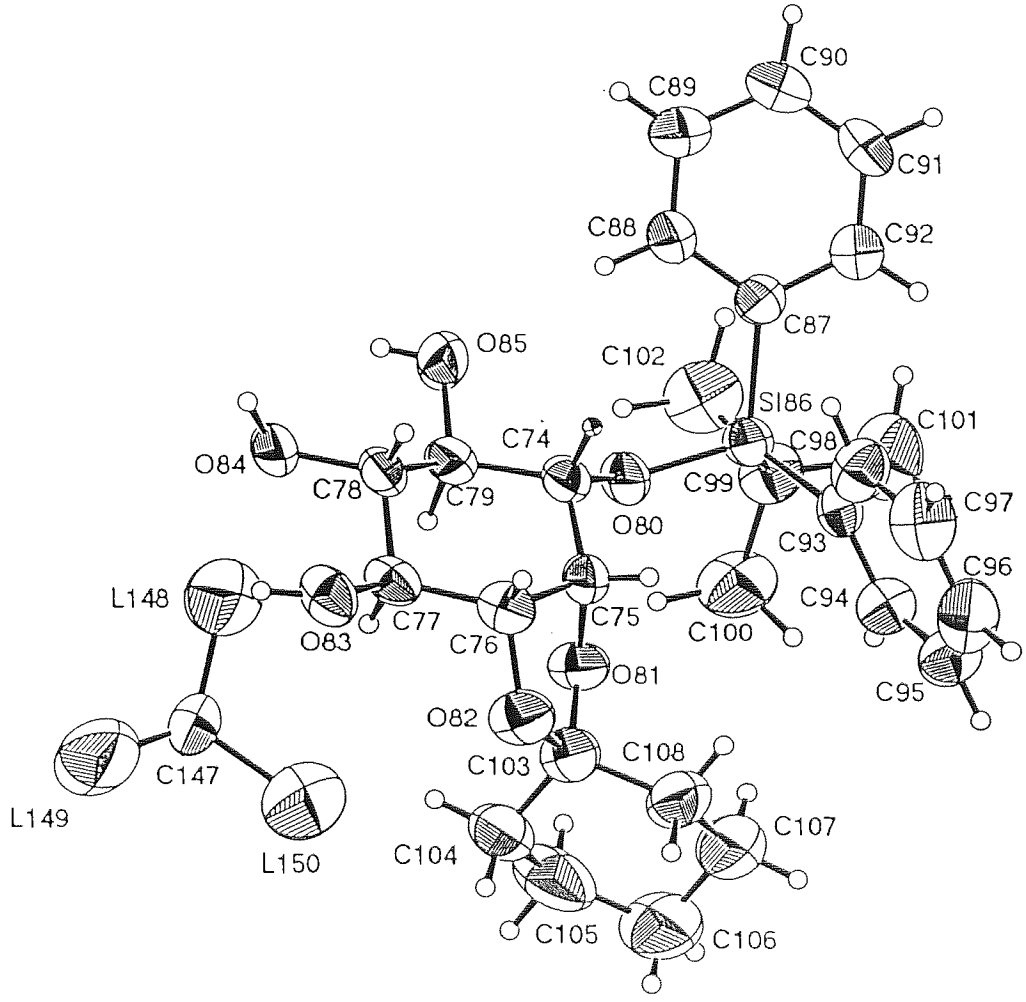

Figure 4.9 : Conformational differences in molecules one and two of D/L-1-*O*-(*tert*-butyldiphenylsilyl)-2,3-*O*-cyclohexylidene *myo*-inositol (**58**)

(a) Molecules one and two are enantiomers

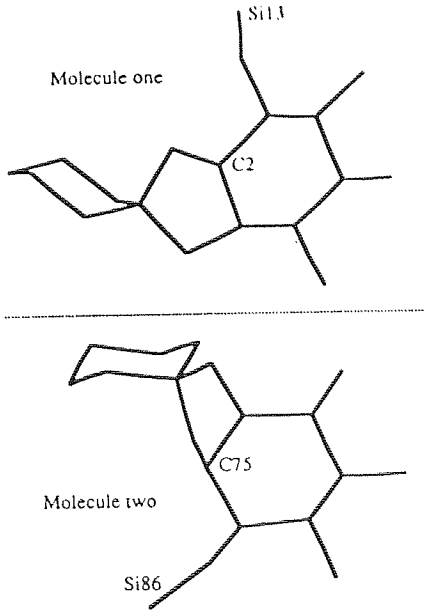

(b) Molecule one has a half chair five membered ring whereas molecule two has an envelope five membered ring

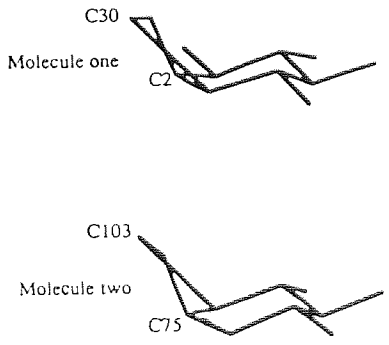

(c) Molecule one has a twisted inositol ring whereas molecule two has a flattened and puckered inositol ring

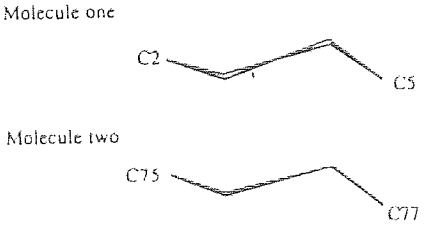

Table 4.13 : Asymmetry parameters for inositol rings of D/L-1-*O*-(*tert*-butyl-diphenylsilyl)-2,3-*O*-cyclohexylidene *myo*-inositol

Molecule 1		Molecule 2	
$\Delta C_s(1)$ =20.18	$\Delta C_2(1\text{-}2)$ =20.31	$\Delta C_s(74)$ =17.33	$\Delta C_2(74\text{-}75)$ =14.27
$\Delta C_s(2)$ = 8.53	$\Delta C_2(2\text{-}3)$ = 2.28	$\Delta C_s(75)$ = 2.85	$\Delta C_2(75\text{-}76)$ = 8.26
$\Delta C_s(3)$ =11.65	$\Delta C_2(3\text{-}4)$ =22.50	$\Delta C_s(76)$ =14.51	$\Delta C_2(76\text{-}77)$ =22.50

ΔC_s = Mirror related asymmetry parameter

ΔC_2 = Two fold related asymmetry parameter

Table 4.14 : Distances of C atoms from least squares plane for D/L-1-*O*-(*tert*-butyldiphenylsilyl)-2,3-*O*-cyclohexylidene *myo*-inositol (SHELXL-93 [Sheldrick, 1993]).

For molecule 1

Atom	Distance
C01	0.190(4) Å
C02	0.110(4) Å
C03	0.116(4) Å
C04	0.206(4) Å
C05	0.298(4) Å
C06	0.287(3) Å

Least squares plane

2.23(2)x - 11.20(3)y + 10.71(4)z = 1.42(2)

Rms deviation of fitted atoms = 0.214

For molecule 2

Atom	Distance
C74	0.161(3) Å
C75	0.106(3) Å
C76	0.139(3) Å
C77	0.232(3) Å
C78	0.297(3) Å
C79	0.259(3) Å

Least squares plane

-4.26(2)x + 12.32(2)y + 10.33(3)z = 10.16(2)

Rms deviation of fitted atoms = 0.211

The bond distances and angles for the silyl substituents are consistent values for both the molecules. The silicon atom Si13 is positioned at similar torsional angles (anticlinal, Appendix 1) from the neighbouring ring atoms C02 and C06 in molecule one, but silicon atom Si86 in molecule two is orientated towards C75 (ie. towards the cyclohexylidene group). The *t*-butyl groups are found to sit closest to their inositol oxygen in both molecules, with the phenyl groups positioned furthest away but closest to one another. In molecule one, the *t*-butyl group is unexpectedly positioned anticlinal to the C01-O07 bond, which places one phenyl group closer and one phenyl group further from the C01-O07 bond than expected. In molecule two, the *t*-butyl group is in the more anticipated *trans* position with the phenyl groups *gauche* to the C74-O80 bond. This allows the bulkier *t*-butyl group to sit furthest from the inositol C-O bond. The *t*-butyl groups of both molecules have one carbon *trans* and two carbons *gauche* to the O-Si bond (Appendix 1). In contrast, the phenyl groups have more flexible orientations to the O-Si bond with the phenyl planes varying in orientation from *trans* to *gauche*.

The three OH groups of both inositol molecules are involved in donating hydrogen bonds (Table 4.15, the values are in good agreement with surveyed data [Steiner & Saenger, 1992]). Two OH groups in each molecule also accept hydrogen bonds (OH

Table 4.15 : Hydrogen bond distances (Å) and hydrogen bond angles (°) for D/L-1-*O*-(*tert*-butyldiphenylsilyl)-2,3-*O*-cyclohexylidene *myo*-inositol with estimated standard deviations in parentheses

	$d_{O\cdots O}$ (Å)	$d_{O\text{-}H\cdots O}$ (Å)	$\alpha_{O\text{-}H\cdots O}$ (°)	Symmetry acceptor [a]
O10-H10...O83	2.707(5)	1.88(6)	170(5)	(-X, 1-Y, 1-Z)
O11-H11...O84	2.767(4)	1.73(8)	156(7)	(X, Y, Z)
O12-H12...O154	3.082(6)	2.24(6)	170(6)	(X, Y, Z)
O83-H83...O10	2.788(5)	1.97(5)	171(5)	(X, Y, Z)
O84-H84...O154	2.696(5)	1.90(5)	172(6)	(1-X, 1-Y, 1-Z)
O85-H85...O11	2.763(5)	2.01(5)	157(4)	(1-X, 1-Y, 1-Z)

[a]Symmetry transformation to be applied to acceptor atom

groups at positions C04/C77 and C05/C78). Oxygens O10 and O83 (OH groups at position C04/C77 in the two triol molecules) are involved in homodromic hydrogen bonding [Jeffrey & Saenger, 1991] with symmetry related molecules forming a tetramer about the centre of symmetry at 0, 0.5, 0.5. A hydrogen bonding tetramer also exists in the crystal structure of *myo*-inositol dihydrate [Lomer *et al.*, 1963] involving hydroxy groups of symmetry related inositols and the two water molecules.

The DMF and chloroform molecules have appropriate bond lengths and angles. The carbonyl oxygen of DMF accepts two hydrogen bonds. The carbonyl group is almost coplanar with the methyl groups [C155-N152-C153-O154 = 173.0(8)]. The chloroform molecule is tetrahedral.

4.2.3 Crystal structure of D/L-1-*O*-(*tert*-butyldiphenylsilyl)-2,3-*O*-cyclohexylidene-4,5,6-tri-*O*-benzoyl *myo*-inositol (59)

4.2.3.1 Experimental

D/L-1-*O*-(*tert*-Butyldiphenylsilyl)-2,3-*O*-cyclohexylidene-4,5,6-tri-*O*-benzoyl *myo*-inositol (**59**) slowly crystallised in diethyl ether and hexane to form colourless rectangular plate crystals. A single crystal (0.40 x 0.25 x 0.05 mm) was chosen for X-ray determination. The data were collected from an Enraf-Nonius CAD4 diffractometer with monochromated graphite Mo-Kα radiation, λ = 0.71069Å at 293 K.

4.2.3.2 Crystal data

D/L-1-*O*-(*tert*-Butyldiphenylsilyl)-2,3-*O*-cyclohexylidene-4,5,6-tri-*O*-benzoyl *myo*-inositol (**59**) ($C_{49}H_{50}O_9Si$) crystallises in the monoclinic space group Pn with a = 14.358(4), b = 11.448(5), c = 14.603(6)Å, α = 90, β = 111.60(2), γ = 90°, Z = 2 and V = 2231.7(15)Å^3. The formula weight is 810.98 (F(000) = 860) and the calculated density D_X = 1.207 Mg m^{-3}. The absorption coefficient μ = 0.107 mm^{-1}.

4.2.3.3 Data collection

Unit cell dimensions were obtained from least squares analysis of setting angles of 25 accurately centred reflections, $8.47 \leq \theta \leq 12.51°$. Intensity data were collected by the ω-2θ scan technique, Bragg angle $2.33 \leq \theta \leq 24.97°$. The ω scan angle was calculated from $[M+N(\tan\theta)]°$, where $M = 0.9$, $N = 0.35$ and increased by 25% on each side for background determination. The ω scan speed was varied from 0.5 to 1.8°min^{-1} depending upon intensity. Six different standard reflections were used during data collection: three intensity reflections (measured every three hours) and three orientation reflections (monitored every 200 reflections). No appreciable loss of intensity or crystal movement was detected during collection. The 5767 reflections were measured for $-17 \leq h \leq 17$, $-1 \leq k \leq 13$, $-17 \leq l \leq 17$ and merged to give 4994 independent reflections ($R_{int} = 0.0423$).

4.2.3.4 Structural determination and refinement

Lorentz, polarisation and intensity corrections (4.5% decay) were applied to the collected data. The space group was determined unambiguously as a result of structure analysis. An initial structure was solved by direct methods using MULTAN-84 [Main *et al.*, 1984] with default options. Normalised structure factors were calculated and phases were determined, from F_{obs} values. The distribution of intensities was found to closely follow the theoretical values for an acentric structure. The phase set with the best combined figure of merit gave an E-map from which a preliminary structure was determined. Using the atomic positions determined from the E-map, the remaining non-hydrogen atoms were located in an electron density map using SHELXL-93 [Sheldrick, 1993].

Full-matrix least-squares refinement of atomic positions and anisotropic temperature factors (for non-hydrogen atoms) on $Fobs^2$ was performed using SHELXL-93 .

From difference electron density maps, hydrogen positions were found for the inositol ring. The other hydrogen atoms were assumed to ride on attached atoms and were

placed in calculated positions, their common temperature factors were set as free variables in chemical groups of similar kind. Further refinement of the structure, which included parameters for atomic co-ordinates, temperature factors (anisotropic for non-hydrogen atoms and isotropic for hydrogen atoms), overall scale factor and an extinction parameter, were carried out. In the weighting scheme $1/[\sigma^2(Fo^2)+(0.1000P)^2+0.0000P]$ where $P=(Fo^2+2Fc^2)/3$, the parameters converged at discrepancy indices R = 0.0475 and Rw = 0.1171 for 2440 observed reflections [$Fo > 4\sigma(Fo)$]. The absolute structure factor was 0.21(29) [Flack, 1983]. The final maximum shift / e.s.d. ratio was 0.006, and the maximum and minimum features on a difference Fourier map were 0.157 and -0.195 e $Å^{-3}$.

4.2.3.5 Results and discussion

Full structural data for the crystal structure of D/L-1-*O*-(*tert*-butyldiphenylsilyl)-2,3-*O*-cyclohexylidene-4,5,6-tri-*O*-benzoyl *myo*-inositol are given in Tables 4.16 (non-hydrogen atomic co-ordinates), 4.17 (bond lengths and angles), 4.18 (anisotropic displacement parameters) and 4.19 (hydrogen atomic co-ordinates and their isotropic temperature factors), and torsional angles are in Appendix 1.

The inositol ring is in a distorted chair conformation with the oxygen at C02 (Figure 4.10) in the expected axial position and the other five oxygen atoms in equatorial positions. All the C-C and C-O bond lengths (Table 4.17) were comparable with those of *myo*-inositol [Rabinowitz & Kraut, 1964]. However, the inositol ring angles (Table 4.17) deviate from expected values (*myo*-inositol has a mean angle of 110.7° [Rabinowitz & Kraut, 1964] and the perfect chair has angles of 111° [Bucourt, 1974]) at positions C02 and C05. The torsion angle O08-C02-C03-O07 = 39.0(7)°, which would normally be closer to 60°, show that the inositol oxygen atoms at the *cis* ring junction have moved closer together to accommodate the acetal linkage which was also seen in the crystal structures of diol **3** and triol **58**. The *cis* junction has expected endocyclic torsion angles which have the same sign and have a similar value [C01-C02-C03-C04 = 43.3(10) and O08-C02-C03-O07 = 39.0(7)°]. The asymmetry parameters of

Table 4.16 : Atomic co-ordinates of non-hydrogen atoms (x 10^4) and equivalent isotropic temperature factors (x 10^3) for D/L-1-*O*-(*tert*-butyldiphenylsilyl)-2,3-*O*-cyclohexylidene-4,5,6-tri-*O*-benzoyl *myo*-inositol (**59**)

	x	y	z	U(eq)
C(01)	1309(5)	2848(7)	10198(6)	52(2)
C(02)	373(5)	3610(7)	9868(6)	51(2)
C(03)	-620(5)	2967(8)	9640(6)	50(2)
C(04)	-551(6)	2032(7)	10412(6)	50(2)
C(05)	333(6)	1231(7)	10556(6)	48(2)
C(06)	1291(6)	1954(7)	10955(6)	50(2)
O(07)	-1274(3)	3887(5)	9695(4)	60(2)
O(08)	357(4)	4393(5)	10615(4)	57(1)
O(09)	2187(3)	3541(5)	10594(3)	51(1)
O(10)	2103(3)	1157(5)	11104(3)	50(1)
O(11)	361(4)	356(5)	11268(4)	54(1)
O(12)	-1455(4)	1336(5)	10039(4)	57(2)
Si(13)	2984(1)	3892(2)	10057(2)	51(1)
C(14)	2765(6)	997(9)	12005(6)	63(2)
O(15)	2795(5)	1536(7)	12715(5)	98(2)
C(16)	3504(5)	51(9)	12030(6)	59(2)
C(17)	3279(6)	-780(8)	11332(7)	63(2)
C(18)	3946(7)	-1678(9)	11374(8)	81(3)
C(19)	4867(8)	-1668(11)	12138(10)	100(4)
C(20)	5132(7)	-821(11)	12846(9)	89(3)
C(21)	4423(6)	57(10)	12815(7)	82(3)
C(22)	562(5)	-744(8)	11058(7)	54(2)
O(23)	633(4)	-1022(5)	10294(4)	71(2)
C(24)	710(5)	-1569(8)	11888(6)	54(2)
C(25)	224(6)	-1406(7)	12553(6)	67(2)
C(26)	366(8)	-2178(10)	13299(8)	85(3)
C(27)	1006(9)	-3099(11)	13409(8)	95(3)
C(28)	1492(8)	-3256(10)	12766(10)	100(4)
C(29)	1318(6)	-2487(8)	12002(8)	73(3)
C(30)	-1995(6)	1279(9)	10613(7)	64(2)
O(31)	-1822(5)	1779(8)	11354(6)	110(3)
C(32)	-2850(6)	477(10)	10179(7)	73(3)

Table 4.16 continued

	x	y	z	U(eq)
C(33)	-3612(7)	464(11)	10579(8)	89(3)
C(34)	-4384(8)	-282(16)	10226(11)	116(5)
C(35)	-4472(8)	-1036(13)	9468(13)	118(5)
C(36)	-3752(8)	-1067(10)	9056(10)	111(4)
C(37)	-2926(6)	-299(9)	9432(8)	81(3)
C(38)	-652(6)	4796(7)	10328(6)	55(2)
C(39)	-916(6)	4934(9)	11233(6)	71(3)
C(40)	-1982(8)	5336(10)	10958(8)	92(3)
C(41)	-2164(9)	6461(10)	10382(9)	105(4)
C(42)	-1906(8)	6332(9)	9478(8)	95(3)
C(43)	-827(6)	5916(8)	9744(7)	69(2)
C(44)	2614(6)	5330(8)	9409(6)	60(2)
C(45)	1923(6)	6048(8)	9613(6)	63(2)
C(46)	1675(8)	7141(9)	9189(8)	80(3)
C(47)	2091(9)	7537(9)	8558(8)	85(3)
C(48)	2780(8)	6859(11)	8336(7)	84(3)
C(49)	3044(7)	5751(9)	8763(6)	77(3)
C(50)	4238(6)	4078(9)	11089(6)	69(2)
C(51)	4112(10)	4975(12)	11800(8)	136(5)
C(52)	5019(8)	4473(18)	10729(10)	191(9)
C(53)	4574(9)	2961(10)	11689(10)	151(7)
C(54)	2940(6)	2712(8)	9147(6)	56(2)
C(55)	3207(6)	1551(8)	9483(7)	64(2)
C(56)	3158(6)	646(10)	8863(8)	79(3)
C(57)	2821(7)	842(11)	7898(8)	79(3)
C(58)	2522(7)	1933(11)	7513(7)	81(3)
C(59)	2576(6)	2853(9)	8143(7)	69(2)

Table 4.17 : Bond lengths (Å) and bond angles (°) for D/L-1-*O*-(*tert*-butyldiphenylsilyl)-2,3-*O*-cyclohexylidene-4,5,6-tri-*O*-benzoyl *myo*-inositol (**59**) with estimated standard deviations in parentheses

Bond	Distance (Å)	Bond	Distance (Å)
C(01)-C(06)	1.514(10)	C(25)-C(26)	1.358(12)
C(01)-O(09)	1.420(9)	C(26)-C(27)	1.369(14)
C(02)-C(01)	1.523(10)	C(27)-C(28)	1.371(14)
C(02)-O(08)	1.419(9)	C(28)-C(29)	1.371(13)
C(03)-C(02)	1.528(11)	C(30)-O(31)	1.168(10)
C(03)-C(04)	1.531(11)	C(30)-C(32)	1.477(13)
C(03)-O(07)	1.433(9)	C(32)-C(37)	1.379(13)
C(04)-O(12)	1.447(9)	C(32)-C(33)	1.417(12)
C(05)-C(04)	1.517(11)	C(33)-C(34)	1.34(2)
C(05)-O(11)	1.433(9)	C(34)-C(35)	1.37(2)
C(06)-C(05)	1.525(11)	C(35)-C(36)	1.37(2)
C(06)-O(10)	1.432(9)	C(36)-C(37)	1.415(14)
O(07)-C(38)	1.459(9)	C(38)-C(43)	1.508(11)
O(08)-C(38)	1.428(9)	C(38)-C(39)	1.511(11)
O(09)-Si(13)	1.658(5)	C(39)-C(40)	1.505(12)
O(10)-C(14)	1.322(9)	C(40)-C(41)	1.507(14)
O(11)-C(22)	1.352(9)	C(41)-C(42)	1.504(14)
O(12)-C(30)	1.336(9)	C(42)-C(43)	1.528(13)
Si(13)-C(44)	1.875(9)	C(44)-C(49)	1.391(11)
Si(13)-C(54)	1.880(9)	C(44)-C(45)	1.402(11)
Si(13)-C(50)	1.887(8)	C(45)-C(46)	1.382(13)
C(14)-O(15)	1.193(10)	C(46)-C(47)	1.347(13)
C(14)-C(16)	1.508(12)	C(47)-C(48)	1.39(2)
C(16)-C(17)	1.343(11)	C(48)-C(49)	1.402(14)
C(16)-C(21)	1.394(11)	C(50)-C(52)	1.474(14)
C(17)-C(18)	1.391(12)	C(50)-C(51)	1.517(14)
C(18)-C(19)	1.381(14)	C(50)-C(53)	1.525(13)
C(19)-C(20)	1.37(2)	C(54)-C(59)	1.373(12)
C(20)-C(21)	1.419(14)	C(54)-C(55)	1.420(12)
C(22)-O(23)	1.200(9)	C(55)-C(56)	1.360(12)
C(22)-C(24)	1.489(11)	C(56)-C(57)	1.330(13)
C(24)-C(29)	1.338(11)	C(57)-C(58)	1.372(14)
C(24)-C(25)	1.401(12)	C(58)-C(59)	1.381(13)

Table 4.17 continued

Bonds	Angles (°)	Bonds	Angles (°)
O(07)-C(03)-C(04)	109.8(6)	C(16)-C(17)-C(18)	121.4(9)
O(07)-C(03)-C(02)	102.3(6)	C(19)-C(18)-C(17)	117.9(11)
C(04)-C(03)-C(02)	112.0(7)	C(20)-C(19)-C(18)	122.3(11)
O(08)-C(02)-C(01)	112.4(6)	C(19)-C(20)-C(21)	118.8(10)
O(08)-C(02)-C(03)	101.1(6)	C(16)-C(21)-C(20)	118.3(11)
C(01)-C(02)-C(03)	115.9(7)	O(23)-C(22)-O(11)	123.7(8)
O(09)-C(01)-C(06)	109.4(6)	O(23)-C(22)-C(24)	123.7(8)
O(09)-C(01)-C(02)	110.8(7)	O(11)-C(22)-C(24)	112.6(8)
C(06)-C(01)-C(02)	111.6(7)	C(29)-C(24)-C(25)	119.2(8)
O(10)-C(06)-C(01)	108.1(6)	C(29)-C(24)-C(22)	119.3(8)
O(10)-C(06)-C(05)	106.4(6)	C(25)-C(24)-C(22)	121.5(8)
C(01)-C(06)-C(05)	110.1(6)	C(26)-C(25)-C(24)	120.2(9)
O(11)-C(05)-C(04)	108.8(6)	C(25)-C(26)-C(27)	119.4(10)
O(11)-C(05)-C(06)	108.7(6)	C(26)-C(27)-C(28)	120.6(10)
C(04)-C(05)-C(06)	108.4(7)	C(27)-C(28)-C(29)	119.2(10)
O(12)-C(04)-C(05)	108.0(6)	C(24)-C(29)-C(28)	121.3(9)
O(12)-C(04)-C(03)	107.6(6)	O(31)-C(30)-O(12)	125.6(8)
C(05)-C(04)-C(03)	110.4(6)	O(31)-C(30)-C(32)	124.2(8)
C(03)-O(07)-C(38)	107.4(5)	O(12)-C(30)-C(32)	110.1(8)
C(02)-O(08)-C(38)	106.3(5)	C(37)-C(32)-C(33)	118.1(10)
C(01)-O(09)-Si(13)	127.4(5)	C(37)-C(32)-C(30)	123.4(8)
C(14)-O(10)-C(06)	119.1(6)	C(33)-C(32)-C(30)	118.4(10)
C(22)-O(11)-C(05)	116.0(6)	C(34)-C(33)-C(32)	120.1(12)
C(30)-O(12)-C(04)	116.0(7)	C(33)-C(34)-C(35)	121.8(12)
O(09)-Si(13)-C(44)	109.5(3)	C(34)-C(35)-C(36)	120.6(12)
O(09)-Si(13)-C(54)	108.1(3)	C(35)-C(36)-C(37)	118.1(13)
C(44)-Si(13)-C(54)	110.2(4)	C(32)-C(37)-C(36)	121.2(10)
O(09)-Si(13)-C(50)	105.7(3)	O(08)-C(38)-O(07)	105.9(6)
C(44)-Si(13)-C(50)	108.3(4)	O(08)-C(38)-C(43)	112.4(7)
C(54)-Si(13)-C(50)	114.8(4)	O(07)-C(38)-C(43)	108.2(6)
O(15)-C(14)-O(10)	125.1(8)	O(08)-C(38)-C(39)	109.3(6)
O(15)-C(14)-C(16)	123.5(8)	O(07)-C(38)-C(39)	109.7(7)
O(10)-C(14)-C(16)	111.4(8)	C(43)-C(38)-C(39)	111.2(7)
C(17)-C(16)-C(21)	121.2(9)	C(40)-C(39)-C(38)	110.9(7)
C(17)-C(16)-C(14)	121.4(7)	C(39)-C(40)-C(41)	111.1(9)
C(21)-C(16)-C(14)	117.4(9)	C(42)-C(41)-C(40)	111.0(9)

Table 4.17 continued

Bonds	Angles (°)	Bonds	Angles (°)
C(41)-C(42)-C(43)	111.2(9)	C(51)-C(50)-C(53)	105.5(9)
C(38)-C(43)-C(42)	110.6(7)	C(52)-C(50)-Si(13)	112.1(7)
C(49)-C(44)-C(45)	117.8(9)	C(51)-C(50)-Si(13)	107.7(7)
C(49)-C(44)-Si(13)	122.1(7)	C(53)-C(50)-Si(13)	111.8(7)
C(45)-C(44)-Si(13)	120.0(7)	C(59)-C(54)-C(55)	115.3(9)
C(46)-C(45)-C(44)	121.4(9)	C(59)-C(54)-Si(13)	124.8(8)
C(47)-C(46)-C(45)	120.3(10)	C(55)-C(54)-Si(13)	119.7(7)
C(46)-C(47)-C(48)	120.4(10)	C(56)-C(55)-C(54)	122.8(9)
C(47)-C(48)-C(49)	120.1(10)	C(57)-C(56)-C(55)	119.1(10)
C(44)-C(49)-C(48)	120.0(10)	C(56)-C(57)-C(58)	121.6(10)
C(52)-C(50)-C(51)	109.5(11)	C(57)-C(58)-C(59)	119.3(9)
C(52)-C(50)-C(53)	110.0(11)	C(54)-C(59)-C(58)	121.9(10)

Table 4.18 : Anisotropic displacement parameters (x 10^3, for non-hydrogen atoms) for D/L-1-*O*-(*tert*-butyldiphenylsilyl)-2,3-*O*-cyclohexylidene-4,5,6-tri-*O*-benzoyl *myo*-inositol (**59**) with estimated standard deviations in parentheses

	U11	U22	U33	U23	U13	U12
C(01)	50(4)	54(5)	48(4)	11(5)	15(4)	0(5)
C(02)	59(5)	49(6)	49(5)	3(5)	25(4)	8(4)
C(03)	53(5)	52(6)	45(5)	-4(5)	19(4)	-1(4)
C(04)	58(5)	48(5)	54(5)	-8(5)	31(4)	-3(4)
C(05)	58(5)	42(5)	49(5)	1(5)	24(4)	2(4)
C(06)	59(5)	46(5)	52(5)	4(5)	28(4)	9(4)
O(07)	53(3)	59(4)	69(3)	-2(3)	24(3)	13(3)
O(08)	56(3)	50(3)	61(3)	-10(3)	16(3)	9(3)
O(09)	54(3)	50(3)	53(3)	-2(3)	23(2)	-9(3)
O(10)	49(3)	52(3)	46(3)	4(3)	15(2)	12(3)
O(11)	64(3)	42(4)	66(3)	9(3)	35(3)	6(3)
O(12)	51(3)	63(4)	66(3)	-1(3)	33(3)	-1(3)
Si(13)	49(1)	51(1)	56(1)	4(1)	21(1)	-2(1)
C(14)	69(5)	68(6)	49(5)	3(5)	19(5)	1(5)
O(15)	104(5)	115(6)	55(4)	-4(5)	5(4)	33(5)
C(16)	45(4)	73(6)	53(5)	24(5)	12(4)	12(5)
C(17)	53(5)	57(6)	81(6)	7(6)	26(5)	4(5)
C(18)	74(6)	62(6)	119(8)	26(7)	49(6)	10(6)
C(19)	69(7)	98(9)	141(10)	43(9)	50(7)	17(7)
C(20)	64(6)	99(9)	98(7)	48(8)	21(6)	12(7)
C(21)	67(6)	92(8)	80(6)	36(7)	17(5)	2(6)
C(22)	47(4)	52(6)	63(6)	-2(5)	20(4)	1(4)
O(23)	103(5)	54(4)	68(4)	-4(4)	43(3)	8(3)
C(24)	50(4)	52(5)	53(5)	5(5)	11(4)	-5(4)
C(25)	80(6)	42(5)	77(6)	13(5)	27(5)	2(5)
C(26)	103(8)	79(7)	74(6)	9(7)	35(6)	-7(7)
C(27)	110(8)	82(9)	83(7)	38(7)	23(7)	-5(7)
C(28)	86(7)	67(7)	148(11)	32(9)	42(8)	13(6)
C(29)	69(5)	56(6)	103(7)	23(6)	42(5)	20(5)
C(30)	59(5)	77(7)	67(6)	-5(6)	37(5)	-7(5)
O(31)	115(5)	154(8)	93(5)	-35(6)	75(4)	-23(5)
C(32)	51(5)	88(7)	79(6)	18(6)	24(5)	7(5)

Table 4.18 continued

	U11	U22	U33	U23	U13	U12
C(33)	60(6)	120(9)	93(7)	39(7)	35(5)	2(7)
C(34)	64(8)	162(15)	129(11)	66(11)	42(8)	5(9)
C(35)	59(7)	116(12)	169(13)	58(11)	30(9)	-21(7)
C(36)	75(7)	83(8)	153(11)	17(9)	16(8)	3(7)
C(37)	53(5)	73(7)	107(8)	9(7)	18(5)	-6(5)
C(38)	60(5)	45(5)	61(5)	0(5)	22(4)	-1(4)
C(39)	76(6)	72(6)	75(6)	-1(6)	37(5)	21(5)
C(40)	95(7)	100(9)	99(7)	8(8)	56(6)	27(7)
C(41)	113(8)	85(8)	126(9)	0(8)	55(8)	44(7)
C(42)	114(8)	67(7)	107(8)	14(7)	45(7)	33(6)
C(43)	82(6)	51(6)	81(6)	9(5)	39(5)	12(5)
C(44)	64(5)	57(6)	55(5)	3(5)	16(4)	-7(5)
C(45)	70(5)	57(6)	60(5)	-3(5)	21(4)	5(5)
C(46)	93(7)	53(7)	82(7)	4(6)	20(6)	-1(6)
C(47)	102(8)	54(7)	77(7)	-3(6)	8(6)	-9(6)
C(48)	98(7)	84(8)	64(6)	18(6)	20(6)	-41(7)
C(49)	81(6)	83(8)	73(6)	7(6)	34(5)	-22(6)
C(50)	57(5)	75(7)	64(5)	2(6)	11(4)	-14(5)
C(51)	147(11)	125(11)	78(7)	-26(9)	-28(7)	-9(9)
C(52)	71(7)	366(27)	112(9)	11(15)	7(7)	-86(12)
C(53)	114(9)	82(9)	169(13)	27(10)	-53(9)	-3(7)
C(54)	46(4)	68(6)	60(5)	-3(5)	25(4)	-9(5)
C(55)	60(5)	64(6)	67(6)	-5(6)	20(4)	4(5)
C(56)	68(6)	82(8)	84(7)	-24(7)	23(5)	-1(5)
C(57)	71(6)	86(9)	86(8)	-30(7)	36(6)	-13(6)
C(58)	86(7)	108(10)	49(5)	-7(7)	25(5)	-24(7)
C(59)	61(5)	74(7)	70(6)	-4(6)	23(5)	-13(5)

Table 4.19 : Hydrogen atomic co-ordinates (x 10^4) and isotropic temperature factors (x 10^3) for D/L-1-*O*-(*tert*-butyldiphenylsilyl)-2,3-*O*-cyclohexylidene-4,5,6-tri-*O*-benzoyl *myo*-inositol (**59**) with estimated standard deviations in parentheses

	x	y	z	U(iso)
H(60)	-916(44)	2618(59)	8999(48)	37(18)
H(61)	375(46)	4011(65)	9282(51)	54(22)
H(62)	1339(63)	2406(83)	9539(68)	97(30)
H(63)	1323(55)	2446(71)	11657(59)	73(23)
H(64)	255(38)	867(54)	9919(43)	23(16)
H(65)	-494(33)	2411(46)	11014(37)	10(14)
H(66)	2664(6)	-754(8)	10810(7)	121(18)
H(67)	3776(7)	-2267(9)	10902(8)	121(18)
H(68)	5323(8)	-2259(11)	12171(10)	121(18)
H(69)	5766(7)	-819(11)	13340(9)	121(18)
H(70)	4568(6)	622(10)	13305(7)	121(18)
H(71)	-197(6)	-768(7)	12484(6)	63(10)
H(72)	31(8)	-2082(10)	13731(8)	63(10)
H(73)	1113(9)	-3623(11)	13924(8)	63(10)
H(74)	1934(8)	-3876(10)	12848(10)	63(10)
H(75)	1630(6)	-2606(8)	11553(8)	63(10)
H(76)	-3578(7)	974(11)	11086(8)	123(20)
H(77)	-4872(8)	-289(16)	10503(11)	123(20)
H(78)	-5023(8)	-1530(13)	9231(13)	123(20)
H(79)	-3806(8)	-1579(10)	8544(10)	123(20)
H(80)	-2425(6)	-317(9)	9171(8)	123(20)
H(81)	-826(6)	4193(9)	11577(6)	97(10)
H(82)	-469(6)	5499(9)	11674(6)	97(10)
H(83)	-2125(8)	5451(10)	11551(8)	97(10)
H(84)	-2432(8)	4738(10)	10566(8)	97(10)
H(85)	-2863(9)	6681(10)	10189(9)	97(10)
H(86)	-1760(9)	7077(10)	10795(9)	97(10)
H(87)	-1993(8)	7077(9)	9141(8)	97(10)
H(88)	-2359(8)	5775(9)	9033(8)	97(10)
H(89)	-695(6)	5790(8)	9147(7)	97(10)
H(90)	-370(6)	6512(8)	10129(7)	97(10)

Table 4.19 continued

	x	y	z	U(iso)
H(91)	1625(6)	5784(8)	10042(6)	100(16)
H(92)	1220(8)	7604(9)	9341(8)	100(16)
H(93)	1914(9)	8269(9)	8270(8)	100(16)
H(94)	3068(8)	7139(11)	7903(7)	100(16)
H(95)	3507(7)	5298(9)	8614(6)	100(16)
H(96)	3603(10)	4717(12)	12033(8)	176(20)
H(97)	3920(10)	5710(12)	11468(8)	176(20)
H(98)	4734(10)	5064(12)	12347(8)	176(20)
H(99)	5098(8)	3905(18)	10280(10)	176(20)
H(100)	5641(8)	4563(18)	11276(10)	176(20)
H(101)	4826(8)	5208(18)	10397(10)	176(20)
H(102)	4061(9)	2708(10)	11921(10)	176(20)
H(103)	5181(9)	3107(10)	12242(10)	176(20)
H(104)	4690(9)	2362(10)	11283(10)	176(20)
H(105)	3424(6)	1402(8)	10155(7)	105(16)
H(106)	3358(6)	-99(10)	9111(8)	105(16)
H(107)	2786(7)	224(11)	7473(8)	105(16)
H(108)	2285(7)	2052(11)	6836(7)	105(16)
H(109)	2360(6)	3588(9)	7880(7)	105(16)

Figure 4.10 : ORTEPII drawing [Johnson, 1976] of D/L-1-*O*-(*tert*-butyldiphenylsilyl)-2,3-*O*-cyclohexylidene-4,5,6-tri-*O*-benzoyl *myo*-inositol (**59**). Thermal ellipsoids are drawn at the 50% probability level.

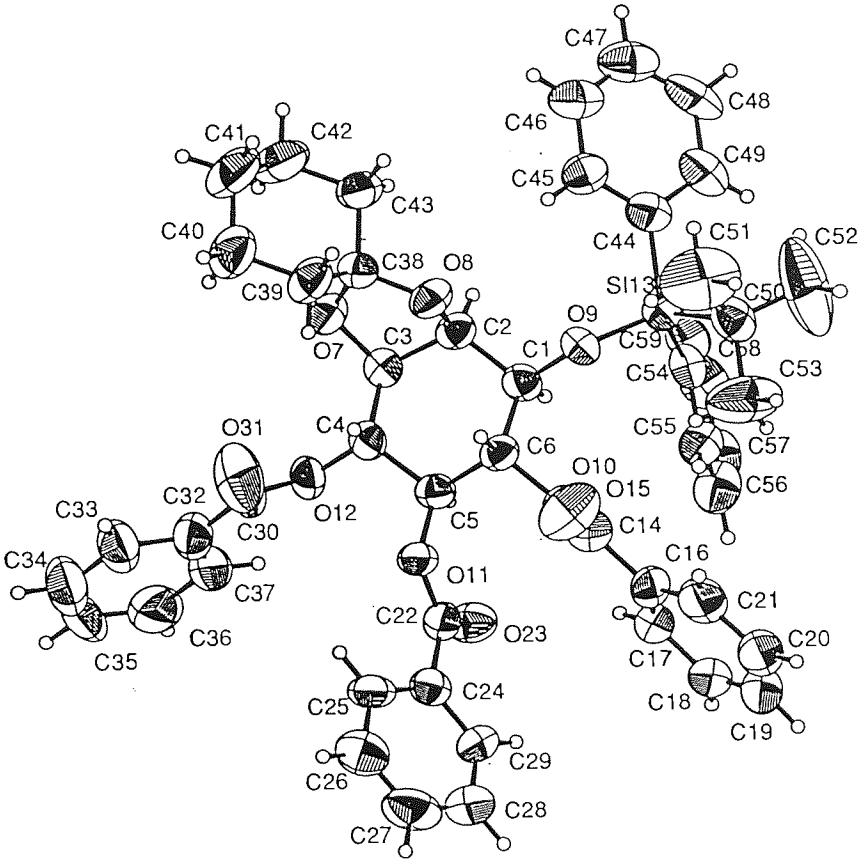

Table 4.20 : Asymmetry parameters for inositol rings of D/L-1-*O*-(*tert*-butyldiphenylsilyl)-2,3-*O*-cyclohexylidene-4,5,6-tri-*O*-benzoyl *myo*-inositol (**59**)

$\Delta C_s(1) = 15.07$	$\Delta C_2(1\text{-}2) = 12.17$
$\Delta C_s(2) = 2.13$	$\Delta C_2(2\text{-}3) = 7.67$
$\Delta C_s(3) = 12.95$	$\Delta C_2(3\text{-}4) = 19.80$

ΔC_s = Mirror related asymmetry parameter
ΔC_2 = Two fold related asymmetry parameter

Table 4.21 : Distances of C atoms from least squares plane for D/L-1-*O*-(*tert*-butyldiphenylsilyl)-2,3-*O*-cyclohexylidene-4,5,6-tri-*O*-benzoyl *myo*-inositol (**59**) (SHELX-93 [Sheldrick, 1993]).

Atom	Distance
C01	0.187(6) Å
C02	0.141(6) Å
C03	0.171(6) Å
C04	0.256(6) Å
C05	0.312(6) Å
C06	0.274(6) Å

Least squares plane
-3.40(5)x + 5.62(4)y + 12.65(3)z = 14.25(2)
Rms deviation of fitted atoms = 0.232

the inositol ring were calculated [Duax & Norton, 1975] and are shown in Table 4.20. The inositol ring is flattened at one end (C02) and puckered at the opposite end (C05), with a good mirror plane retained $\Delta C_S(2) = 2.28$. The distances of ring atoms from the least squares plane (Table 4.30) confirm this distortion, showing that C02 is pulled in much closer to the plane and that C05 is pushed out further away from the plane. The puckering and flattening, of the ring instead of twisting, may be explained by the steric

hindrance caused by the presence of the bulky silyl protecting group and the three benzoyl groups.

The cyclohexylidene ring is in the chair conformation with its ring and torsion angles similar to that of a perfect chair [Bucourt, 1974].

The acetal five-membered ring adopts the conformation of an envelope, with the C02 atom below a O08-C03-O09-C30 plane, with $\Delta C_S(2) = 0.67$.

The bond distances and angles for the silyl substituent are consistent with those of triol **58**. The silicon atom Si13 is orientated towards C02 (ie. towards the cyclohexylidene group) which is again similar to molecule two of triol **58**. The *t*-butyl group is found to sit closest to the inositol ring oxygen and the phenyl groups are positioned furthest away. In contrast to triol **58**, the *t*-butyl group is found to be closer to one of the phenyl groups than the phenyl groups are to each other. The *t*-butyl group is unexpectedly positioned anticlinal to the C01-O09 bond which places one phenyl group closer and one phenyl group further away from the C01-O07 bond than expected, which is similar to molecule one of triol **58.** The *t*-butyl group has one carbon *trans* and two carbons *gauche* to the O-Si bond (Appendix 1). The phenyl groups of the silyl substituent are more flexible in orientation to the O-Si bond, with phenyl (C44-C49) *trans* and phenyl (C55-C59) *gauche*.

The three benzoyl groups have bond lengths and bond angles which are in good agreement with each other, and the carbonyl linkages are similar to the structure of 1,2,3,4,5,6-hexa-*O*-acetyl *myo*-inositol [Abboud *et al.*, 1990]. The carbonyl carbons linked to positions C04 and C06 are orientated towards C05 which allows the benzoyl groups to be as far away as posssible from the silyl and cyclohexylidene substituents. The carbonyl carbon linked to position C05 is orientated towards C06. The C=O bonds of the benzoyl groups point in the same direction as the C-H bonds on the inositol ring [O15(C06), O31(C04) above and O23(C05) below] and are approximately coplanar with their corresponding inositol C-O bonds (C-O-C-O torsion angles range from 3.2 to 6.3°) which is also seen in the crystal structure of 1,2,3,4,5,6-hexa-*O*-acetyl-*myo*-inositol [Abboud *et al.*, 1990]. This s-*trans* conformation is best explained by a secondary electronic effect, where the ether oxygen has an electron pair which is

oriented anti periplanar to the C-O σ bond of the carbonyl group. This electron pair orbital can therefore overlap with the antibonding orbital σ* of that bond, and is suggested to result in approximately 3 kcal/mol increase in stability [Deslongchamps, 1983]. The phenyl groups of the benzoyl substituents are all positioned *trans* with respect to their corresponding inositol C-O bond and with respect to their corresponding O-C carbonyl linkage. The phenyl groups are therefore orientated so that they cause least steric hindrance in the fully protected inositol.

4.2.4 Crystal structure of 4,5,6-tri-*O*-benzoyl *myo*-inositol 1,2,3-tris(dibenzyl phosphate) (61)

4.2.4.1 Experimental

4,5,6-Tri-*O*-benzoyl *myo*-inositol 1,2,3-tris(dibenzyl phosphate) (**61**) slowly crystallised in chloroform and hexane to form colourless lath crystals. A single crystal (0.75 x 0.325 x 0.225 mm) was chosen for X-ray determination. The data were collected from an Enraf-Nonius CAD4 diffractometer with monochromated graphite Mo-Kα radiation, λ = 0.71069Å at 293 K.

4.2.4.2 Crystal data

4,5,6-Tri-*O*-benzoyl *myo*-inositol 1,2,3-tris(dibenzyl phosphate) (**61**) crystallises in the monoclinic space group $P2_1$ with a = 15.564(3), b = 18.835(2), c = 22.738(6)Å, α = 90, β = 95.04(2), γ = 90°, Z = 4 and V = 6639.8(23)Å^3. The formula weight is 1291.12 (F(000) = 2704) and the calculated density D_X = 1.292 Mg m^{-3}. The absorption coefficient μ = 0.162 mm^{-1}.

4.2.4.3 Data collection

Unit cell dimensions were obtained from least squares analysis of setting angles of 25 accurately centred reflections, $9.50 \leq \theta \leq 14.31°$. Intensity data were collected by the ω-2θ scan technique, Bragg angle $2.10 \leq \theta \leq 24.97°$. The ω scan angle was calculated from $[M+N(\tan\theta)]°$, where $M = 0.96$, $N = 0.35$ and increased by 25% on each side for background determination. The ω scan speed was varied from 0.8 to 2.8°min^{-1} depending upon intensity. Six different standard reflections were used during data collection: three intensity reflections (measured every three hours) and three orientation reflections (monitored every 200 reflections). No appreciable loss of intensity or crystal movement was detected during collection. The 14315 reflections were measured for $-18 \leq h \leq 1$, $-22 \leq k \leq 1$, $-26 \leq l \leq 27$ and merged to give 12807 independent reflections ($R_{int} = 0.0537$).

4.2.4.4 Structural determination and refinement

Lorentz, polarisation and intensity corrections (5% decay) were applied to the collected data. The space group was determined unambiguously as a result of structure analysis. An initial structure was solved by direct methods using SHELXS-86 (Sheldrick, 1985) with default options from F_{obs} values. Using the atomic positions determined from the E-map, most of the remaining non-hydrogen atoms were located in an electron density map using SHELXL-93 [Sheldrick, 1993].

Full-matrix least-squares refinement of atomic positions and anisotropic temperature factors (for non-hydrogen atoms) on F_{obs}^2 using SHELXL-93 showed that in each asymmetric unit there are two molecules of **61** and two molecules of water. From difference electron density maps, all non-hydrogen atom positions were found except the benzoyl phenyl atoms which were placed in calculated positions (the six atoms were fitted to a regular hexagon with a distance of 1.39 Å from each other) and subsequently refined as rigid bodies. All the hydrogen atoms (except water) were assumed to ride on attached atoms and were placed in calculated positions; their common temperature

factors were set at 1.5 times the value of the riding atom. Hydrogen atoms for the two water molecules were not found and were not placed in calculated positions. Further refinement of the structure, which included parameters for atomic co-ordinates, temperature factors (anisotropic for non-hydrogen atoms and isotropic for hydrogen atoms), overall scale factor and an extinction parameter, were carried out. Refinement of the structure was blocked into two separate blocks of data (one block for each molecule) because the number of parameters in this large structure exceeded limits for single refinement. In the weighting scheme $1/[\sigma^2(Fo^2)+(0.1000P)^2+0.0000P]$ where $P=(Fo^2+2Fc^2)/3$, the parameters converged at discrepancy indices R = 0.0566 and Rw = 0.1429 for 7032 observed reflections [$Fo > 4\sigma(Fo)$]. The absolute structure factor was -0.07(13) [Flack, 1983]. The final maximum shift / e.s.d. ratio was -0.049 and the maximum and minimum features on a difference Fourier map were 0.428 and -0.241 e $Å^{-3}$.

4.2.4.5 Results and discussion

Full structural data for the crystal structure of 4,5,6-tri-*O*-benzoyl *myo*-inositol 1,2,3-tris(dibenzyl phosphate) are given in Tables 4.22 (non-hydrogen atomic co-ordinates), 4.23 (bond lengths and angles), 4.24 (anisotropic displacement parameters) and 4.25 (hydrogen atomic co-ordinates and their isotropic temperature factors), and torsional angles are in Appendix 1.

The inositol rings for both inositol molecules (in one asymmetric unit) are in a distorted chair conformation with the oxygen at C02 and C92 (Figures 4.11 and 4.12) in the expected axial position and the other five oxygen atoms in equatorial positions for each molecule. All the C-C, and C-O bond lengths and angles (Table 4.23) were comparable with those of *myo*-inositol [Rabinowitz & Kraut, 1964]. The asymmetry parameters of the inositol ring were calculated [Duax & Norton, 1975] and are shown in Table 4.26. The inositol rings of the two molecules are slightly distorted in a similar way but through different inositol atoms. In this meso compound, one would expect a conserved

Table 4.22 : Atomic co-ordinates of non-hydrogen atoms (x 10^4) and equivalent isotropic temperature factors (x 10^3) for 4,5,6-tri-*O*-benzoyl *myo*-inositol 1,2,3-tris(dibenzyl phosphate) (**61**) and two water molecules with estimated standard deviations in parentheses

	x	y	z	U(eq)
C(01)	3027(4)	5135(4)	2546(3)	41(2)
C(02)	3470(4)	4836(4)	3121(3)	40(2)
C(03)	2824(4)	4786(4)	3575(3)	38(2)
C(04)	2391(4)	5502(4)	3663(3)	41(2)
C(05)	1997(4)	5793(4)	3074(3)	45(2)
C(06)	2692(4)	5868(4)	2662(3)	43(2)
O(07)	3649(3)	5177(3)	2109(2)	44(1)
O(08)	4146(3)	5314(2)	3322(2)	42(1)
O(09)	3281(3)	4570(3)	4126(2)	46(1)
O(10)	1722(3)	5402(3)	4054(2)	46(1)
O(11)	1648(3)	6488(3)	3187(2)	47(1)
O(12)	2350(3)	6190(3)	2116(2)	53(1)
P(13)	3598(1)	4669(1)	1558(1)	48(1)
O(14)	3058(3)	4046(3)	1622(2)	62(2)
O(15)	4561(3)	4514(3)	1464(2)	58(1)
C(16)	5020(6)	3943(6)	1781(5)	80(3)
C(17)	5867(6)	3834(6)	1543(4)	73(3)
C(18)	6317(7)	4367(8)	1311(6)	117(5)
C(19)	7122(9)	4259(11)	1125(8)	149(6)
C(20)	7467(8)	3594(13)	1166(7)	135(7)
C(21)	7052(9)	3045(10)	1394(7)	132(6)
C(22)	6233(7)	3171(7)	1585(6)	105(4)
O(23)	3316(3)	5178(3)	1043(2)	58(1)
C(24)	3368(5)	4901(5)	436(3)	65(2)
C(25)	2624(5)	5177(6)	33(4)	67(2)
C(26)	1780(6)	4991(5)	111(4)	73(3)
C(27)	1129(6)	5206(7)	-279(5)	91(3)
C(28)	1267(8)	5589(8)	-770(6)	113(4)
C(29)	2081(9)	5780(9)	-865(5)	126(5)
C(30)	2784(7)	5577(7)	-452(4)	92(4)

Table 4.22 continued

	x	y	z	U(eq)
P(31)	5135(1)	5097(1)	3378(1)	50(1)
O(32)	5271(4)	4349(4)	3414(4)	113(3)
O(33)	5524(4)	5561(6)	3888(3)	111(3)
C(34)	5283(6)	5594(8)	4469(4)	99(4)
C(35)	6062(5)	5667(6)	4898(4)	68(3)
C(36)	6378(7)	6303(7)	5077(5)	97(4)
C(37)	7029(9)	6390(10)	5477(7)	124(5)
C(38)	7431(8)	5848(14)	5729(6)	124(6)
C(39)	7157(9)	5179(11)	5572(6)	122(5)
C(40)	6439(7)	5077(7)	5151(5)	97(3)
O(41)	5539(4)	5409(4)	2868(3)	100(2)
C(42)	5436(6)	6058(6)	2593(5)	93(3)
C(43)	6201(6)	6280(5)	2276(3)	57(2)
C(44)	7004(7)	6007(6)	2422(5)	94(3)
C(45)	7708(8)	6277(7)	2150(7)	122(5)
C(46)	7600(9)	6808(7)	1754(6)	98(4)
C(47)	6818(10)	7087(7)	1612(5)	103(4)
C(48)	6126(7)	6829(6)	1886(4)	81(3)
P(49)	3022(1)	3909(1)	4490(1)	50(1)
O(50)	2640(4)	3328(3)	4141(2)	69(2)
O(51)	2453(3)	4238(3)	4942(2)	58(1)
C(52)	1883(6)	3796(7)	5276(4)	91(3)
C(53)	2354(6)	3452(6)	5790(4)	70(3)
C(54)	2449(8)	2720(6)	5840(5)	95(3)
C(55)	2853(11)	2400(9)	6312(7)	133(5)
C(56)	3187(10)	2829(11)	6761(8)	133(6)
C(57)	3129(9)	3535(10)	6748(6)	128(5)
C(58)	2691(7)	3861(7)	6248(5)	91(3)
O(59)	3878(3)	3733(3)	4874(2)	58(1)
C(60)	4550(6)	3330(6)	4614(4)	78(3)
C(61)	5196(6)	3081(5)	5111(5)	75(3)
C(62)	4953(7)	2934(6)	5650(5)	95(3)
C(63)	5566(11)	2650(7)	6096(6)	128(5)
C(64)	6371(11)	2507(9)	5943(10)	143(7)

Table 4.22 continued

	x	y	z	U(eq)
C(65)	6622(10)	2684(9)	5431(10)	140(7)
C(66)	6030(7)	2953(7)	4997(7)	126(5)
C(67)	1809(5)	5742(5)	4572(3)	53(2)
C(68)	2401(4)	6136(4)	4716(3)	88(2)
C(69)	1123(3)	5575(3)	4958(2)	56(2)
C(70)	394(4)	5190(4)	4756(2)	71(3)
C(71)	-245(3)	5054(4)	5131(3)	101(4)
C(72)	-156(4)	5303(5)	5708(3)	109(4)
C(73)	572(5)	5688(5)	5911(2)	105(4)
C(74)	1212(4)	5824(4)	5536(3)	88(3)
C(75)	807(5)	6587(5)	3008(4)	62(2)
C(76)	363(4)	6160(4)	2745(4)	118(3)
C(77)	508(4)	7308(3)	3163(3)	61(2)
C(78)	-375(3)	7433(4)	3090(3)	87(3)
C(79)	-700(4)	8094(4)	3228(3)	104(4)
C(80)	-141(6)	8631(3)	3438(3)	99(4)
C(81)	742(5)	8506(3)	3511(3)	119(4)
C(82)	1067(3)	7845(3)	3373(3)	77(3)
C(83)	2768(6)	6768(5)	1931(4)	68(2)
O(84)	3381(6)	7017(5)	2225(4)	134(4)
C(85)	2408(4)	7053(3)	1372(2)	70(3)
C(86)	2672(5)	7721(3)	1200(3)	112(4)
C(87)	2374(6)	7990(4)	650(4)	132(5)
C(88)	1814(6)	7591(5)	272(3)	115(5)
C(89)	1550(5)	6923(4)	445(3)	108(4)
C(90)	1847(4)	6654(3)	995(3)	73(3)
C(91)	2679(4)	2256(4)	1720(3)	37(2)
C(92)	1912(4)	2319(4)	2082(3)	43(2)
C(93)	1467(4)	3015(4)	1925(3)	40(2)
C(94)	1159(4)	3044(4)	1273(3)	41(2)
C(95)	1905(4)	2926(4)	887(3)	41(2)
C(96)	2410(4)	2261(4)	1063(3)	43(2)
O(97)	3118(3)	1595(3)	1866(2)	50(1)
O(98)	1317(3)	1734(3)	1928(2)	51(1)

Table 4.22 continued

	x	y	z	U(eq)
C(99)	708(3)	3057(3)	2250(2)	47(1)
C(100)	819(3)	3743(3)	1149(2)	47(1)
C(101)	1505(3)	2882(3)	294(2)	47(1)
C(102)	3197(3)	2249(3)	772(2)	44(1)
P(103)	4110(1)	1541(1)	2024(1)	55(1)
C(105)	4217(4)	952(3)	2502(3)	75(2)
C(106)	3949(6)	1077(8)	3087(4)	99(4)
C(107)	4664(6)	840(6)	3528(4)	73(3)
C(108)	5180(8)	1339(7)	3844(5)	98(4)
C(109)	5864(8)	1106(8)	4249(5)	101(4)
C(110)	5986(7)	414(8)	4333(5)	90(3)
C(111)	5513(7)	-61(7)	4020(5)	99(4)
C(112)	4846(6)	145(7)	3624(5)	91(3)
O(113)	4407(3)	1145(4)	1481(3)	79(2)
C(114)	5305(7)	926(7)	1466(6)	112(4)
C(115)	5339(8)	162(7)	1271(7)	98(4)
C(116)	4859(12)	-48(10)	765(8)	141(5)
C(117)	4963(14)	-807(12)	572(9)	172(7)
C(118)	5465(15)	-1225(10)	947(11)	178(8)
C(119)	5912(14)	-975(10)	1434(14)	209(11)
C(120)	5821(11)	-290(9)	1635(9)	163(7)
O(104)	4532(4)	2208(4)	2158(3)	95(2)
P(121)	990(2)	1230(2)	2405(1)	87(1)
O(122)	1438(10)	1243(8)	2959(5)	233(8)
O(123)	802(8)	523(5)	2042(5)	145(4)
C(124)	1396(13)	202(9)	1675(8)	150(6)
C(125)	2123(12)	-247(8)	1989(9)	127(5)
C(126)	2906(16)	-291(10)	1726(8)	151(6)
C(127)	3558(19)	-734(14)	1990(14)	206(11)
C(128)	3473(16)	-1087(11)	2506(12)	177(8)
C(129)	2685(19)	-1003(17)	2726(12)	229(13)
C(130)	1975(15)	-606(13)	2442(10)	174(7)
O(131)	86(7)	1372(7)	2492(8)	218(7)
C(132)	-557(8)	1685(9)	2245(7)	160(8)

Table 4.22 continued

	x	y	z	U(eq)
C(133)	-1385(7)	1448(8)	2512(5)	89(3)
C(134)	-1584(9)	780(8)	2499(5)	109(4)
C(135)	-2315(12)	481(12)	2664(8)	150(7)
C(136)	-2845(11)	902(18)	2902(9)	157(8)
C(137)	-2710(16)	1626(18)	2989(11)	193(9)
C(138)	-1938(15)	1892(11)	2768(11)	185(8)
P(139)	458(1)	3735(1)	2598(1)	48(1)
O(140)	1134(3)	4267(3)	2689(3)	64(2)
O(141)	-385(3)	3970(3)	2236(2)	59(1)
C(142)	-809(6)	4627(5)	2372(4)	76(3)
C(143)	-1376(5)	4572(5)	2865(4)	64(2)
C(144)	-2046(7)	4093(7)	2826(5)	92(3)
C(145)	-2585(8)	4056(10)	3288(8)	128(5)
C(146)	-2482(11)	4546(13)	3746(8)	141(8)
C(147)	-1827(12)	4997(11)	3781(6)	134(6)
C(148)	-1257(7)	5035(7)	3333(5)	93(3)
O(149)	101(3)	3420(4)	3154(2)	68(2)
C(150)	696(7)	3083(9)	3599(5)	113(4)
C(151)	181(7)	2898(6)	4108(4)	78(3)
C(152)	-536(9)	3204(8)	4246(6)	127(5)
C(153)	-938(13)	3024(11)	4744(8)	172(8)
C(154)	-607(16)	2539(13)	5121(8)	157(9)
C(155)	133(14)	2214(10)	5007(7)	139(6)
C(156)	507(9)	2370(8)	4483(6)	116(4)
C(157)	15(5)	3777(5)	884(3)	53(2)
O(158)	-412(4)	3286(4)	724(3)	80(2)
C(159)	-283(4)	4520(3)	795(3)	63(2)
C(160)	-957(4)	4651(4)	366(3)	95(4)
C(161)	-1272(4)	5337(5)	279(3)	123(5)
C(162)	-913(5)	5892(4)	621(4)	124(5)
C(163)	-239(5)	5761(3)	1050(4)	110(4)
C(164)	76(4)	5075(4)	1137(3)	77(3)
C(165)	1893(6)	3189(5)	-150(3)	54(2)
O(166)	2636(4)	3382(4)	-86(3)	72(2)

Table 4.22 continued

	x	y	z	U(eq)
C(167)	1322(4)	3251(4)	-693(2)	57(2)
C(168)	1635(4)	3606(4)	-1167(3)	90(3)
C(169)	1108(6)	3700(5)	-1687(2)	112(4)
C(170)	269(5)	3439(5)	-1734(2)	108(4)
C(171)	-43(4)	3084(5)	-1261(3)	117(5)
C(172)	484(4)	2990(4)	-740(2)	85(3)
C(173)	3283(5)	1780(6)	345(4)	67(3)
O(174)	2739(5)	1369(6)	200(4)	142(4)
C(175)	4127(3)	1821(4)	103(3)	65(2)
C(176)	4768(4)	2290(4)	319(3)	87(3)
C(177)	5563(4)	2291(5)	83(4)	126(5)
C(178)	5716(4)	1823(6)	-368(4)	153(8)
C(179)	5075(6)	1354(5)	-584(3)	126(6)
C(180)	4280(5)	1353(4)	-349(3)	102(4)
W(1)	3171(5)	3058(5)	3027(3)	111(3)
W(2)	5114(9)	2934(5)	3199(5)	177(5)

Note : W = Oxygen atom of a water molecule

Table 4.23 : Bond lengths (Å) and bond angles (°) for 4,5,6-tri-*O*-benzoyl *myo*-inositol 1,2,3-tris(dibenzyl phosphate) (**61**) and two water molecules with estimated standard deviations in parentheses

Bond	Distance (Å)	Bond	Distance (Å)
C(01)-O(07)	1.448(8)	C(26)-C(27)	1.35(1)
C(01)-C(06)	1.51(1)	C(27)-C(28)	1.36(2)
C(01)-C(02)	1.531(9)	C(28)-C(29)	1.35(2)
C(02)-O(08)	1.429(8)	C(29)-C(30)	1.43(2)
C(02)-C(03)	1.506(9)	P(31)-O(32)	1.426(7)
C(03)-O(09)	1.443(7)	P(31)-O(41)	1.488(7)
C(03)-C(04)	1.53(1)	P(31)-O(33)	1.534(8)
C(04)-O(10)	1.440(8)	O(33)-C(34)	1.41(1)
C(04)-C(05)	1.525(9)	C(34)-C(35)	1.49(1)
C(05)-O(11)	1.451(9)	C(35)-C(40)	1.36(2)
C(05)-C(06)	1.50(1)	C(35)-C(36)	1.34(2)
C(06)-O(12)	1.442(8)	C(36)-C(37)	1.31(2)
O(07)-P(13)	1.573(5)	C(37)-C(38)	1.30(2)
O(08)-P(31)	1.587(5)	C(38)-C(39)	1.37(2)
O(09)-P(49)	1.567(5)	C(39)-C(40)	1.42(2)
O(10)-C(67)	1.338(9)	O(41)-C(42)	1.38(1)
O(11)-C(75)	1.348(9)	C(42)-C(43)	1.50(1)
O(12)-C(83)	1.36(1)	C(43)-C(48)	1.36(1)
P(13)-O(14)	1.458(6)	C(43)-C(44)	1.37(1)
P(13)-O(23)	1.546(6)	C(44)-C(45)	1.40(2)
P(13)-O(15)	1.559(5)	C(45)-C(46)	1.35(2)
O(15)-C(16)	1.45(1)	C(46)-C(47)	1.34(2)
C(16)-C(17)	1.48(1)	C(47)-C(48)	1.38(1)
C(17)-C(22)	1.37(2)	P(49)-O(50)	1.448(6)
C(17)-C(18)	1.36(2)	P(49)-O(51)	1.546(6)
C(18)-C(19)	1.37(2)	P(49)-O(59)	1.563(5)
C(19)-C(20)	1.36(2)	O(51)-C(52)	1.47(1)
C(20)-C(21)	1.35(2)	C(52)-C(53)	1.48(1)
C(21)-C(22)	1.40(2)	C(53)-C(58)	1.36(1)
O(23)-C(24)	1.485(9)	C(53)-C(54)	1.39(2)
C(24)-C(25)	1.50(1)	C(54)-C(55)	1.34(2)
C(25)-C(30)	1.38(1)	C(55)-C(56)	1.37(2)
C(25)-C(26)	1.39(1)	C(56)-C(57)	1.33(2)

Table 4.23 continued

Bond	Distance (Å)	Bond	Distance (Å)
C(57)-C(58)	1.41(2)	C(91)-C(96)	1.52(1)
O(59)-C(60)	1.46(1)	C(92)-O(98)	1.463(9)
C(60)-C(61)	1.52(1)	C(92)-C(93)	1.51(1)
C(61)-C(66)	1.37(2)	C(93)-O(99)	1.450(8)
C(61)-C(62)	1.34(2)	C(93)-C(94)	1.52(1)
C(62)-C(63)	1.43(2)	C(94)-O(100)	1.438(8)
C(63)-C(64)	1.36(2)	C(94)-C(95)	1.53(1)
C(64)-C(65)	1.30(2)	C(95)-O(101)	1.438(8)
C(65)-C(66)	1.39(2)	C(95)-C(96)	1.51(1)
C(67)-O(68)	1.21(1)	C(96)-O(102)	1.442(8)
C(67)-C(69)	1.474(9)	O(97)-P(103)	1.556(5)
C(69)-C(70)	1.39	O(98)-P(121)	1.560(6)
C(69)-C(74)	1.39	O(99)-P(139)	1.569(5)
C(70)-C(71)	1.39	O(100)-C(157)	1.341(9)
C(71)-C(72)	1.39	O(101)-C(165)	1.351(9)
C(72)-C(73)	1.39	O(102)-C(173)	1.33(1)
C(73)-C(74)	1.39	P(103)-O(104)	1.438(7)
C(75)-O(76)	1.19(1)	P(103)-O(113)	1.547(7)
C(75)-C(77)	1.49(1)	P(103)-O(105)	1.553(6)
C(77)-C(78)	1.39	O(105)-C(106)	1.45(1)
C(77)-C(82)	1.39	C(106)-C(107)	1.50(1)
C(78)-C(79)	1.39	C(107)-C(112)	1.35(2)
C(79)-C(80)	1.39	C(107)-C(108)	1.39(2)
C(80)-C(81)	1.39	C(108)-C(109)	1.41(2)
C(81)-C(82)	1.39	C(109)-C(110)	1.33(2)
C(83)-O(84)	1.21(1)	C(110)-C(111)	1.33(2)
C(83)-C(85)	1.445(9)	C(111)-C(112)	1.37(1)
C(85)-C(86)	1.39	O(113)-C(114)	1.46(1)
C(85)-C(90)	1.39	C(114)-C(115)	1.51(2)
C(86)-C(87)	1.39	C(115)-C(120)	1.37(2)
C(87)-C(88)	1.39	C(115)-C(116)	1.37(2)
C(88)-C(89)	1.39	C(116)-C(117)	1.51(3)
C(89)-C(90)	1.39	C(117)-C(118)	1.36(2)
C(91)-O(97)	1.445(8)	C(118)-C(119)	1.34(2)
C(91)-C(92)	1.51(1)	C(119)-C(120)	1.38(2)

Table 4.23 continued

Bond	Distance (Å)	Bond	Distance (Å)
P(121)-O(122)	1.39(1)	C(150)-C(151)	1.51(1)
P(121)-O(131)	1.46(1)	C(151)-C(156)	1.38(2)
P(121)-O(123)	1.58(1)	C(151)-C(152)	1.32(2)
O(123)-C(124)	1.43(2)	C(152)-C(153)	1.38(2)
C(124)-C(125)	1.54(2)	C(153)-C(154)	1.33(3)
C(125)-C(130)	1.27(2)	C(154)-C(155)	1.35(2)
C(125)-C(126)	1.41(2)	C(155)-C(156)	1.40(2)
C(126)-C(127)	1.41(3)	C(157)-O(158)	1.18(1)
C(127)-C(128)	1.36(3)	C(157)-C(159)	1.48(1)
C(128)-C(129)	1.37(3)	C(159)-C(160)	1.39
C(129)-C(130)	1.44(3)	C(159)-C(164)	1.39
O(131)-C(132)	1.25(2)	C(160)-C(161)	1.39
C(132)-C(133)	1.54(2)	C(161)-C(162)	1.39
C(133)-C(138)	1.37(2)	C(162)-C(163)	1.39
C(133)-C(134)	1.29(2)	C(163)-C(164)	1.39
C(134)-C(135)	1.35(2)	C(165)-O(166)	1.208(9)
C(135)-C(136)	1.30(3)	C(165)-C(167)	1.462(9)
C(136)-C(137)	1.39(3)	C(167)-C(168)	1.39
C(137)-C(138)	1.43(3)	C(167)-C(172)	1.39
P(139)-O(140)	1.456(6)	C(168)-C(169)	1.39
P(139)-O(149)	1.543(6)	C(169)-C(170)	1.39
P(139)-O(141)	1.551(5)	C(170)-C(171)	1.39
O(141)-C(142)	1.45(1)	C(171)-C(172)	1.39
C(142)-C(143)	1.49(1)	C(173)-O(174)	1.17(1)
C(143)-C(148)	1.38(1)	C(173)-C(175)	1.471(9)
C(143)-C(144)	1.38(1)	C(175)-C(176)	1.39
C(144)-C(145)	1.40(2)	C(175)-C(180)	1.39
C(145)-C(146)	1.39(2)	C(176)-C(177)	1.39
C(146)-C(147)	1.32(2)	C(177)-C(178)	1.39
C(147)-C(148)	1.41(2)	C(178)-C(179)	1.39
O(149)-C(150)	1.46(1)	C(179)-C(180)	1.39

Table 4.23 continued

Bonds	Angles (°)	Bonds	Angles (°)
O(07)-C(01)-C(06)	109.4(6)	C(17)-C(18)-C(19)	122(1)
O(07)-C(01)-C(02)	109.1(5)	C(20)-C(19)-C(18)	119(2)
C(06)-C(01)-C(02)	108.9(6)	C(19)-C(20)-C(21)	122(1)
O(08)-C(02)-C(03)	109.7(5)	C(20)-C(21)-C(22)	118(2)
O(08)-C(02)-C(01)	107.8(5)	C(17)-C(22)-C(21)	121(1)
C(03)-C(02)-C(01)	109.3(5)	C(24)-O(23)-P(13)	116.8(5)
O(09)-C(03)-C(02)	107.8(5)	O(23)-C(24)-C(25)	110.1(7)
O(09)-C(03)-C(04)	109.0(5)	C(30)-C(25)-C(26)	118.7(9)
C(02)-C(03)-C(04)	111.3(6)	C(30)-C(25)-C(24)	119.6(8)
O(10)-C(04)-C(05)	109.4(5)	C(26)-C(25)-C(24)	121.5(8)
O(10)-C(04)-C(03)	108.4(5)	C(27)-C(26)-C(25)	120.4(9)
C(05)-C(04)-C(03)	110.5(6)	C(28)-C(27)-C(26)	122(1)
O(11)-C(05)-C(06)	109.2(6)	C(29)-C(28)-C(27)	119(1)
O(11)-C(05)-C(04)	107.3(6)	C(28)-C(29)-C(30)	120(1)
C(06)-C(05)-C(04)	109.0(6)	C(25)-C(30)-C(29)	119(1)
O(12)-C(06)-C(05)	110.2(6)	O(32)-P(31)-O(41)	111.4(5)
O(12)-C(06)-C(01)	110.0(6)	O(32)-P(31)-O(33)	118.2(6)
C(05)-C(06)-C(01)	107.6(6)	O(41)-P(31)-O(33)	101.4(5)
C(01)-O(07)-P(13)	121.5(4)	O(32)-P(31)-O(08)	113.5(3)
C(02)-O(08)-P(31)	123.0(4)	O(41)-P(31)-O(08)	108.0(3)
C(03)-O(09)-P(49)	123.5(4)	O(33)-P(31)-O(08)	103.2(3)
C(67)-O(10)-C(04)	117.3(6)	C(34)-O(33)-P(31)	128.0(8)
C(75)-O(11)-C(05)	116.1(6)	O(33)-C(34)-C(35)	110.5(8)
C(83)-O(12)-C(06)	117.0(6)	C(40)-C(35)-C(36)	117.8(9)
O(14)-P(13)-O(23)	116.5(3)	C(40)-C(35)-C(34)	120(1)
O(14)-P(13)-O(15)	115.6(3)	C(36)-C(35)-C(34)	122(1)
O(23)-P(13)-O(15)	103.0(3)	C(37)-C(36)-C(35)	124(1)
O(14)-P(13)-O(07)	113.5(3)	C(38)-C(37)-C(36)	121(2)
O(23)-P(13)-O(07)	102.5(3)	C(37)-C(38)-C(39)	119(1)
O(15)-P(13)-O(07)	104.0(3)	C(38)-C(39)-C(40)	121(1)
C(16)-O(15)-P(13)	120.6(5)	C(35)-C(40)-C(39)	117(1)
C(17)-C(16)-O(15)	109.7(8)	C(42)-O(41)-P(31)	131.7(8)
C(22)-C(17)-C(18)	118(1)	O(41)-C(42)-C(43)	113.6(9)
C(22)-C(17)-C(16)	119(1)	C(48)-C(43)-C(44)	117.9(9)
C(18)-C(17)-C(16)	123(1)	C(48)-C(43)-C(42)	119.9(9)

Table 4.23 continued

Bonds	Angles (°)	Bonds	Angles (°)
C(44)-C(43)-C(42)	121.7(9)	C(70)-C(69)-C(74)	120.0
C(43)-C(44)-C(45)	120(1)	C(70)-C(69)-C(67)	121.7(5)
C(46)-C(45)-C(44)	121(1)	C(74)-C(69)-C(67)	118.3(5)
C(47)-C(46)-C(45)	121(1)	C(69)-C(70)-C(71)	120.0
C(46)-C(47)-C(48)	119(1)	C(72)-C(71)-C(70)	120.0
C(43)-C(48)-C(47)	122(1)	C(73)-C(72)-C(71)	120.0
O(50)-P(49)-O(51)	115.9(4)	C(72)-C(73)-C(74)	120.0
O(50)-P(49)-O(59)	115.8(3)	C(73)-C(74)-C(69)	120.0
O(51)-P(49)-O(59)	102.9(3)	O(76)-C(75)-O(11)	124.4(8)
O(50)-P(49)-O(09)	115.0(3)	O(76)-C(75)-C(77)	123.9(7)
O(51)-P(49)-O(09)	102.8(3)	O(11)-C(75)-C(77)	111.7(8)
O(59)-P(49)-O(09)	102.6(3)	C(78)-C(77)-C(82)	120.0
C(52)-O(51)-P(49)	121.4(7)	C(78)-C(77)-C(75)	116.9(5)
O(51)-C(52)-C(53)	112.1(8)	C(82)-C(77)-C(75)	123.1(5)
C(58)-C(53)-C(54)	118(1)	C(77)-C(78)-C(79)	120.0
C(58)-C(53)-C(52)	119(1)	C(80)-C(79)-C(78)	120.0
C(54)-C(53)-C(52)	123(1)	C(79)-C(80)-C(81)	120.0
C(55)-C(54)-C(53)	123(1)	C(82)-C(81)-C(80)	120.0
C(54)-C(55)-C(56)	117(1)	C(81)-C(82)-C(77)	120.0
C(57)-C(56)-C(55)	124(2)	O(84)-C(83)-O(12)	121.1(8)
C(56)-C(57)-C(58)	118(2)	O(84)-C(83)-C(85)	124.6(8)
C(53)-C(58)-C(57)	120(1)	O(12)-C(83)-C(85)	114.3(7)
C(60)-O(59)-P(49)	119.4(5)	C(86)-C(85)-C(90)	120.0
O(59)-C(60)-C(61)	108.1(8)	C(86)-C(85)-C(83)	118.8(6)
C(66)-C(61)-C(62)	119(1)	C(90)-C(85)-C(83)	121.1(6)
C(66)-C(61)-C(60)	119(1)	C(87)-C(86)-C(85)	120.0
C(62)-C(61)-C(60)	121.4(9)	C(86)-C(87)-C(88)	120.0
C(61)-C(62)-C(63)	120(1)	C(89)-C(88)-C(87)	120.0
C(64)-C(63)-C(62)	118(2)	C(88)-C(89)-C(90)	120.0
C(65)-C(64)-C(63)	122(2)	C(89)-C(90)-C(85)	120.0
C(64)-C(65)-C(66)	120(2)	O(97)-C(91)-C(92)	108.7(6)
C(61)-C(66)-C(65)	121(2)	O(97)-C(91)-C(96)	108.4(6)
O(68)-C(67)-O(10)	123.3(7)	C(92)-C(91)-C(96)	111.9(5)
O(68)-C(67)-C(69)	123.1(7)	O(98)-C(92)-C(93)	109.2(5)
O(10)-C(67)-C(69)	113.6(7)	O(98)-C(92)-C(91)	108.9(6)

Table 4.23 continued

Bonds	Angles (°)	Bonds	Angles (°)
C(93)-C(92)-C(91)	107.8(6)	C(114)-O(113)-P(103)	120.7(7)
O(99)-C(93)-C(92)	107.7(6)	C(115)-C(114)-O(113)	110(1)
O(99)-C(93)-C(94)	107.1(5)	C(120)-C(115)-C(116)	124(2)
C(92)-C(93)-C(94)	111.2(6)	C(120)-C(115)-C(114)	117(2)
O(100)-C(94)-C(93)	107.7(6)	C(116)-C(115)-C(114)	119(1)
O(100)-C(94)-C(95)	107.8(6)	C(115)-C(116)-C(117)	117(2)
C(93)-C(94)-C(95)	111.3(5)	C(118)-C(117)-C(116)	116(2)
O(101)-C(95)-C(96)	111.8(6)	C(119)-C(118)-C(117)	123(2)
O(101)-C(95)-C(94)	104.9(5)	C(118)-C(119)-C(120)	123(2)
C(96)-C(95)-C(94)	111.8(6)	C(115)-C(120)-C(119)	117(2)
O(102)-C(96)-C(95)	109.5(6)	O(122)-P(121)-O(131)	107(1)
O(102)-C(96)-C(91)	106.3(5)	O(122)-P(121)-O(98)	116.9(5)
C(95)-C(96)-C(91)	110.9(6)	O(131)-P(121)-O(98)	111.0(6)
C(91)-O(97)-P(103)	123.2(4)	O(122)-P(121)-O(123)	123.1(9)
C(92)-O(98)-P(121)	122.0(5)	O(131)-P(121)-O(123)	95.1(8)
C(93)-O(99)-P(139)	123.4(4)	O(98)-P(121)-O(123)	101.9(4)
C(157)-O(100)-C(94)	116.4(6)	C(124)-O(123)-P(121)	124(1)
C(165)-O(101)-C(95)	119.4(6)	O(123)-C(124)-C(125)	117(2)
C(173)-O(102)-C(96)	119.4(6)	C(130)-C(125)-C(126)	123(2)
O(104)-P(103)-O(113)	115.2(4)	C(130)-C(125)-C(124)	119(2)
O(104)-P(103)-O(105)	117.2(4)	C(126)-C(125)-C(124)	118(2)
O(113)-P(103)-O(105)	101.1(4)	C(127)-C(126)-C(125)	118(2)
O(104)-P(103)-O(97)	114.7(3)	C(128)-C(127)-C(126)	122(3)
O(113)-P(103)-O(97)	102.0(3)	C(127)-C(128)-C(129)	114(3)
O(105)-P(103)-O(97)	104.5(3)	C(128)-C(129)-C(130)	125(3)
C(106)-O(105)-P(103)	120.3(7)	C(125)-C(130)-C(129)	117(2)
O(105)-C(106)-C(107)	108.1(7)	C(132)-O(131)-P(121)	140(1)
C(112)-C(107)-C(108)	118(1)	O(131)-C(132)-C(133)	111(1)
C(112)-C(107)-C(106)	122(1)	C(138)-C(133)-C(134)	116(2)
C(108)-C(107)-C(106)	120(1)	C(138)-C(133)-C(132)	125(2)
C(107)-C(108)-C(109)	120(1)	C(134)-C(133)-C(132)	119(2)
C(110)-C(109)-C(108)	119(1)	C(135)-C(134)-C(133)	127(2)
C(111)-C(110)-C(109)	121(1)	C(136)-C(135)-C(134)	116(2)
C(110)-C(111)-C(112)	121(1)	C(135)-C(136)-C(137)	124(2)
C(107)-C(112)-C(111)	121(1)	C(136)-C(137)-C(138)	114(3)

Table 4.23 continued

Bonds	Angles (°)	Bonds	Angles (°)
C(133)-C(138)-C(137)	121(2)	C(160)-C(159)-C(164)	120.0
O(140)-P(139)-O(149)	117.2(3)	C(160)-C(159)-C(157)	118.1(5)
O(140)-P(139)-O(141)	116.5(4)	C(164)-C(159)-C(157)	121.9(5)
O(149)-P(139)-O(141)	101.3(3)	C(159)-C(160)-C(161)	120.0
O(140)-P(139)-O(99)	115.1(3)	C(160)-C(161)-C(162)	120.0
O(149)-P(139)-O(99)	102.9(3)	C(161)-C(162)-C(163)	120.0
O(141)-P(139)-O(99)	101.6(3)	C(162)-C(163)-C(164)	120.0
C(142)-O(141)-P(139)	120.7(6)	C(163)-C(164)-C(159)	120.0
O(141)-C(142)-C(143)	114.2(8)	O(166)-C(165)-O(101)	121.6(7)
C(148)-C(143)-C(144)	121(1)	O(166)-C(165)-C(167)	125.6(7)
C(148)-C(143)-C(142)	119(1)	O(101)-C(165)-C(167)	112.8(7)
C(144)-C(143)-C(142)	119.5(9)	C(168)-C(167)-C(172)	120.0
C(143)-C(144)-C(145)	119(1)	C(168)-C(167)-C(165)	117.7(5)
C(146)-C(145)-C(144)	119(2)	C(172)-C(167)-C(165)	122.3(5)
C(147)-C(146)-C(145)	120(2)	C(167)-C(168)-C(169)	120.0
C(146)-C(147)-C(148)	121(2)	C(170)-C(169)-C(168)	120.0
C(143)-C(148)-C(147)	118(1)	C(169)-C(170)-C(171)	120.0
C(150)-O(149)-P(139)	118.9(6)	C(172)-C(171)-C(170)	120.0
O(149)-C(150)-C(151)	106.7(8)	C(171)-C(172)-C(167)	120.0
C(156)-C(151)-C(152)	116(1)	O(174)-C(173)-O(102)	121.9(8)
C(156)-C(151)-C(150)	117(1)	O(174)-C(173)-C(175)	125.1(8)
C(152)-C(151)-C(150)	127(1)	O(102)-C(173)-C(175)	112.9(7)
C(151)-C(152)-C(153)	123(2)	C(176)-C(175)-C(180)	120.0
C(154)-C(153)-C(152)	121(2)	C(176)-C(175)-C(173)	122.6(6)
C(153)-C(154)-C(155)	119(2)	C(180)-C(175)-C(173)	117.4(6)
C(154)-C(155)-C(156)	120(2)	C(175)-C(176)-C(177)	120.0
C(151)-C(156)-C(155)	121(2)	C(178)-C(177)-C(176)	120.0
O(158)-C(157)-O(100)	125.4(8)	C(177)-C(178)-C(179)	120.0
O(158)-C(157)-C(159)	122.5(7)	C(180)-C(179)-C(178)	120.0
O(100)-C(157)-C(159)	112.1(8)	C(179)-C(180)-C(175)	120.0

Table 4.24 : Anisotropic displacement parameters (x 10^3, for non-hydrogen atoms) for 4,5,6-tri-*O*-benzoyl *myo*-inositol 1,2,3-tris(dibenzyl phosphate) (**61**) and two water molecules with estimated standard deviations in parentheses

	U11	U22	U33	U23	U13	U12
C(01)	30(3)	54(5)	40(4)	-1(4)	4(3)	-5(4)
C(02)	36(4)	40(4)	43(4)	-3(3)	1(3)	-3(3)
C(03)	29(3)	46(4)	38(4)	5(3)	-4(3)	-3(3)
C(04)	34(4)	50(5)	38(4)	5(3)	-2(3)	0(3)
C(05)	42(4)	40(4)	53(5)	6(4)	3(4)	4(4)
C(06)	39(4)	52(5)	37(4)	10(4)	-5(3)	0(4)
O(07)	41(3)	54(3)	40(3)	1(2)	11(2)	-8(2)
O(08)	34(2)	43(3)	49(3)	-5(2)	-6(2)	-3(2)
O(09)	44(3)	53(3)	41(3)	7(2)	-6(2)	-3(3)
O(10)	39(3)	55(3)	44(3)	-1(3)	7(2)	0(2)
O(11)	38(3)	43(3)	59(3)	-2(2)	2(2)	5(2)
O(12)	50(3)	55(3)	53(3)	11(3)	-1(2)	0(3)
P(13)	44(1)	54(1)	47(1)	-4(1)	14(1)	-8(1)
O(14)	60(3)	64(4)	67(3)	-16(3)	27(3)	-20(3)
O(15)	44(3)	64(4)	69(3)	1(3)	27(3)	1(3)
C(16)	72(6)	75(7)	98(7)	17(6)	32(5)	28(5)
C(17)	53(5)	96(8)	72(6)	-10(6)	15(4)	4(6)
C(18)	71(7)	122(11)	167(12)	33(10)	65(8)	18(7)
C(19)	80(9)	184(18)	189(16)	35(14)	48(10)	6(11)
C(20)	58(8)	207(20)	144(13)	-57(13)	24(8)	18(11)
C(21)	78(9)	153(15)	167(14)	-78(12)	15(9)	28(10)
C(22)	65(7)	105(10)	147(11)	-35(8)	18(7)	14(7)
O(23)	63(3)	69(4)	43(3)	2(3)	5(2)	-2(3)
C(24)	66(5)	92(7)	38(4)	-5(4)	14(4)	0(5)
C(25)	62(5)	94(7)	47(5)	12(5)	15(4)	-3(5)
C(26)	61(6)	82(7)	80(6)	17(6)	24(5)	7(5)
C(27)	56(6)	115(9)	101(8)	15(8)	6(6)	-1(6)
C(28)	86(8)	155(12)	94(9)	29(9)	-17(7)	-2(9)
C(29)	117(10)	194(15)	65(7)	56(9)	-3(7)	-15(11)
C(30)	81(7)	145(11)	52(6)	10(6)	13(5)	-22(7)
P(31)	35(1)	57(1)	58(1)	1(1)	3(1)	-1(1)
O(32)	48(4)	60(4)	229(9)	1(5)	3(5)	10(3)

Table 4.24 continued

	U11	U22	U33	U23	U13	U12
O(33)	49(3)	204(9)	80(5)	-49(5)	-5(3)	-3(5)
C(34)	60(6)	173(12)	62(6)	-38(7)	-2(5)	-7(7)
C(35)	51(5)	98(8)	54(5)	-9(6)	-2(4)	-3(6)
C(36)	80(7)	105(10)	103(8)	-5(7)	-14(7)	-18(7)
C(37)	84(9)	152(15)	133(12)	-46(11)	-3(9)	-29(10)
C(38)	62(8)	221(20)	86(9)	-53(12)	-7(6)	1(11)
C(39)	101(10)	171(16)	96(10)	12(10)	12(8)	52(11)
C(40)	83(7)	101(9)	109(9)	-2(8)	12(7)	7(7)
O(41)	60(4)	114(6)	128(6)	56(5)	19(4)	-3(4)
C(42)	60(6)	87(8)	132(9)	30(7)	7(6)	-15(6)
C(43)	65(6)	56(5)	50(5)	8(4)	1(4)	-16(5)
C(44)	81(7)	73(7)	133(10)	13(7)	36(7)	5(6)
C(45)	98(9)	86(9)	195(14)	24(10)	81(9)	10(7)
C(46)	109(10)	76(8)	116(9)	15(7)	52(8)	-13(7)
C(47)	123(10)	82(8)	110(9)	26(7)	38(8)	-24(8)
C(48)	88(7)	78(7)	76(7)	2(6)	0(6)	-5(6)
P(49)	48(1)	51(1)	49(1)	11(1)	-2(1)	1(1)
O(50)	75(4)	64(4)	63(4)	5(3)	-12(3)	-10(3)
O(51)	57(3)	65(4)	53(3)	15(3)	14(3)	9(3)
C(52)	70(6)	119(9)	87(7)	56(7)	21(5)	-7(6)
C(53)	72(6)	73(7)	66(6)	17(5)	20(5)	1(5)
C(54)	110(9)	80(9)	98(9)	12(7)	21(7)	-3(7)
C(55)	181(15)	103(11)	112(11)	46(10)	8(11)	21(11)
C(56)	143(13)	136(15)	123(13)	70(12)	17(10)	26(12)
C(57)	136(12)	151(16)	93(10)	9(10)	-7(8)	-22(11)
C(58)	99(8)	85(8)	89(8)	19(7)	5(6)	-4(7)
O(59)	56(3)	65(4)	51(3)	11(3)	-1(2)	13(3)
C(60)	76(6)	78(7)	78(6)	6(6)	3(5)	30(6)
C(61)	55(6)	52(6)	117(9)	-14(6)	-6(6)	8(5)
C(62)	88(8)	90(8)	100(9)	8(7)	-22(7)	14(7)
C(63)	149(13)	88(9)	134(11)	33(8)	-57(10)	9(9)
C(64)	83(11)	99(11)	236(22)	11(13)	-53(13)	13(9)
C(65)	75(9)	105(12)	236(21)	24(13)	-9(12)	40(9)
C(66)	60(7)	92(9)	223(16)	-12(10)	-7(8)	22(7)
C(67)	51(5)	60(5)	48(5)	-11(4)	9(4)	1(4)
O(68)	84(4)	105(5)	74(4)	-34(4)	14(4)	-29(5)

Table 4.24 continued

	U11	U22	U33	U23	U13	U12
C(69)	50(5)	68(6)	51(5)	5(4)	2(4)	15(4)
C(70)	52(5)	94(7)	69(6)	-9(5)	14(4)	5(5)
C(71)	62(6)	151(11)	95(8)	17(8)	32(6)	-5(7)
C(72)	90(8)	135(12)	107(10)	49(9)	45(7)	34(8)
C(73)	106(9)	152(12)	61(6)	6(7)	36(7)	30(9)
C(74)	85(7)	121(9)	59(6)	-12(6)	8(5)	6(7)
C(75)	50(5)	63(6)	72(6)	3(5)	2(4)	8(5)
O(76)	59(4)	67(5)	217(9)	-41(6)	-48(5)	13(4)
C(77)	60(5)	63(6)	61(5)	-1(5)	12(4)	22(5)
C(78)	55(6)	79(7)	127(9)	8(7)	12(6)	17(5)
C(79)	87(8)	102(9)	128(10)	1(8)	35(7)	39(8)
C(80)	130(10)	75(8)	94(8)	-11(6)	26(7)	52(8)
C(81)	136(11)	60(8)	162(12)	-28(7)	17(9)	26(7)
C(82)	74(6)	70(7)	86(7)	-17(5)	7(5)	4(6)
C(83)	64(6)	64(6)	73(6)	26(5)	-6(5)	-11(5)
O(84)	134(7)	113(6)	139(7)	75(6)	-73(6)	-68(6)
C(85)	52(5)	73(7)	84(6)	26(6)	1(5)	9(5)
C(86)	122(10)	77(8)	132(10)	45(8)	-14(8)	-6(7)
C(87)	152(13)	122(11)	122(11)	89(10)	4(9)	5(10)
C(88)	117(10)	132(12)	94(9)	55(9)	-3(7)	40(9)
C(89)	143(11)	108(10)	72(7)	29(7)	5(7)	40(8)
C(90)	77(6)	88(7)	53(5)	20(5)	0(5)	6(6)
C(91)	31(4)	43(4)	37(4)	1(3)	-4(3)	4(3)
C(92)	31(4)	47(5)	50(4)	-1(4)	-5(3)	3(4)
C(93)	29(3)	40(4)	52(4)	-7(4)	9(3)	6(3)
C(94)	32(4)	37(4)	54(4)	3(4)	2(3)	-1(3)
C(95)	31(4)	47(5)	45(4)	1(4)	1(3)	3(3)
C(96)	29(4)	43(4)	57(5)	-2(4)	10(3)	-6(3)
O(97)	43(3)	48(3)	59(3)	3(3)	-1(2)	10(3)
O(98)	40(3)	50(3)	66(3)	7(3)	8(2)	-2(3)
O(99)	36(3)	54(3)	55(3)	0(3)	18(2)	1(2)
O(100)	33(3)	44(3)	63(3)	6(3)	1(2)	6(2)
O(101)	42(3)	59(3)	39(3)	1(3)	1(2)	-2(3)
O(102)	35(3)	48(3)	51(3)	-12(3)	11(2)	2(2)
P(103)	43(1)	56(1)	64(1)	2(1)	-5(1)	13(1)
O(105)	74(4)	81(5)	69(4)	9(3)	1(3)	31(4)

Table 4.24 continued

	U11	U22	U33	U23	U13	U12
C(106)	66(6)	147(11)	85(7)	17(7)	13(5)	40(7)
C(107)	68(6)	90(8)	61(6)	28(6)	16(5)	34(6)
C(108)	116(10)	101(10)	81(8)	18(7)	27(7)	35(8)
C(109)	90(8)	116(11)	95(8)	-6(8)	-2(7)	0(8)
C(110)	75(7)	122(11)	71(7)	28(7)	-10(5)	19(8)
C(111)	93(8)	97(9)	104(9)	31(7)	-9(7)	16(7)
C(112)	69(6)	105(9)	96(8)	30(7)	-17(6)	6(6)
O(113)	51(3)	99(5)	87(4)	0(4)	12(3)	34(4)
C(114)	78(7)	97(9)	165(12)	-10(8)	40(8)	35(7)
C(115)	82(7)	88(9)	128(10)	18(8)	38(7)	30(7)
C(116)	179(15)	126(14)	120(12)	31(10)	27(11)	13(12)
C(117)	191(19)	144(18)	189(18)	12(16)	65(15)	16(15)
C(118)	196(20)	103(13)	228(23)	-38(15)	-19(16)	69(14)
C(119)	178(19)	103(14)	334(32)	-53(17)	-50(19)	61(13)
C(120)	153(14)	101(12)	226(19)	6(12)	-29(13)	48(11)
O(104)	49(4)	83(5)	146(6)	-12(5)	-30(4)	8(4)
P(121)	94(2)	73(2)	97(2)	25(2)	29(2)	-18(2)
O(122)	307(16)	287(17)	97(7)	100(9)	-26(8)	-167(14)
O(123)	193(10)	81(6)	170(9)	6(6)	62(8)	-47(6)
C(124)	213(18)	87(11)	162(15)	-16(11)	84(15)	-17(12)
C(125)	158(15)	72(9)	159(15)	-10(10)	56(13)	-34(10)
C(126)	208(19)	104(13)	148(14)	-10(11)	67(15)	-56(14)
C(127)	254(30)	119(17)	253(29)	16(18)	71(24)	6(18)
C(128)	177(20)	109(14)	241(26)	-1(16)	-11(18)	-24(14)
C(129)	159(19)	272(33)	256(27)	100(25)	21(20)	-48(22)
C(130)	173(19)	177(19)	175(18)	33(16)	34(15)	-17(16)
O(131)	100(7)	193(12)	377(20)	134(13)	104(10)	14(8)
C(132)	84(9)	171(15)	209(15)	123(13)	-82(10)	-63(10)
C(133)	54(6)	99(9)	113(9)	16(7)	-1(6)	-22(7)
C(134)	103(9)	115(11)	111(10)	10(8)	15(7)	-36(9)
C(135)	124(13)	187(19)	145(14)	-18(13)	40(11)	-63(14)
C(136)	96(12)	235(27)	144(15)	25(17)	24(10)	-16(16)
C(137)	157(20)	195(24)	232(24)	15(21)	46(17)	22(19)
C(138)	146(16)	137(16)	271(25)	31(17)	15(17)	2(15)
P(139)	37(1)	58(1)	51(1)	-6(1)	10(1)	2(1)
O(140)	46(3)	65(4)	83(4)	-21(3)	7(3)	-8(3)

Table 4.24 continued

	U11	U22	U33	U23	U13	U12
C(141)	43(3)	69(4)	66(3)	-3(3)	13(3)	18(3)
C(142)	62(5)	72(6)	97(7)	5(6)	31(5)	20(5)
C(143)	43(5)	73(6)	76(6)	-11(5)	6(4)	16(5)
C(144)	59(6)	120(10)	98(8)	-4(7)	16(6)	6(7)
C(145)	66(8)	179(16)	142(12)	50(13)	28(9)	18(9)
C(146)	83(10)	235(23)	111(12)	30(14)	37(10)	68(13)
C(147)	129(12)	193(18)	74(8)	-29(10)	-16(9)	81(13)
C(148)	73(6)	111(9)	92(8)	-18(7)	-2(6)	27(7)
C(149)	58(3)	96(5)	54(3)	5(3)	16(3)	13(3)
C(150)	72(7)	176(14)	91(8)	30(9)	8(6)	9(8)
C(151)	90(7)	83(7)	62(6)	3(6)	13(6)	-2(6)
C(152)	142(11)	127(11)	124(11)	23(9)	79(9)	25(10)
C(153)	226(20)	178(17)	131(13)	32(13)	124(14)	23(16)
C(154)	236(23)	163(19)	81(10)	-11(11)	64(14)	-77(18)
C(155)	189(17)	126(14)	99(11)	50(10)	-9(11)	-71(13)
C(156)	114(10)	123(11)	107(10)	14(9)	-2(8)	-34(9)
C(157)	37(4)	71(6)	52(5)	-4(5)	5(4)	4(5)
O(158)	45(3)	72(5)	118(5)	-11(4)	-22(3)	10(3)
C(159)	52(5)	63(6)	76(6)	6(5)	14(5)	16(5)
C(160)	48(5)	125(10)	108(8)	32(8)	-15(5)	31(6)
C(161)	79(8)	129(12)	161(13)	80(11)	7(8)	38(9)
C(162)	90(9)	91(10)	196(15)	72(10)	32(9)	45(8)
C(163)	110(9)	73(8)	157(12)	38(8)	65(9)	24(7)
C(164)	80(6)	72(7)	82(6)	24(6)	29(5)	38(6)
C(165)	59(5)	58(5)	48(5)	2(4)	16(4)	-7(5)
O(166)	67(4)	87(5)	64(4)	12(3)	21(3)	-14(4)
C(167)	68(6)	58(5)	45(5)	0(4)	3(4)	9(5)
C(168)	114(8)	96(8)	62(6)	11(6)	19(6)	-8(7)
C(169)	148(11)	137(11)	48(6)	14(7)	-2(7)	-6(10)
C(170)	121(10)	140(12)	60(7)	14(7)	-13(7)	11(9)
C(171)	94(8)	174(14)	78(8)	23(9)	-15(7)	-22(9)
C(172)	86(7)	119(9)	48(5)	11(6)	-4(5)	-12(7)
C(173)	46(5)	98(8)	56(5)	-27(5)	6(4)	-3(5)
O(174)	79(5)	188(10)	165(8)	-138(8)	43(5)	-44(6)
C(175)	64(6)	87(7)	47(5)	-4(5)	17(4)	27(5)
C(176)	59(6)	123(9)	83(7)	19(7)	24(5)	-6(7)

Table 4.24 continued

	U11	U22	U33	U23	U13	U12
C(177)	63(7)	205(16)	117(10)	23(11)	47(7)	28(9)
C(178)	101(10)	220(20)	147(14)	82(14)	67(10)	66(12)
C(179)	114(10)	202(16)	69(7)	39(8)	52(7)	108(11)
C(180)	91(7)	143(11)	72(6)	-9(7)	5(6)	65(8)
W(1)	117(6)	110(6)	104(6)	-33(5)	-3(5)	-3(5)
W(2)	303(15)	91(7)	143(8)	-16(6)	42(9)	-32(9)

Note : W = Oxygen atom of a water molecule

Table 4.25 : Hydrogen atomic co ordinates (x 10^4) and isotropic temperature factors (x 10^3) for 4,5,6 tri *O*-benzoyl *myo*-inositol 1,2,3-tris(dibenzyl-phosphate) (**61**) and two water molecules with estimated standard deviations in parentheses

	x	y	z	U(iso)
H(01)	2547(4)	4826(4)	2402(3)	62
H(02)	3709(4)	4365(4)	3050(3)	60
H(03)	2385(4)	4431(4)	3451(3)	57
H(04)	2819(4)	5839(4)	3840(3)	61
H(05)	1541(4)	5476(4)	2904(3)	67
H(06)	3161(4)	6161(4)	2847(3)	64
H(16A)	5105(6)	4059(6)	2198(5)	121
H(16B)	4683(6)	3509(6)	1739(5)	121
H(18)	6074(7)	4818(8)	1278(6)	176
H(19)	7425(9)	4632(11)	974(8)	223
H(20)	8007(8)	3517(13)	1032(7)	203
H(21)	7301(9)	2596(10)	1424(7)	198
H(22)	5934(7)	2799(7)	1743(6)	158
H(24A)	3354(5)	4386(5)	441(3)	97
H(24B)	3908(5)	5049(5)	290(3)	97
H(26)	1662(6)	4716(5)	434(4)	110
H(27)	566(6)	5090(7)	-210(5)	136
H(28)	807(8)	5717(8)	-1038(6)	170
H(29)	2183(9)	6043(9)	-1198(5)	189
H(30)	3344(7)	5714(7)	-510(4)	139
H(34A)	4971(6)	5166(8)	4556(4)	148
H(34B)	4904(6)	5997(8)	4508(4)	148
H(36)	6119(7)	6707(7)	4906(5)	146
H(37)	7208(9)	6847(10)	5583(7)	185
H(38)	7895(8)	5914(14)	6010(6)	185
H(39)	7444(9)	4787(11)	5743(6)	184
H(40)	6234(7)	4624(7)	5053(5)	146
H(42A)	5332(6)	6416(6)	2886(5)	140
H(42B)	4931(6)	6040(6)	2311(5)	140
H(44)	7083(7)	5645(6)	2699(5)	141
H(45)	8255(8)	6088(7)	2244(7)	184

Table 4.25 continued

	x	y	z	U(iso)
H(46)	8073(9)	6983(7)	1577(6)	147
H(47)	6743(10)	7448(7)	1333(5)	155
H(48)	5588(7)	7038(6)	1800(4)	121
H(52A)	1618(6)	3433(7)	5016(4)	137
H(52B)	1426(6)	4089(7)	5409(4)	137
H(54)	2220(8)	2437(6)	5529(5)	143
H(55)	2904(11)	1909(9)	6334(7)	199
H(56)	3469(10)	2617(11)	7093(8)	200
H(57)	3372(9)	3808(10)	7061(6)	192
H(58)	2632(7)	4352(7)	6232(5)	137
H(60A)	4834(6)	3626(6)	4341(4)	116
H(60B)	4299(6)	2925(6)	4399(4)	116
H(62)	4387(7)	3017(6)	5734(5)	142
H(63)	5417(11)	2565(7)	6477(6)	192
H(64)	6758(11)	2276(9)	6213(10)	215
H(65)	7196(10)	2630(9)	5357(10)	210
H(66)	6202(7)	3049(7)	4623(7)	190
H(70)	335(5)	5024(5)	4369(3)	107
H(71)	-732(4)	4796(6)	4995(5)	152
H(72)	-584(6)	5211(7)	5959(4)	163
H(73)	632(7)	5854(7)	6298(2)	157
H(74)	1699(5)	6082(5)	5672(4)	133
H(78)	-749(4)	7074(5)	2950(5)	130
H(79)	-1290(4)	8178(6)	3180(5)	156
H(80)	-358(8)	9073(4)	3531(5)	148
H(81)	1116(7)	8865(4)	3652(5)	178
H(82)	1658(3)	7761(5)	3422(5)	115
H(86)	3047(7)	7988(5)	1453(5)	168
H(87)	2551(8)	8436(4)	535(5)	199
H(88)	1615(8)	7770(6)	-95(3)	172
H(89)	1175(6)	6656(6)	192(4)	162
H(90)	1671(6)	6207(4)	1110(4)	109
H(91)	3075(4)	2652(4)	1817(3)	56
H(92)	2102(4)	2306(4)	2505(3)	65

Table 4.25 continued

	x	y	z	U(iso)
H(93)	1856(4)	3413(4)	2031(3)	60
H(94)	709(4)	2687(4)	1181(3)	62
H(95)	2292(4)	3338(4)	921(3)	62
H(96)	2064(4)	1839(4)	954(3)	64
H(10A)	3427(6)	813(8)	3140(4)	148
H(10B)	3832(6)	1578(8)	3139(4)	148
H(108)	5075(8)	1821(7)	3789(5)	147
H(109)	6223(8)	1434(8)	4455(5)	151
H(110)	6412(7)	259(8)	4617(5)	136
H(111)	5636(7)	-541(7)	4070(5)	148
H(112)	4513(6)	-199(7)	3417(5)	137
H(11A)	5587(7)	1225(7)	1193(6)	167
H(11B)	5608(7)	978(7)	1855(6)	167
H(116)	4487(12)	263(10)	552(8)	211
H(117)	4699(14)	-978(12)	218(9)	258
H(118)	5500(15)	-1706(10)	863(11)	267
H(119)	6300(14)	-1276(10)	1645(14)	314
H(120)	6075(11)	-144(9)	2001(9)	244
H(12A)	1657(13)	575(9)	1457(8)	225
H(12B)	1070(13)	-98(9)	1389(8)	225
H(126)	2991(16)	-34(10)	1387(8)	226
H(127)	4065(19)	-788(14)	1807(14)	309
H(128)	3912(16)	-1362(11)	2693(12)	266
H(129)	2604(19)	-1218(17)	3086(12)	343
H(130)	1432(15)	-613(13)	2583(10)	261
H(13A)	-604(8)	1580(9)	1826(7)	241
H(13B)	-485(8)	2194(9)	2293(7)	241
H(134)	-1180(9)	473(8)	2360(5)	164
H(135)	-2431(12)	-1(12)	2610(8)	225
H(136)	-3350(11)	707(18)	3023(9)	236
H(137)	-3089(16)	1914(18)	3175(11)	289
H(138)	-1811(15)	2373(11)	2799(11)	277
H(14A)	-1153(6)	4788(5)	2021(4)	114
H(14B)	-372(6)	4985(5)	2473(4)	114

Table 4.25 continued

	x	y	z	U(iso)
H(144)	-2140(7)	3799(7)	2498(5)	138
H(145)	-3008(8)	3707(10)	3288(8)	192
H(146)	-2875(11)	4556(13)	4031(8)	212
H(147)	-1742(12)	5296(11)	4106(6)	200
H(148)	-811(7)	5365(7)	3354(5)	139
H(15A)	1161(7)	3405(9)	3726(5)	169
H(15B)	941(7)	2658(9)	3440(5)	169
H(152)	-782(9)	3556(8)	3999(6)	190
H(153)	-1452(13)	3247(11)	4815(8)	258
H(154)	-878(16)	2426(13)	5457(8)	236
H(155)	393(14)	1888(10)	5274(7)	208
H(156)	985(9)	2113(8)	4387(6)	173
H(160)	-1197(6)	4280(5)	138(4)	142
H(161)	-1723(5)	5425(7)	-8(4)	185
H(162)	-1124(8)	6351(4)	563(6)	187
H(163)	1(7)	6133(4)	1279(5)	165
H(164)	527(5)	4988(5)	1424(3)	115
H(168)	2196(5)	3780(6)	-1135(4)	135
H(169)	1317(7)	3938(6)	-2003(3)	168
H(170)	-83(7)	3502(7)	-2082(3)	163
H(171)	-604(4)	2910(7)	-1292(4)	175
H(172)	275(6)	2753(6)	-424(3)	127
H(176)	4666(6)	2603(5)	621(4)	131
H(177)	5992(5)	2604(6)	228(6)	189
H(178)	6248(5)	1823(8)	-526(5)	229
H(179)	5177(8)	1040(6)	-887(4)	189
H(180)	3851(6)	1039(5)	-494(4)	154

Figure 4.11 : ORTEPII drawing [Johnson, 1976] of molecule one of 4,5,6-tri-*O*-benzoyl *myo*-inositol 1,2,3-tris(dibenzyl phosphate) (**61**), showing the labelling scheme for non-H atoms (phenyl rings have been omitted for clarity). Thermal ellipsoids are drawn at the 50% probability level.

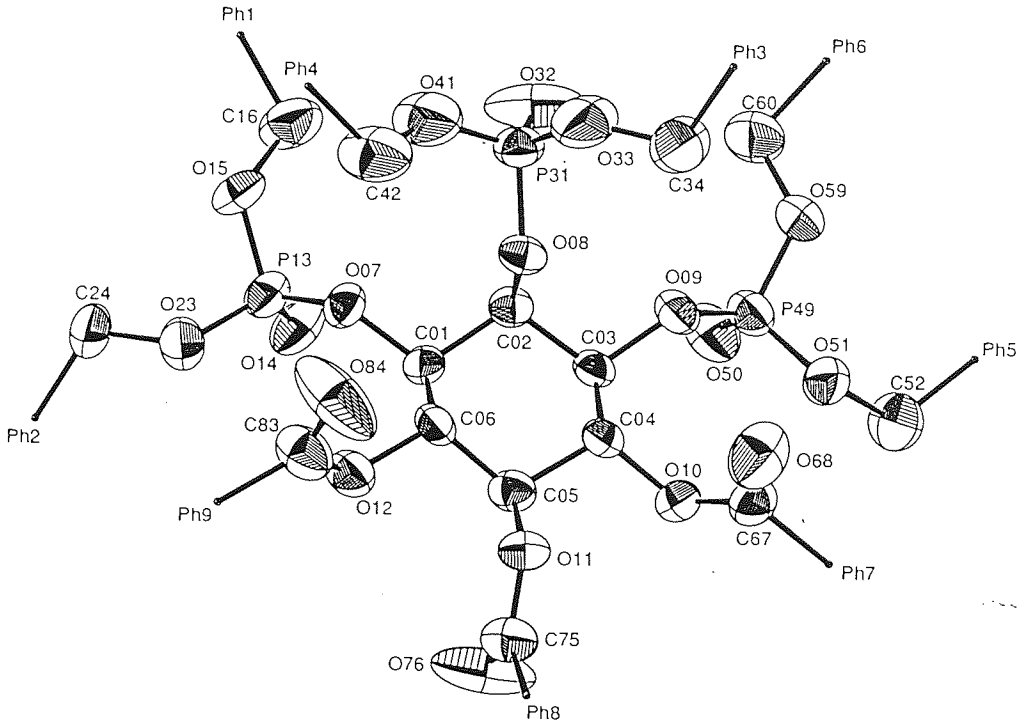

Ph1 = Phenyl ring atoms C17->C22
Ph2 = Phenyl ring atoms C25->C30
Ph3 = Phenyl ring atoms C35->C40
Ph4 = Phenyl ring atoms C43->C48
Ph5 = Phenyl ring atoms C53->C58
Ph6 = Phenyl ring atoms C61->C66
Ph7 = Phenyl ring atoms C69->C74
Ph8 = Phenyl ring atoms C77->C82
Ph9 = Phenyl ring atoms C85->C90

Figure 4.12 : ORTEPII drawing [Johnson, 1976] of molecule two of 4,5,6-tri-*O*-benzoyl *myo*-inositol 1,2,3-tris(dibenzyl phosphate) (**61**), showing the labelling scheme for non-H atoms (phenyl rings have been omitted for clarity). Thermal ellipsoids are drawn at the 50% probability level.

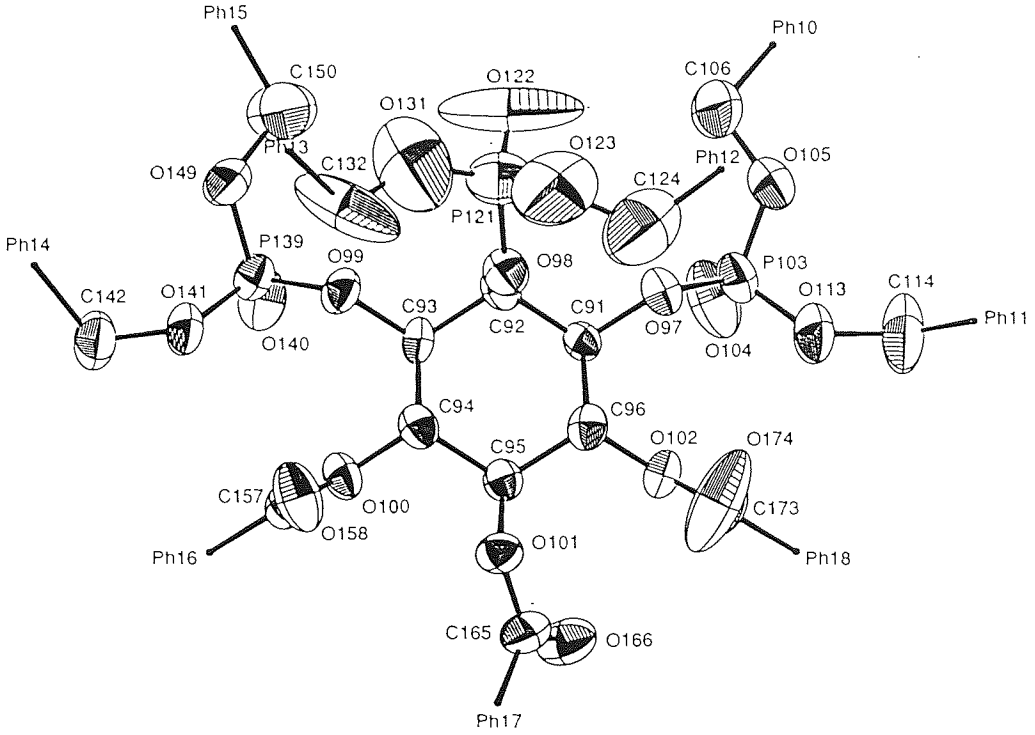

Ph10 = Phenyl ring atoms C107->C112
Ph11 = Phenyl ring atoms C115->C120
Ph12 = Phenyl ring atoms C125->C130
Ph13 = Phenyl ring atoms C133->C138
Ph14 = Phenyl ring atoms C143->C148
Ph15 = Phenyl ring atoms C151->C156
Ph16 = Phenyl ring atoms C159->C164
Ph17 = Phenyl ring atoms C167->C172
Ph18 = Phenyl ring atoms C175->C180

Table 4.26 : Asymmetry parameters for inositol rings of 4,5,6-tri-*O*-benzoyl *myo*-inositol 1,2,3-tris(dibenzyl phosphate)

Molecule 1		Molecule 2	
$\Delta C_s(1) = 6.55$	$\Delta C_2(1\text{-}2) = 10.50$	$\Delta C_s(91) = 5.95$	$\Delta C_2(91\text{-}92) = 4.15$
$\Delta C_s(2) = 8.30$	$\Delta C_2(2\text{-}3) = 7.10$	$\Delta C_s(92) = 0.39$	$\Delta C_2(92\text{-}93) = 4.61$
$\Delta C_s(3) = 1.76$	$\Delta C_2(3\text{-}4) = 3.40$	$\Delta C_s(93) = 6.24$	$\Delta C_2(93\text{-}94) = 8.56$

ΔC_s = Mirror related asymmetry parameter

ΔC_2 = Two fold related asymmetry parameter

Table 4.27 : Distances of C atoms from least squares plane for 4,5,6-tri-*O*-benzoyl *myo*-inositol 1,2,3-tris(dibenzyl phosphate)
(SHELXL-93 [Sheldrick, 1993])

For Molecule 1

Atom	**Distance**
C01	0.280(5) Å
C02	0.237(5) Å
C03	0.211(5) Å
C04	0.220(5) Å
C05	0.264(5) Å
C06	0.297(5) Å

Least squares plane
10.81(4)x + 11.73(5)y + 6.78(7)z = 11.30(2)
Rms deviation of fitted atoms = 0.253

For Molecule 2

Atom	**Distance**
C91	0.253(5) Å
C92	0.269(5) Å
C93	0.253(5) Å
C94	0.217(5) Å
C95	0.198(5) Å
C96	0.217(5) Å

Least squares plane
0.96(4)x + 14.38(4)y + 3.34(7)z = 6.13(1)
Rms deviation of fitted atoms = 0.236

mirror symmetry through the C02-C05 and C92-C95 plane. The ring of molecule one is actually flattened at C03 and puckered at the opposite end (C06), with a good mirror plane retained through C03-C06 [$\Delta C_S(3) = 1.76$] and not C02-C05. The ring of molecule two on the other hand is flattened at C95 and puckered at the opposite end (C92), with a good mirror plane retained through C92-C95 [$\Delta C_S(92) = 1.76$] as expected. The distances of ring atoms from the least squares plane (Table 4.27) confirm this distortion, showing that C03 and C95 are pulled in closer to the plane and that C06 and C92 are pushed out further away from the plane. The symmetry of molecule two is also conveyed in the distance from the least squares plane with the mirror symmetry related pairs C91, C93 and C94, C96 having the same values. The differences in ring distortion for the same chemical structure are probably caused by crystal packing and hydrogen bonding, and were also seen for the two enantiomeric inositol molecules in the crystal structure of triol **61**.

All the phosphorus atoms are positioned with similar angles to the inositol C-O bonds, and are comparable with the angles of $InsP_6$ [Blank *et al.*, 1975] and *myo*-inositol 2-phosphate [Yoo *et al.*, 1974]. Molecule one has P13 and P49 orientated in the same direction towards C02 and C04 respectively, whereas P31 is orientated in the opposite direction towards C01. Molecule two has P103 orientated towards C96, whereas P121 and P139 are orientated in the opposite direction towards C93 and C94 respectively. This shows that in both molecules the phosphorus atoms are not positioned in such a way as to conserve the expected mirror symmetry through the C02-C05 and C92-C95 planes. In *myo*-inositol 2-phosphate [Yoo *et al.*, 1974], the phosphorus atom was positioned towards C3 and again the possible mirror symmetry was lost. Yoo and co-workers attributed the symmetry loss to an asymmetrical hydrogen bonding environment. In 4,5,6-tri-*O*-benzoyl *myo*-inositol 1,2,3-tris(dibenzyl phosphate), the position of the phosphorus atoms in both molecules could be affected by hydrogen bonding (see later) between water molecules and P=O groups, but also could be influenced by the high steric crowding around the inositol ring. The P-O and P=O bond distances are in good agreement with one another, except for bonds P121=O122 and P121-O131, which are much shorter than expected. Bond O131-C132 is also short and

the angles between P121, O131 and C132 are unusually large. These unexpected distances and angles are most likely caused by vibration of these atoms, evident by high temperature factors (Figure 4.12). It is difficult to get reasonable bond lengths and angles in regions of high movement because a single value does not express all possible atomic positions. The phosphate groups are essentially tetrahedral with O-P-O angles ranging from 101.6(3) to 116.9(5), similar to $InsP_6$ [99.0(4)-115.0(4), Blank *et al.*, 1975] and *myo*-inositol 2-phosphate [107.3(1)-115.7(1), Yoo *et al.*, 1974]. All the P=O bonds are angled close to the inositol C-O bond (-15.3 to 14.8) which allows the bulkier benzyl groups to be positioned furthest away.

The six P-O-benzyl groups attached to inositol each have three bonds through which rotation may occur and consequently they exhibit conformational flexibility. In the crystal structure of (+/-)-3,4-di-*O*-acetyl-1,2,5,6-tetra-*O*-benzyl *myo*-inositol [Steiner *et al.*, 1993], this flexibility of benzyl groups may have contributed to the phase transitions between three different crystal forms and to the disorder observed in a benzyl group. Also the benzyl groups in the latter structure exhibited large thermal parameters which suggested extensive thermal vibrations. Here, the benzyl groups of both molecules of **61** have bond distances and angles which are comparable with one another. There is some deviation from expected values, but this is not surprising when the thermal displacements are considered. The benzyl CH_2 groups have angles varying from *trans* to *gauche* with respect to the P-O bond. The phenyl groups are also orientated between *gauche* and *trans* with respect to both the O-CH_2 and the CH_2-C(Ph) bonds, which emphasises the flexibility of these side groups.

The three benzoyl groups have bond lengths and bond angles which are in good agreement with each other and the carbonyl linkages are similar to the structure of 1,2,3,4,5,6-hexa-*O*-acetyl *myo*-inositol [Abboud *et al.*, 1990]. The carbonyl carbons of molecule one, C75 and C83 are orientated towards C06 and C01 respectively, whereas C67 is orientated in the opposite direction towards C03. The carbonyl carbons of molecule two, C157 and C173 are positioned towards C95, with C165 angled towards C96. The C=O bonds of the benzoyl groups point in the same direction as the C-H bonds on the inositol ring and are approximately coplanar with their corresponding

inositol C-O bonds (C-O-C-O torsion angles range from 3.7 to 14.2°). This *s-trans* conformation was seen both for the fully protected inositol **59** and in the crystal structure of 1,2,3,4,5,6-hexa-*O*-acetyl-*myo*-inositol [Abboud *et al.*, 1990]. The phenyl groups of the benzoyl substituents are all positioned *trans* with respect to both their corresponding inositol C-O bond and O-C carbonyl linkage. The phenyl groups are therefore orientated so that they cause least steric hindrance which again was also observed in the crystal structure of **59**.

The two water molecules (only oxygen positions found) have contact distances from electronegative atoms that would be acceptable for hydrogen bond distances. Water molecule W1 is 2.778(8)Å from O50 (P=O) and 3.02(2)Å from water molecule W2 with an angle of 105.7(3)° between these two contacts. The two water molecules therefore form a dimer which was also seen in the crystal structure of *myo*-inositol dihydrate [Lomer *et al.*, 1963]. W2 is 2.82(1)Å from O104 (P=O) and 2.72(1)Å from O32 (P=O), with an angle of 130.2(5)° between these two contacts. Hence water molecule W2 forms a water bridge between the two inositol molecules.

4.2.5 Crystal structure of monosodium tetra(cyclohexylammonium) *myo*-inositol 1,2,3-trisphosphate (57)

4.2.5.1 Experimental

Monosodium tetra(cyclohexylammonium) *myo*-inositol 1,2,3-trisphosphate (**57**) slowly crystallised in methanol, water and acetone to form tabular colourless crystals. A single crystal (0.45 x 0.25 x 0.15 mm) was chosen for X-ray determination. The density of the crystals was determined by flotation in *m*-xylene and bromobenzene. The data were collected from an Enraf-Nonius CAD4 diffractometer with monochromated graphite Mo-Kα radiation, λ = 0.71069Å at 293 K.

4.2.5.2 Crystal data

Monosodium tetra(cyclohexylammonium) *myo*-inositol 1,2,3-trisphosphate (**57**) $(C_6H_{14}N^+)_4Na^+C_6H_{10}O_{15}P_3^{5-}.6.5H_2O.CH_3OH)$ crystallises in the triclinic space group $P\bar{1}$ with a = 12.355(2), b = 14.803(2), c = 15.101(2)Å, α = 102.90(1), β = 112.570(13), γ = 93.380(11)°, Z = 2 and V = 2453.6(6)Å^3. The formula weight is 987.41 (F(000) = 1065) and the measured density D_m = 1.319 Mg m^{-3} with the calculated density D_X = 1.336 Mg m^{-3}. The absorption coefficient μ = 0.209 mm^{-1}.

4.2.5.3 Data collection

Unit cell dimensions were obtained from least squares analysis of setting angles of 25 accurately centred reflections, $8.49 \leq \theta \leq 14.79°$. Intensity data were collected by the ω-2θ scan technique, Bragg angle $2.12 \leq \theta \leq 25.04°$. The ω scan angle was calculated from $[M+N(\tan\theta)]°$, where M=1, N=0.35 and increased by 25% on each side for background determination. The ω scan speed was varied from 0.5 to 2.8°min^{-1} depending upon intensity. Six different standard reflections were used during data collection: three intensity reflections (measured every three hours) and three orientation reflections (monitored every 200 reflections). No crystal movement was detected during collection. The 9291 reflections were measured for $-14 \leq h \leq 14$, $-17 \leq k \leq 1$, $-17 \leq l \leq 17$ and merged to give 8607 independent reflections (R_{int} = 0.0514).

4.2.5.4 Structural determination and refinement

Lorentz, polarisation and intensity corrections (10.5% decay) were applied to the collected data. The space group was determined unambiguously as a result of structure analysis. An initial structure was solved by direct methods using MULTAN-84 [Main *et al.*, 1984) with default options. Normalised structure factors were calculated and phases were determined from F_{obs} values. The distribution of intensities was found to closely follow the theoretical values for a centric structure. The phase set with the best

combined figure of merit gave an E-map from which a preliminary structure was determined. Using the atomic positions determined from the E-map, the remaining non-hydrogen atoms were located for the inositol molecule in an electron density map using SHELXL-93 [Sheldrick, 1993]. Four cyclohexylammonium cations and one sodium were also located in the electon density map, showing the inositol molecule existed as its sodium tetra(cyclohexylammonium) salt.

Full-matrix least-squares refinement of atomic positions and anisotropic temperature factors (for non-hydrogen atoms) on $Fobs^2$ using SHELXL-93 [Sheldrick, 1993], located seven molecules of water and a molecule of methanol in one asymmetric unit. One of the cyclohexylammonium cations was found to be disordered. The best fit model for this disorder was two half-occupied rings with three of the ring carbon atoms having two different positions each. The cyclohexane ring bond distances were restrained to 1.5Å with an estimated standard deviation of 0.03. Hamilton's test (Hamilton, 1974) was performed to show that the introduction of three more carbon atoms (i.e. 27 more parameters) into the structure refinement, gave a reduction in the R value that was significantly greater than that expected just from an increase in the degrees of freedom. Comparison of the weighted R values from SHELXL-93 [Sheldrick, 1993] for three and six carbon atom sites gave a ratio of 1.024:1. The expected ratio from the introduction of 27 more degrees of freedom was 1.003:1 (α = 0.01). This shows that the extra three carbon atoms make a significant difference in the R value at a 99% probability. One of the water molecules was found to sit in a special position and so its site was also half-occupied. From difference electron density maps, hydrogen positions were found for 2 x OH (inositol), OH methanol and water hydrogen positions. The other hydrogen atoms were placed in calculated positions and their temperature factors were set at 1.5 times the value of the riding atom. Further refinement of the structure, which included parameters for atomic co-ordinates, temperature factors (anisotropic for non-hydrogen atoms and isotropic for hydrogen atoms), overall scale factor and an extinction parameter, were carried out. In the weighting scheme $1/[\sigma^2(Fo^2)+(0.1000P)^2+0.0000P]$ where $P=(Fo^2+2Fc^2)/3$, the parameters converged at discrepancy indices R = 0.0704 and Rw = 0.1764 for 4267

observed reflections [Fo > 4σ(Fo)]. The final maximum shift / e.s.d. ratio was 0.004 and the maximum and minimum features on a difference Fourier map were 0.906 and -0.666 e $Å^{-3}$.

4.2.5.5 Results and discussion

Full structural data for the crystal structure of monosodium tetra(cyclohexylammonium) *myo*-inositol 1,2,3-trisphosphate are given in Tables 4.28 (non-hydrogen atomic co-ordinates), 4.29 (bond lengths and angles), 4.30 (anisotropic displacement parameters), 4.31 (hydrogen atomic co-ordinates and their isotropic temperature factors) and torsional angles are in Appendix 1.

The *myo*-inositol ring possesses the expected chair conformation with 1-axial/5-equatorial oxygen positions (Figure 4.13). The inositol ring and phosphate groups have bond distances and angles (Table 4.29) that are consistent with those of *myo*-inositol 2-phosphate [Yoo *et al.*, 1974]. The asymmetry parameters for the inositol ring (Table 4.32) are very small for all planes and the estimated standard deviations for the ring torsional angles involved (Appendix 1) are significant when considering such small distortions, therefore it is difficult to describe the type of ring distortion present. The inositol ring is slightly distorted from an ideal cyclohexane chair, the presence or absence of phosphate groups making little difference to the ring conformation. The distances of inositol ring atoms from a least squares plane are shown in Table 4.33 and emphasize that no particular carbon atom sits exceptionally near to or far from the plane, which is consistent with the very small deviations in asymmetry parameters from zero.

The phosphorus atoms are all found to be orientated in the same direction towards C04. The phosphate groups are essentially tetrahedral with O-P-O angles ranging from 101.8(2) to 118.7(2), similar to fully protected inositol **61**, $InsP_6$ [Blank *et al.*, 1975] and *myo*-inositol 2-phosphate [Yoo *et al.*, 1974]: these large ranges are normally observed in flexible phosphate geometry. The ester P-O bond lengths [1.607(4)-

Table 4.28 : Atomic co-ordinates of non-hydrogen atoms (x 10^4) and equivalent isotropic temperature factors (x 10^3) for monosodium tetra(cyclohexylammonium) *myo*-inositol 1,2,3-trisphosphate (**57**) and solvents (seven water molecules and methanol) with estimated standard deviations in parentheses. U(eq) is defined as one third of the trace of the orthogonalized U_{ij} tensor.

	x	y	z	U(eq)
C(01)	2906(4)	675(4)	3245(3)	25(1)
C(02)	3766(4)	500(4)	2749(3)	24(1)
C(03)	4704(4)	-18(4)	3325(3)	26(1)
C(04)	4150(4)	-943(4)	3382(4)	26(1)
C(05)	3299(4)	-747(4)	3868(4)	28(1)
C(06)	2330(4)	-231(4)	3318(3)	26(1)
O(07)	5538(3)	-144(2)	2885(2)	28(1)
O(08)	3149(3)	-56(2)	1737(2)	27(1)
O(09)	1976(3)	1133(3)	2700(2)	32(1)
O(10)	1556(4)	-43(3)	3797(3)	40(1)
O(11)	2805(4)	-1597(3)	3945(3)	42(1)
O(12)	5028(3)	-1404(3)	3960(3)	40(1)
P(13)	6955(1)	45(1)	3563(1)	31(1)
P(14)	2892(1)	379(1)	796(1)	28(1)
P(15)	2124(1)	2260(1)	2983(1)	38(1)
O(13A)	7179(3)	-668(3)	4171(3)	37(1)
O(13B)	7292(3)	1035(3)	4225(3)	40(1)
O(13C)	7456(3)	-123(3)	2783(3)	38(1)
O(14A)	3217(4)	1436(3)	1173(3)	42(1)
O(14B)	1584(3)	75(3)	160(3)	45(1)
O(14C)	3633(4)	-41(3)	278(3)	44(1)
O(15A)	2552(4)	2642(3)	4077(3)	53(1)
O(15B)	942(4)	2438(3)	2327(3)	50(1)
O(15C)	3123(4)	2573(3)	2676(4)	52(1)
CA1	-62(5)	2042(4)	-374(4)	38(1)
CA2	894(6)	2894(5)	112(5)	57(2)
CA3	675(7)	3562(5)	-563(6)	70(2)
CA4	-554(7)	3821(5)	-812(7)	79(3)
CA5	-1492(6)	2949(5)	-1297(6)	66(2)
CA6	-1274(5)	2306(5)	-623(5)	51(2)

Table 4.28 continued

	x	y	z	U(eq)
NA1	147(4)	1425(3)	308(3)	42(1)
CB1	4694(5)	1982(4)	-568(4)	41(1)
CB2	5288(6)	2272(4)	-1190(5)	52(2)
CB3	5544(7)	3354(5)	-921(7)	75(2)
CB4	4442(8)	3762(6)	-1059(7)	81(3)
CB5	3857(11)	3466(6)	-454(9)	109(4)
CB6	3591(7)	2410(5)	-702(7)	72(2)
NB1	4406(4)	941(3)	-833(3)	35(1)
CC1	5446(6)	3912(4)	5809(5)	47(2)
CC2	6747(7)	4033(6)	6447(7)	92(3)
CC3	7188(8)	5052(5)	7122(8)	101(4)
CC4	6474(11)	5282(6)	7732(7)	103(4)
CC5	5186(10)	5146(7)	7082(8)	117(4)
CC6	4769(9)	4131(6)	6418(7)	97(3)
NC1	5019(4)	2926(3)	5154(3)	44(1)
CD1	-1191(10)	3575(7)	2872(7)	102(3)
CD2	-1541(13)	3757(7)	1906(8)	132(5)
CD3	-2024(19)	4682(10)	1863(14)	206(8)
CD4A	-1096(35)	5451(27)	2525(22)	182(24)
CD5A	-567(33)	5278(15)	3536(19)	162(14)
CD6A	-224(18)	4303(12)	3544(17)	108(9)
CD4B	-1149(45)	5443(22)	2686(28)	352(65)
CD5B	-1704(40)	5168(19)	3328(39)	217(24)
CD6B	-1282(53)	4282(28)	3655(21)	286(29)
ND1	-894(5)	2651(4)	2866(4)	63(2)
SOD1	9455(2)	-222(2)	3208(2)	70(1)
WO2	2829(4)	-1196(3)	-1641(4)	54(1)
WO3	5545(5)	2353(4)	1959(4)	62(1)
WO4	422(4)	-101(4)	-1853(3)	71(2)
WO5	6288(5)	2617(4)	3988(4)	70(2)
WO6	8237(6)	-2227(5)	4411(6)	114(2)
WO7	9633(18)	8110(7)	3134(8)	204(5)
WO8	0	0	5000	222(7)
MC1	9315(12)	2391(10)	4714(10)	154(5)
MO1	9508(9)	1501(7)	4256(7)	169(4)

Note : W = Oxygen atom of water SOD = Sodium atom

Table 4.29 : Bond lengths (Å) and bond angles (°) for monosodium tetra(cyclohexylammonium) *myo*-inositol 1,2,3-trisphosphate (**57**) and solvents (seven water molecules and methanol) with estimated standard deviations in parentheses.

Bond	Distance (Å)	Bond	Distance (Å)
C(02)-C(01)	1.521(7)	CA5-CA6	1.506(9)
C(03)-C(02)	1.522(6)	CB1-NB1	1.487(7)
C(03)-C(04)	1.529(7)	CB1-CB6	1.498(9)
C(03)-C(06)	1.526(7)	CB1-CB2	1.509(8)
C(05)-C(04)	1.504(7)	CB2-CB3	1.542(9)
C(06)-C(05)	1.528(7)	CB3-CB4	1.482(11)
C(01)-O(09)	1.440(6)	CB4-CB5	1.482(11)
C(02)-O(08)	1.437(5)	CB5-CB6	1.508(11)
C(03)-O(07)	1.426(6)	CC1-CC6	1.464(10)
C(04)-O(12)	1.425(6)	CC1-CC2	1.499(10)
C(05)-O(11)	1.413(6)	CC1-NC1	1.499(7)
C(06)-O(10)	1.409(6)	CC2-CC3	1.550(11)
O(07)-P(13)	1.622(3)	CC3-CC4	1.503(14)
O(08)-P(14)	1.619(3)	CC4-CC5	1.487(14)
O(09)-P(15)	1.607(4)	CC5-CC6	1.539(11)
O(10)-SOD1#1	2.375(5)	CD1-CD6A	1.43(2)
P(13)-O(13B)	1.508(4)	CD1-ND1	1.437(10)
P(13)-O(13C)	1.510(4)	CD1-CD6B	1.44(3)
P(13)-O(13A)	1.518(4)	CD1-CD2	1.447(12)
P(14)-O(14C)	1.495(4)	CD2-CD3	1.53(2)
P(14)-O(14B)	1.506(4)	CD3-CD4A	1.44(2)
P(14)-O(14A)	1.512(4)	CD3-CD4B	1.48(3)
P(15)-O(15A)	1.486(4)	CD4A-CD5A	1.50(3)
P(15)-O(15B)	1.495(4)	CD5A-CD6A	1.53(2)
P(15)-O(15C)	1.556(5)	CD4B-CD5B	1.49(3)
O(13C)-SOD1	2.323(4)	CD5B-CD6B	1.55(3)
CA1-NA1	1.485(7)	SOD1-WO4#2	2.261(5)
CA1-CA6	1.496(8)	SOD1-O(10)#3	2.375(5)
CA1-CA2	1.507(8)	SOD1-WO8#3	2.462(3)
CA2-CA3	1.535(9)	SOD1-WO7#4	2.473(11)
CA3-CA4	1.513(10)	SOD1-MO1	2.668(11)
CA4-CA5	1.515(10)	MC1-MO1	1.423(14)

Table 4.29 continued

Bonds	Angles (°)	Bonds	Angles (°)
O(07)-C(03)-C(02)	108.7(4)	O(14C)-P(14)-O(14B)	112.0(2)
O(07)-C(03)-C(04)	112.7(4)	O(14C)-P(14)-O(14A)	112.0(2)
C(02)-C(03)-C(04)	111.8(4)	O(14B)-P(14)-O(14A)	111.8(2)
O(08)-C(02)-C(03)	109.4(4)	O(14C)-P(14)-O(08)	106.7(2)
O(08)-C(02)-C(01)	110.5(4)	O(14B)-P(14)-O(08)	105.2(2)
C(03)-C(02)-C(01)	108.8(4)	O(14A)-P(14)-O(08)	108.8(2)
O(09)-C(01)-C(02)	110.6(4)	O(15A)-P(15)-O(15B)	118.7(2)
O(09)-C(01)-C(06)	108.1(4)	O(15A)-P(15)-O(15C)	107.8(3)
C(02)-C(01)-C(06)	112.4(4)	O(15B)-P(15)-O(15C)	111.7(3)
O(10)-C(06)-C(01)	111.0(4)	O(15A)-P(15)-O(09)	110.0(2)
O(10)-C(06)-C(05)	111.1(4)	O(15B)-P(15)-O(09)	103.0(2)
C(01)-C(06)-C(05)	109.3(4)	O(15C)-P(15)-O(09)	104.7(2)
O(11)-C(05)-C(04)	109.6(4)	P(13)-O(13C)-SOD1	121.1(2)
O(11)-C(05)-C(06)	111.3(4)	NA1-CA1-CA6	109.9(5)
C(04)-C(05)-C(06)	112.2(4)	NA1-CA1-CA2	109.0(5)
O(12)-C(04)-C(05)	107.9(4)	CA6-CA1-CA2	111.7(5)
O(12)-C(04)-C(03)	111.6(4)	CA1-CA2-CA3	110.1(6)
C(05)-C(04)-C(03)	109.3(4)	CA4-CA3-CA2	110.3(6)
C(03)-O(07)-P(13)	121.3(3)	CA3-CA4-CA5	110.7(6)
C(02)-O(08)-P(14)	122.6(3)	CA6-CA5-CA4	110.3(6)
C(01)-O(09)-P(15)	120.2(3)	CA1-CA6-CA5	110.6(6)
C(06)-O(10)-SOD1#1	133.1(3)	NB1-CB1-CB6	110.2(5)
O(13B)-P(13)-O(13C)	114.4(2)	NB1-CB1-CB2	110.1(5)
O(13B)-P(13)-O(13A)	111.2(2)	CB6-CB1-CB2	111.1(5)
O(13C)-P(13)-O(13A)	113.8(2)	CB1-CB2-CB3	108.9(6)
O(13B)-P(13)-O(07)	108.4(2)	CB4-CB3-CB2	111.2(6)
O(13C)-P(13)-O(07)	101.8(2)	CB5-CB4-CB3	111.2(7)
O(13A)-P(13)-O(07)	106.3(2)	CB4-CB5-CB6	110.9(7)

Table 4.29 continued

Bonds	Angles (°)	Bonds	Angles (°)
CB1-CB6-CB5	111.2(7)	CD3-CD4B-CD5B	87(3)
CC6-CC1-CC2	111.0(7)	CD4B-CD5B-CD6B	112(3)
CC6-CC1-NC1	110.3(6)	CD1-CD6B-CD5B	113(2)
CC2-CC1-NC1	109.8(5)	WO4#2-SOD1-O(13C)	97.5(2)
CC1-CC2-CC3	109.7(7)	WO4#2-SOD1-O(10)#3	83.2(2)
CC4-CC3-CC2	110.2(8)	O(13C)-SOD1-O(10)#3	170.0(2)
CC5-CC4-CC3	110.9(8)	WO4#2-SOD1-WO8#3	155.6(2)
CC4-CC5-CC6	109.9(9)	O(13C)-SOD1-WO8#3	96.25(12)
CC1-CC6-CC5	110.8(7)	O(10)#3-SOD1-WO8#3	79.87(13)
CD6A-CD1-ND1	112.9(11)	WO4#2-SOD1-WO7#4	109.2(3)
ND1-CD1-CD6B	130(2)	O(13C)-SOD1-WO7#4	106.1(5)
CD6A-CD1-CD2	106.0(14)	O(10)#3-SOD1-WO7#4	82.9(5)
ND1-CD1-CD2	112.5(8)	WO8#3-SOD1-WO7#4	86.0(3)
CD6B-CD1-CD2	118(2)	WO4#2-SOD1-MO1	100.3(3)
CD1-CD2-CD3	113.2(11)	O(13C)-SOD1-MO1	77.0(3)
CD4A-CD3-CD2	109(2)	O(10)#3-SOD1-MO1	93.0(3)
CD4B-CD3-CD2	108(2)	WO8#3-SOD1-MO1	63.5(2)
CD3-CD4A-CD5A	109(2)	WO7#4-SOD1-MO1	149.4(3)
CD4A-CD5A-CD6A	115(3)	SOD1#6-WO8-SOD1#1	180.0
CD1-CD6A-CD5A	112(2)	MC1-MO1-SOD1	169.8(9)

Symmetry transformations used to generate equivalent atoms

#1	X-1, Y, Z	#2	1-X, -Y, -Z	#3	X+1, Y, Z
#4	X, Y-1, Z	#5	X, Y+1, Z	#6	1-X, -Y, 1-Z

Note : W = Oxygen atom of water SOD = Sodium atom

Table 4.30 : Anisotropic displacement parameters (x 10^3, for non-hydrogen atoms) for monosodium tetra(cyclohexylammonium) *myo*-inositol 1,2,3-trisphosphate (**57**) and solvents (seven water molecules and methanol) with estimated standard deviations in parentheses

	U11	U22	U33	U23	U13	U12
C(01)	20(3)	33(3)	18(2)	9(2)	3(2)	6(2)
C(02)	23(3)	31(3)	17(2)	9(2)	5(2)	3(2)
C(03)	24(3)	36(3)	20(3)	10(2)	8(2)	5(2)
C(04)	28(3)	30(3)	22(3)	12(2)	9(2)	6(2)
C(05)	29(3)	32(3)	21(3)	7(2)	11(2)	-1(2)
C(06)	21(3)	43(3)	17(2)	5(2)	11(2)	4(2)
O(07)	21(2)	45(2)	21(2)	12(2)	10(2)	9(2)
O(08)	33(2)	28(2)	17(2)	7(2)	6(2)	1(2)
O(09)	21(2)	40(2)	30(2)	12(2)	3(2)	10(2)
O(10)	24(2)	70(3)	29(2)	18(2)	11(2)	11(2)
O(11)	58(3)	41(3)	38(3)	15(2)	29(2)	0(2)
O(12)	34(2)	48(3)	50(2)	30(2)	18(2)	14(2)
P(13)	24(1)	48(1)	24(1)	13(1)	10(1)	8(1)
P(14)	26(1)	39(1)	20(1)	14(1)	6(1)	5(1)
P(15)	37(1)	34(1)	34(1)	5(1)	6(1)	11(1)
O(13A)	34(2)	49(2)	29(2)	17(2)	10(2)	13(2)
O(13B)	35(2)	48(3)	34(2)	12(2)	13(2)	-3(2)
O(13C)	29(2)	66(3)	25(2)	12(2)	16(2)	11(2)
O(14A)	56(3)	34(2)	32(2)	15(2)	13(2)	2(2)
O(14B)	32(2)	65(3)	31(2)	22(2)	1(2)	2(2)
O(14C)	54(3)	60(3)	38(2)	27(2)	29(2)	24(2)
O(15A)	59(3)	43(3)	36(2)	-4(2)	6(2)	15(2)
O(15B)	45(3)	50(3)	48(2)	16(2)	7(2)	29(2)
O(15C)	53(3)	33(3)	66(3)	7(2)	23(3)	1(2)
CA1	38(3)	41(4)	33(3)	9(3)	12(3)	10(3)
CA2	38(4)	62(5)	71(5)	22(4)	18(3)	3(3)
CA3	69(5)	58(5)	76(5)	28(4)	20(4)	-2(4)
CA4	67(5)	60(5)	104(7)	45(5)	16(5)	13(4)
CA5	53(4)	59(5)	80(5)	36(4)	10(4)	17(4)
CA6	37(4)	55(4)	51(4)	15(3)	7(3)	8(3)
NA1	36(3)	43(3)	42(3)	12(2)	10(2)	7(2)
CB1	48(4)	40(4)	38(3)	16(3)	19(3)	3(3)

Table 4.30 continued

	U11	U22	U33	U23	U13	U12
CB2	56(4)	44(4)	73(5)	25(3)	37(4)	10(3)
CB3	78(6)	59(5)	98(6)	28(5)	46(5)	-4(4)
CB4	109(7)	52(5)	105(7)	38(5)	57(6)	28(5)
CB5	161(10)	65(6)	172(10)	58(7)	125(9)	55(6)
CB6	75(5)	56(5)	125(7)	45(5)	69(5)	33(4)
NB1	39(3)	45(3)	26(2)	16(2)	15(2)	8(2)
CC1	57(4)	30(3)	44(4)	15(3)	8(3)	2(3)
CC2	73(6)	52(5)	97(6)	1(5)	-10(5)	-6(4)
CC3	82(6)	43(5)	120(8)	9(5)	-10(6)	-17(4)
CC4	164(11)	59(6)	61(6)	10(5)	30(7)	-23(6)
CC5	118(9)	91(8)	109(8)	-40(6)	55(7)	-27(6)
CC6	104(7)	76(6)	87(6)	-35(5)	54(6)	-35(5)
NC1	52(3)	34(3)	36(3)	12(2)	7(2)	3(2)
CD1	149(10)	89(7)	86(7)	32(6)	61(7)	45(7)
CD2	221(14)	76(7)	110(9)	41(6)	68(9)	41(8)
CD3	293(24)	105(11)	194(17)	77(12)	47(17)	61(14)
CD4A	215(41)	195(48)	89(22)	46(25)	22(24)	-77(33)
CD5A	209(35)	77(20)	97(19)	-28(15)	-15(20)	6(20)
CD6A	113(17)	59(12)	74(14)	-15(10)	-27(12)	8(11)
CD4B	667(154)	82(31)	219(64)	119(40)	43(73)	77(55)
CD5B	217(40)	56(18)	379(68)	-35(28)	169(47)	40(22)
CD6B	388(78)	369(75)	62(19)	69(32)	48(35)	23(67)
ND1	59(4)	73(4)	66(4)	28(3)	30(3)	13(3)
SOD1	32(1)	134(3)	49(2)	30(2)	17(1)	22(2)
WO2	64(3)	51(3)	45(3)	16(2)	21(2)	7(2)
WO3	58(3)	72(4)	49(3)	13(3)	19(3)	5(3)
WO4	36(3)	132(5)	41(3)	38(3)	5(2)	-2(3)
WO5	89(4)	73(4)	52(3)	22(3)	27(3)	22(3)
WO6	95(5)	93(5)	161(7)	52(5)	47(5)	32(4)
WO7	337(18)	137(9)	138(8)	52(7)	84(9)	64(9)

Note : W = Oxygen atom of water SOD = Sodium atom

Table 4.31 : Hydrogen atomic co-ordinates (x 10^4) and isotropic temperature factors (x 10^3) for monosodium tetra(cyclohexylammonium) *myo*-inositol 1,2,3 trisphosphate (**57**) and solvents (seven water molecules and methanol) with estimated standard deviations in parentheses

	x	y	z	U(iso)
H(01)	3343(4)	1086(4)	3919(3)	37
H(02)	4151(4)	1103(4)	2759(3)	36
H(03)	5126(4)	383(4)	4005(3)	39
H(04)	3720(4)	-1356(4)	2709(4)	39
H(05)	3751(4)	-344(4)	4544(4)	41
H(06)	1868(4)	-631(4)	2643(3)	40
H(10)	1841(59)	30(48)	4296(48)	49(24)
H(11)	2803(48)	-1448(38)	4446(40)	22(16)
H(12)	5680(10)	-1205(34)	3992(42)	60
H(15C)	3005(53)	2233(44)	2051(47)	45(19)
HA1	-15(5)	1697(4)	-989(4)	58
HA2A	1664(6)	2702(5)	233(5)	86
HA2B	896(6)	3217(5)	747(5)	86
HA3A	1265(7)	4126(5)	-228(6)	104
HA3B	752(7)	3261(5)	-1171(6)	104
HA4A	-694(7)	4221(5)	-1260(7)	118
HA4B	-608(7)	4168(5)	-209(7)	118
HA5A	-2272(6)	3127(5)	-1436(6)	99
HA5B	-1474(6)	2623(5)	-1923(6)	99
HA6A	-1347(5)	2617(5)	-16(5)	76
HA6B	-1867(5)	1743(5)	-949(5)	76
HA1A	869(4)	1270(3)	454(3)	63
HA1B	-395(4)	907(3)	15(3)	63
HA1C	91(4)	1728(3)	865(3)	63
HB1	5247(5)	2205(4)	134(4)	61
HB2A	4774(6)	2026(4)	-1891(5)	78
HB2B	6025(6)	2021(4)	-1063(5)	78
HB3A	6109(7)	3592(5)	-233(7)	112
HB3B	5895(7)	3545(5)	-1338(7)	112
HB4A	4632(8)	4441(6)	-868(7)	121

Table 4.31 continued

	x	y	z	U(iso)
HB4B	3900(8)	3562(6)	-1756(7)	121
HB5A	3124(11)	3721(6)	-579(9)	163
HB5B	4372(11)	3713(6)	247(9)	163
HB6A	3245(7)	2233(5)	-275(7)	108
HB6B	3016(7)	2168(5)	-1386(7)	108
HB1A	5067(4)	695(3)	-751(3)	52
HB1B	3889(4)	730(3)	-1465(3)	52
HB1C	4090(4)	776(3)	-442(3)	52
HC1	5323(6)	4344(4)	5385(5)	70
HC2A	7182(7)	3901(6)	6030(7)	138
HC2B	6890(7)	3595(6)	6856(7)	138
HC3A	8020(8)	5120(5)	7560(8)	152
HC3B	7110(8)	5486(5)	6714(8)	152
HC4A	6605(11)	4881(6)	8179(7)	154
HC4B	6737(11)	5929(6)	8131(7)	154
HC5A	5045(10)	5580(7)	6668(8)	175
HC5B	4739(10)	5275(7)	7489(8)	175
HC6A	4870(9)	3700(6)	6833(7)	145
HC6B	3931(9)	4050(6)	5990(7)	145
HC1A	5436(4)	2802(3)	4787(3)	65
HC1B	4254(4)	2865(3)	4757(3)	65
HC1C	5113(4)	2527(3)	5530(3)	65
HD1	-1855(10)	3634(7)	3073(7)	152
HD2A	-2144(13)	3246(7)	1411(8)	198
HD2B	-859(13)	3773(7)	1736(8)	198
HD3A	-2306(19)	4745(10)	1189(14)	309
HD3B	-2686(19)	4687(10)	2058(14)	309
HD4A	-1417(35)	6034(27)	2568(22)	274
HD4B	-488(35)	5504(27)	2273(22)	274
HD5A	-1133(33)	5368(15)	3837(19)	242
HD5B	136(33)	5744(15)	3948(19)	242
HD6A	444(18)	4247(12)	3359(17)	162
HD6B	22(18)	4229(12)	4213(17)	162
HD4C	-1243(45)	6068(22)	2598(28)	528

Table 4.31 continued

	x	y	z	U(iso)
HD4D	-330(45)	5345(22)	2868(28)	528
HD5C	-2560(40)	5047(19)	2966(39)	326
HD5D	-1507(40)	5685(19)	3915(39)	326
HD6C	-512(53)	4465(28)	4213(21)	430
HD6D	-1835(53)	4017(28)	3878(21)	430
HD1A	-686(5)	2569(4)	3473(4)	94
HD1B	-291(5)	2586(4)	2684(4)	94
HD1C	-1520(5)	2224(4)	2437(4)	94
W(2HA)	2664(73)	-874(57)	-2002(61)	80
W(2HB)	3081(66)	-876(53)	-937(62)	80
W(3HA)	4957(79)	2197(67)	1668(69)	92
W(3HB)	5908(75)	1915(59)	1674(62)	92
W(4HA)	-390	-200	-1917	107
W(4HB)	865	-200	-1270	107
W(5HA)	6105(81)	2557(65)	3373(70)	106
W(5HB)	6559(80)	2054(65)	4064(66)	106
W(6HA)	8459	-2000	3818	171
W(6HB)	7599	-1800	4226	171
W(7HA)	8777	8000	2976	492(245)
W(7HB)	9760	8400	2819	30(17)
W(8HA)	0	600	5026	333
HC1D	10059(12)	2749(10)	5208(10)	231
HC1E	8783(12)	2302(10)	5023(10)	231
HC1F	8974(12)	2721(10)	4219(10)	231
HO1	9436	1482	3686	253

Figure 4.13 : ORTEPII drawing [Johnson, 1976] of *myo*-inositol 1,2,3-trisphosphate (**57**) and sodium cation, showing the labelling scheme for non-H atoms (water, methanol and cyclohexylammonium cations are omitted for clarity). Thermal ellipsoids are drawn at the 50% probability level.

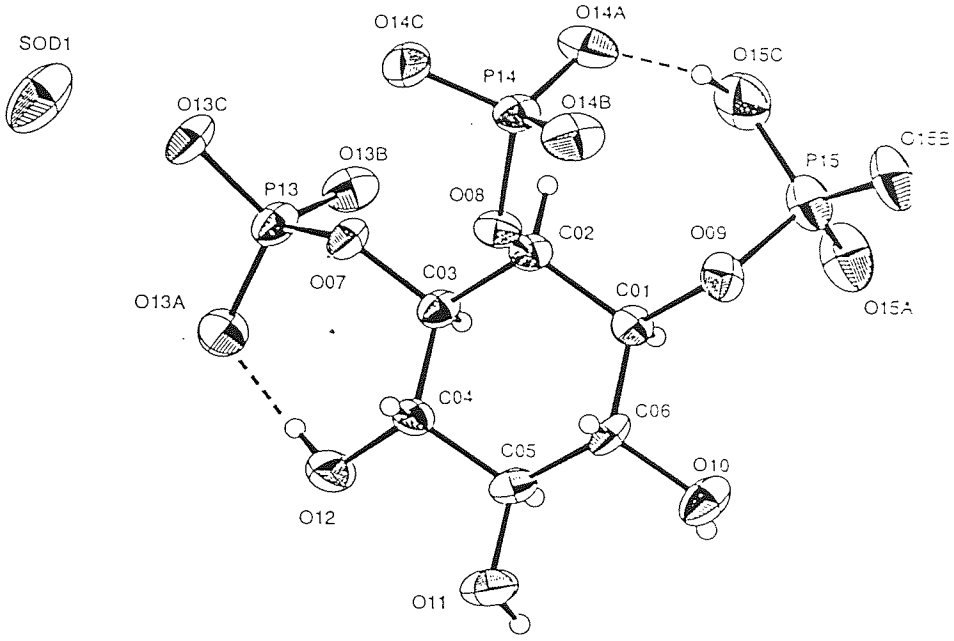

Table 4.32 : Asymmetry parameters for inositol rings of monosodium tetra(cyclohexylammonium) *myo*-inositol 1,2,3-trisphosphate (**57**)

$\Delta C_s(1) = 1.05$	$\Delta C_2(1\text{-}2) = 1.30$
$\Delta C_s(2) = 1.45$	$\Delta C_2(2\text{-}3) = 1.77$
$\Delta C_s(3) = 0.48$	$\Delta C_2(3\text{-}4) = 0.47$

ΔC_s = Mirror related asymmetry parameter
ΔC_2 = Two fold related asymmetry parameter

Table 4.33 : Distances of C atoms from least squares plane for monosodium tetra(cyclohexylammonium) *myo*-inositol 1,2,3-trisphosphate (**57**) (SHELXL-93 [Sheldrick, 1993]).

Atom	Distance
C01	0.245(4) Å
C02	0.242(4) Å
C03	0.235(4) Å
C04	0.230(4) Å
C05	0.235(4) Å
C06	0.243(4) Å

Least squares plane
1.52(3)x + 5.02(3)y + 10.49(2)z = 3.95(1)
Rms deviation of fitted atoms = 0.238

1.622(3)Å] are longer than for fully protected inositol **61** [1.556(5)-1.587(5)Å] and 1.586(2)Å for *myo*-inositol 2-phosphate [Yoo *et al.*, 1974] but are similar to $InsP_6$ [1.616(5)-1.647(6)Å, Blank *et al.*, 1975]. The P-O^- bond lengths are in between those expected for P=O and P-O-H which shows that they have some double bond character. The P15-O15 bond is longer which is expected for a POH group. The phosphate oxygens for P13 and P15 are positioned in the anticipated *gauche* and *trans* orientation to the C-O inositol bond. In contrast, P14 has an oxygen (O14A) angled close (9.1°) to the C-O inositol bond and its other two oxygens angled anticlinal. These latter oxygens are rotated to allow O14A to accept the hydrogen bond from O15C (Figure 4.13).

Overall the expected structural symmetry through C02-C05 is conserved in the inositol ring but is lost when including the phosphate groups. The phosphate group positioning is most likely influenced by the hydrogen bonding environment and sodium cation co-ordination (see below).

The high thermal displacements of the cyclohexylammonium atoms give rise to variable bond lengths and angles. Cyclohexylammonium ring D (atoms ND1 to CD6B) had the worst geometry but this is because it is disordered with the best fit model being two half-occupied rings, with three of the ring carbon atoms having two different positions each. The model does not completely describe the disorder but does represent the positions where the atoms are most likely to be found. The water molecules also have high temperature displacements.

The ions and solvent molecules are linked by numerous hydrogen bonds (Figures 4.14, 4.15, 4.16 and 4.17). Geometric data for hydrogen bonds involving atoms of **57** as both donors and acceptors (Table 4.34) are in good agreement with surveyed data [Steiner & Saenger, 1992]. Oxygen anions of phosphate groups are the best acceptors, receiving up to three hydrogen bonds each, whereas the oxygen of the POH group does not accept any hydrogen bonds. Phosphate groups P13 and P14 accept hydrogen bonds from water, cyclohexylammonium cations and hydroxy groups whereas P15 accepts only from cyclohexylammonium cations. The oxygen atom of methanol accepts a hydrogen bond from water molecule WO8 and four water molecules also function as hydrogen bond acceptors. Water molecules WO5 and WO2 accept hydrogen bonds from cyclohexylammonium cations. WO2, WO3 and WO7 accept hydrogen bonds from neighbouring water molecules (WO2 accepting two hydrogen bonds overall). Only one of the inositol hydroxyl groups (O12) accepts a hydrogen and this is from a cyclohexylammonium cation. Inositol hydroxyl group O12, which is adjacent to phosphate (P13), forms an intramolecular hydrogen bond but the other two hydroxyl groups prefer intermolecular bonding to the same symmetry related phosphate (P15). Another intramolecular interaction occurs between the two phosphate groups P14 and P15 (O15C-H15C and O14A), whose bond is particularly short and strong. The four cyclohexylammonium groups each donate three hydrogen bonds. All the water

Figure 4.14 : ORTEPII drawing [Johnson, 1976] showing the position of the cyclohexylammonium A cation with respect to *myo*-inositol 1,2,3-trisphosphate (**57**) and its labelling scheme for non-H atoms. Other cations, water molecules and selective hydrogen bonding are also shown. Thermal ellipsoids are drawn at the 50% probability level.

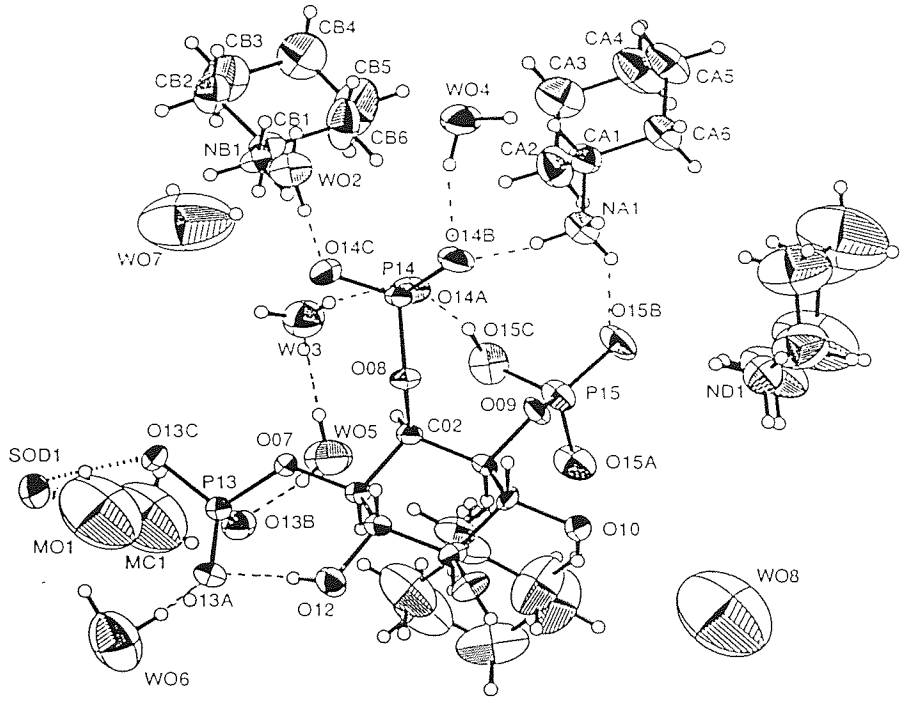

Figure 4.15 : ORTEPII drawing [Johnson, 1976] showing the position of the cyclohexylammonium B cation with respect to *myo*-inositol 1,2,3-trisphosphate (**57**) and its labelling scheme for non-H atoms. Other cations, water molecules and selective hydrogen bonding are also shown. Thermal ellipsoids are drawn at the 50% probability level.

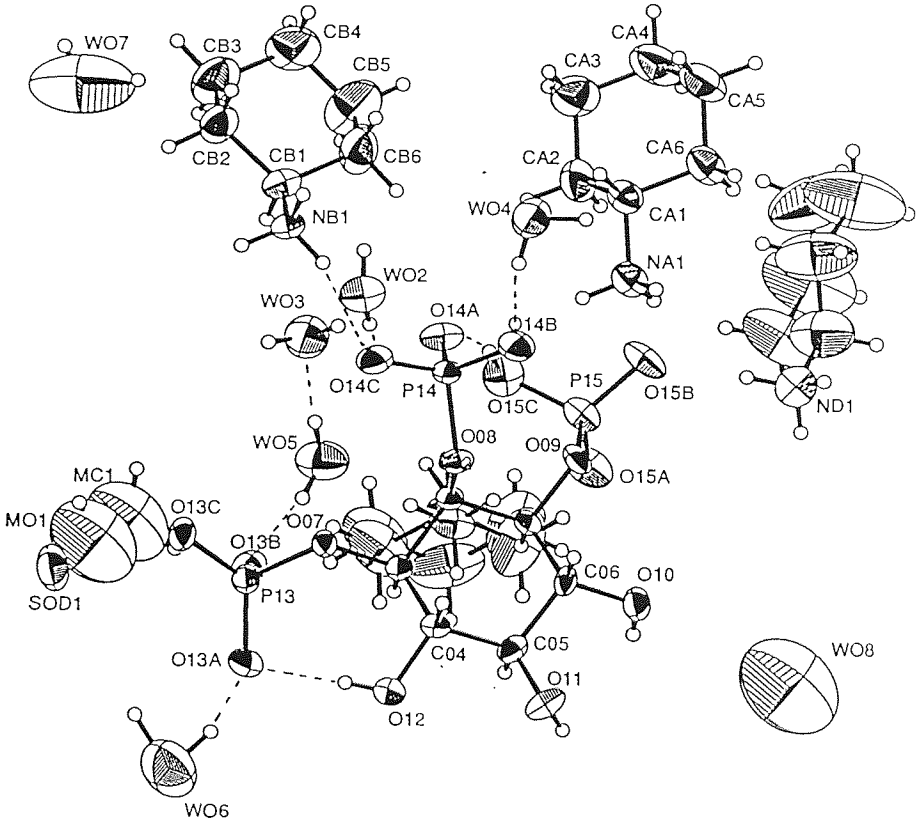

Figure 4.16 : ORTEPII drawing [Johnson, 1976] showing the position of the cyclohexylammonium C cation with respect to *myo*-inositol 1,2,3-trisphosphate (**57**) and its labelling scheme for non-H atoms. Other cations, water molecules and selective hydrogen bonding are also shown. Thermal ellipsoids are drawn at the 50% probability level.

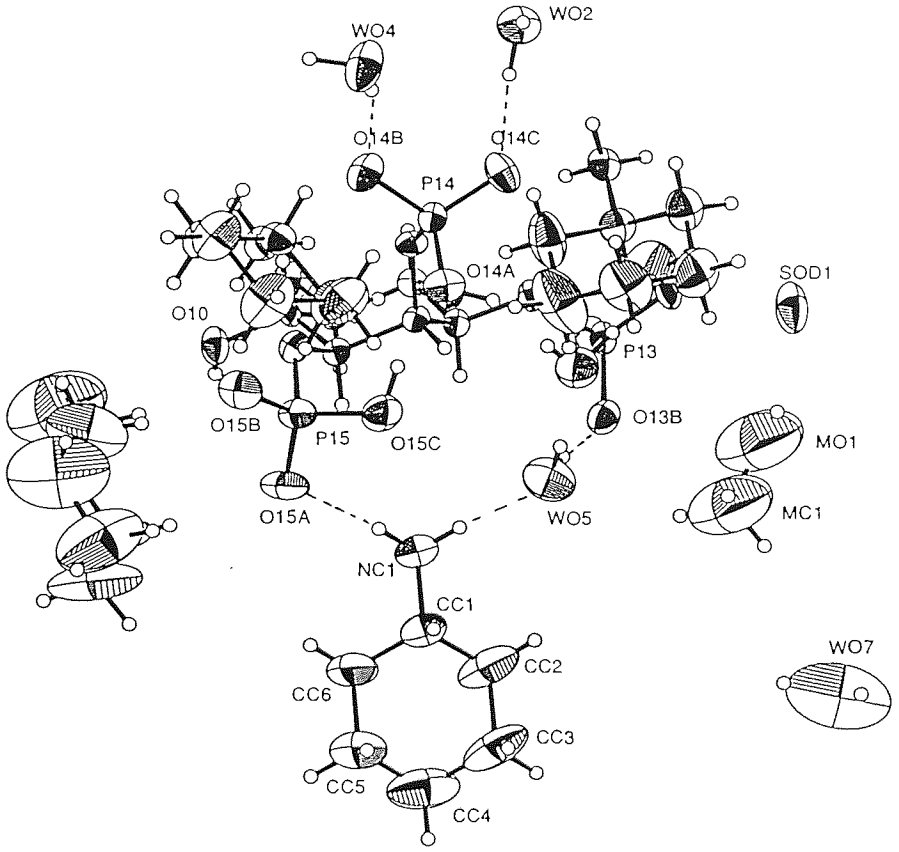

Figure 4.17 : ORTEPII drawing [Johnson, 1976] showing the position of the cyclohexylammonium D cation with respect to *myo*-inositol 1,2,3-trisphosphate (**57**) and its labelling scheme for non-H atoms. Other cations, water molecules and selective hydrogen bonding are also shown. Thermal ellipsoids are drawn at the 50% probability level.

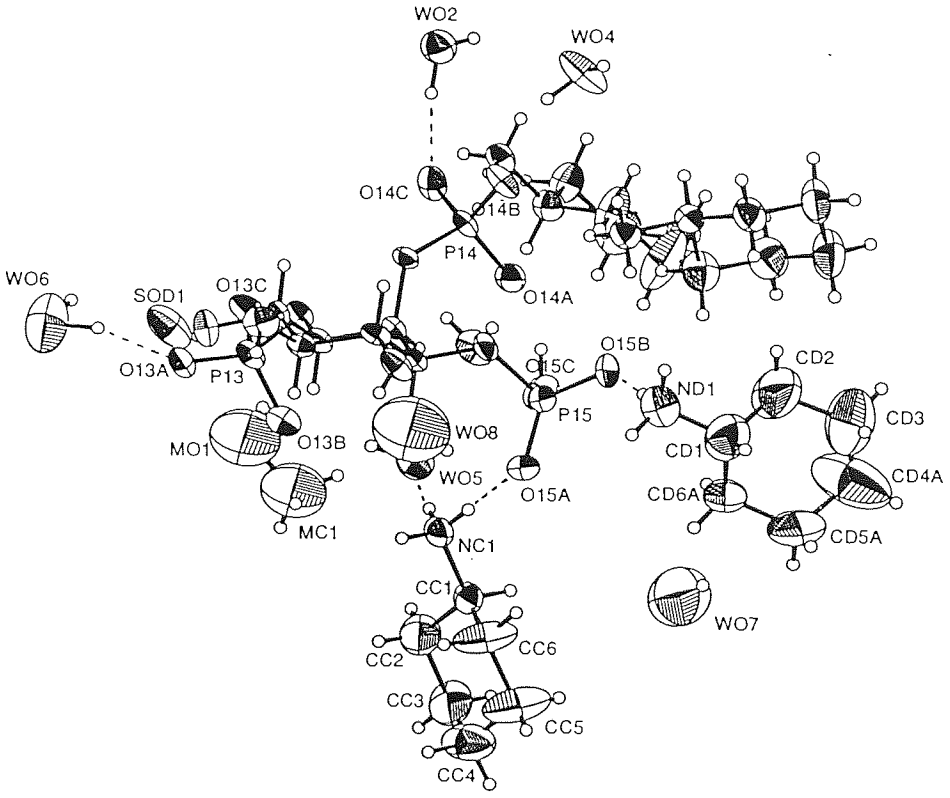

Table 4.34 : Hydrogen bond distances (Å) and hydrogen bond angles (°) for monosodium tetra(cyclohexylammonium) *myo*-inositol 1,2,3-trisphosphate (**57**) and solvents (seven water molecules and methanol) with estimated standard deviations in parentheses

	$d_{O/N.....O}$ (Å)	$d_{O/N-H.....O}$ (Å)	$a_{O/N-H.....O}$ (°)	Sym. accep.[a]
O10-H10...O13A	2.766(6)	2.111(65)	163(8)	1-X, -Y, 1-Z
O11-H11...O13B	2.754(6)	2.014(56)	177(6)	1-X, -Y, 1-Z
O12-H12[b]...O13A	2.685(5)	1.867(8)	175(7)	X, Y, Z
O15C-H15C...O14A	2.553(6)	1.680(64)	158(6)	X, Y, Z
NA1-HA1B...O14B	2.753(6)	1.903(6)	159(0)	-X, -Y, -Z
NA1-HA1A...O14B	2.779(6)	2.061(6)	137(0)	X, Y, Z
NA1-HA1C...O15B	2.826(6)	2.033(6)	148(0)	X, Y, Z
NB1-HB1A...O14C	2.770(6)	1.908(6)	162(0)	1-X, -Y, -Z
NB1-HB1B...O13C	2.882(6)	2.004(6)	169(0)	1-X, -Y, -Z
NB1-HB1C...O14C	2.827(6)	1.984(6)	158(0)	X, Y, Z
NC1-HC1A...WO5	2.760(8)	1.871(8)	176(0)	X, Y, Z
NC1-HC1B...O15A	2.801(7)	1.922(7)	170(0)	X, Y, Z
NC1-HC1C...O12	2.875(6)	2.008(6)	164(0)	1-X, -Y, 1-Z
ND1-HD1B...O15B	2.701(7)	1.811(7)	179(0)	X, Y, Z
ND1-HDIC...WO2	2.827(8)	1.943(8)	172(0)	-X, -Y, -Z
ND1-HD1A...MO1	2.906(12)	2.150(12)	142(0)	X-1, Y, Z
WO2-W2HA...O13C	2.833(6)	2.085(88)	167(9)	1-X, -Y, -Z
WO2-W2HB...O14C	2.770(7)	1.796(90)	165(7)	X, Y, Z
WO3-W3HA...O14A	2.779(6)	2.134(91)	159(11)	X, Y, Z
WO3-W3HB...WO2	2.825(8)	1.951(86)	156(7)	1-X, -Y, -Z
WO4-W4HA...O09	2.904(6)	2.078(3)	142(0)	-X, -Y, -Z
WO4-W4HB...O14B	2.760(5)	1.926(4)	155(0)	X, Y, Z
WO5-W5HA...WO3	2.765(7)	1.919(95)	174(9)	X, Y, Z
WO5-W5HB...O13B	2.743(7)	1.820(93)	172(8)	X, Y, Z
WO6-W6HA...WO7	3.134(18)	2.097(18)	150(0)	X, Y-1, Z
WO6-W6HB...O13A	2.745(7)	1.794(4)	151(0)	X, Y, Z
WO8-W8HA...MO1	2.705(10)	1.935(10)	145(0)	X-1, Y, Z

a) Symmetry operation to be applied to the acceptor atom.

b) Calculated hydrogen position based on electron density and subjected to rotating group refinement

molecules except WO8, WO7 and WO4 donate a hydrogen bond to both a neighbouring water molecule and a phosphate oxygen anion. Water molecule WO4 hydrogen bonds to both O09 and O14B, forming a water bridge between two symmetry related molecules whereas WO7 does not donate any hydrogen bonds.

The sodium cation is surrounded by six oxygen atoms in essentially octahedral co-ordination: one from phosphate O13C, one from hydroxyl O10, three from water and one from methanol (Table 4.52). The sodium oxygen contact distances are comparable with those of $InsP_6$ (2.191-2.899Å) [Blank *et al.*, 1975]. The phosphate and hydroxyl co-ordinate at opposite ends, and water molecule WO8 bridges between symmetry related sodium cations.

Table 4.35 : Sodium cation contact distances (Å) for monosodium tetra(cyclohexylammonium) *myo*-inositol 1,2,3-trisphosphate (**57**) with estimated standard deviations in parentheses

	*d*Na.....O (Å)	Symm.ligand
SOD1...WO4	2.261(5)	1-X, -Y, -Z
SOD1...WO7	2.473(11)	X, Y-1, Z
SOD1...O13C	2.323(4)	X, Y, Z
SOD1...WO8	2.462(3)	X+1, Y, Z
SOD1...O10	2.375(5)	X+1, Y, Z
SOD1...MO1	2.668(11)	X, Y, Z

Overall the phosphate group positions are stabilised by both intramolecular hydrogen bonding and also by two cyclohexylammonium cation bridges in which P14 has all its oxygens participating. Stabilisation also comes from hydrogen bonding of the phosphate groups with water molecules and symmetry related hydroxyl group.

The protonation sequences of *myo*-inositol 1,4,5-trisphosphate and related compounds have been analysed by potentiometric and ^{31}P NMR spectroscopy measurements [Schmitt *et al.*, 1993, a]. It was suggested that vicinal phosphate groups repel each other to minimise charge interactions: This brings the phosphate groups into close proximity with neighbouring hydroxyl groups, resulting in hydrogen bonding and a reduction in

the phosphate basicity. This is verified in the crystal structure of **57** by the intramolecular hydrogen bonding between the O12 hydroxyl and O13A-P13 phosphate group (Figure 4.18 and Table 4.51), and by the existence of sodium cation co-ordination to O13C-P13 even after treatment with Dowex-H^+. The first protonation site of fully ionised *myo*-inositol 1,4,5-trisphosphate was estimated to be shared between the phosphate groups at positions 4 and 5 [Schmitt *et al.*, 1993, a]. The first protonation site of *myo*-inositol 1,2,6-trisphosphate, with three vicinal phosphate groups, was also suggested to be stabilised by strong hydrogen bonding [Mernissi-Arifi *et al.*, 1994]. The intramolecular hydrogen bond between the neighbouring P15 and P14 phosphate groups of **57** (Figure 4.18) adds support to proton sharing, and accounts for the high sixth pKa value (reported as 9.56 [Schmitt, 1993, b]) of *myo*-inositol 1,2,3-trisphosphate.

The two possible chair conformations for *myo*-inositol 1,2,3-trisphosphate (fully ionised) were optimised using semi-empirical molecular orbital calculations. AM1 parameters were used in MOPAC [Stewart, 1990] through CHEM-X [Chemical Design, 1994] with GNORM = 0.5 and CHARGE = -6. The initial structures were adapted from crystal structure geometry. The heat of formation values obtained were -173.9 kcal mol^{-1} (1-ax/5-eq) and -151.3 kcal mol^{-1} (5-ax/1-eq) confirming that the equatorial-axial-equatorial orientation of the three phosphate groups is the more stable conformation.

4.2.6 Crystal structure of D/L-*cis*-1,2-*O*-cyclohexylidene-3,4,5,6-tetra-*O*-benzyl *myo*-inositol

4.2.6.1 Experimental

D/L-*cis*-1,2-*O*-Cyclohexylidene-3,4,5,6-tetra-*O*-benzyl *myo*-inositol slowly crystallised from ethyl acetate and hexane to form colourless rectangular plate crystals. A single crystal (0.48 x 0.43 x 0.35 mm) was chosen for X-ray determination. The data were

collected from an Enraf-Nonius CAD4 diffractometer with monochromated graphite Mo-Kα radiation, λ = 0.71069Å at 293 K.

4.2.6.2 Crystal data

D/L-*cis*-1,2-*O*-Cyclohexylidene-3,4,5,6-tetra-*O*-benzyl *myo*-inositol ($C_{40}H_{44}O_6$) crystallises in the monoclinic space group $P2_1/c$ with a = 10.608(3), b = 19.147(6), c = 17.448(5)Å, α = 90, β = 107.22(2), γ = 90°, Z = 4 and V = 3385.0(17)Å^3. The formula weight is 620.75 (F(000) = 1328) and the calculated density D_X = 1.218 Mg m^{-3}. The absorption coefficient μ = 0.081 mm^{-1}.

4.2.6.3 Data collection

Unit cell dimensions were obtained from least squares analysis of setting angles of 25 accurately centred reflections, 9.78 ≤ θ ≤ 13.96°. Intensity data were collected by the ω-2θ scan technique, Bragg angle 2.01 ≤ θ ≤ 24.97°. The ω scan angle was calculated from [*M*+*N*(tanθ)]°, where *M* = 0.9, *N* = 0.35 and increased by 25% on each side for background determination. The ω scan speed was varied from 0.9 to 2.8°min^{-1} depending upon intensity. Six different standard reflections were used during data collection: three intensity reflections (measured every three hours) and three orientation reflections (monitored every 200 reflections). No appreciable loss of intensity or crystal movement was detected during collection. The 5893 reflections were measured for -12 ≤ h ≤ 5, -22 ≤ k ≤ 0, -20 ≤ l ≤ 20 and merged to give 5893 independent reflections (R_{int} = 0.0261).

4.2.6.4 Structural determination and refinement.

Lorentz, polarisation and intensity corrections (4.4% decay) were applied to the collected data. The space group was determined unambiguously as a result of structure analysis. An initial structure was solved by direct methods using MULTAN-84 [Main

et al., 1984] with default options. Normalised structure factors were calculated and phases were determined, from Fobs values. The distribution of intensities was found to closely follow the theoretical values for a centric structure. The phase set with the best combined figure of merit gave an E-map from which a preliminary structure was determined. Using the atomic positions determined from the E-map, the remaining non-hydrogen atoms were located in an electron density map using SHELXL-93 [Sheldrick, 1993].

Full-matrix least-squares refinement of atomic positions and anisotropic temperature factors (for non-hydrogen atoms) on $Fobs^2$ was performed using SHELXL-93.

From difference electron density maps, hydrogen positions were found for all groups except one benzyl group which had its hydrogen atoms placed in calculated positions to ride on attached atoms, with common temperature factors set as free variables in chemical groups of similar kind. Further refinement of the structure, which included parameters for atomic co-ordinates, temperature factors (anisotropic for non-hydrogen atoms and isotropic for hydrogen atoms), overall scale factor and an extinction parameter, were carried out. In the weighting scheme $1/[s^2(Fo^2)+(0.1000P)^2+0.0000P]$ where $P=(Fo^2+2Fc^2)/3$, the parameters converged at discrepancy indices R = 0.0525 and Rw = 0.1389 for 2702 observed reflections [$Fo > 4\sigma(Fo)$]. The final maximum shift / e.s.d. ratio was 0.000 and the maximum and minimum features on a difference Fourier map were 0.226 and -0.178 e $Å^{-3}$.

4.2.6.5 Results and discussion

Full structural data for the crystal structure of D/L-*cis*-1,2-*O*-cyclohexylidene-3,4,5,6-tetra-*O*-benzyl *myo*-inositol are given in Tables 4.36 (non-hydrogen atomic co-ordinates), 4.37 (bond lengths and angles), 4.38 (anisotropic displacement parameters), 4.39 (hydrogen atomic co-ordinates and their isotropic temperature factors) and torsional angles are in Appendix 1.

The inositol ring is in a distorted chair conformation with the oxygen at C02 (Figure 4.18) in the expected axial position and the other five oxygen atoms in equatorial

positions. All the C-C and C-O bond lengths (Table 4.37) were comparable with those of *myo*-inositol [Rabinowitz & Kraut, 1964]. However the inositol ring angles (Table 4.37) deviate from expected values except for position C06 (*myo*-inositol has a mean angle of 110.7° [Rabinowitz & Kraut, 1964], and 111° expected for the perfect chair [Bucourt, 1974]) with the largest deviation at position C02. The torsion angle O08-C02-C03-O09 = 38.6(3)° which would normally be closer to 60°, shows that the inositol oxygen atoms at the *cis* ring junction have moved closer together to accommodate the acetal linkage which was also seen in the crystal structures of diol **3**, triol **58** and fully protected inositol **59**. The *cis* junction has expected endocyclic torsion angles which have the same sign and have a similar value [C1-C2-C3-C4 = 39.3(4)° and O8-C2-C3-O7 = 38.6(3)°]. The asymmetry parameters of the inositol ring were calculated [Duax & Norton, 1975] and are shown in Table 4.40. The inositol ring is twisted with a good two-fold axis retained [ΔC_2(2-3) = 3.17], which is in contrast to the fully protected inositol **59** which had a flattened/puckered ring. The benzyl groups appear to impose less steric hindrance onto the inositol ring than the bulky silyl and benzoyl groups of **59** and therefore allow twisting of the ring to accommodate the five-membered acetal ring linkage. The distances of ring atoms from best fit planes (Table 4.41) confirm the ring distortion, showing that the inositol carbon atoms C02 and C03 are pulled in much closer to the plane, and C05 and C06 are pushed further away from the plane.

The cyclohexylidene ring is in the chair conformation with ring and torsion angles slightly deviating from that of the perfect chair [Bucourt, 1974]. The slight distortion is expected as compensation for the acetal linkage.

The acetal five-membered ring adopts a distorted envelope with atom C02 below a C03, O08, O09, C20 plane with $\Delta C_S(3)$ = 1.60.

The four P-O-benzyl groups have three bonds through which rotation may occur and consequently they exhibit conformational flexibility as shown in both the crystal structures of (+/-)-3,4-di-*O*-acetyl-1,2,5,6-tetra-*O*-benzyl *myo*-inositol [Steiner *et al.*, 1993] and **61**. The benzyl groups have bond distances and angles which are comparable with one another. The CH_2 groups C40 and C33 are orientated towards C05, and the

Table 4.36 : Atomic co-ordinates of non-hydrogen atoms (x 10^4) and equivalent isotropic temperature factors (x 10^3) for D/L-*cis*-1,2-*O*-cyclohexylidene-3,4,5,6-tetra-*O*-benzyl *myo*-inositol with estimated standard deviations in parentheses

	x	y	z	U(eq)
C(01)	454(3)	2984(2)	1147(2)	62(1)
C(02)	1825(3)	3287(2)	1486(2)	60(1)
C(03)	1950(3)	4067(2)	1400(2)	63(1)
C(04)	810(4)	4485(2)	1530(2)	62(1)
C(05)	-522(3)	4175(2)	1086(2)	61(1)
C(06)	-593(3)	3422(2)	1345(2)	59(1)
O(07)	349(2)	2291(1)	1412(1)	68(1)
O(08)	2285(2)	3204(1)	2338(1)	64(1)
O(09)	3160(2)	4207(1)	2013(1)	70(1)
O(10)	896(2)	5191(1)	1293(1)	72(1)
O(11)	-1506(2)	4574(1)	1290(1)	70(1)
O(12)	-1859(2)	3131(1)	963(1)	68(1)
C(13)	1154(4)	1799(2)	1166(3)	83(1)
C(14)	591(4)	1077(2)	1189(2)	67(1)
C(15)	1413(5)	541(3)	1592(3)	94(1)
C(16)	925(6)	-142(2)	1571(4)	102(2)
C(17)	-358(6)	-262(3)	1144(3)	98(2)
C(18)	-1173(6)	272(3)	781(3)	101(1)
C(19)	-685(5)	933(3)	811(3)	92(1)
C(20)	3376(3)	3664(2)	2609(2)	61(1)
C(21)	4678(4)	3300(2)	2655(3)	76(1)
C(22)	5851(4)	3767(3)	3005(3)	90(1)
C(23)	5855(5)	4036(4)	3814(3)	107(2)
C(24)	4577(6)	4426(3)	3761(3)	106(2)
C(25)	3389(4)	3959(2)	3406(3)	79(1)
C(26)	-2576(5)	4807(3)	645(3)	92(1)
C(27)	-3357(4)	5305(2)	979(2)	76(1)
C(28)	-2953(5)	5992(2)	1136(3)	90(1)
C(29)	-3613(5)	6442(3)	1499(3)	97(1)

Table 4.36 continued

	x	y	z	U(eq)
C(30)	-4694(5)	6214(2)	1705(3)	93(1)
C(31)	-5106(5)	5541(2)	1546(3)	94(1)
C(32)	-4442(5)	5092(3)	1188(3)	89(1)
C(33)	957(6)	5680(2)	1906(3)	91(1)
C(34)	924(4)	6408(2)	1588(2)	66(1)
C(35)	1703(4)	6623(2)	1130(2)	73(1)
C(36)	1673(5)	7307(2)	868(3)	82(1)
C(37)	858(5)	7771(2)	1063(3)	84(1)
C(38)	68(5)	7577(2)	1500(3)	85(1)
C(39)	108(4)	6900(2)	1769(3)	81(1)
C(40)	-2587(5)	2983(4)	1492(3)	147(3)
C(41)	-3742(4)	2522(2)	1101(2)	76(1)
C(42)	-3810(7)	1874(4)	1381(4)	134(2)
C(43)	-4930(11)	1464(3)	1086(5)	165(3)
C(44)	-5945(7)	1731(4)	508(4)	127(2)
C(45)	-5893(5)	2358(4)	232(3)	115(2)
C(46)	-4801(5)	2765(2)	529(3)	96(1)

Table 4.37 : Bond lengths (Å) and bond angles (°) for D/L-*cis*-1,2-*O*-cyclohexylidene-3,4,5,6-tetra-*O*-benzyl *myo*-inositol with estimated standard deviations in parentheses

Bond	Distance (Å)	Bond	Distance (Å)
C(01)-C(02)	1.513(5)	C(20)-C(21)	1.528(5)
C(01)-C(06)	1.511(5)	C(21)-C(22)	1.507(6)
C(01)-O(07)	1.419(4)	C(22)-C(23)	1.502(7)
C(02)-C(03)	1.512(5)	C(23)-C(24)	1.526(7)
C(02)-O(08)	1.429(4)	C(24)-C(25)	1.519(6)
C(03)-C(04)	1.522(5)	C(26)-C(27)	1.491(6)
C(03)-O(09)	1.432(4)	C(27)-C(32)	1.367(6)
C(04)-C(05)	1.518(5)	C(27)-C(28)	1.385(6)
C(04)-O(10)	1.424(4)	C(28)-C(29)	1.377(6)
C(05)-C(06)	1.520(5)	C(29)-C(30)	1.371(6)
C(05)-O(11)	1.422(4)	C(30)-C(31)	1.362(6)
C(06)-O(12)	1.424(4)	C(31)-C(32)	1.373(6)
O(07)-C(13)	1.420(4)	C(33)-C(34)	1.497(5)
O(08)-C(20)	1.419(4)	C(34)-C(35)	1.372(5)
O(09)-C(20)	1.440(4)	C(34)-C(39)	1.378(5)
O(10)-C(33)	1.410(5)	C(35)-C(36)	1.384(6)
O(11)-C(26)	1.413(5)	C(36)-C(37)	1.351(6)
O(12)-C(40)	1.398(5)	C(37)-C(38)	1.341(6)
C(13)-C(14)	1.512(5)	C(38)-C(39)	1.376(6)
C(14)-C(19)	1.347(5)	C(40)-C(41)	1.500(6)
C(14)-C(15)	1.394(6)	C(41)-C(42)	1.344(7)
C(15)-C(16)	1.404(7)	C(41)-C(46)	1.346(6)
C(16)-C(17)	1.364(7)	C(42)-C(43)	1.390(10)
C(17)-C(18)	1.367(7)	C(43)-C(44)	1.339(10)
C(18)-C(19)	1.363(6)	C(44)-C(45)	1.301(8)
C(20)-C(25)	1.497(5)	C(45)-C(46)	1.365(7)

Bonds	Angles (°)	Bonds	Angles (°)
C(03)-C(02)-C(01)	116.3(3)	C(01)-C(06)-C(05)	110.7(3)
C(02)-C(03)-C(04)	114.0(3)	C(06)-C(01)-C(02)	112.6(3)

Table 4.37 continued

Bonds	Angles (°)	Bonds	Angles (°)
C(05)-C(04)-C(03)	112.2(3)	C(25)-C(20)-C(21)	111.4(3)
C(04)-C(05)-C(06)	109.9(3)	C(22)-C(21)-C(20)	112.1(4)
O(07)-C(01)-C(02)	113.0(3)	C(23)-C(22)-C(21)	110.9(4)
O(07)-C(01)-C(06)	108.1(3)	C(22)-C(23)-C(24)	110.9(4)
O(08)-C(02)-C(03)	101.6(3)	C(25)-C(24)-C(23)	110.7(5)
O(08)-C(02)-C(01)	110.9(3)	C(20)-C(25)-C(24)	112.3(4)
O(09)-C(03)-C(02)	101.3(3)	O(11)-C(26)-C(27)	107.4(3)
O(09)-C(03)-C(04)	111.4(3)	C(32)-C(27)-C(28)	117.8(4)
O(10)-C(04)-C(03)	109.4(3)	C(32)-C(27)-C(26)	121.5(4)
O(10)-C(04)-C(05)	110.7(3)	C(28)-C(27)-C(26)	120.6(5)
O(11)-C(05)-C(06)	109.3(3)	C(29)-C(28)-C(27)	121.0(5)
O(11)-C(05)-C(04)	107.6(3)	C(30)-C(29)-C(28)	120.0(5)
O(12)-C(06)-C(01)	109.4(3)	C(31)-C(30)-C(29)	119.4(5)
O(12)-C(06)-C(05)	110.7(3)	C(30)-C(31)-C(32)	120.5(5)
C(13)-O(07)-C(01)	114.2(3)	C(27)-C(32)-C(31)	121.3(5)
C(20)-O(08)-C(02)	105.8(2)	O(10)-C(33)-C(34)	110.2(3)
C(03)-O(09)-C(20)	108.7(2)	C(35)-C(34)-C(39)	117.2(4)
C(33)-O(10)-C(04)	113.7(3)	C(35)-C(34)-C(33)	122.9(4)
C(26)-O(11)-C(05)	116.4(3)	C(39)-C(34)-C(33)	119.9(4)
C(40)-O(12)-C(06)	113.5(3)	C(34)-C(35)-C(36)	121.1(4)
O(07)-C(13)-C(14)	108.7(3)	C(37)-C(36)-C(35)	119.6(5)
C(19)-C(14)-C(15)	119.0(4)	C(38)-C(37)-C(36)	121.0(5)
C(19)-C(14)-C(13)	121.4(4)	C(37)-C(38)-C(39)	119.6(5)
C(15)-C(14)-C(13)	119.6(4)	C(34)-C(39)-C(38)	121.6(4)
C(14)-C(15)-C(16)	120.1(5)	O(12)-C(40)-C(41)	110.8(4)
C(17)-C(16)-C(15)	118.1(5)	C(42)-C(41)-C(46)	117.8(5)
C(18)-C(17)-C(16)	121.3(5)	C(42)-C(41)-C(40)	120.1(5)
C(19)-C(18)-C(17)	119.7(5)	C(46)-C(41)-C(40)	121.6(5)
C(14)-C(19)-C(18)	121.6(5)	C(41)-C(42)-C(43)	121.3(6)
O(08)-C(20)-O(09)	105.5(2)	C(44)-C(43)-C(42)	118.1(6)
O(08)-C(20)-C(25)	109.0(3)	C(45)-C(44)-C(43)	121.2(6)
O(09)-C(20)-C(25)	110.7(3)	C(44)-C(45)-C(46)	120.8(5)
O(08)-C(20)-C(21)	111.7(3)	C(41)-C(46)-C(45)	120.8(5)
O(09)-C(20)-C(21)	108.4(3)		

Table 4.38 : Anisotropic displacement parameters (x 10^3, for non-hydrogen atoms) for D/L-*cis*-1,2-*O*-cyclohexylidene-3,4,5,6-tetra-*O*-benzyl *myo*-inositol with estimated standard deviations in parentheses

	U11	U22	U33	U23	U13	U12
C(01)	65(2)	52(2)	71(2)	-1(2)	26(2)	-2(2)
C(02)	58(2)	55(2)	73(2)	-4(2)	28(2)	3(2)
C(03)	71(3)	51(2)	71(2)	1(2)	26(2)	-5(2)
C(04)	70(2)	51(2)	67(2)	2(2)	24(2)	3(2)
C(05)	68(2)	57(2)	60(2)	0(2)	23(2)	11(2)
C(06)	60(2)	56(2)	62(2)	-4(2)	20(2)	0(2)
O(07)	69(2)	46(1)	96(2)	-3(1)	38(1)	-2(1)
O(08)	58(1)	58(1)	75(2)	5(1)	18(1)	-4(1)
O(09)	60(2)	57(1)	91(2)	6(1)	21(1)	-7(1)
O(10)	104(2)	45(1)	71(2)	2(1)	30(1)	3(1)
O(11)	70(2)	66(2)	71(1)	1(1)	15(1)	22(1)
O(12)	59(1)	73(2)	74(2)	-2(1)	22(1)	-4(1)
C(13)	78(3)	55(2)	126(4)	-8(2)	44(3)	2(2)
C(14)	77(3)	49(2)	83(2)	-3(2)	35(2)	4(2)
C(15)	75(3)	85(4)	123(4)	-8(3)	31(3)	10(3)
C(16)	106(4)	64(3)	146(4)	10(3)	54(4)	23(3)
C(17)	113(4)	63(3)	137(4)	-13(3)	65(4)	-12(3)
C(18)	106(4)	85(3)	112(3)	5(3)	31(3)	-18(3)
C(19)	78(3)	89(3)	104(3)	19(3)	21(3)	-12(3)
C(20)	59(2)	51(2)	75(2)	5(2)	22(2)	-1(2)
C(21)	63(3)	71(3)	98(3)	7(2)	27(2)	2(2)
C(22)	58(3)	105(3)	101(3)	7(3)	16(2)	-1(3)
C(23)	77(3)	132(5)	100(4)	-1(3)	7(3)	-19(3)
C(24)	116(4)	106(4)	90(3)	-26(3)	21(3)	-15(3)
C(25)	76(3)	74(3)	88(3)	-6(2)	27(2)	5(2)
C(26)	96(4)	93(4)	76(3)	5(3)	9(3)	39(3)
C(27)	71(3)	69(3)	77(2)	11(2)	7(2)	22(2)
C(28)	72(3)	80(3)	120(3)	13(3)	33(3)	5(3)
C(29)	90(3)	61(3)	143(4)	4(3)	41(3)	10(3)
C(30)	80(3)	78(3)	125(4)	2(3)	36(3)	19(3)
C(31)	76(3)	72(3)	138(4)	12(3)	39(3)	5(3)

Table 4.38 continued

	U11	U22	U33	U23	U13	U12
C(32)	80(3)	62(3)	120(4)	6(2)	20(3)	8(3)
C(33)	141(5)	56(2)	71(3)	-7(2)	24(3)	-5(3)
C(34)	82(3)	53(2)	60(2)	-10(2)	18(2)	-2(2)
C(35)	74(3)	67(3)	75(2)	-10(2)	20(2)	7(2)
C(36)	93(3)	75(3)	82(3)	-6(2)	30(3)	-16(3)
C(37)	111(4)	47(2)	83(3)	-6(2)	13(3)	-1(3)
C(38)	92(3)	60(3)	101(3)	-21(2)	25(3)	9(2)
C(39)	86(3)	74(3)	90(3)	-17(2)	40(2)	-11(2)
C(40)	92(3)	249(7)	109(4)	-39(4)	45(3)	-84(5)
C(41)	65(2)	89(3)	78(2)	3(2)	32(2)	-4(2)
C(42)	141(5)	113(5)	134(5)	31(4)	21(4)	22(4)
C(43)	267(10)	83(4)	155(6)	31(4)	78(7)	-21(5)
C(44)	144(6)	137(6)	126(5)	-44(4)	80(5)	-73(5)
C(45)	81(3)	149(5)	107(4)	-33(4)	15(3)	-6(4)
C(46)	104(4)	83(3)	88(3)	6(2)	9(3)	5(3)

Table 4.39 : Hydrogen atomic co-ordinates (x 10^4) and isotropic temperature factors (x 10^3) for D/L-*cis*-1,2-*O*-cyclohexylidene-3,4,5,6-tetra-*O*-benzyl *myo*-inositol with estimated standard deviations in parentheses

	x	y	z	U(iso)
H(47)	257(29)	2990(16)	592(19)	58(9)
H(48)	2420(30)	3038(16)	1246(17)	59(9)
H(49)	2025(27)	4201(15)	864(18)	55(8)
H(50)	858(32)	4429(18)	2084(22)	77(11)
H(51)	-664(26)	4191(14)	525(18)	47(8)
H(52)	-470(25)	3402(13)	1922(17)	42(7)
H(53)	1162(40)	1922(23)	516(28)	123(15)
H(54)	2157(62)	1818(32)	1582(36)	182(24)
H(55)	2208(47)	603(24)	1823(26)	105(17)
H(56)	1421(57)	-557(33)	1862(34)	167(22)
H(57)	-833(52)	-677(30)	1066(31)	146(21)
H(58)	-2202(68)	228(35)	491(41)	198(28)
H(59)	-1283(53)	1357(28)	524(31)	154(20)
H(60)	4608(37)	3159(20)	2043(25)	97(12)
H(61)	4774(36)	2912(22)	3023(22)	89(12)
H(62)	5784(42)	4211(25)	2556(27)	121(15)
H(63)	6678(43)	3520(21)	3017(22)	98(13)
H(64)	6574(51)	4391(25)	4019(27)	125(17)
H(65)	5964(47)	3674(27)	4256(32)	135(19)
H(66)	4391(43)	4865(25)	3387(27)	118(16)
H(67)	4472(40)	4604(22)	4296(28)	110(14)
H(68)	2529(39)	4231(20)	3329(20)	86(12)
H(69)	3458(34)	3529(21)	3793(22)	83(11)
H(70)	-3012(56)	4358(30)	448(33)	152(22)
H(71)	-2226(42)	5020(25)	267(28)	110(17)
H(72)	-2187(40)	6123(20)	981(21)	88(12)
H(73)	-3320(39)	6936(23)	1586(23)	101(13)
H(74)	-5099(40)	6542(22)	2048(23)	103(13)
H(75)	-5829(50)	5351(24)	1708(28)	125(17)
H(76)	-4721(44)	4632(26)	1107(26)	113(16)
H(77)	107(65)	5620(33)	2132(39)	190(27)

Table 4.39 continued

	x	y	z	U(iso)
H(78)	1609(56)	5624(28)	2409(36)	153(22)
H(79)	2252(36)	6314(20)	995(21)	82(12)
H(80)	2240(45)	7397(24)	599(27)	112(17)
H(81)	842(40)	8203(24)	886(23)	94(13)
H(82)	-482(38)	7904(21)	1626(22)	89(12)
H(83)	-360(33)	6781(18)	2089(20)	67(11)
H(84)	-2900(5)	3415(4)	1661(3)	279(33)
H(85)	-2025(5)	2752(4)	1965(3)	279(33)
H(86)	-3093(7)	1696(4)	1780(4)	190(12)
H(87)	-4974(11)	1016(3)	1284(5)	190(12)
H(88)	-6701(7)	1463(4)	301(4)	190(12)
H(89)	-6608(5)	2530(4)	-172(3)	190(12)
H(90)	-4789(5)	3216(2)	333(3)	190(12)

Figure 4.18 : ORTEPII drawing [Johnson, 1976] of D/L-*cis*-1,2-*O*-cyclohexylidene-3,4,5,6-tetra-*O*-benzyl *myo*-inositol. Thermal ellipsoids are drawn at the 50% probability level.

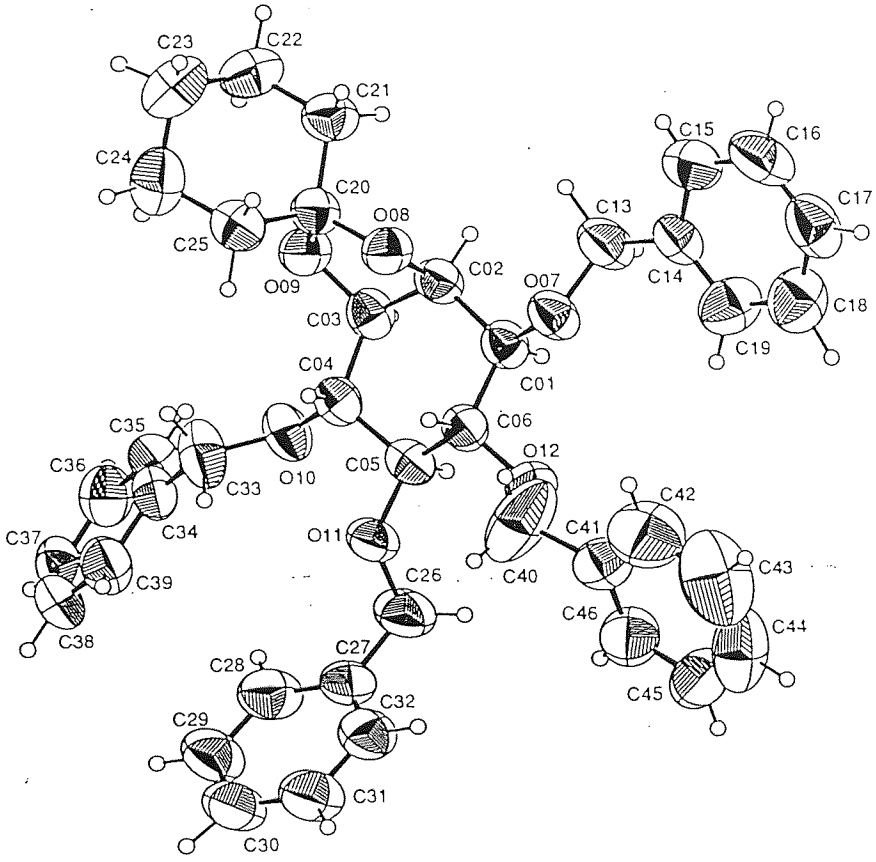

Table 4.40 : Asymmetry parameters for inositol rings of D/L-*cis*-1,2-*O*-cyclohexylidene-3,4,5,6-tetra-*O*-benzyl *myo*-inositol

$\Delta C_s(1) = 15.49$	$\Delta C_2(1\text{-}2) = 14.85$
$\Delta C_s(2) = 5.52$	$\Delta C_2(2\text{-}3) = 3.17$
$\Delta C_s(3) = 9.97$	$\Delta C_2(3\text{-}4) = 18.00$

ΔC_s = Mirror related asymmetry parameter
ΔC_2 = Two fold related asymmetry parameter

Table 4.41 : Distances of C atoms from least squares plane for D/L-*cis*-1,2-*O*-cyclohexylidene-3,4,5,6-tetra-*O*-benzyl *myo*-inositol (SHELX-93, [Sheldrick, 1993]).

Atom	Distance
C01	0.189(3) Å
C02	0.129(3) Å
C03	0.142(3) Å
C04	0.219(3) Å
C05	0.286(3) Å
C06	0.270(3) Å

Least squares plane
-1.66(2)x + 1.29(3)y + 17.23(1)z = 1.71(1)
Rms deviation of fitted atoms = 0.214

CH_2 group C26 is orientated towards C06. The acetal linkage creates space which allows the CH_2 group C13 to orientate towards C02, and this reduces crowding with the other benzyl groups. All phenyl groups are orientated trans with respect to the inositol C-O bond which suggests a concerted orientation for these groups. Their phenyl planes are orientated *gauche* with respect to the CH_2-Ph bonds.

4.3 CONCLUSION

The crystal structures of six *myo*-inositol compounds have been solved by X-ray diffraction. All of the compounds had structures consistent with the assignments determined by experimental analysis (Chapter 5). In all cases, the inositol rings adopted the five equatorial / 1 axial conformation, in contrast to phytic acid's unusual 5 axial / 1 equatorial conformation in the dodecasodium salt form [Blank, 1975].

The presence of an acetal cyclohexylidene ring linkage caused large distortions to the inositol ring. This protecting group twists the inositol ring at the linkage site or flattens/puckers the ring if further bulky substituents are present. The distortion imposed on the inositol ring makes the cyclohexylidene group a useful and popular protecting group, as it not only protects but also introduces differences in hydroxy group reactivity around the ring. Other substituents alone caused only slight distortions in the inositol ring, even when bulky groups such as dibenzyl phosphates were attached in crowded environments. Small ring distortions could partly be attributed to hydrogen bonding environments and crystal packing requirements. These small ring distortions are consistent with those of reported structures for fully protected inositols, 1,2,3,4,5,6-hexa-*O*-acetyl-*myo*-inositol [Abboud *et al.*, 1990] and D/L-3,4-di-*O*-acetyl-1,2,5,6-tetra-*O*-benzyl-*myo*-inositol [Steiner *et al.*, 1993].

Extensive hydrogen bonding networks exist with inositol compounds that have free hydroxy groups. Most hydroxy groups accept and all donate hydrogen bonds in the structures studied. An unusual intermolecular hydrogen bonding system has been illustrated in the crystal structure of D/L-1,2;4,5-di-O-cyclohexylidene *myo*-inositol (**3**) at both room and low (150K) temperatures. The possible flip-flop disorder has only been reported once before and this was in the more complex cyclodextrin/water system [Saenger *et al.*, 1982]. The two molecules of triol **58** also exhibited intermolecular hydrogen bonding between symmetry related molecules, but in this case, homodromic rather than disordered bonding was present as well as standard hydrogen bonding. *myo*-Inositol 1,2,3-trisphosphate was shown to exhibit both inter- and intramolecular hydrogen bonding. The intramolecular hydrogen bonding present in the structure

confirmed reports [Schmitt *et al.*, 1993, a] of proton sharing between neighbouring phosphate groups, and between inositol hydroxy and phosphate groups.

In the structures of D/L-1-*O*-(*tert*-butyldiphenylsilyl)-2,3-*O*-cyclohexylidene-4,5,6-tri-*O*-benzoyl *myo*-inositol (**59**) and D/L-1-*O*-(*tert*-butyldiphenylsilyl)-2,3-*O*-cyclohexylidene *myo*-inositol (**58**), two molecules of the compounds existed within the asymmetric unit. The two molecules in both cases had different conformations which illustrates that care must be taken when extrapolating precise details from crystal structures. It also demonstrates that other factors, such as crystal packing forces and hydrogen bonding environments, can alter the conformation of the compounds even for the same chemical structure. In contrast, the crystal structure of *myo*-inositol itself [Rabinowitz & Kraut, 1964] had two inositol molecules in the asymmetric unit which were almost identical.

The inositol ring has been shown to be capable of large distortions, although natural substituents such as phosphates seem to cause little distortion unless stabilised by ion bridging and hydrogen bonding, as in the case of $InsP_6$ [Blank *et al.*, 1975]. Metal ion binding, to magnesium [Blank, 1973] and calcium [Cook & Bugg, 1973] has also been reported between *cis* vicinal inositol hydroxy groups and was shown to introduce strain into the inositol ring at the site of co-ordination. Calcium ions were also found to bind to equatorial / equatorial hydroxy groups [Cook & Bugg, 1973]. The flexibility of the inositol ring should allow compounds to adopt the structural requirements of biological environments and illustrates why the inositol molecule is involved in many biochemical events.

CHAPTER 5

Chemistry experimental

5.1 EXPERIMENTAL DETAILS

NMR spectra were recorded on a Bruker AC-250 spectrometer for ^{1}H (250.1 MHz), ^{31}P (101.3 MHz) and ^{13}C (62.9 MHz) data or on a Varian Unity 500 spectrometer for ^{1}H (499.9 MHz) data. ^{1}H spectra were referenced to tetramethylsilane unless otherwise stated, ^{31}P NMR spectra were referenced to 85% phosphoric acid (chemical shifts are denoted as negative when upfield from this reference) and ^{13}C NMR spectra were referenced to $CDCl_3$ or d_6-DMSO in D_2O. All ^{13}C and ^{31}P NMR spectra were ^{1}H decoupled unless otherwise stated. Infra-red spectra were recorded on a FT-IR Mattson 3000 Series spectrometer. Mass spectrometry data were recorded by the EPSRC mass spectrometry service centre uncorrected, Chemistry Department, Swansea University using a V.G. 7070E instrument. FAB spectra were recorded with a 3-nitrobenzyl alcohol or PEG matrix, while CI mass spectra were recorded using NH_3 as carrier gas. Melting points were measured on a Kofler Reichert-Jung hot stage with the aid of a microscope (Cambridge Instruments). Elemental analyses were performed by Butterworths Laboratories, Middlesex. Flash column chromatography [Still *et al.*, 1978] was performed using Sorbsil C60 40/60H silica gel. TLC was performed using plastic-backed Kieselgel 60 silica gel plates containing a fluorescent indicator. Spots were visualised under 254 nm UV light or with the aid of iodine. Optical rotation were measured on a AA-100 polarimeter, manufactured by Optical Activity Ltd. The following solvents were dried by heating under reflux over the appropriate drying agent followed by distillation: dichloromethane (P_2O_5), THF (sodium, benzophenone), toluene (sodium, benzophenone) and triethylamine (KOH). Chemicals were obtained from Aldrich Chemical Company, including anhydrous solvents: pyridine, ethanol, diethyl ether and DMF.

5.2 SYNTHESIS OF D-*MYO*-INOSITOL 3-PHOSPHATE

5.2.1 Synthesis of 1,1-diethoxycyclohexane (43) [Dreef *et al.*, 1991]

To a solution of cyclohexanone (51.7 ml, 0.5 mol) and triethyl orthoformate (83.05 ml, 0.5 mol) in dry ethanol (100 ml) was added *p*-toluenesulphonic acid monohydrate

(0.10g, 0.53 mmol). The exothermic reaction was stirred for 3 hours at 20°C. The crude product was neutralized with sodium ethoxide and concentrated *in vacuo*. Distillation (80°C-90°C/42 mbar) of the crude product afforded 1,1-diethoxycyclohexane (51.1 g, 59.4 %), as a colourless liquid. ^{1}H-NMR data (250.1 MHz, $CDCl_3$): δ 1.07 (t, 6 H, J_{HH} 7.1 Hz, CH_3), 1.2-1.6 (m, 10 H, CH_2 of cyclohexylidene), 3.35 (q, 4 H, J_{HH} 7.1 Hz, OCH_2). ^{13}C-NMR (62.9 MHz, $CDCl_3$): δ 15.36 (CH_3), 22.8, 25.5, 33.6 (CH_2 of cyclohexylidene), 54.6 (OCH_2), 99.7 (C1 of cyclohexylidene).

5.2.2 Synthesis of D/L-1,2;4,5-di-*O*-cyclohexylidene-*myo*-inositol (3) [Dreef *et al.*, 1991]

A mixture of *myo*-inositol (27g, 0.150 mol), 1,1-diethoxycyclohexane (67.5g, 0.392 mol) and *p*-toluenesulphonic acid monohydrate (0.5g, 2.63 mmol) in dry DMF (375 ml) was stirred for 2 hours at 95°C. The cooled reaction mixture was diluted with CH_2Cl_2 (300 ml) and washed with H_2O (300 ml), 1M $NaHCO_3$ (300 ml) and H_2O (300 ml). The organic layer was dried over $MgSO_4$ and concentrated *in vacuo*. Crystallisation of a small amount of crude product from acetone/hexane afforded compound **3** as rectangular plate crystals which were used for X-ray diffraction structure determination (Chapter 4). One of the crystals was used to seed the crystallisation of the remainder of compound **3** (6.78 g, 17.9 %), mp 176-179°C; Lit.= 172-174°C [Dreef *et al.*, 1991]. R_f = 0.47 ethyl acetate/hexane (1:1). ^{1}H-NMR (250.1 MHz, $CDCl_3$, assigned with the aid of a COSY spectrum and decoupling experiments): δ 1.4-1.8 (m, 20 H, CH_2), 2.51 (d, 1 H, J_{HH} 8.8 Hz, 3-OH), 2.76 (s, 1 H, 6-OH), 3.27 (dd, 1 H, J_{HH} 9.4 Hz, J_{HH} 10.6 Hz, H-5), 3.78 (dd, 1 H, J_{HH} 10 Hz, J_{HH} 11.8 Hz, H-4), 3.84 (ddd, 1 H, J_{HH} 2.9 Hz, J_{HH} 6.4 Hz, J_{HH} 10.6 Hz, H-6), 3.97 (dd, 1 H, J_{HH} 4.4 Hz, J_{HH} 9.3 Hz, H-3), 4.03 (dd, 1 H, J_{HH} 5.0 Hz, J_{HH} 6.4 Hz, H-1), 4.43 (t, 1 H, J_{HH} = 4.8 Hz, H-2). ^{13}C-NMR data (62.9 MHz, $CDCl_3$, assignments made with the aid of a DEPT spectrum): δ 24.0, 24.1, 24.1, 24.4, 25.3, 25.4, 35.5, 36.9, 38.2 (CH_2, 1 overlapping), 70.4, 75.6, 77.6, 78.1, 78.4, 81.9 (inositol CH), 111.3, 113.7 (C1 of cyclohexylidene). IR data (KBr): υ_{max} 3285, 3410 cm^{-1} (OH).

5.2.3 Synthesis of (2R, 4S, 5R)-2-chloro-3,4-dimethyl-5-phenyl-1,3,2-oxazaphospholidin-2-one (Major, 37)

A procedure similar to a reported method [Cooper *et al.*, 1977] was used.

Hydrated (-)-ephedrine [(1R,2S)-2-methylamino-1-phenylpropan-1-ol)] (9.16g, 0.05 mol) was dried by heating at reflux for 3 hours in toluene (100 ml) with a Dean-Stark apparatus and concentrated *in vacuo* when cool. Phosphorus oxychloride (4.66 ml, 0.05 mol) in dry CH_2Cl_2 (25 ml) was added dropwise over 15 min to a cooled (0°C-ice bath) stirred solution of the residue and triethylamine (13.94 ml, 0.1 mol) in dry CH_2Cl_2 (150 ml) under argon. After stirring for 2 hours at room temperature, the solid triethylammonium hydrochloride was removed by filtration and the remaining solution was concentrated *in vacuo*. A small sample was removed for ^{31}P-NMR ($CDCl_3$) analysis which showed the presence of the two diastereoisomers: δ 21.32 (s) major (**37**) and δ 25.08 (s) minor [(2S, 4S, 5R)-2-chloro-3,4-dimethyl-5-phenyl-1,3,2-oxazaphospholidin-2-one, **38**]. TLC in ethyl acetate/hexane (2:1) showed the two diastereoisomers of R_f = 0.43 (minor) and R_f = 0.3 (major). The major diastereoisomer (8.51 g, 69.3 %) was separated from the minor (0.95 g, 7.7 %) by flash chromatography eluting with ethyl acetate/hexane (2:1). Mp = 92-93°C; Lit.= 88-89°C [Cooper *et al.*, 1977]. ^{1}H-NMR (250.1 MHz, $CDCl_3$): δ 0.83 (d, 3 H, J_{HH} 6.8 Hz, CHC*H*$_3$), 2.83 (d, 3 H, J_{PH} 12.5 Hz, NCH_3), 3.77 (ddq, 1 H, J_{PH} 26.7 Hz, J_{HH} 6.2 Hz, J_{HH} 6.8 Hz, C*H*CH_3), 5.85 (d, 1 H, J_{HH} 6.2 Hz, C*H*Ph), 7.3-7.4 (m, 5 H, Ph). ^{13}C-NMR (62.9 MHz, $CDCl_3$): δ 12.3 (CH*C*H_3), 29.5 (d, J_{PC} 5.5 Hz, NCH_3), 61.0 (d, J_{PC} 13.6 Hz, *C*HCH_3), 83.5 (*C*HPh), 126.1, 129.3 (CH of Ph), 135.3 (d, J_{PC} 8.8 Hz, C-1 of Ph).

5.2.4 Synthesis of 1,2:4,5-di-*O*-cyclohexylidene-3-[(2'S, 4'S, 5'R)-3',4'-dimethyl-5'-phenyl-1',3',2'-oxazaphospholidin-2'-one]-*myo*-inositol (40)

D/L-1,2:4,5-Di-*O*-cyclohexylidene-*myo*-inositol **3** (2g, 5.88 mmol) and 95 % NaH (0.155g, 6.47 mmol) in dry DMF (10 ml) was stirred for 1 hour at 0°C under argon. To this reaction mixture was added dropwise a solution of (2R, 4S, 5R)-2-chloro-3,4-dimethyl-5-phenyl-1,3,2-oxazaphospholidin-2-one **37** (1.44g, 5.88 mmol) in dry DMF (6 ml) and the mixture was stirred for 2 hours, allowing the temperature to rise to 20°C.

A small sample of the crude material was removed for ^{31}P-NMR ($CDCl_3$) analysis which showed the presence of four diastereoisomers (see Figure 2.17) : δ 19.4 (s), 19.1 (s), 18.9 (s) and 18.7 (s), together with starting material, δ 20.9 (s) [the first two diastereoisomers were major products]. The reaction mixture was concentrated *in vacuo* and was subjected to flash chromatography eluting with ethyl acetate, which separated the products from the starting material. Several slow crystallisations in acetone/hexane afforded diastereoisomer **40** (0.669g, 16.8 %), mp 212.5-214°C. R_f = 0.12 ethyl acetate / hexane (1:1). ^{1}H-NMR data (499.9 MHz, $CDCl_3$, assigned with the aid of COSY spectra and decoupling experiments): δ 0.80 (d, 3 H, J_{HH} 6.6 Hz, $CHCH_3$), 1.3-1.8 (m, 20 H, CH_2), 2.60 (d, 1 H, J_{HH} 3 Hz, 6-OH), 2.75 (d, 3 H, J_{PH} 10.4 Hz, NCH_3), 3.39 (dd, 1 H, $J_{H\,H}$ 9.5 Hz, $J_{H\,H}$ 10.7 Hz, H-5), 3.75 (ddq, 1 H, J_{PH} 23.6 Hz, J_{CHCH_3,CH_3}~$J_{CHCH_3,CHPh}$~6.6 Hz, $CHCH_3$), 3.89 (ddd, 1 H, J_{HH} 10.7 Hz, J_{HH} 9.6 Hz, $J_{6,6\text{-}OH}$ 3.0 Hz, H-6), 4.0-4.1 (m, 2 H, H-1/H-4), 4.61 (t, 1 H, J_{HH} 4.7 Hz, H-2), 4.87 (ddd, 1 H, J_{HH} 4.5 Hz, J_{HH} 9.6 Hz, J_{PH} 10.7 Hz, H-3), 5.64 (dd, 1 H, J_{PH} 3.7 Hz, J_{HH} 6.5 Hz, $CHPh$), 7.3-7.4 (m, 5 H, Ph). ^{13}C-NMR data (62.9 MHz, $CDCl_3$, assignments made with the aid of a DEPT spectrum): δ 14.1 (d, CCH_3, J_{PC} 1.9 Hz), 23.8, 24.0, 24.2, 24.4, 25.3, 35.1, 36.6, 36.8, 38.4 (CH_2, 1 overlapping), 29.2 (d, NCH_3, J_{PC} 4.9 Hz), 59.6 (d, $CHCH_3$, J_{PC} 13.9 Hz), [75.2 (d, J_{PC} 6.2 Hz), 75.5, 75.8 (d, J_{PC} 6.7 Hz), 76.9, 78.1, 81.2 (d, J_{PC} 2.3 Hz), inositol CH], 81.74 ($CHPh$), 111.3, 113.6 (C-1 of cyclohexylidene), (126.5, 128.6, CH of Ph), [136.5 (d, J_{PC} 6.7 Hz), C-1 of Ph]. ^{31}P-NMR data (101.3 MHz, $CDCl_3$): δ 19.9 (s). IR data (KBr): υ_{max} 3410 (OH), 1240 (P=O) cm^{-1}. MS data (CI): observed accurate mass 550.257 (M + H$^+$), $C_{28}H_{41}NO_8P$ requires 550.257 (M + H$^+$). Calcd for $C_{28}H_{40}NO_8P$: C, 61.19; H, 7.34; N, 2.55 %. Found C, 60.47; H, 7.30: N, 2.58 %.

5.2.5 Synthesis of (1'R, 2'S)-P-(2'-methylamino-1'-phenylpropyl)-*myo*-inositol 3-phosphate (42)

The acid hydrolysis was conducted using a procedure similar to a reported method [Seidel *et al.*, 1990]. Diastereoisomer **40** (1.45 g, 2.64 mmol) in THF (3.1 ml) was stirred with trifluoroacetic acid (0.95 ml, 12.41 mmol) and H_2O (2.5 ml) for 15 minutes

at 20°C. The crude product was concentrated *in vacuo* which afforded zwitterion **42** (1.05 g, 97.9 %), mp 150-152°C. ^{1}H-NMR data (250.1 MHz, D_2O, referenced to acetone at 2.22 ppm, assigned with the aid of a COSY spectrum and decoupling experiments): δ 1.18 (d, 3 H, J_{HH} 6.8 Hz, $CHCH_3$), 2.78 (s, 3 H, NCH_3), 3.24 (t, 1 H, J_{HH} 9.3 Hz, H-5), 3.45 (dd, 1 H, J_{HH} 10.0 Hz, J_{HH} 2.7 Hz, H-1), 3.55-3.65 (m, 2 H, H-6/$CHCH_3$), 3.71 (t, 1 H, J_{HH} 9.6 Hz, H-4), 3.93 (ddd, 1 H, J_{HH} 10.2 Hz, J_{PH} 7.5 Hz, J_{HH} 2.7 Hz, H-3), 4.11 (t, 1 H, J_{HH} 2.7 Hz, H-2), 5.56 (dd, 1 H, J_{PH} 9.0 Hz, J_{HH} 2.9 Hz, $CHPh$), 7.4-7.5 (m, 5 H, Ph). ^{13}C-NMR data (62.9 MHz, D_2O, referenced to d_6-DMSO at 39.7 ppm, assignments made with the aid of a DEPT spectrum): δ 18.3 ($CHCH_3$), 38.9 (NCH_3), 68.9 (d, $CHCH_3$, J_{PC} = 6.1 Hz), [79.3, 80.0, 80.1, 80.8, 82.6, 84.9 (d, J_{PC} = 5.2 Hz) (inositol CH)], 85.2 (d, $CHPh$, J_{PC} = 6 Hz), [135.1, 137.4, 137.5 (CH of Ph], 144.4 (C-1 of Ph). ^{31}P-NMR data (101.3 MHz, D_2O): δ -0.54. IR data (KBr): υ_{max} 3500-3000 (OH), 1210 (P=O) cm^{-1}. MS data (positive ion FAB): observed accurate mass 408.1423 (M+ H$^+$), $C_{16}H_{27}NO_9P$ requires 408.1423 (M+ H$^+$). Calcd for $C_{16}H_{26}NO_9P.4H_2O$: C, 40.09; H, 6.31; N, 2.92 %. Found: C, 40.09; H, 5.02; N, 2.47 %.

5.2.6 Synthesis of D-*myo*-inositol 3-phosphate (17)

A method for hydrogenolysis was used similar to that previously described by Berlin and co-workers [Berlin *et al.*, 1991]. A solution of zwitterion **42** (0.081g, 0.20 mmol) in methanol/water (8:2, 30ml) with palladium-on-carbon (40mg, 10 %) was shaken in a Parr pressure reaction-apparatus under an atmosphere of hydrogen (50 PSI) for 16 hours at 20°C. The catalyst was removed by filtration through celite and the product was evaporated *in vacuo*. The residue was dissolved in water (4ml) and stirred with cyclohexylamine (2ml) for 4 hours at 20°C. Extraction with ether removed excess cyclohexylamine and the aqueous solution was concentrated *in vacuo*, yielding a colourless solid, which was recrystallised from water/acetone to give the bis(cyclohexylammonium) salt of D-*myo*-inositol 3-phosphate (0.087g, 95 %), mp 191.4-193.2°C; Lit. = 192-193°C [Berlin *et al.*, 1991]. ^{1}H-NMR data (250.1 MHz, D_2O, referenced to acetone at 2.22 ppm, assigned with the aid of a COSY spectrum and decoupling experiments): δ [1.1-1.4 (m, 10 H), 1.59 (d, 2 H, J_{HH} 11.8 Hz), 1.73 (s, 4

H), 1.91 (s, 4 H), 3.08 (s, 2 H), (2 x cyclohexylammonium)], 3.27 (t, 1 H, J_{HH} = 8.8 Hz, H-5), 3.48-3.62 (m, 2 H, H-1/H-6), 3.69 (t, 1H, J_{HH} = 9.4 Hz, H-4), 3.84 (br t, 1 H, $J_{3,4}$~J_{PH}~9.9 Hz, H-3), 4.16 (br s, 1 H, H-2). ^{13}C-NMR data (62.9 MHz, D_2O, referenced to d_6-DMSO at 39.7 ppm, assignments made with the aid of a DEPT spectrum): δ [26.7 (4 x CH_2, C-3 & C-5 of cyclohexylamine), 27.2 (2 x CH_2, C-4 of cyclohexylamine), 33.3 (4 x CH_2, C-2 & C-6 of cyclohexylamine), 53.2 (2 x CH, C-1 of cyclohexylamine), [73.7, 74.6 (d, J_{PC} = 2.9 Hz), 75.2 (d, J_{PC} = 4.3 Hz), 75.2, 77.2 (d, J_{PC} = 5.2 Hz), 77.3 (inositol CH). ^{31}P-NMR data (101.3 MHz, D_2O): δ 4.68. ^{31}P-NMR data (101.3 MHz, D_2O, ^{1}H coupled): δ 4.68 (d, J_{PH} 7.8 Hz).

For the monocyclohexylammonium salt of D-*myo*-inositol 3-phosphate (produced by repeating the above synthesis but with the addition of less cyclohexylamine) ; MS data (positive ion FAB): observed accurate mass 259.0215 ($M + H^+$), $C_6H_{12}NO_9P$ requires 259.0219 ($M + H^+$). Calcd for $C_{12}H_{26}NO_9P$: C, 40.11; H, 7.29; N, 3.90 % and for $C_{12}H_{26}NO_9P.H_2O$: C, 38.20; H, 7.48; N, 3.71 %. Found: C, 38.36; H, 7.47; N, 4.31 % and C, 39.45; H, 7.47; N, 4.46 %, Butterworths Laboratories were unable to obtain a reliable replicate.

To determine the optical rotation of both the free acid and the bis(cyclohexylammonium) salt of D-*myo*-inositol 3-phosphate, the following procedure was performed. A solution of the mono(cyclohexylammonium) salt of D-*myo*-inositol 3-phosphate was dissolved in water (3 cm^3) and applied to a cation exchange column (Dowex 50-X8, mesh 20-50, 50 cm^3, Na^+ form) which was eluted with water (150 cm^3). The water was evaporated under vacuum to give the free acid of D-*myo*-inositol 3-phosphate as a colourless gum (16.2 mg). The free acid of D-*myo*-inositol 3-phosphate (16.2 mg) was dissolved in double distilled water (2 cm^3) and added to a 1 dm length polarimeter cell (capacity 1.3 cm^3). The optical rotation was measured at 19.5 °C. Two separate readings were recorded, +0.073° and +0.071°, an average of +0.072°, which gives $[\alpha]_D$ = + 8.9° (pH 1.63). Lit. = + 9.3° (pH 2) [Ballou & Pizer, 1960]. Cyclohexylamine (28.5 µl, 4 equiv.) was then added to the free acid solution. The optical rotation readings were -0.052° and -0.048°, an average of -0.050°, which gives $[\alpha]_D$ = -3.56° (pH 11.14). Lit. = -3.2° (pH 9) [Ballou & Pizer, 1960], -3.4° (pH 9)

[Pietrusiewicz *et al.*, 1992], -2.8° (pH 9) [Berlin *et al.*, 1991], -3.45° (pH 9) [Billington *et al.*, 1987], -4.9±1.0 (pH 9) [Mercier *et al.*, 1969].

5.3 SYNTHESIS OF *MYO*-INOSITOL THIOPHOSPHATE DERIVATIVES

5.3.1 NMR data of (2R, 4R, 5S)-2-chloro-3,4-dimethyl-5-phenyl-1,3,2-oxazaphospholidin-2-sulfide 98 % (39)

This compound was obtained from Aldrich chemical company.

^{31}P-NMR data (101.3 MHz, $CDCl_3$): δ 75.6 (s). ^{1}H-NMR (250.1 MHz, $CDCl_3$): δ 0.87 (d, 3 H, J_{HH} 6.8 Hz, CHC*H*$_3$), 2.91 (d, 3 H, J_{PH} 14.7 Hz, NCH_3), 3.83 (ddq, 1 H, J_{PH} 29 Hz, J_{HH} 6.3 Hz, J_{HH} 6.8 Hz, C*H*CH_3), 5.82 (d, 1 H, J_{HH} = 6.2 Hz, C*H*Ph), 7.3-7.4 (m, 5H, Ph). ^{13}C-NMR (62.9 MHz, $CDCl_3$): δ 12.5 (CH*C*H_3), 29.8 (d, J_{PC} 6.7 Hz, NCH_3), 61.2 (d, J_{PC} 9.9 Hz, *C*HCH_3), 84.3 (d, J_{PC} 3.4 Hz, C*H*Ph), [126.1, 129.0 (d, J_{PC} 2.1 Hz), CH of Ph], 135.1 (d, J_{PC} 7.9 Hz, C-1 of Ph).

5.3.2 Synthesis of D/L-1,2:4,5-di-*O*-cyclohexylidene-3-[(2'S, 4'R, 5'S)-3',4'-dimethyl-5'-phenyl-1',3',2'-oxazaphospholidin-2'-sulfide)]-*myo*-inositol (48)

D/L-1,2:4,5-Di-*O*-cyclohexylidene-*myo*-inositol **3** (0.51g, 1.5 mmol) and 95 % NaH (0.036g, 1.5 mmol) in dry DMF (5 ml) was stirred for 1 hour at 0°C under argon. To this reaction mixture was added dropwise (2R, 4R, 5S)-2-chloro-3,4-dimethyl-5-phenyl-1,3,2-oxazaphospholidin-2-sulfide **39** (0.393g, 1.5 mmol) in dry DMF (2 ml). The mixture was stirred for 2 hours allowing the temperature to rise to room 20°C. A small sample of the crude material was removed for ^{31}P-NMR ($CDCl_3$) analysis which showed the presence of four diastereoisomers: δ 83.1 (s), 82.5 (s), 82.4 (s) and 80.8 (s), and starting material δ 75.2 (s). The reaction mixture was concentrated *in vacuo* and was subjected to flash chromatography eluting with ethyl acetate/hexane (1:3). The diastereoisomeric pair D/L-1,2:4,5-di-*O*-cyclohexylidene-3-[(2'S, 4'R, 5'S)-3',4'-dimethyl-5'-phenyl-1',3',2'-oxazaphospholidin-2'-sulfide)]-*myo*-inositol (**48**) was isolated (0.22g, 25.9 %), R_f = 0.18 ethyl acetate/hexane (1:3). Mp 78-80°C. ^{1}H-NMR

data (250.1 MHz, $CDCl_3$): δ 0.81 (d, 3 H, J_{HH} 6.6 Hz, $CHCH_3$, diastereoisomer B†), 0.82 (d, 3 H, J_{HH} 6.6 Hz, $CHCH_3$, diastereoisomer A†), 1.2-1.7 (m, 20 H, CH_2, both diastereoisomers), 2.73 (d, 3 H, J_{PH} 12.6 Hz, NCH_3, diastereoisomer B), 2.74 (d, 3 H, J_{PH} 12.6 Hz, NCH_3, diastereoisomer A), 2.93 (s, 1 H, 6-OH, both diastereoisomers), 3.40 (dd, 1H, J_{HH} 9.5 Hz, J_{HH} 10.7 Hz, H-5, both diastereoisomers), 3.68 (ddq, 1 H, J_{PH} 21.2 Hz, J_{4,CH_3}~$J_{4,5}$~6.6 Hz, $CHCH_3$, both diastereoisomers), 3.8-3.9 (m, 1 H, H-6, both diastereoisomers), 4.0-4.1 (m, 2 H, H-1/H-4, both diastereoisomers), 4.54 (t, 1 H, J_{HH} 4.6 Hz, H-2, diastereoisomer B), 4.67 (t, 1 H, J_{HH} 4.6 Hz, H-2, 1 diastereoisomer A), 4.8-5.1 (m, 1 H, H-3, both diastereoisomers), 5.6-5.7 (m, 1 H, CHPh, both diastereoisomers), 7.3-7.4 (m, 5 H, Ph, both diastereoisomers). ^{13}C-NMR data (62.9 MHz, $CDCl_3$, assignments made with the aid of a DEPT spectrum): δ [14.2 (diastereoisomer A), 14.8 (diastereoisomer B), $CHCH_3$], [23.9, 23.9, 24.1, 24.1, 24.2, 24.4, 25.3, 25.4, 35.1, 35.2, 36.6, 36.7, 36.9, 38.3, 38.4 (CH_2, 5 overlapping, both diastereoisomers)], 29.6 (d, J_{PC} 6.3 Hz, NCH_3, diastereoisomer A), 29.9 (d, J_{PC} 6.6 Hz, NCH_3, diastereoisomer B), 59.8 (d, J_{PC} = 11.4 Hz, $CHCH_3$, diastereoisomer B), 60.1 (d, J_{PC} 11.4 Hz, $CHCH_3$, diastereoisomer A), [75.3, 75.4, 75.6, 75.7, 76.0, 76.1, 76.3, 76.8, 78.1, 78.2, 81.7, 81.7 (inositol CH, both diastereoisomers)], [82.7 (diastereoisomer A), 82.8 (diastereoisomer B), CHPh], 111.0, 111.2, 113.6 (C-1 of cyclohexylidene for both diastereoisomers, 1 overlapping), [126.43, 126.84, 128.45, 128.51, 128.56 (CH of Ph, both diastereoisomers)], 136.44 (d, J_{PC} 6.7 Hz, C-1 of Ph, both diastereoisomers). ^{31}P-NMR data (101.3 MHz, $CDCl_3$): δ 81.1 (s, diastereoisomer A), 82.8 (s, diastereoisomer B). IR data (KBr): υ_{max} 3410 (OH) cm^{-1}. MS data (positive ion FAB): observed accurate mass 566.2341 ($M + H^+$), $C_{28}H_{41}NO_7PS$ requires 566.2341 ($M + H^+$). Calcd for $C_{28}H_{40}NO_7PS.H_2O$: C, 57.62; H, 7.25; N, 2.40 %. Found: C, 57.64; H, 7.26; N, 2.28 %.

† Diastereoisomer A : diastereoisomer B have peak heights 3 : 2 respectively.

5.3.3 Synthesis of (1'S, 2'R)-P'-(2'-methylamino-1'-phenylpropyl)-(D/L)-*myo*-inositol -(3R)-thiophosphate (50)

The acid hydrolysis was performed using a procedure similar to a reported method [Seidel *et al.*, 1990]. Diastereoisomers **48** (0.220g, 0.388 mmol) in THF (0.5 ml) were stirred with trifluoroacetic acid (0.15 ml, 1.94 mmol) and H_2O (0.4 ml) for 15 minutes at 20°C. The crude product was concentrated *in vacuo* which afforded zwitterions **50** (113.6g, 69 %). ^{1}H-NMR data (250.1 MHz, D_2O, referenced to acetone at 2.22 ppm): δ 1.09 (d, 3 H, J_{HH} 6.7 Hz, C*H*CH_3), 2.74 (s, 3 H, NCH_3), 3.28 (t, 1 H, J_{HH} 9.3 Hz, H-5), 3.45 (dd, 1H, J_{HH} 2.3 Hz, J_{HH} 10.1 Hz, H-1), 3.5-3.8 (m, 3 H), 4.1-4.2 (m, 2 H), 5.6-5.7 (m, 1 H, C*H*Ph), 7.3-7.4 (m, 5 H, Ph). ^{13}C-NMR (D_2O, referenced to d_6-DMSO at 39.7 ppm, assignments made with the aid of a DEPT spectrum): δ [12.4 (zwitterion B¶), 12.6 (zwitterion A¶), CH*C*H_3], [34.0 (zwitterion B), 34.1 (zwitterion A), NCH_3], 63.0 (d, J_{PC} 5.7 Hz, C*H*CH_3, zwitterion B), 63.13 (d, J_{PC} 5.7 Hz, C*H*CH_3, zwitterion A), [73.5, 74.0, 74.2, 74.3, 75.1, 76.8, 77.0, 79.5, 79.6, 79.7, 79.8, 79.9, 80.0 (inositol ring and C*H*Ph for both zwitterions), 129.42, 131.65 (CH of Ph, both zwitterions), 138.75 (C-1 of Ph, both zwitterions). ^{31}P-NMR data (101.3 MHz, D_2O): δ 56.5 (s, zwitterion A), 56.9 (s, zwitterion B).

¶ Zwitterion A : zwitterion B have peak height 3 : 2 respectively.

5.4 SYNTHESIS OF *MYO*-INOSITOL 1,2,3-TRISPHOSPHATE

5.4.1 Synthesis of D/L-*cis*-1,2-*O*-cyclohexylidene-*myo*-inositol (6)

D/L-*cis*-1,2-*O*-cyclohexylidene-*myo*-inositol **6** was prepared by adapting the method described by Baker and co-workers [Baker *et al.*, 1991]. A mixture of bis(cyclohexylidene) acetals of *myo*-inositol (74.3 g, 0.218 mol) (compounds **3**, **4** and **5** see section 5.2.2 above), was dissolved in toluene (200 mL), hexane (200 mL) and ethanol (100 mL). *p*-Toluenesulfonic acid (2.4 g, 12.6 mmol) was added and the mixture was maintained at 4°C for 2 hours. Triethylamine (2.4 mL, 17.2 mmol) was added and the solution was stored at -20°C for 24 hours. Compound **6** (30.1 g, 53 %)

was isolated by filtration, mp 179-181°C, Lit. mp 181-183°C [Baker *et al.*, 1991]. R_f = 0.14 chloroform / methanol (4:1). ^{1}H-NMR data (250.1 MHz, D_2O, referenced to acetone 2.22 ppm): δ 1.4-1.8 (m, 10 H, cyclohexylidene), 3.26 (t, 1 H, J_{HH} 9.9 Hz, H-5), 3.58 (dd, 1 H, J_{HH} 10.3 Hz, J_{HH} 7.8 Hz, H-6), 3.64 (t, 1 H, J_{HH} 9.6 Hz, H-4), 3.85 (dd, 1 H, J_{HH} 4.1 Hz, J_{HH} 9.8 Hz, H-3), 4.05 (dd, 1 H, J_{HH} 4.8 Hz, J_{HH} 7.8 Hz, H-1), 4.47 (t, 1 H, J_{HH} 4.5 Hz, H-2). ^{13}C-NMR data (62.9 MHz, D_2O, referenced to d_6-DMSO at 39.7 ppm, assignments made with the aid of a DEPT spectrum): δ 20.5, 20.8, 21.5, 31.8, 34.7 (CH_2), 66.8, 69.5, 69.9, 72.3, 72.9, 75.4 (inositol CH), 108.7 (C1 of cyclohexylidene). IR data (KBr): υ_{max} 3600-3000 cm^{-1} (OH).

5.4.2 Synthesis of D/L-1-*O*-(*tert*-butyldiphenylsilyl)-2,3-*O*-cyclohexylidene-*myo*-inositol (58)

D/L-1-*O*-(*tert*-butyldiphenylsilyl)-2,3-*O*-cyclohexylidene-*myo*-inositol **58** was prepared utilising the procedure developed by Bruzik and Tsai [Bruzik & Tsai, 1992]. *tert*-Butyldiphenylsilyl chloride (5.1 mL, 19.4 mmol) was added to a stirred solution of D/L-*cis*-1,2-*O*-cyclohexylidene-*myo*-inositol (5 g, 19.2 mmol) and imidazole (1.96 g, 28.8 mmol) in pyridine (70 mL) at -10°C. After 24 hours, the reaction mixture was concentrated *in vacuo*. The residue was dissolved in CH_2Cl_2 (100 mL), washed with H_2O (100 mL), 1M $NaHCO_3$ (100 mL) and H_2O (100 mL), dried ($MgSO_4$) and concentrated *in vacuo*. Crystallisation from DMF/$CHCl_3$/hexane afforded **58** as colourless plate crystals (5.34 g, 57.6 %), which were used for X-ray diffraction structure determination (Chapter 4), mp 98-100°C. R_f = 0.56 ethyl acetate. ^{1}H-NMR data (250.1 MHz, $CDCl_3$, assigned with the aid of a COSY spectrum and decoupling experiments): δ 1.09 (s, 9 H, Bu^t), 1.2-1.7 (m, 10 H, cyclohexylidene), 2.52 (d, 1 H, J_{HH} 2.3 Hz, OH), 2.74 (s, 1 H, OH), 2.90 (s, 1 H, OH), 3.12 (t, 1 H, J_{HH} 9.5 Hz, H-5), 3.55-3.75 (m, 3 H, H-1/3/4), 3.85-3.9 (m, 2 H, H-2/6), 7.3-7.5 (m, 6 H, Ph), 7.7-7.8 (m, 4 H, Ph). ^{13}C-NMR data (62.9 MHz, $CDCl_3$,): δ 19.8 (CMe_3), 24.1, 24.3, 25.3 (CH_2), 27.3 (CMe_3), 35.2, 38.7 (CH_2), 73.0, 73.1, 73.3, 76.0, 76.2, 78.6 (inositol CH), 111.0 (C1 of cyclohexylidene), 128.0, 128.3, 130.3, 130.4, 133.4, 133.7, 136.1, 136.3 (phenyl). IR

data (KBr): υ_{max} 3600-3100 cm^{-1} (OH). MS data (CI): observed accurate mass 499.2516 ($M + H^+$), $C_{28}H_{39}O_6Si$ requires 499.2516 ($M + H^+$).

5.4.3 Synthesis of D/L-1-*O*-(*tert*-butyldiphenylsilyl)-2,3-*O*-cyclohexylidene-4,5,6-tri-*O*-benzoyl *myo*-inositol (59)

Benzoyl chloride (7.70 mL, 66.4 mmol) was added to a solution of triol **58** (3.54 g, 7.1 mmol) and 4-dimethylaminopyridine (DMAP) (0.43 g, 3.5 mmol) in pyridine (50 mL) at room temperature under argon. The mixture was heated at reflux for 20 hours and then concentrated *in vacuo*. The residue was diluted with CH_2Cl_2 (100 mL), washed with H_2O (100 mL), 1M $NaHCO_3$ (100 mL) and H_2O (100 mL), dried ($MgSO_4$) and concentrated *in vacuo* . The crude product was subjected to flash chromatography on silica gel eluting with diethyl ether / hexane (1:3). Colourless plate crystals of **59**, suitable for X-ray crystallography (Chapter 4), were isolated (4.23 g, 73.4 %), mp 173.5-175°C. R_f = 0.76 diethyl ether / hexane (2:1). ^{1}H-NMR data (250.1 MHz, $CDCl_3$, assigned with the aid of a COSY spectrum and decoupling experiments): δ 0.95 (s, 9 H, Bu^t), 1.15-2.1 (m, 10 H, cyclohexylidene), 4.05-4.2 (m, 2 H, H-2/3), 4.30 (dd, 1 H, $J_{1/2}$ 3.9 Hz, $J_{1/6}$ 9.3 Hz, H-1), 5.36 (t, 1 H, $J_{5/4} \sim J_{5/6} \sim$ 9.8 Hz, H-5), 5.79 (dd, 1 H, $J_{4/5}$ 10.3 Hz, $J_{4/3}$ 7.0 Hz, H-4), 6.03 (t, 1 H, $J_{6/1} \sim J_{6/5} \sim$ 9.4 Hz, H-6), 7.1-7.9 (m, 25 H, Ph). ^{13}C-NMR data (62.9 MHz, $CDCl_3$): δ 19.0 (CMe_3), 23.8, 23.9, 24.9 (CH_2), 26.5 (CMe_3), 34.7, 37.7 (CH_2), 70.1, 71.1, 72.2, 73.7, 75.5, 75.6 (inositol CH), 111.4 (C1 of cyclohexylidene), 127.5, 127.6, 128.0, 128.1, 128.7, 129.3, 129.6, 129.7, 129.9, 132.3, 132.8, 132.9, 133.6, 135.9 (phenyl), 165.3, 165.4, 165.7 (3 x C=O). IR data (KBr): υ_{max} 1735 cm^{-1} (C=O). MS data (positive ion FAB): observed accurate mass 833.3103 ($M + Na^+$), $C_{49}H_{50}O_9SiNa$ requires 833.3122 ($M + Na^+$). Calcd for $C_{49}H_{50}O_9Si$: C, 72.57; H, 6.21 %. Found C, 72.51; H, 6.13 %.

5.4.4 Synthesis of D/L-1-*O*-(*tert*-butyldiphenylsilyl)-4,5,6-tri-*O*-benzoyl *myo*-inositol (61)

Trifluoroacetic acid (0.8 ml) was added to a solution of D/L-1-O-(*tert*-butyldiphenylsilyl)-2,3-*O*-cyclohexylidene-4,5,6-tri-*O*-benzoyl *myo*-inositol (**59**) (0.2 g, 0.25 mmol) in chloroform (3.2 mL). After 24 hours at room temperature, the solution was diluted with chloroform (5 mL), washed with H_2O (10 mL), 1M $NaHCO_3$ (10 mL) and H_2O (10 mL), dried ($MgSO_4$) and concentrated *in vacuo* . The crude product was subjected to flash chromatography on silica gel eluting with diethyl ether / hexane (2:1), and D/L-1-*O*-(*tert*-butyldiphenylsilyl)-4,5,6-tri-*O*-benzoyl *myo*-inositol (**61**) was isolated (0.112 g, 62.1 %). R_f = 0.30 diethyl ether / hexane (2:1). ^{1}H-NMR data (250.1 MHz, $CDCl_3$): δ 0.96 (s, 9 H, Bu^t), 3.17 (br s, 2H, 2 x OH), 3.68 (br d, 1H, J_{HH} 9.7 Hz, H-1), 4.0-4.3 (m, 2H, H-2/3), 5.52 (t, 1H, J_{HH} 10 Hz, H-5), 5.84 (t, 1H, J_{HH} 10 Hz, H-6), 6.12 (t, 1H, J_{HH} 9.8 Hz, H-4), 7.2-7.9 (m, 25 H, Ph). ^{13}C-NMR data (62.9 MHz, $CDCl_3$, assignments made with the aid of a DEPT spectrum): δ 19.8 (CMe_3), 27.4 (CMe_3), 71.6, 71.8, 72.9, 73.1, 73.3, 74.2 (inositol CH), 128.4, 128.7, 128.8, 128.9, 129.6, 129.9, 130.3, 130.4, 130.5, 130.7, 131.0, 132.5, 133.5, 133.7, 133.8, 136.4, 136.5 (phenyl), 166.3, 166.6, 167.4 (3 x C=O). MS data (positive ion FAB): observed accurate mass 753.2505 ($M + Na^+$), $C_{43}H_{42}O_9SiNa$ requires 753.2496 ($M + Na^+$).

5.4.5 Synthesis of 4,5,6-tri-*O*-benzoyl *myo*-inositol (60)

A solution of **59** (200 mg, 0.25 mmol) in trifluoroacetic acid (70 %)/water (8 mL) was stirred at 50°C for 2 days. The reaction mixture was concentrated *in vacuo*, the residue diluted with diethyl ether (20 mL) and washed with H_2O (3 x 20 mL), dried ($MgSO_4$) and concentrated *in vacuo*. A small amount of diethyl ether was added and **60** precipitated overnight at 4 °C, which was further purified by precipitation from diethyl ether (59 mg, 49 %); mp 100.5-103°C. R_f = 0.25 methanol / dichloromethane (1:10). ^{1}H NMR data (250.1 MHz, CD_3OD, assignments made with the aid of a COSY spectrum): δ 4.02 (dd, 2 H, $J_{1/2}$ 2.7 Hz, $J_{1/6}$ 9.7 Hz, H-1/3), 4.19 (t, 1 H, $J_{2/1}$ 2.7 Hz, H-2), 5.67 (t, 1 H, $J_{5/4}$ 9.9 Hz, H-5), 5.85 (t, 2 H, $J_{4/5}$ 9.9 Hz, H-4/6), 7.2-7.5 (m, 9 H, Ph),

7.6 7.75 (m, 2 H, Ph), 7.9-7.95 (m, 4 H, Ph). ^{1}H-NMR data (250.1 MHz, DMSO-d_6): δ 3.9 4.1 (m, 3 H, H-1/2), 5.27 (d, 2 H, J_{HH} 6.1 Hz, OH-1/3, exchangeable with D_2O), 5.50 (d, 1 H, J_{HH} 2.9 Hz, OH-2, exchangeable with D_2O), 5.6-5.8 (m, 3 H, H-4/5), 7.3-7.9 (m, 15 H, Ph). ^{13}C-NMR (62.9 MHz, DMSO-d_6): δ 69.1 (2 x C), 72.8, 73.1, 73.7 (2 x C) (inositol CH), 128.8, 128.9, 129.1, 129.3, 129.9, 133.5, 133.6 (phenyl), 165.3 (C=O), 165.6 (2 x C=O). IR data (KBr): υ_{max} 3475 (OH), 3415 (OH), 1727 (C=O) cm^{-1} MS data (CI): observed accurate mass 493.1499 (M + H$^+$), $C_{27}H_{25}O_9$ requires 493.1499 (M + H$^+$). Calcd for $C_{27}H_{24}O_9$: C, 65.85; H, 4.91 % and for $C_{27}H_{24}O_9.0.5H_2O$: C, 64.67; H, 5.02 %. Found C, 64.52; H, 4.74 %.

5.4.6 Synthesis of *N,N*-diisopropylphosphorochloridate (63) [Tanaka *et al.*, 1986]

Phosphorus trichloride (4.36ml, 0.05 mol) was dissolved in dry diethyl ether (50ml) under argon at -78°C. Diisopropylamine (14.15ml, 0.1 mol) was addded dropwise over 30 minutes during which time a white precipitate formed. On complete addition of the amine, the solution was allowed to warm to room temperature and react for a further 3 hours. The precipitate was removed by filtration and the mixture was concentrated *in vacuo*. The resultant pale yellow oil was distilled under reduced pressure (74-77°C @7mm Hg) to give *N,N*-diisopropylphosphorochloridate (13.34g, 85.4 %). ^{1}H-NMR data (250.1 MHz, $CDCl_3$): δ 1.27 (d, 12 H, J_{HH} 6.8 Hz, CH_3), 3.91 (sept, 2 H, J_{HH} 6.4 Hz, CH). ^{13}C-NMR data (62.9 MHz, $CDCl_3$): δ 23.3 (d, J_{PC} 8.4 Hz, CH_3), 48.1 (d, J_{PC} 14.1 Hz, CH). ^{31}P-NMR data (101.3 MHz, $CDCl_3$): δ 169.9 (s).

5.4.7 Synthesis of dibenzyl *N,N*-diisopropylphosphoramidite (14) [Yu & Fraser-Reid, 1988]

N,N-Diisopropylphosphorochloridate (0.50g, 2.47 mmol) was dissolved in dry diethyl ether (20ml) under argon at -78°C. A solution of benzyl alcohol (0.51ml, 4.95 mmol) and triethylamine (0.76ml, 5.44 mmol) in dry diethyl ether (12.5ml) was added dropwise over 60 minutes, and a colourless precipitate of triethylammonium

hydrochloride formed. On complete addition, the resultant solution was allowed to warm to room temperature and stirred for a further 2 hours. The precipitate was removed by filtration and the mixture was concentrated *in vacuo*. The crude oil was subjected to flash chromatography eluting with hexane/ethyl acetate/triethylamine (31:3:1), which gave pure dibenzyl *N,N*-diisopropylphosphoramidite (0.42g, 49.6 %). R_f = 0.68 hexane / ethyl acetate / triethylamine (7:3:1). ^{1}H-NMR data (250.1 MHz, $CDCl_3$): δ 1.40 (d, 12 H, J_{HH} 6.7 Hz, CH_3), 3.90 (sept, 2 H, J_{HH} 6.7 Hz, CH), 4.9-5.0 (m, 4 H, CH_2), 7.4-7.6 (m, 10 H, Ph). ^{13}C-NMR data (62.9 MHz, $CDCl_3$): δ 24.7 (d, J_{PC} 7.2 Hz, CH_3), 43.2 (d, J_{PC} 12.4 Hz, CH), 65.5 (d, J_{PC} 18.1 Hz, CH_2), 127.1, 127.3, 128.3 (CH of Ph), 139.6 (d, J_{PC} 7.4 Hz, C1 of Ph).^{31}P-NMR data (101.3 MHz, $CDCl_3$): δ 148.4(s).

5.4.8 Synthesis of 4,5,6-tri-*O*-benzoyl *myo*-inositol 1,2,3-tris(dibenzyl phosphate) (61)

4,5,6-Tri-*O*-benzoyl *myo*-inositol 1,2,3-tris(dibenzyl phosphate) **61** was prepared using a phosphorylation method similar to that described by Yu and Fraser-Reid [Yu & Fraser-Reid, 1988].

Dibenzyl *N,N*-diisopropylphosphoramidite (1.69 g, 4.87 mmol) was added to a solution of triol **60** (0.40 g, 0.81 mmol) and 1*H*-tetrazole (0.68 g, 9.76 mmol) in CH_2Cl_2 (40 mL). The reaction mixture was stirred under argon at room temperature for 2 hours to give the trisphosphite **64** (see Figure 3.15), ^{31}P-NMR data (101.3 MHz, $CDCl_3$): δ 140.9 (s, 2P), 139.9 (s, P). The reaction mixture was cooled to -40°C and a solution of *meta*-chloroperoxybenzoic acid (1.4 g, ~ 6.5 mmol) in CH_2Cl_2 (40 mL) was added. The reaction mixture was stirred at 0°C for 1 hour, after which time the solution was concentrated *in vacuo*. Crystallisation from diethyl ether/hexane afforded **61** (0.57 g, 55.5 %) as colourless laths. The crystal structure was solved by X-ray diffraction and shown to contain one molecule of water per formula unit (Chapter 4). Mp 131.5-132.5°C. R_f = 0.30 methanol / dichloromethane (1:10). ^{1}H-NMR data (250.1 MHz, $CDCl_3$, assignments were made with the aid of a COSY spectrum): δ 4.45 (dd, 2 H, J_{gem} 11.7 Hz, J_{PH} 8.9 Hz, 2 x P-O-CH_AH$_B$Ph), 4.66 (dd, 2 H, J_{gem} 11.8 Hz, J_{PH} 7.5 Hz,

2 x P-O-CH_AH_BPh), 4.9-5.05 (m, 6 H, 2 x P-O-CH_2Ph, H-1), 5.22 (d, 4 H, J_{PH} 6.1 Hz, 2 x P-O-CH_2Ph), 5.56 (br d, 1 H, J_{PH} 9.3 Hz, H-2), 5.75 (t, 1 H, $J_{5/4}$ 10.0 Hz, H-5), 6.16 (t, 2 H, $J_{4/3} \sim J_{4/5} \sim$ 10.1 Hz, H-4), 6.81 (d, 4 H, J_{HH} 7.1 Hz, Ph), 7.05-7.5 (m, 35 H, Ph), 7.79 (d, 2 H, J_{HH} 7.3 Hz, Ph), 7.91 (d, 4 H, J_{HH} 7.3 Hz, Ph). ^{13}C-NMR data (62.9 MHz, $CDCl_3$, assignments made with the aid of a DEPT spectrum): δ 69.5 (d, J_{PC} 5.7 Hz, 2 x PhCH_2OP), 69.65 (d, J_{PC} 5.3 Hz, 2 x PhCH_2OP), 69.85 (d, J_{PC} 6.2 Hz, 2 x PhCH_2OP), 70.0 (d, J_{PC} 3.8 Hz, 2 x inositol CH), 70.3 (s, inositol CH), 73.8 (br s, 2 x inositol CH), 77.1 (br s, inositol CH), 127.5, 128.0, 128.05, 128.2, 128.3, 128.35, 128.45, 129.7, 129.9, 133.25 (all s, aromatic CH), 128.8 [s, 3 x quaternary aromatic PhC(O)], 135.0 (d, J_{PC} 6.7 Hz, 2 x quaternary aromatic PhCH_2OP), 135.4 (d, J_{PC} 8.6 Hz, 2 x quaternary aromatic PhCH_2OP), 135.6 (d, J_{PC} 8.6 Hz, 2 x quaternary aromatic PhCH_2OP), 165.3 (C=O), 165.4 (2 x C=O). ^{31}P-NMR data (101.3 MHz, $CDCl_3$): δ -1.06 (s, P-1/3), -2.22 (s, P-2). ^{31}P-NMR data (101.3 MHz, $CDCl_3$, ^{1}H coupled): δ -1.18 (sextet, J_{PH} 8.3 Hz), -2.30 (br sextet, $J_{PH} \sim$ 6.8 Hz). IR data (KBr): υ_{max} 1733 (C=O), 1269 (P=O) cm^{-1}. MS data (positive ion FAB): observed accurate mass 1273.3311 ($M + H^+$), $C_{69}H_{64}P_3O_{18}$ requires 1273.3306 ($M + H^+$). Calcd for $C_{69}H_{63}P_3O_{18}.H_2O$: C, 64.19; H, 5.07 % and for $C_{69}H_{63}P_3O_{18}.2H_2O$: C, 63.30 H, 5.00 %. Found: C, 63.82; H, 4.89 %.

5.4.9 Synthesis of monosodium tetra(cyclohexylammonium) *myo*-inositol 1,2,3-trisphosphate (57)

A solution of **61** (130 mg, 0.102 mmol) and Pd-C catalyst (10 %, 30 mg) in ethanol (20 mL) was stirred under an atmosphere of hydrogen for 24 h at room temperature. The catalyst was removed by filtration through Celite® to give the free acid, ^{31}P-NMR data (101.3 MHz, CD_3OD): δ 1.80 (s, 1P), 1.43 (s, 2P). The reaction mixture was concentrated under vacuum and the residue was reacted for 12 hours at room temperature with 0.5 M sodium hydroxide (20 mL). The solution was applied to a cation exchange column (Dowex 50-X8, mesh 20-50, 20 mL, H^+ form), which was eluted with water (60 mL) {Extrapolating back from the X-ray crystal structure (Chapter 4) and elemental analysis data of the final product, suggests that the monosodium salt of *myo*-inositol 1,2,3-trisphosphate is present at this stage,

presumably attributable to the low pKa of the first ionisation: for phytic acid this pKa (at C-2) is 1.1 [Costello *et al.*, 1976]}. The by-product, benzoic acid, was removed by extraction into chloroform and the pH of the aqueous layer was adjusted to 11 with cyclohexylamine. The solution was concentrated under vacuum, the residue was redissolved in water (2mL) and acetone was added to crystallise **57** as its hydrated monosodium tetra(cyclohexylammonium) salt (73 mg, 82 %) as confirmed by X-ray crystallography [Chapter 4]. {The monosodium tetra(cyclohexylammonium) salt of **57** is formed presumably due to the very high sixth pKa value: for phytic acid the highest pKa value (at C-3) is 12.0 [Costello *et al.*, 1976] and the pKa of cyclohexylamine is 10.64 [James & Lord, 1992]. The highest pKa value for *myo*-inositol 1,2,3-trisphosphate has been measured as 9.56 [Schmitt, 1993]}. Mp 165-166.5 °C. ^{1}H-NMR data (250.1 MHz, D_2O, referenced to acetone at 2.22 ppm): δ [1.1-1.45 (m, 20 H), 1.64 (br d, 4 H, J_{HH} 11.9 Hz), 1.79 (br d, 8 H, J_{HH} 3.8 Hz), 1.97 (br s, 8 H), 3.0-3.25 (m, 4 H), 4 x cyclohexylammonium], 3.39 (t, 1 H, $J_{4/5}$ 9.2 Hz, H-5), 3.83 (t, 2 H, $J_{4/3} \sim J_{4/5} \sim$ 9.5 Hz, H-4/-6), 3.98 (br t, 2 H, $J_{1/6} \sim J_{PH} \sim$ 8.9 Hz, H-1/-3), 4.72 (br d, 1 H, J_{PH} 9.8 Hz, H-2). ^{13}C-NMR data (62.9 MHz, D_2O, referenced to d_6-DMSO at 39.7 ppm): δ 23.1, 23.6, 29.7 (all s, ratio 2:1:2, CH_2 of cyclohexylammonium), 49.5 (CH of cyclohexylammonium), 71.2 (d, J_{PC} 3.8 Hz, 2 x inositol CH), 73.2 (br s, 2 x inositol CH), 73.7 (s, inositol CH), 74.3 (br s, inositol CH). ^{31}P-NMR data (101.3 MHz, D_2O): δ 1.70 (s, P-2), 3.62 (s, P-1/3). ^{31}P-NMR data (101.3 MHz, D_2O, ^{1}H coupled): δ 1.70 (d, J_{PH} 8.5 Hz), 3.62 (d, J_{PH} 6.1 Hz). MS data (positive ion FAB): 421 (38 %, $C_6H_{16}O_{15}P_3$, free acid + H), 443 (100 %, $C_6H_{15}O_{15}P_3Na$, free acid + Na), 465 (22 %, $C_6H_{14}O_{15}P_3Na_2$, free acid + 2Na - H), 520 (25 %, free acid + cyclohexylammonium). Calcd for $C_{30}H_{66}N_4O_{15}P_3Na.2H_2O$: C, 41.19; H, 8.06; N, 6.40 %. Found: C, 41.42; H, 8.41; N, 6.42 %.

CHAPTER 6

References

Abboud K. A., Simonsen S. H., Voll R. J. and Younathan, E. S., Structure of 1,2,3,4,5,6-hexa-*O*-acetyl-*myo*-inositol, *Acta. Cryst.*, 1990, **C46**, 2208-2210.

Akiyama T., Takechi N. and Ozaki S., Chiral synthesis of D-*myo*-inositol 1-phosphate starting from L-quebrachitol, *Tet. Lett.*, 1990, **31**, 1433-1434.

Allison J. H. and Stewart M. A., Reduced brain inositol in lithium-treated rats, *Nature*, 1971, **233**, 267-268.

Arnold J. R. P., Bethel R. C. and Lowe G., Chiral inorganic [^{16}O, ^{17}O, ^{18}O] *Bioorg. Chem.*, 1987, **15**, 250-261.

Arnone A. and Perutz M. F., Structure of inositol hexaphosphate - human deoxyhaemoglobin complex, *Nature*, 1974, **249**, 34-36.

Atack J. R., Broughton H. B. and Pollack S. J., Inositol monophosphatase - a putative target for Li^+ in the treatment of bipolar disorder, *TINS*, 1995, **18**, 343-349.

Baker R., Kulagowski J. J., Billington D. C., Leeson P. D., Lennon I. C. and Liverton N. J., Synthesis of 2- and 6-deoxyinositol 1-phosphate and the role of the adjacent hydroxy groups in the mechanism of inositol monophosphatase, *J. Chem. Soc., Chem. Commun.*, 1989, 1383-1385.

Baker R., Leeson P. D., Liverton N. J. and Kulagowski J. J., Identification of (1S)-phosphoryloxy-(2R,4S)-dihydroxycyclohexane as a potent inhibitor of inositol monophosphatase, *J. Chem. Soc., Chem. Commun.*, 1990, 462-464.

Baker G. R. and Gani D., Inositol dependant phosphate-oxygen ligand exchange catalysed by inositol monophosphatase, *Bioorg. Med. Chem. Lett.*, 1991, **1**, 193-196.

Baker G. R., Billington D. C. and Gani D., Chemical and enzymic syntheses of D- and L-*myo*-inositol 1-phosphorothioate, substrates for inositol monophosphatase: D-glucose 6-phosphorothioate is not a substrate for inositol synthase, *Bioorg. Med. Chem. Lett.*, 1991 a, **1**, 17-20.

Baker G. R., Billington D. C. and Gani D., Synthesis of D- and L-*myo*-inositol 1-phosphorothioate, substrates for inositol monophosphatase, *Tetrahedron*, 1991 b, **47**, 3895-3908.

Baker R., Carrick C., Leeson P. D., Lennon I. C. and Liverton N. J., Design and synthesis of 6α-substituted 2β,4α-dihydroxy-1β-phosphoryloxycyclohexanes, potent inhibitors of inositol monophosphatase, *J. Chem. Soc., Chem. Commun.*, 1991 c, 298-300.

Ballou C. E. and Pizer L. I., The absolute configuration of the *myo*-inositol 1-phosphates and a confirmation of the bornesitol configurations, *J. Am. Chem. Soc.*, 1960, **82**, 3333-3335.

Barker C. J., Wright J., Kirk C. J. and Michell R. H., Inositol 1,2,3-trisphosphate is a product of $InsP_6$ dephosphorylation in WRK-1 rat mammary epithelial cells and exhibits transient concentration changes during the cell cycle, *Biochem. Soc. Trans.*, 1995, **23**, 169S.

Barker C. J., French P. J., Moore A. J., Nilsson J., Berggren P.-O., Bunce C. M., Kirk C. J. and Michell R. H., Inositol 1,2,3-trisphosphate and inositol 1,2- and/or 2,3-bisphosphate are normal constituents of mammalian cells, *Biochem. J.*, 1995, **306**, 557-564.

Berlin W. K., Zhang W.-S. and Shen T. Y., Glycosyl-inositol derivatives III. Synthesis of hexosamine-inositol-phosphates related to putative insulin mediators, *Tetrahedron*, 1991, **47**, 1-20.

Berridge M. J., Downes C. P. and Hanley M. R., Lithium amplifies agonist-dependent phosphatidylinositol responses in brain and salivary glands, *Biochem. J.*, 1982, **206**, 587-595.

Berridge M. J., Downes C. P. and Hanley M. R., Neural and developmental actions of lithium: A unifying hypothesis, *Cell*, 1989, **59**, 411-419.

Berridge M. J., The molecular basis of communication within the cell, *Scientific American*, 1985, **253**, 124-134.

Berridge M. J., Inositol trisphosphate and calcium signalling, *Nature*, 1993, **361**, 315-325.

Billington D. C., Baker R., Kulagowski J. J. and Mawer I. M., Synthesis of *myo*-inositol 1-phosphate and 4-phosphate, and their individual enantiomers, *J. Chem. Soc., Chem. Commun.*, 1987, 314-316.

Billington D. C., Recent developments in the synthesis of *myo*-inositol phosphates, *Chem. Soc. Rev.*, 1989, **18**, 83-122.

Billington D. C., *The inositol phosphates: Chemical synthesis and biological significance*, VCH, Weinheim, 1993.

Blank G. E., Magnesium ion binding to *myo*-Inositol: The crystal structure of *myo*-inositol-magnesium chloride-hydrate (1:1:4), *Acta Cryst.*, 1973, **B29**, 1677-1683.

Blank G. E., Pletcher J. and Sax M., Hemoglobin cofactors. I. The crystal structure of *myo*-inositol hexaphosphate dodecasodium salt octatriacontahydrate, *Acta Cryst.*, 1975, **B31**, 2584-2591.

Blank G. E., Pletcher J. and Sax M., Hemoglobin cofactors. II. The crystal structure of *myo*-inositol hexasulfate hexacyclohexylamine salt, *A. C. A. Summer Meeting Program and Abstracts*, 1976, 74.

Blattler W. A. and Knowles J. R., Phosphoglycerate mutases: Stereochemical course of the phosphoryl group transfers catalyzed by the cofactor-dependent enzyme from rabbit muscle and the cofactor-independent enzyme from wheat germ, *Biochemistry*, 1980, **19**, 738-743.

Bone R., Springer J. P. and Atack J. R., Structure of inositol monophosphatase, the putative target of lithium therapy, *Proc. Natl. Acad. Sci. USA*, 1992, **89**, 10031-10035.

Bone R., Frank L., Springer J. P., Pollack S. J., Osbourne S., Atack J. R., Knowles M. R., McAllister G., Ragan C. I., Broughton H. B., Baker R. and Fletcher S. R., Structural analysis of inositol monophosphatase complexes with substrates, *Biochemistry*, 1994 a, **33**, 9460-9467.

Bone R., Frank L., Springer J. P. and Atack J. R., Structural studies of metal binding by inositol monophosphatase: Evidence for two-metal ion catalysis, *Biochemistry*, 1994 b, **33**, 9468-9476.

Bruzik K. S. and Tsai M.-D., Efficient and systematic syntheses of enantiomerically pure and regiospecifically protected *myo*-inositols, *J. Am. Chem. Soc.*, 1992, **114**, 6361-6381.

Bucourt R., The torsion angle concept in conformational analysis, *Topics in stereochemistry*, 1974, **8**, 159, eds. E. L. Eliel and N. L. Allinger, New York, Wiley-Interscience.

Burkitt M. J. and Gilbert B. C., Model studies of the iron-catalysed Haber-Weiss cycle and the ascorbate-driven Fenton reaction, *Free Rad. Res. Comms.*, 1990, **10**, 265-280.

Burkitt M. J. and Gilbert B. C., The autoxidation of iron (II) in aqueous systems: The effects of iron chelation by physiological, non-physiological and therapeutic chelators on the generation of reactive oxygen species and the inducement of biomolecular damage, *Free Rad. Res. Comms.*, 1991, **14**, 107-123.

Carpenter D., Hanley M. R., Hawkins P. T., Jackson T. R., Stephens L. R. and Vallejo M., The metabolism and functions of inositol pentakisphosphate and inositol hexakisphosphate, *Biochem. Soc. Trans.*, 1989, **17**, 3-5.

Chemical Design Ltd., CHEMX, Oxford, England, 1994.

Chung S.-K. and Chang Y.-T., Base-catalysed acyl migrations in *myo*-inositol dibenzoates, *J. Chem. Soc., Chem. Commun.*, 1995 a, 13-14.

Chung S.-K. and Chang Y.-T., Synthesis of all possible regioisomers of *myo*-inositol tetrakisphosphates, *J. Chem. Soc., Chem. Commun.*, 1995 b, 11-12.

Cohn M. and Hu A., Isotopic (^{18}O) shift in ^{31}P nuclear magnetic resonance applied to a study of enzyme-catalysed phosphate-phosphate exchange and phosphate (oxygen)-water exchange reactions, *Proc. Natl. Acad. Sci. USA*, 1978, **75**, 200-203.

Cohn M. and Hu A., Isotopic ^{18}O shifts in ^{31}P NMR of adenine nucleotides synthesized with ^{18}O in various positions, *J. Am. Chem. Soc.*, 1980, **102**, 913-916.

Cole A. G. and Gani D., Active conformation of the inositol monophosphatase substrates adenosine 2'-phosphate and inositol phosphate: Role of the ribofuranosyl O-atom and inositol O-atoms in chelating a second magnesium ion, *J. Chem. Soc., Chem. Commun.*, 1994, 1139-1141.

Cook W. and Bugg C., Effects of calcium interactions on the conformation of sugars: Crystal structure of *myo*-inositol-calcium bromide pentahydrate, *Acta Cryst.*, 1973, **B29**, 2404-2411.

Cooke A. M., Gigg R. and Potter B. V. L., Synthesis of DL-*myo*-inositol 1,4,5-trisphosphate, *Biochem. Soc. Trans.*, 1987 a, 904-906.

Cooke A. M., Gigg R. and Potter B. V. L., *myo*-Inositol 1,4,5-trisphosphorothioate: A novel analogue of a biological second messenger, *J. Chem. Soc., Chem. Commun.*, 1987 b, 1525-1526.

Cooke F., Poyner D. R., Hawkins P. T., Erlebach C. B. and Hanley M. R., Inositol hexakisphosphate-membrane interactions: the role of metal ions, *Biochem. Soc. Trans.*, 1991, **19**, 152S.

Cooper D. B., Hall C. R., Harrison J. M. and Inch T. D., 1,3,2-Oxazaphospholidines from (-)-ephedrine. Intermediates for the stereospecific synthesis of optically active dialkyl alkylphosphono - thioates and -selenoates, trialkyl phosphoro -thioates and -selenoates, dialkyl methylphosphonates, and trialkyl phosphates, *J. Chem. Soc., Perkin Trans. 1*, 1977, 1969-1980.

Cosgrove D. J., *Inositol Phosphates, their Chemistry, Biochemistry and Physiology*, Elsevier, Amsterdam, 1980.

Costello A. J. R., Glonek T. and Myers T. C., ^{31}P nuclear magnetic resonance-pH titrations of *myo*-inositol hexaphosphate, *Carbohydr. Res.*, 1976, **46**, 159-171.

Cowart R. E., Swope S., Loh T. T., Chasteen N. D. and Bates G. W., The exchange of Fe^{3+} between pyrophosphate and transferrin, *J. Biol. Chem.*, 1986, **261**, 4607-4614.

Cullis P. M., Iagrossi A. and Rous A. J., Thiophosphoryl-transfer reactions: A general synthesis and configurational analysis of O-substituted [^{16}O, ^{18}O] thiophosphates, *J. Am. Chem. Soc.*, 1986, **108**, 7869-7870.

Cullis P. M., Iagrossi A., Rous A. J. and Schilling M. B., Epimerisation and non-stereospecific reactions of 1,3,2-oxazaphospholidin-2-ones and -2-thiones, *J. Chem. Soc., Chem. Commun.*, 1987, 996-998.

Davies E. K., CHEMX, Chemical Design Ltd., Oxford, England, 1986.

Deighton N. and Hider R. C., Intracellular low molecular weight iron, *Biochem. Soc. Trans.*, **17**, 490.

Desai T., Fernandez-Mayoralas A., Gigg J., Gigg R., Jaramillo C., Payne S., Penades S. and Schnetz N., Preparation of optically active *myo*-inositol derivatives as intermediates for the synthesis of inositol phosphates in *Inositol phosphates and derivatives: Synthesis, biochemistry and therapeutic potential*, Ed. A. B. Reitz, ACS Symposium Series 463 , 1991, Chapter 6, 86-102.

Deslongchamps P., *Stereoelectronic Effects in Organic Chemistry*, Pergamon Press, 1983.

Dodd G. H., Golding B. T. and Ioannou P. V., Limitations of t-butyldimethylsilyl as a protecting group for hydroxy-functions, *J. Chem. Soc., Chem. Commun.*, 1975, 249-250.

Dreef C. E., Tulnman R. J., Lefeber A. W. M., Elle C. J. J., van der Marel G. A. and van Boom J. H., Synthesis of racemic 3-methylphosphonate analogues of *myo*-inositol 3,4-bis- and 1,3,4-trisphosphate, *Tetrahedron*, 1991, **47**, 4709-4722.

Duax W. L. and Norton D. A. , *Atlas of Steroid Structure*, Plenum Press, 1975, 16-22.

Emsley J. and Niazi S., The structure of *myo*-inositol hexaphosphate in solution - P-31 NMR investigation, *Phosphorus Sulfur Relat. Elem.*, 1981, **10**, 401-408.

Evans W. J. and Martin C. J., Heat of complex formation of Al(III) and Cd(II) with phytic acid. IX., *J. Inorg. Biochem.*, 1988, **34**, 11-18.

Evans W. J. and Martin C. J., The interactions of inositol hexaphosphate with Fe(III) and Cr(III). A calorimetric investigation. XV., *J. Inorg. Biochem.*, 1991, **41**, 245-252.

Flack H. D., On Enantiomorph-polarity estimation, *Acta Cryst.*, 1983, **A39**, 876-881.

Floyd R. A. and Lewis C. A., Hydroxyl free radical formation from hydrogen peroxide by ferrous iron-nucleotide complexes, *Biochemistry,* 1983, **22**, 2645-2649.

Frey P. A., Chiral phosphorothioates: Stereochemical analysis of enzymatic substitution at phosphorus in *Advances in Enzymology, and related areas of molecular biology*, Ed. A. Meister, Interscience, New York, 1989, **62**, 119-201.

Gani D., Downes C. P., Batty I. and Bramham J., Lithium and myo-inositol homeostasis, *Biochem. Biophys. Acta.*, 1993, **1177**, 253-269.

Gani D. and Wilkie J., Stereochemical, mechanistic, and structural features of enzyme-catalysed phosphate monoester hydrolyses, *Chem. Soc. Rev.*, 1995, 55-63.

Ganzhorn A. J. and Chanal M.-C., Kinetic studies with *myo*-inositol monophosphatase from bovine brain, *Biochemistry*, 1990, **29**, 6065-6071.

Gigg J., Gigg R., Payne S. and Conant R., The allyl group for protection in carbohydrate chemistry. Part 18. Allyl and benzyl ethers of *myo*-inositol. Intermediates for the synthesis of *myo*-inositol trisphosphates, *J. Chem. Soc., Perkin Trans. 1*, 1987, 423-429.

Graf E., Mahoney J. R., Bryant R. G. and Eaton J. W., Iron-catalysed hydroxyl radical formation, *J. Biol. Chem.*, 1984, **259**, 3620-3624.

Graf E. and Empson K. L., Phytic acid: A natural antioxidant, *J. Biol. Chem.*, 1987, **262**, 11647-50.

Graf E. and Eaton J. W., Antioxidant functions of phytic acid, *Free Radical Biology & Medicine*, 1990, **8**, 61-69.

Greasley P. J. and Gore M. G., Bovine inositol monophosphatase. Studies on the binding interactions with magnesium, lithium and phosphate ions, *FEBS Lett.*, 1993, **331**, 114-118.

Hallcher L. M. and Sherman W. R., The effects of lithium ion and other agents on the activity of *myo*-inositol 1-phosphatase from bovine brain, *J. Biol. Chem.*, 1980, **255**, 10896-10901.

Halliwell B., Superoxide-dependent formation of hydroxyl radicals in the presence of iron chelates, *FEBS Lett.*, 1978, **92**, 321-326.

Halliwell B. and Gutteridge J. M. C., *Free Radicals in Biology and Medicine*, 2nd edition, Clarendon Press, Oxford, 1989.

Hamilton W. C., Tests for statistical significance, *International tables for X-ray crystallography*, 1974, **4**, Section 4, eds. J. A. Ibers and W. C. Hamilton, Kynoch Press, Birmingham.

Hanessian S. and Lavallee P., The preparation and synthetic utility of *tert*-Butyldiphenylsilyl ethers, *Can. J. Chem.*, 1975, **53**, 2975-2977.

Hawkins P. T., Poyner D. R., Jackson T. R., Letcher A. J., Lander D. A. and Irvine R. F., Inhibition of iron-catalysed hydroxyl radical formation by inositol polyphosphates: a possible physiological function for *myo*-inositol hexakisphosphate, *Biochem. J.*, 1993, **294**, 929-934.

Hokin M. R. and Hokin L. E., Enzyme secretion and the incorporation of ^{32}P into phospholipides of pancreas slices, *J. Biol. Chem.*, 1953, **203**, 967-977.

Isaacks R. E. and Harkness D. R., Erythrocyte organic phosphates and hemoglobin function in birds, reptiles, and fishes, *Amer. Zool.*, 1980, **20**, 115-129.

Isbrandt L. R. and Oertel R. P., Conformational states of *myo*-inositol hexakis(phosphate) in aqueous solution. A ^{13}C NMR, ^{31}P NMR, and Raman spectroscopic investigation., *J. Am. Chem. Soc.*, 1980, **102**, 3144-3148.

James A. M. and Lord M. P., *Macmillan's Chemical and Physical Data*, Macmillan, 1992.

Jeffrey G. A. and Saenger W., *Hydrogen bonding in biological structures*, Heildelberg, Springer-Verlag, 1991.

Johnson C. K., ORTEPII, Report ORNL-5138, Oak Ridge National Laboratory, Tennessee, USA, 1976.

Johnson C. R., Elliot R. C. and Penning T. D., Determination of enantiomeric purities of alcohols and amines by a ^{31}P NMR technique, *J. Am. Chem. Soc.*, 1984, **106**, 5019-5020.

Klein S. M., Cohen G. and Cederbaum A. I., Production of formaldehyde during metabolism of dimethyl sulfoxide by hydroxyl radical generating systems, *Biochemistry*, 1981, **20**, 6006-6012.

Koppitz B., Vogel F. and Mayr G. W., Mammalian aldolases are isomer-selective high-affinity inositol polyphosphate binders, *Eur. J. Biochem.*, 1986, **161**, 421-433.

Kulagowski J. J., Baker R. and Fletcher S. R., Inhibitors of *myo*-inositol monophosphatase containing methylenebisphosphonic acid as a replacement for a phosphate group, *J. Chem. Soc., Chem. Commun.*, 1991, 1649-1650.

Leech A. P., Baker G. R., Shute J. K., Cohen M. A. and Gani D., Chemical and kinetic mechanism of the inositol monophosphate reaction and its inhibition by Li^+, *Eur. J. Biochem.*, 1993, **212**, 693-704.

Lewin L. M., Yannai Y., Sulimovici S. and Kraicer P. F., Studies on the metabolic role of *myo*-inositol, *Biochem. J.*, 1976, **156**, 375-380.

Lomer T. R., Miller A. and Beevers C. A., The crystal structure of *myo*-inositol dihydrate, *Acta Cryst.*, 1963, **16**, 264-268.

Main P., Germain G. and Woolfson M. M., MULTAN 84. A system of computer programs for the automatic solution of crystal structures from X-ray diffraction data, Universities of York, England and Louvain, Belgium, 1984.

Majerus P. W., Inositol phosphate biochemistry, *Ann. Rev. Biochem.*, 1992, **61**, 225-250.

McConnell F. M., Shears S. B., Lane P. J. L., Scheibel M. S. and Clark E. A., Relationships between the degree of cross-linking of surface immunoglobulin and the associated inositol 1,4,5-trisphosphate and Ca^{2+} signals in human B cells, *Biochem. J.*, 1992, **284**, 447-445.

Menniti F. S., Oliver K. G., Putney Jr. J. W. and Shears S. B., Inositol phosphates and cell signalling: New views of $InsP_5$ and $InsP_6$. *TIBS*, 1993, **18**. 53-56.

Mercier D., Barnett J. E. G. and Gero S. D., Synthesis of optically active derivatives of *myo*-inositol: Preparation of 1L-*myo*-inositol 1-phosphate, *Tetrahedron*, 1969, **25**, 5681-5687.

Mernissi-Arifi K., Wehrer C., Schlewer G. and Spiess B., Complexation studies of inositol-phosphates - V. Cu^{2+}, Zn^{2+}, Fe^{2+} and Fe^{3+} complexes of some *myo*-inositol triphosphates, *J. Inorg. Biochem.*, 1994, **55**, 263-277.

Michell R.H, Inositol phospholipids and cell surface receptor function, *Biochim. Biophys. Acta*, 1975, **415**, 81-147.

Morgan E. H., Iron exchange between transferrin molecules mediated by phosphate compounds and other cell metabolites, *Biochim. Biophys. Acta.*, 1977, **499**, 169-177.

Mueller E. G., Crowder M. W., Averill B. A. and Knowles J. R., Purple acid phosphatase: A diiron enzyme that catalyzes a direct phospho group transfer to water, *J. Am. Chem. Soc.*, 1993, **115**, 2974-2975.

Nahorski S. R., Jenkinson S. and Challiss R. A. J., Disruption of phosphoinositide signalling by lithium, *Biochem. Soc. Trans.*, 1992, **20**, 430-434.

Nash T., The colorimetric estimation of formaldehyde by means of the Hantzsch reaction, *Biochem. J.*, 1953, **55**, 416-421.

Neilands J. B., Siderophores, *Archives of Biochemistry and Biophysics*, 1993, **302**, 1-3.

Noble N. J., Cooke A. M. and Potter B. V. L., Synthesis of (±)-*myo*-inositol 1,4,5-trisphosphate and the novel analogue (±)-*myo*-inositol 1,4-bisphosphate 5-phosphorothioate, *Carbohydr. Res.*, 1992, **234**, 177-187.

Ozaki S. and Watanabe Y., Synthesis of inositol polyphosphates and their derivatives in *Inositol phosphates and derivatives: Synthesis, biochemistry and therapeutic potential*, Ed. A. B. Reitz, ACS Symposium Series 463, 1991, Chapter 4, 42-65.

Pietrusiewicz K. M., Salamonczyk G. M. and Bruzik K. S., The synthesis of homochiral inositol phosphates from *myo*-inositol, *Tetrahedron*, 1992, **48**, 5523-5542.

Pippard M. J., Johnson D. K. and Finch C. A., Hepatocyte iron kinetics in the rat explored with an iron chelator, *Brit. J. Haem.*, 1982, **52**, 211-224.

Pizer F. L. and Ballou C. E., Studies on *myo*-inositol phosphates of natural origin, *J. Am. Chem. Soc.*, 1959, **81**, 915-920.

Pollack S. J., Knowles M. R., Atack J. R., Broughton H. B., Ragan C. I., Osbourne S. and McAllister G., Probing the role of metal ions in the mechanism of inositol monophosphatase by site-directed mutagenesis, *Eur. J. Biochem.*, 1993, **217**, 281-287.

Pollack S. J., Atack J. R., Knowles M. R., McAllister G., Ragan C. I., Baker R., Fletcher S. R., Iversen L. L. and Broughton H. B., Mechanism of inositol monophosphatase, the putative target of lithium therapy, *Proc. Natl. Acad. Sci. USA*, 1994, **91**, 5766-5770.

Poole K., Neshat S. and Heinrichs D., Pyoverdine-mediated iron transport in *Pseudomonas aeruginosa*: involvement of a high-molecular-mass outer membrane protein, *Federation of European Microbiological Societies, Microbiology Letters*, 1991, **78**, 1-6.

Potter B. V. L., Recent advances in the chemistry and biochemistry of inositol phosphates of biological interest, *Nat. Prod. Rep.*, 1990, **7**, 1-24.

Potter B. V. L. and Lampe D., Chemistry of inositol lipid mediated cellular signalling, *Angew. Chem. Int. Ed. Engl.*, 1995, **34**, 1933-1972.

Poyner D. R., Cooke F., Hanley M. R., Reynolds D. J. M. and Hawkins P. T., Characterization of metal ion-induced [^{3}H]inositol hexakisphosphate binding to rat cerebellar membranes, *J. Biol. Chem.*, 1993, **268**, 1032-1038.

Rabinowitz I. N. and Kraut J., The crystal structure of *myo*-inositol, *Acta. Cryst.*, 1964, **17**, 159-168.

Reese C. B. and Ward J. G., Synthesis of D-*myo*-Inositol 1,4,5-triphosphate, *Tet. Lett.*, 1987, **28**, 2309-2312.

Saenger W., Betzel Ch., Hingerty B. and Brown G. M., Flip-flop hydrogen bonding in a partially disordered system, *Nature*, 1982, **296**, 581-583.

Saenger W., Betzel Ch., Hingerty B. and Brown G. M., Flip-flop hydrogen bonds in β-cyclodextrin- A generally valid principle in polysaccharides, *Angew. Chem. Int. Ed. Engl.*, 1983, **22**, 883-884.

Schmitt L., Bortmann P., Schlewer G. and Spiess B., *Myo*-inositol 1,4,5-triphosphate and related compounds protonation sequence- potentiometric and P-31 NMR studies, *J. Chem. Soc., Perkin Trans. 2*, 1993 a, 2257-2263.

Schmitt L., PhD Thesis, Université Louis Pasteur de Strasbourg, France, 1993 b.

Seidel H. M., Freeman S., Schwalbe C. H. and J. R. Knowles, Phosphonate biosynthesis: The stereochemical course of phosphoenolpyruvate mutase, *J. Am. Chem. Soc.*, 1990, **112**, 8149-8155.

Shamsuddin A. M., Inositol phosphates have novel anticancer function, *J. Nutr.*, 1995, **125**, 725S-732S.

Sheldrick G. M., SHELX-76, Program for Crystal Structure Determination. University of Cambridge, England, 1976.

Sheldrick G. M., SHELXS-86, Program for the Solution of Crystal Structures, University of Göttingen, Germany, 1986.

Sheldrick G. M., SHELXL-93, Program for Crystal Structure Refinement, University of Göttingen, Germany, 1993.

Shute J. K., Baker R., Billington D. C. and Gani D., Mechanism of the *myo*-inositol phosphatase reaction, *J. Chem. Soc., Chem. Commun.*, 1988, 626-628.

Shvets V. I., Stepanov A. E., Schmitt L., Spiess B. and Schlewer G., Synthesis and complexation properties of inositol-phosphates in *Inositol phosphates and derivatives: Synthesis, biochemistry and therapeutic potential*, Ed. A. B. Reitz, ACS Symposium Series 463, 1991, Chapter 12, 155-171.

Smith A. W., Poyner D. R., Hughes H. K. and Lambert P. A., Siderophore activity of *myo*-inositol hexakisphosphate in Pseudomonas aeruginosa, *J. Bacteriol.*, 1994, **176**, 3455-3459.

Smith S. E. and Dürmüller N., Inositol hexakisphosphate is convulsant in mice and rats in the nanomolar range, *Eur.J.Pharmacol.*, 1990, **191**, 337-343.

Spiers I. D., Barker C. J., Chung S.-K., Chang Y.-T., Freeman S., Gardiner J. M., Hirst P. H., Lambert P. A., Michell R. H., Poyner D. R., Schwalbe C. H., Smith A. W. and Solomons K. R. H., Synthesis and iron binding studies of *myo*-inositol 1,2,3-trisphosphate and D/L-*myo*-inositol 1,2-bisphosphate, and iron binding studies of all *myo*-inositol tetrakisphosphates, *Carbohydr. Res.*, 1996, in press.

Steiner T. and Saenger W., Geometric analysis of nonionic O-H...O hydrogen bonds and nonbonding arrangements in neutron-diffraction studies of carbohydrates, *Acta. Cryst.*, 1992, **B48**, 819-827.

Steiner T., Hinrichs W., Saenger W. and Gigg R., 'Jumping Crystals': X-ray structures of the three crystalline phases of D/L-3,4-di-*O*-acetyl-1,2,5,6-tetra-*O*-benzyl-myo-inositol, *Acta Cryst.*, 1993, **B49**, 708-718.

Stephens L. R. and Irvine R. F., Stepwise phosphorylation of *myo*-inositol leading to *myo*-inositol hexakisphosphate in Dictyostelium, *Nature*, 1990, **346**, 580-583.

Stephens L. R., Hawkins P. T., Stanley A. F., Moore T., Poyner D. R., Morris P. J., Stanley M. R., Kay R. R. and Irvine R. F., *myo*-Inositol pentakisphosphates, *Biochem. J.*, 1991, **275**, 485-499.

Stephens L., Radenberg T., Thiel U., Vogel G., Khoo K.-H., Dell A., Jackson T. R., Hawkins P. T. and Mayr G.W., The detection, purification, structural characterization, and metabolism of diphosphoinositol pentakisphosphate(s) and bisdiphosphoinositol tetrakisphosphate(s), *J. Biol. Chem.*, 1993, **268**, 4009-4015.

Stewart J. J. P., MOPAC. A semi-empirical molecular orbital program, *J. Comp.-Aided Mol. Design*, 1990, **4**, 1-105.

Still W. C., Khan M. and Mitra A., Rapid chromatographic technique for preparative separations with moderate resolution, *J. Org. Chem.*, 1978, **43**, 2923-2925.

Streb H., Irvine R. F., Berridge M. J. and Schulz I., Release of Ca^{2+} from a nonmitochondrial intracellular store in pancreatic acinar cells by inositol-1,4,5-trisphosphate, *Nature*, 1983, **306**, 67-69.

Sun M-K., Wahlestedt C. and Reis D. J., Inositol hexakisphosphate excites rat medullary sympathoexcitatory neurons *in vivo*, *Eur.J.Pharmacol.*, 1992, **215**, 9-16.

Szwergold B. S., Graham R. A. and Brown T. B., Observation of inositol pentakis-and hexakis-phosphates in mammalian tissues by ^{31}P NMR, *Biochem. Biophys. Res. Commun.*, 1987, **149**, 874-881.

Tanaka T., Tamatsukuri S. and Ikehara M., New approach to the synthesis of deoxynucleoside-phosphoramidite derivatives, *Tet. Lett.*, 1986, **27**, 199-202.

Tegge W. and Ballou C. E., Chiral syntheses of D- and L-*myo*-inositol 1,4,5-trisphosphate, *Proc. Natl. Acad. Sci. USA*, 1989, **86**, 94-98.

Tsai M.-D., Use of phosphorus-31 nuclear magnetic resonance to distinguish bridge and nonbridge oxygens of oxygen-17-enriched nucleoside trisphosphates. Stereochemistry of acetate activation by acetyl coenzyme A synthetase, *Biochemistry*, 1979, **18**, 1468-1472.

Tsai M.-D., Stereochemistry of the hydrolysis of adenosine 5'-thiophosphate catalysed by venom 5'-nucleotidase, *Biochemistry*, 1980, **19**, 5310-5316.

Vacca J. P., deSolms S. J., Huff J. R., Billington D. C., Baker R., Kulagowski J. J. and Mawer I. M., The total synthesis of *myo*-inositol polyphosphates, *Tetrahedron*, 1989, **45**, 5679-5701.

Vacca J. P., deSolms S. J., Young S. D., Huff J. R., Billington D. C., Baker R., Kulagowski J. J. and Mawer I. M., Synthesis of *myo*-inositol polyphosphates in *Inositol phosphates and derivatives: Synthesis, biochemistry and therapeutic potential*, Ed. A. B. Reitz, ACS Symposium Series 463, 1991, Chapter 5, 66-85.

Vallejo M., Jackson T., Lightman S. and Hanley M. R., Occurrence and extracellular actions of inositol pentakis- and hexakisphosphate in mammalian brain, *Nature*, 1987, **330**, 656-658.

Watanabe Y., Nakahira H., Bunya M. and Ozaki S., An efficient method for polyphosphorylation of inositol derivatives, *Tet. Lett.*, 1987, **28**, 4179-4180.

Watanabe Y., Komoda Y., Ebisuya K. and Ozaki S., An efficient phosphorylation method using a new phosphitylation agent, 2-diethylamino-1,3,2-benzodioxaphosphepane, *Tet. Lett.*, 1990, **31**, 255-256.

Weaver J. and Pollack S., Low -M_r iron isolated from guinea pig reticulocytes as AMP-Fe and ATP-Fe complexes, *Biochem. J.*, 1989, **261**, 787-792.

Webb M. R. and Trentham D. R., Analysis of chiral inorganic [^{16}O, ^{17}O, ^{18}O] thiophosphate and the stereochemistry of the 3-phosphoglycerate kinase reaction, *J. Biol. Chem.*, 1980, **255**, 1775-1779.

Wilkie J., Cole A. G. and Gani D., 3-Dimensional interactions between inositol monophosphatase and its substrates, inhibitors and metal ion cofactors, *J. Chem. Soc. Perkin Trans. 1*, 1995, 2709-2727.

Wong Y.-H. H., Kalmbach S. J., Hartman B. K. and Sherman W. R., Immunohistochemical staining and enzyme activity measurements show *myo*-inositol 1-phosphate synthase to be localized in the vasculature of brain, *J. Neurochem.*, 1987, **48**, 1434-1442.

Yoo C. S., Blank G., Pletcher J. and Sax M., The crystal structure of *myo*-inositol 2-phosphate monohydrate, *Acta Cryst.*, 1974, **B30**, 1983-1987.

Yu K.-L. and Fraser-Reid B., A novel reagent for the synthesis of *myo*-inositol phosphates: *N,N*-diisopropyl dibenzyl phosphoramidite, *Tet. Lett.*, 1988, **29**, 979-982.

Zhang Y., Liang J.-Y. and Lipscomb W. N., Structural similarities between fructose 1,6-bisphosphatase and inositol monophosphatase, *Biochem. Biophys. Res. Commun.*, 1993, **190**, 1080-1083.

APPENDIX 1

Table A1 : Bond torsional angles (°) for D/L-1,2;4,5-di-*O*-cyclohexylidene *myo*-inositol at 293K and 150K with estimated standard deviations in parentheses

Bond				Angles (°)		Bond				Angles (°)	
				273K	150K					273K	150K
C01	C02	C03	C04	40.6(2)	40.6(3)	C13	C14	C15	C16	53.5(2)	53.3(4)
C01	C02	C03	O09	163.0(1)	163.1(2)	C14	C13	C18	C17	51.6(2)	52.0(4)
C01	C02	O08	C19	41.5(1)	42.5(3)	C14	C15	C16	C17	-56.1(2)	-55.4(4)
C01	O07	C19	C20	125.0(1)	125.3(3)	C15	C16	C17	C18	56.2(2)	55.5(4)
C01	O07	C19	C24	-111.8(1)	-111.1(3)	C16	C17	C18	C13	-54.3(2)	-54.2(4)
C01	O07	C19	O08	7.4(2)	7.8(3)	C18	C13	C14	C15	-51.0(2)	-51.4(4)
C02	C01	O07	C19	17.5(1)	17.7(3)	C19	C20	C21	C22	-53.9(2)	-53.0(4)
C02	O08	C19	C20	-150.3(1)	-151.0(2)	C20	C19	C24	C23	-55.3(2)	-56.0(4)
C02	O08	C19	C24	86.8(1)	86.0(3)	C20	C21	C22	C23	54.2(3)	52.8(4)
C02	O08	C19	O07	-31.6(1)	-32.3(3)	C21	C22	C23	C24	-55.3(2)	-54.6(4)
C03	C02	O08	C19	167.8(1)	168.5(2)	C22	C23	C24	C19	55.8(2)	56.0(4)
C03	C04	C05	C06	72.0(2)	71.2(3)	C24	C19	C20	C21	54.4(2)	54.3(4)
C03	C04	C05	O11	-163.5(1)	-164.2(2)	O07	C01	C02	C03	-156.8(1)	-157.3(2)
C03	C04	O10	C13	145.8(1)	146.5(2)	O07	C01	C02	O08	-35.9(1)	-36.6(2)
C04	C05	C06	C01	-61.2(2)	-61.0(3)	O07	C19	C20	C21	176.5(2)	176.9(2)
C04	C05	C06	O12	179.1(1)	179.2(2)	O07	C19	C24	C23	-178.0(1)	-179.1(2)
C04	C05	O11	C13	41.1(1)	41.8(3)	O08	C02	C03	C04	-75.3(1)	-75.1(3)
C04	O10	C13	C14	-121.8(1)	-121.9(2)	O08	C02	C03	O09	47.1(2)	47.5(3)
C04	O10	C13	C18	115.2(1)	115.2(3)	O08	C19	C20	C21	-68.1(2)	-68.1(3)
C04	O10	C13	O11	-2.3(2)	-2.6(3)	O08	C19	C24	C23	66.2(2)	65.5(3)
C05	C04	C03	C02	-56.5(2)	-56.1(3)	O10	C04	C03	C02	-170.7(1)	-169.9(2)
C05	C04	C03	O09	-178.2(1)	-177.6(2)	O10	C04	C03	O09	67.7(2)	68.7(3)
C05	C04	O10	C13	27.2(1)	27.7(3)	O10	C04	C05	C06	-166.5(1)	-167.3(2)
C05	C06	C01	C02	42.9(2)	43.5(3)	O10	C04	C05	O11	-41.9(1)	-42.7(3)
C05	C06	C01	O07	158.9(1)	159.4(2)	O10	C13	C14	C15	-172.3(2)	-172.5(2)
C05	O11	C13	C14	92.8(1)	92.9(2)	O10	C13	C18	C17	172.5(1)	172.9(2)
C05	O11	C13	C18	-142.8(1)	-142.6(2)	O11	C05	C06	C01	-176.2(1)	-176.4(2)
C05	O11	C13	O10	-25.1(1)	-25.1(3)	O11	C05	C06	O12	64.1(2)	63.8(3)
C06	C01	C02	C03	-35.7(2)	-36.2(4)	O11	C13	C14	C15	71.7(2)	71.5(3)
C06	C01	C02	O08	85.3(1)	84.5(3)	O11	C13	C18	C17	-72.3(2)	-71.7(3)
C06	C01	O07	C19	-106.5(1)	-106.1(2)	O12	C06	C01	C02	165.6(1)	166.6(2)
C06	C05	O11	C13	161.8(1)	162.7(2)	O12	C06	C01	O07	78.4(1)	-77.5(3)

Table A2 : Bond torsional angles (°) for D/L-1-*O*-(*tert*-butyldiphenylsilyl)-2,3-*O*-cyclohexylidene *myo*-inositol with estimated standard deviations in parentheses

Bond				Angle (°)	Bond				Angle (°)
O07	C01	C02	O08	-48.8(5)	C26	Si13	C20	C25	-114.2(5)
C06	C01	C02	O08	76.4(5)	O07	Si13	C20	C21	-52.3(5)
O07	C01	C02	C03	-166.5(4)	C14	Si13	C20	C21	-171.6(4)
C06	C01	C02	C03	-41.3(6)	C26	Si13	C20	C21	66.0(5)
O08	C02	C03	O09	30.6(5)	C25	C20	C21	C22	-0.5(8)
C01	C02	C03	O09	153.7(4)	Si13	C20	C21	C22	179.3(5)
O08	C02	C03	C04	-88.0(5)	C20	C21	C22	C23	0.9(10)
C01	C02	C03	C04	35.1(6)	C21	C22	C23	C24	-0.1(12)
O09	C03	C04	O10	82.3(5)	C22	C23	C24	C25	-1.0(13)
C02	C03	C04	O10	-162.7(4)	C23	C24	C25	C20	1.4(13)
O09	C03	C04	C05	-157.9(4)	C21	C20	C25	C24	-0.7(10)
C02	C03	C04	C05	-42.9(6)	Si13	C20	C25	C24	179.5(6)
O10	C04	C05	O11	-60.0(5)	O07	Si13	C26	C29	59.3(4)
C03	C04	C05	O11	178.1(4)	C14	Si13	C26	C29	176.5(4)
O10	C04	C05	C06	179.5(4)	C20	Si13	C26	C29	-62.3(4)
C03	C04	C05	C06	57.7(5)	O07	Si13	C26	C28	179.3(4)
O07	C01	C06	O12	-58.5(5)	C14	Si13	C26	C28	-63.6(4)
C02	C01	C06	O12	176.4(4)	C20	Si13	C26	C28	57.7(4)
O07	C01	C06	C05	-180.0(4)	O07	Si13	C26	C27	-60.5(4)
C02	C01	C06	C05	54.9(5)	C14	Si13	C26	C27	56.6(4)
O11	C05	C06	O12	53.3(5)	C20	Si13	C26	C27	177.9(3)
C04	C05	C06	O12	175.8(4)	C03	O09	C30	O08	-9.8(5)
O11	C05	C06	C01	173.9(3)	C03	O09	C30	C31	-126.5(4)
C04	C05	C06	C01	-63.6(5)	C03	O09	C30	C35	111.2(4)
C06	C01	O07	Si13	122.3(4)	C02	O08	C30	O09	30.3(5)
C02	C01	O07	Si13	-111.1(4)	C02	O08	C30	C31	149.0(4)
C01	C02	O08	C30	-162.8(3)	C02	O08	C30	C35	-88.7(4)
C03	C02	O08	C30	-37.6(5)	O09	C30	C31	C32	-172.7(4)
C04	C03	O09	C30	110.0(4)	O08	C30	C31	C32	71.7(5)
C02	C03	O09	C30	-12.8(5)	C35	C30	C31	C32	-51.5(6)
C01	O07	Si13	C14	100.4(4)	C30	C31	C32	C33	55.2(6)
C01	O07	Si13	C20	-18.2(4)	C31	C32	C33	C34	-56.0(6)
C01	O07	Si13	C26	-141.7(4)	C32	C33	C34	C35	55.0(7)
O07	Si13	C14	C19	0.0(5)	C33	C34	C35	C30	-53.9(6)
C20	Si13	C14	C19	120.5(4)	O09	C30	C35	C34	173.3(4)
C26	Si13	C14	C19	-114.7(4)	O08	C30	C35	C34	-69.5(5)
O07	Si13	C14	C15	179.7(4)	C31	C30	C35	C34	51.1(6)
C20	Si13	C14	C15	-59.8(5)	O80	C74	C75	O81	-46.5(5)
C26	Si13	C14	C15	65.0(5)	C79	C74	C75	O81	76.9(4)
C19	C14	C15	C16	-0.5(8)	O80	C74	C75	C76	-162.0(4)
Si13	C14	C15	C16	179.8(4)	C79	C74	C75	C76	-38.6(6)
C14	C15	C16	C17	0.8(9)	O81	C75	C76	O82	37.4(4)
C15	C16	C17	C18	-1.0(9)	C74	C75	C76	O82	157.7(4)
C16	C17	C18	C19	1.0(8)	O81	C75	C76	C77	-83.4(4)
C17	C18	C19	C14	-0.8(8)	C74	C75	C76	C77	36.9(6)
C15	C14	C19	C18	0.5(7)	O82	C76	C77	O83	73.9(4)
Si13	C14	C19	C18	-179.8(4)	C75	C76	C77	O83	-170.6(3)
O07	Si13	C20	C25	127.5(5)	O82	C76	C77	C78	-161.9(4)
C14	Si13	C20	C25	8.2(6)	C75	C76	C77	C78	-46.5(5)

Table A2 continued

Bond				Angle (°)	Bond				Angle (°)
O83	C77	C78	O84	-58.1(5)	O80	Si86	C93	C94	88.1(4)
C76	C77	C78	O84	-179.8(4)	C87	Si86	C93	C94	-152.6(4)
O83	C77	C78	C79	-179.2(4)	C99	Si86	C93	C94	-27.9(4)
C76	C77	C78	C79	59.0(5)	C98	C93	C94	C95	-0.9(7)
O80	C74	C79	O85	-62.9(4)	Si86	C93	C94	C95	-176.8(4)
C75	C74	C79	O85	173.3(4)	C93	C94	C95	C96	1.2(8)
O80	C74	C79	C78	174.2(3)	C94	C95	C96	C97	-0.6(8)
C75	C74	C79	C78	50.4(5)	C95	C96	C97	C98	-0.2(8)
O84	C78	C79	O85	57.6(5)	C96	C97	C98	C93	0.4(8)
C77	C78	C79	O85	178.7(4)	C94	C93	C98	C97	0.1(7)
O84	C78	C79	C74	177.5(3)	Si86	C93	C98	C97	176.1(4)
C77	C78	C79	C74	-61.4(5)	O80	Si86	C99	C100	-49.0(4)
C79	C74	O80	Si86	148.8(3)	C87	Si86	C99	C100	-166.7(4)
C75	C74	O80	Si86	-86.1(4)	C93	Si86	C99	C100	71.1(4)
C74	C75	O81	C103	-165.1(3)	O80	Si86	C99	C101	-173.0(4)
C76	C75	O81	C103	-40.0(4)	C87	Si86	C99	C101	69.3(4)
C77	C76	O82	C103	101.0(4)	C93	Si86	C99	C101	-52.9(4)
C75	C76	O82	C103	-21.6(5)	O80	Si86	C99	C102	69.9(4)
C74	O80	Si86	C87	-64.9(4)	C87	Si86	C99	C102	-47.7(4)
C74	O80	Si86	C93	53.2(4)	C93	Si86	C99	C102	-169.9(3)
C74	O80	Si86	C99	175.7(3)	C75	O81	C103	O82	27.4(4)
O80	Si86	C87	C88	-13.7(5)	C75	O81	C103	C104	145.8(4)
C93	Si86	C87	C88	-133.7(4)	C75	O81	C103	C108	-90.5(4)
C99	Si86	C87	C88	100.4(4)	C76	O82	C103	O81	-2.3(5)
O80	Si86	C87	C92	168.4(4)	C76	O82	C103	C104	-119.7(4)
C93	Si86	C87	C92	48.4(5)	C76	O82	C103	C108	117.1(4)
C99	Si86	C87	C92	-77.5(5)	O81	C103	C104	C105	68.7(6)
C92	C87	C88	C89	-1.6(8)	O82	C103	C104	C105	-176.0(5)
Si86	C87	C88	C89	-179.6(4)	C108	C103	C104	C105	-54.6(7)
C87	C88	C89	C90	1.5(8)	C103	C104	C105	C106	56.2(7)
C88	C89	C90	C91	-0.1(9)	C104	C105	C106	C107	-56.8(8)
C89	C90	C91	C92	-1.0(9)	C105	C106	C107	C108	56.1(8)
C90	C91	C92	C87	0.8(9)	C106	C107	C108	C103	-54.6(7)
C88	C87	C92	C91	0.5(8)	O81	C103	C108	C107	-68.2(5)
Si86	C87	C92	C91	178.5(4)	O82	C103	C108	C107	176.0(4)
O80	Si86	C93	C98	-87.6(4)	C104	C103	C108	C107	53.8(6)
C87	Si86	C93	C98	31.7(4)	C155	N152	C153	O154	173.0(8)
C99	Si86	C93	C98	156.3(3)	C156	N152	C153	O154	-13.0(12)

Table A3 : Bond torsional angles (°) D/L-1-*O*-(tert-butyldiphenylsilyl)-2,3-*O*-cyclohexylidene-4,5,6-tri-*O*-benzoyl *myo*-inositol with estimated standard deviations in parentheses

Bond				Angle (°)	Bond				Angle (°)
O07	C03	C02	O08	39.0(7)	C14	C16	C21	C20	-179.5(8)
C04	C03	C02	O08	-78.5(8)	C19	C20	C21	C16	-3.4(14)
O07	C03	C02	C01	160.8(7)	C05	O11	C22	O23	-6.2(11)
C04	C03	C02	C01	43.3(10)	C05	O11	C22	C24	172.5(6)
O08	C02	C01	O09	-51.5(9)	O23	C22	C24	C29	28.3(12)
C03	C02	C01	O09	-167.1(7)	O11	C22	C24	C29	-150.4(7)
O08	C02	C01	C06	70.7(9)	O23	C22	C24	C25	-151.6(8)
C03	C02	C01	C06	-44.8(9)	O11	C22	C24	C25	29.7(10)
O09	C01	C06	O10	-66.3(8)	C29	C24	C25	C26	-0.5(13)
C02	C01	C06	O10	170.6(6)	C22	C24	C25	C26	179.4(8)
O09	C01	C06	C05	177.9(6)	C24	C25	C26	C27	1.6(14)
C02	C01	C06	C05	54.8(9)	C25	C26	C27	C28	-0.9(16)
O10	C06	C05	O11	60.3(7)	C26	C27	C28	C29	-0.9(17)
C01	C06	C05	O11	177.1(6)	C25	C24	C29	C28	-1.4(13)
O10	C06	C05	C04	178.4(6)	C22	C24	C29	C28	178.7(8)
C01	C06	C05	C04	-64.7(8)	C27	C28	C29	C24	2.1(15)
O11	C05	C04	O12	-61.6(8)	C04	O12	C30	O31	3.6(14)
C06	C05	C04	O12	-179.6(6)	C04	O12	C30	C32	-175.9(6)
O11	C05	C04	C03	-178.9(6)	O31	C30	C32	C37	-165.1(10)
C06	C05	C04	C03	63.0(9)	O12	C30	C32	C37	14.5(13)
O07	C03	C04	O12	77.6(8)	O31	C30	C32	C33	12.0(15)
C02	C03	C04	O12	-169.5(6)	O12	C30	C32	C33	-168.5(8)
O07	C03	C04	C05	-164.8(6)	C37	C32	C33	C34	-0.4(15)
C02	C03	C04	C05	-51.9(9)	C30	C32	C33	C34	-177.7(9)
C04	C03	O07	C38	94.6(7)	C32	C33	C34	C35	-1.0(17)
C02	C03	O07	C38	-24.4(8)	C33	C34	C35	C36	1.4(20)
C01	C02	O08	C38	-163.7(6)	C34	C35	C36	C37	-0.3(18)
C03	C02	O08	C38	-39.5(7)	C33	C32	C37	C36	1.5(13)
C06	C01	O09	Si13	132.7(6)	C30	C32	C37	C36	178.6(9)
C02	C01	O09	Si13	-103.8(7)	C35	C36	C37	C32	-1.2(15)
C01	C06	O10	C14	124.4(7)	C02	O08	C38	O07	25.2(8)
C05	C06	O10	C14	-117.4(8)	C02	O08	C38	C43	-92.7(8)
C04	C05	O11	C22	137.6(7)	C02	O08	C38	C39	143.3(7)
C06	C05	O11	C22	-104.5(7)	C03	O07	C38	O08	1.0(8)
C05	C04	O12	C30	117.7(8)	C03	O07	C38	C43	121.7(7)
C03	C04	O12	C30	-123.1(8)	C03	O07	C38	C39	-116.8(7)
C01	O09	Si13	C44	92.9(6)	O08	C38	C39	C40	-178.9(8)
C01	O09	Si13	C54	-27.2(7)	O07	C38	C39	C40	-63.2(10)
C01	O09	Si13	C50	-150.6(6)	C43	C38	C39	C40	56.4(11)
C06	O10	C14	O15	-6.3(13)	C38	C39	C40	C41	-56.6(12)
C06	O10	C14	C16	174.7(6)	C39	C40	C41	C42	56.5(13)
O15	C14	C16	C17	157.8(9)	C40	C41	C42	C43	-55.8(14)
O10	C14	C16	C17	-23.2(11)	O08	C38	C43	C42	-178.4(7)
O15	C14	C16	C21	-21.0(13)	O07	C38	C43	C42	65.0(9)
O10	C14	C16	C21	158.0(7)	C39	C38	C43	C42	-55.5(10)
C21	C16	C17	C18	1.2(13)	C41	C42	C43	C38	55.4(12)
C14	C16	C17	C18	-177.6(8)	O09	Si13	C44	C49	-169.2(6)
C16	C17	C18	C19	-2.4(13)	C54	Si13	C44	C49	-50.4(7)
C17	C18	C19	C20	0.6(15)	C50	Si13	C44	C49	75.9(7)
C18	C19	C20	C21	2.2(16)	O09	Si13	C44	C45	14.4(7)
C17	C16	C21	C20	1.7(13)	C54	Si13	C44	C45	133.2(6)

Table A3 continued

Bond				Angle (°)	Bond				Angle (°)
C50	Si13	C44	C45	-100.4(7)	C44	Si13	C50	C53	177.2(9)
C49	C44	C45	C46	-0.1(12)	C54	Si13	C50	C53	-59.2(9)
Si13	C44	C45	C46	176.4(6)	O09	Si13	C54	C59	112.5(7)
C44	C45	C46	C47	0.6(13)	C44	Si13	C54	C59	-7.1(8)
C45	C46	C47	C48	-0.8(14)	C50	Si13	C54	C59	-129.8(7)
C46	C47	C48	C49	0.4(15)	O09	Si13	C54	C55	-61.2(7)
C45	C44	C49	C48	-0.2(12)	C44	Si13	C54	C55	179.2(6)
Si13	C44	C49	C48	-176.7(7)	C50	Si13	C54	C55	56.5(8)
C47	C48	C49	C44	0.1(13)	C59	C54	C55	C56	3.3(12)
O09	Si13	C50	C52	-176.1(10)	Si13	C54	C55	C56	177.6(6)
C44	Si13	C50	C52	-58.8(11)	C54	C55	C56	C57	-1.9(14)
C54	Si13	C50	C52	64.9(11)	C55	C56	C57	C58	0.1(14)
O09	Si13	C50	C51	-55.6(8)	C56	C57	C58	C59	0.3(15)
C44	Si13	C50	C51	61.8(8)	C55	C54	C59	C58	-2.9(12)
C54	Si13	C50	C51	-174.6(7)	Si13	C54	C59	C58	-176.9(7)
O09	Si13	C50	C53	59.9(9)	C57	C58	C59	C54	1.3(14)

Table A4 : Bond torsional angles (°) for 4,5,6-tri-*O*-benzoyl *myo*-inositol 1,2,3-tris(dibenzyl phosphate) with estimated standard deviations in parentheses

Bond				Angle (°)	Bond				Angle (°)
O07	C01	C02	O08	61.2(7)	C16	C17	C22	C21	-176.9(11)
C06	C01	C02	O08	-58.1(7)	C20	C21	C22	C17	-0.2(21)
O07	C01	C02	C03	-179.6(6)	O14	P13	O23	C24	-67.0(6)
C06	C01	C02	C03	61.0(7)	O15	P13	O23	C24	60.7(6)
O08	C02	C03	O09	-56.5(7)	O07	P13	O23	C24	168.5(5)
C01	C02	C03	O09	-174.4(6)	P13	O23	C24	C25	143.3(6)
O08	C02	C03	C04	63.0(7)	O23	C24	C25	C30	120.3(10)
C01	C02	C03	C04	-55.0(7)	O23	C24	C25	C26	-65.0(12)
O09	C03	C04	O10	-67.2(6)	C30	C25	C26	C27	-0.8(16)
C02	C03	C04	O10	174.1(5)	C24	C25	C26	C27	-175.5(10)
O09	C03	C04	C05	172.9(5)	C25	C26	C27	C28	2.3(19)
C02	C03	C04	C05	54.1(7)	C26	C27	C28	C29	-2.1(22)
O10	C04	C05	O11	64.2(7)	C27	C28	C29	C30	0.3(23)
C03	C04	C05	O11	-176.5(5)	C26	C25	C30	C29	-1.0(18)
O10	C04	C05	C06	-177.8(6)	C24	C25	C30	C29	173.9(11)
C03	C04	C05	C06	-58.5(8)	C28	C29	C30	C25	1.2(22)
O11	C05	C06	O12	-59.0(8)	C02	O08	P31	O32	-20.9(7)
C04	C05	C06	O12	-175.9(6)	C02	O08	P31	O41	103.2(6)
O11	C05	C06	C01	-178.9(5)	C02	O08	P31	O33	-150.0(6)
C04	C05	C06	C01	64.3(7)	O32	P31	O33	C34	-68.8(11)
O07	C01	C06	O12	55.0(7)	O41	P31	O33	C34	169.2(10)
C02	C01	C06	O12	174.2(5)	O08	P31	O33	C34	57.4(11)
O07	C01	C06	C05	175.1(5)	P31	O33	C34	C35	141.1(9)
C02	C01	C06	C05	-65.8(7)	O33	C34	C35	C40	-93.4(14)
C06	C01	O07	P13	-131.2(5)	O33	C34	C35	C36	91.2(14)
C02	C01	O07	P13	109.8(5)	C40	C35	C36	C37	0.5(18)
C03	C02	O08	P31	124.4(5)	C34	C35	C36	C37	176.0(11)
C01	C02	O08	P31	-116.7(5)	C35	C36	C37	C38	0.9(22)
C02	C03	O09	P49	-125.5(5)	C36	C37	C38	C39	-0.5(23)
C04	C03	O09	P49	113.6(6)	C37	C38	C39	C40	-1.2(22)
C05	C04	O10	C67	-122.6(7)	C36	C35	C40	C39	-2.0(16)
C03	C04	O10	C67	116.8(7)	C34	C35	C40	C39	-177.7(10)
C06	C05	O11	C75	117.3(7)	C38	C39	C40	C35	2.5(19)
C04	C05	O11	C75	-124.7(7)	O32	P31	O41	C42	165.1(9)
C05	C06	O12	C83	127.2(7)	O33	P31	O41	C42	-68.2(10)
C01	C06	O12	C83	-114.3(7)	O08	P31	O41	C42	39.9(11)
C01	O07	P13	O14	-17.1(6)	P31	O41	C42	C43	155.8(8)
C01	O07	P13	O23	109.5(5)	O41	C42	C43	C48	166.3(9)
C01	O07	P13	O15	-143.5(5)	O41	C42	C43	C44	-22.2(15)
O14	P13	O15	C16	-38.8(7)	C48	C43	C44	C45	-2.7(16)
O23	P13	O15	C16	-167.1(7)	C42	C43	C44	C45	-174.4(11)
O07	P13	O15	C16	86.2(7)	C43	C44	C45	C46	0.9(20)
P13	O15	C16	C17	170.9(6)	C44	C45	C46	C47	-0.1(21)
O15	C16	C17	C22	-152.5(10)	C45	C46	C47	C48	1.1(20)
O15	C16	C17	C18	30.8(15)	C44	C43	C48	C47	3.7(15)
C22	C17	C18	C19	-0.5(20)	C42	C43	C48	C47	175.6(10)
C16	C17	C18	C19	176.2(13)	C46	C47	C48	C43	-3.0(18)
C17	C18	C19	C20	1.2(26)	C03	O09	P49	O50	31.6(6)
C18	C19	C20	C21	-1.4(28)	C03	O09	P49	O51	-95.2(5)
C19	C20	C21	C22	0.9(26)	C03	O09	P49	O59	158.2(5)
C18	C17	C22	C21	0.0(18)	O50	P49	O51	C52	37.5(7)

Table A4 continued

Bond				Angle (°)	Bond				Angle (°)
O59	P49	O51	C52	-89.9(6)	C06	O12	C83	C85	178.2(7)
O09	P49	O51	C52	163.8(6)	O84	C83	C85	C86	-11.8(14)
P49	O51	C52	C53	81.4(11)	O12	C83	C85	C86	167.1(6)
O51	C52	C53	C58	66.7(13)	O84	C83	C85	C90	164.4(10)
O51	C52	C53	C54	-115.4(12)	O12	C83	C85	C90	-16.7(11)
C58	C53	C54	C55	-0.1(19)	C90	C85	C86	C87	0.0
C52	C53	C54	C55	-177.9(12)	C83	C85	C86	C87	176.2(7)
C53	C54	C55	C56	-0.3(23)	C85	C86	C87	C88	0.0
C54	C55	C56	C57	-0.1(27)	C86	C87	C88	C89	0.0
C55	C56	C57	C58	0.8(27)	C87	C88	C89	C90	0.0
C54	C53	C58	C57	0.9(16)	C88	C89	C90	C85	0.0
C52	C53	C58	C57	178.8(10)	C86	C85	C90	C89	0.0
C56	C57	C58	C53	-1.3(21)	C83	C85	C90	C89	-176.2(8)
O50	P49	O59	C60	45.1(7)	O97	C91	C92	O98	-61.9(6)
O51	P49	O59	C60	172.5(6)	C96	C91	C92	O98	57.8(8)
O09	P49	O59	C60	-81.0(7)	O97	C91	C92	C93	179.7(5)
P49	O59	C60	C61	-166.2(6)	C96	C91	C92	C93	-60.6(8)
O59	C60	C61	C66	-153.7(10)	O98	C92	C93	O99	59.0(7)
O59	C60	C61	C62	31.2(13)	C91	C92	C93	O99	177.2(5)
C66	C61	C62	C63	0.2(17)	O98	C92	C93	C94	-58.1(7)
C60	C61	C62	C63	175.3(10)	C91	C92	C93	C94	60.1(7)
C61	C62	C63	C64	-3.0(20)	O99	C93	C94	O100	67.9(6)
C62	C63	C64	C65	6.9(28)	C92	C93	C94	O100	-174.7(5)
C63	C64	C65	C66	-7.6(32)	O99	C93	C94	C95	-174.2(6)
C62	C61	C66	C65	-0.7(19)	C92	C93	C94	C95	-56.8(8)
C60	C61	C66	C65	-176.0(13)	O100	C94	C95	O101	-68.9(7)
C64	C65	C66	C61	4.4(27)	C93	C94	C95	O101	173.2(6)
C04	O10	C67	O68	2.1(11)	O100	C94	C95	C96	169.7(5)
C04	O10	C67	C69	-176.6(6)	C93	C94	C95	C96	51.9(8)
O68	C67	C69	C70	171.9(7)	O101	C95	C96	O102	74.1(7)
O10	C67	C69	C70	-9.4(9)	C94	C95	C96	O102	-168.7(5)
O68	C67	C69	C74	-7.1(11)	O101	C95	C96	C91	-169.0(6)
O10	C67	C69	C74	171.6(5)	C94	C95	C96	C91	-51.7(7)
C74	C69	C70	C71	0.0	O97	C91	C96	O102	-64.0(7)
C67	C69	C70	C71	-179.0(6)	C92	C91	C96	O102	176.1(6)
C69	C70	C71	C72	0.0	O97	C91	C96	C95	177.1(5)
C70	C71	C72	C73	0.0	C92	C91	C96	C95	57.2(8)
C71	C72	C73	C74	0.0	C92	C91	O97	P103	-130.8(5)
C72	C73	C74	C69	0.0	C96	C91	O97	P103	107.4(6)
C70	C69	C74	C73	0.0	C93	C92	O98	P121	-115.7(6)
C67	C69	C74	C73	179.0(6)	C91	C92	O98	P121	126.8(5)
C05	O11	C75	O76	-3.7(13)	C92	C93	O99	P139	133.6(5)
C05	O11	C75	C77	178.1(6)	C94	C93	O99	P139	-106.7(6)
O76	C75	C77	C78	12.1(12)	C93	C94	O100	C157	-126.4(6)
O11	C75	C77	C78	-169.6(5)	C95	C94	O100	C157	113.4(6)
O76	C75	C77	C82	-168.0(9)	C96	C95	O101	C165	-98.0(7)
O11	C75	C77	C82	10.3(10)	C94	C95	O101	C165	140.6(6)
C82	C77	C78	C79	0.0	C95	C96	O102	C173	-109.7(7)
C75	C77	C78	C79	179.9(6)	C91	C96	O102	C173	130.5(7)
C77	C78	C79	C80	0.0	C91	O97	P103	O104	14.8(7)
C78	C79	C80	C81	0.0	C91	O97	P103	O113	-110.5(5)
C79	C80	C81	C82	0.0	C91	O97	P103	O105	144.5(5)
C80	C81	C82	C77	0.0	O104	P103	O105	C106	58.2(8)
C78	C77	C82	C81	0.0	O113	P103	O105	C106	-175.7(7)
C75	C77	C82	C81	-179.8(7)	O97	P103	O105	C106	-70.0(7)
C06	O12	C83	O84	-2.8(14)	P103	O105	C106	C107	-132.4(8)

Table A4 continued

Bond				Angle (°)
O105	C106	C107	C112	-72.2(13)
O105	C106	C107	C108	106.1(12)
C112	C107	C108	C109	-0.2(16)
C106	C107	C108	C109	-178.6(9)
C107	C108	C109	C110	-1.9(18)
C108	C109	C110	C111	4.0(20)
C109	C110	C111	C112	-4.0(19)
C108	C107	C112	C111	0.3(16)
C106	C107	C112	C111	178.6(10)
C110	C111	C112	C107	1.8(18)
O104	P103	O113	C114	60.2(9)
O105	P103	O113	C114	-67.2(9)
O97	P103	O113	C114	-174.8(8)
P103	O113	C114	C115	132.1(10)
O113	C114	C115	C120	-125.3(14)
O113	C114	C115	C116	51.3(16)
C120	C115	C116	C117	-7.5(23)
C114	C115	C116	C117	176.2(13)
C115	C116	C117	C118	5.6(26)
C116	C117	C118	C119	-6.1(36)
C117	C118	C119	C120	8.1(44)
C116	C115	C120	C119	8.9(27)
C114	C115	C120	C119	-174.7(18)
C118	C119	C120	C115	-8.9(38)
C92	O98	P121	O122	-15.3(11)
C92	O98	P121	O131	107.3(9)
C92	O98	P121	O123	-152.4(7)
O122	P121	O123	C124	-84.4(15)
O131	P121	O123	C124	161.9(14)
O98	P121	O123	C124	49.1(14)
P121	O123	C124	C125	80.2(15)
O123	C124	C125	C130	34.8(22)
O123	C124	C125	C126	-150.8(14)
C130	C125	C126	C127	-2.1(28)
C124	C125	C126	C127	-176.3(17)
C125	C126	C127	C128	-3.8(34)
C126	C127	C128	C129	3.3(37)
C127	C128	C129	C130	2.5(41)
C126	C125	C130	C129	7.4(31)
C124	C125	C130	C129	-178.5(20)
C128	C129	C130	C125	-8.0(42)
O122	P121	O131	C132	144.1(25)
O98	P121	O131	C132	15.7(28)
O123	P121	O131	C132	-89.1(25)
P121	O131	C132	C133	164.8(18)
O131	C132	C133	C138	121.9(21)
O131	C132	C133	C134	-58.1(21)
C138	C133	C134	C135	6.1(24)
C132	C133	C134	C135	-174.0(13)
C133	C134	C135	C136	-5.4(27)
C134	C135	C136	C137	0.6(33)
C135	C136	C137	C138	2.6(40)
C134	C133	C138	C137	-2.1(30)
C132	C133	C138	C137	178.0(19)
C136	C137	C138	C133	-1.9(38)
C93	O99	P139	O140	-13.4(6)
C93	O99	P139	O149	-142.1(5)
C93	O99	P139	O141	113.3(5)
O140	P139	O141	C142	-48.5(7)
O149	P139	O141	C142	79.8(6)
O99	P139	O141	C142	-174.3(6)
P139	O141	C142	C143	-82.7(9)
O141	C142	C143	C148	126.5(9)
O141	C142	C143	C144	-58.0(12)
C148	C143	C144	C145	-3.4(16)
C142	C143	C144	C145	-178.8(10)
C143	C144	C145	C146	6.0(19)
C144	C145	C146	C147	-6.9(23)
C145	C146	C147	C148	5.0(24)
C144	C143	C148	C147	1.4(15)
C142	C143	C148	C147	176.9(10)
C146	C147	C148	C143	-2.3(20)
O140	P139	O149	C150	-56.7(9)
O141	P139	O149	C150	175.4(9)
O99	P139	O149	C150	70.6(9)
P139	O149	C150	C151	174.4(7)
O149	C150	C151	C156	158.1(10)
O149	C150	C151	C152	-24.5(18)
C156	C151	C152	C153	1.2(22)
C150	C151	C152	C153	-176.2(15)
C151	C152	C153	C154	1.8(29)
C152	C153	C154	C155	-0.9(31)
C153	C154	C155	C156	-3.0(29)
C152	C151	C156	C155	-5.1(18)
C150	C151	C156	C155	172.6(13)
C154	C155	C156	C151	6.2(24)
C94	O100	C157	O158	-3.6(11)
C94	O100	C157	C159	178.1(6)
O158	C157	C159	C160	-19.4(10)
O100	C157	C159	C160	158.9(5)
O158	C157	C159	C164	158.8(7)
O100	C157	C159	C164	-22.8(9)
C164	C159	C160	C161	0.0
C157	C159	C160	C161	178.3(7)
C159	C160	C161	C162	0.0
C160	C161	C162	C163	0.0
C161	C162	C163	C164	0.0
C162	C163	C164	C159	0.0
C160	C159	C164	C163	0.0
C157	C159	C164	C163	-178.2(7)
C95	O101	C165	O166	14.2(11)
C95	O101	C165	C167	-166.0(6)
O166	C165	C167	C168	-4.8(11)
O101	C165	C167	C168	175.4(5)
O166	C165	C167	C172	177.3(8)
O101	C165	C167	C172	-2.4(9)
C172	C167	C168	C169	0.0
C165	C167	C168	C169	-177.9(7)
C167	C168	C169	C170	0.0
C168	C169	C170	C171	0.0
C169	C170	C171	C172	0.0
C170	C171	C172	C167	0.0

Table A4 continued

Bond				Angle (°)	Bond				Angle (°)
C168	C167	C172	C171	0.0	C180	C175	C176	C177	0.0
C165	C167	C172	C171	177.8(7)	C173	C175	C176	C177	178.2(7)
C96	O102	C173	O174	-0.7(14)	C175	C176	C177	C178	0.0
C96	O102	C173	C175	-178.5(6)	C176	C177	C178	C179	0.0
O174	C173	C175	C176	-175.7(10)	C177	C178	C179	C180	0.0
O102	C173	C175	C176	2.0(10)	C178	C179	C180	C175	0.0
O174	C173	C175	C180	2.5(13)	C176	C175	C180	C179	0.0
O102	C173	C175	C180	-179.8(6)	C173	C175	C180	C179	-178.3(7)

Table A5 : Bond torsional angles (°) for monosodium tetra(cyclohexylammonium) *myo*-inositol 1,2,3-trisphosphate with estimated standard deviations in parentheses

Bond				Angle (°)	Bond				Angle (°)
O07	C03	C02	O08	61.7(5)	CA2	CA3	CA4	CA5	-56.8(9)
C04	C03	C02	O08	-63.3(5)	CA3	CA4	CA5	CA6	57.8(9)
O07	C03	C02	C01	-177.5(4)	NA1	CA1	CA6	CA5	178.8(5)
C04	C03	C02	C01	57.5(5)	CA2	CA1	CA6	CA5	57.7(7)
O08	C02	C01	O09	-57.7(5)	CA4	CA5	CA6	CA1	-57.6(8)
C03	C02	C01	O09	-177.8(4)	NB1	CB1	CB2	CB3	178.4(5)
O08	C02	C01	C06	63.3(5)	CB6	CB1	CB2	CB3	56.0(8)
C03	C02	C01	C06	-56.8(5)	CB1	CB2	CB3	CB4	-56.7(9)
O09	C01	C06	O10	-58.7(5)	CB2	CB3	CB4	CB5	57.6(10)
C02	C01	C06	O10	178.9(4)	CB3	CB4	CB5	CB6	-56.8(12)
O09	C01	C06	C05	178.4(4)	NB1	CB1	CB6	CB5	-179.0(7)
C02	C01	C06	C05	56.0(5)	CB2	CB1	CB6	CB5	-56.8(9)
O10	C06	C05	O11	57.7(6)	CB4	CB5	CB6	CB1	56.3(11)
C01	C06	C05	O11	-179.4(4)	CC6	CC1	CC2	CC3	-57.9(10)
O10	C06	C05	C04	-179.1(4)	NC1	CC1	CC2	CC3	179.9(7)
C01	C06	C05	C04	-56.2(5)	CC1	CC2	CC3	CC4	56.3(11)
O11	C05	C04	O12	-57.2(5)	CC2	CC3	CC4	CC5	-56.9(11)
C06	C05	C04	O12	178.7(4)	CC3	CC4	CC5	CC6	57.2(11)
O11	C05	C04	C03	-178.6(4)	CC2	CC1	CC6	CC5	59.0(10)
C06	C05	C04	C03	57.2(5)	NC1	CC1	CC6	CC5	-179.1(8)
O07	C03	C04	O12	59.9(5)	CC4	CC5	CC6	CC1	-58.3(12)
C02	C03	C04	O12	-177.4(4)	CD6A	CD1	CD2	CD3	-64.2(18)
O07	C03	C04	C05	179.1(4)	ND1	CD1	CD2	CD3	172.0(12)
C02	C03	C04	C05	-58.2(5)	CD6B	CD1	CD2	CD3	-3.0(34)
C02	C03	O07	P13	135.9(3)	CD1	CD2	CD3	CD4A	64.2(24)
C04	C03	O07	P13	-99.6(4)	CD1	CD2	CD3	CD4B	52.9(29)
C03	C02	O08	P14	106.9(4)	CD2	CD3	CD4A	CD5A	-52.4(41)
C01	C02	O08	P14	-133.4(4)	CD3	CD4A	CD5A	CD6A	49.4(51)
C02	C01	O09	P15	-91.3(4)	ND1	CD1	CD6A	CD5A	-179.9(21)
C06	C01	O09	P15	145.2(3)	CD2	CD1	CD6A	CD5A	56.5(28)
C01	C06	O10	SOD1	104.2(5)	CD4A	CD5A	CD6A	CD1	-52.5(45)
C05	C06	O10	SOD1	-133.9(4)	CD2	CD3	CD4B	CD5B	-84.1(31)
C03	O07	P13	O13B	-56.0(4)	CD3	CD4B	CD5B	CD6B	78.7(42)
C03	O07	P13	O13C	-176.9(4)	ND1	CD1	CD6B	CD5B	-176.5(27)
C03	O07	P13	O13A	63.7(4)	CD2	CD1	CD6B	CD5B	-2.5(57)
C02	O08	P14	O14C	111.9(4)	CD4B	CD5B	CD6B	CD1	-40.6(63)
C02	O08	P14	O14B	-129.0(4)	P13	O13C	SOD1	WO4	-159.1(3)
C02	O08	P14	O14A	-9.1(4)	P13	O13C	SOD1	O10	-65.8(12)
C01	O09	P15	O15A	-47.1(4)	P13	O13C	SOD1	WO8	0.7(3)
C01	O09	P15	O15B	-174.5(4)	P13	O13C	SOD1	WO7	88.4(4)
C01	O09	P15	O15C	68.5(4)	P13	O13C	SOD1	MO1	-60.2(3)
O13B	P13	O13C	SOD1	73.7(3)	WO4	SOD1	MO1	MC1	85.7(50)
O13A	P13	O13C	SOD1	-55.6(3)	O13C	SOD1	MO1	MC1	-9.7(49)
O07	P13	O13C	SOD1	-169.6(2)	O10	SOD1	MO1	MC1	169.3(50)
NA1	CA1	CA2	CA3	-178.1(6)	WO8	SOD1	MO1	MC1	-113.6(50)
CA6	CA1	CA2	CA3	-56.5(8)	WO7	SOD1	MO1	MC1	-109.5(50)
CA1	CA2	CA3	CA4	55.8(8)					

Table A6 : Bond torsional angles (°) for D/L-*cis*-1,2-*O*-cyclohexylidene-3,4,5,6-tetra-*O*-benzyl *myo*-inositol with estimated standard deviations in parentheses

Bond				Angle (°)	Bond				Angle (°)
O07	C01	C02	O08	-50.7(4)	C02	O08	C20	C25	144.6(3)
C06	C01	C02	O08	72.1(4)	C02	O08	C20	C21	-91.9(3)
O07	C01	C02	C03	-166.0(3)	C03	O09	C20	O08	0.2(3)
C06	C01	C02	C03	-43.3(4)	C03	O09	C20	C25	-117.6(3)
O08	C02	C03	O09	38.6(3)	C03	O09	C20	C21	119.9(3)
C01	C02	C03	O09	159.1(3)	O08	C20	C21	C22	-175.4(3)
O08	C02	C03	C04	-81.2(4)	O09	C20	C21	C22	68.8(4)
C01	C02	C03	C04	39.3(4)	C25	C20	C21	C22	-53.3(5)
O09	C03	C04	O10	76.7(4)	C20	C21	C22	C23	55.5(6)
C02	C03	C04	O10	-169.4(3)	C21	C22	C23	C24	-57.1(6)
O09	C03	C04	C05	-160.0(3)	C22	C23	C24	C25	56.6(6)
C02	C03	C04	C05	-46.1(4)	O08	C20	C25	C24	176.6(4)
O10	C04	C05	O11	-61.3(4)	O09	C20	C25	C24	-67.7(5)
C03	C04	C05	O11	176.2(3)	C21	C20	C25	C24	52.9(5)
O10	C04	C05	C06	179.8(3)	C23	C24	C25	C20	-54.8(6)
C03	C04	C05	C06	57.3(4)	C05	O11	C26	C27	-170.9(4)
O07	C01	C06	O12	-58.4(4)	O11	C26	C27	C32	-95.5(5)
C02	C01	C06	O12	176.1(3)	O11	C26	C27	C28	80.3(6)
O07	C01	C06	C05	179.3(3)	C32	C27	C28	C29	0.7(6)
C02	C01	C06	C05	53.8(4)	C26	C27	C28	C29	-175.3(4)
O11	C05	C06	O12	59.4(4)	C27	C28	C29	C30	-0.4(7)
C04	C05	C06	O12	177.2(3)	C28	C29	C30	C31	-0.2(8)
O11	C05	C06	C01	-179.2(3)	C29	C30	C31	C32	0.5(7)
C04	C05	C06	C01	-61.3(4)	C28	C27	C32	C31	-0.4(6)
C06	C01	O07	C13	171.8(3)	C26	C27	C32	C31	175.5(4)
C02	C01	O07	C13	-63.0(4)	C30	C31	C32	C27	-0.2(7)
C03	C02	O08	C20	-40.1(3)	C04	O10	C33	C34	-175.0(4)
C01	C02	O08	C20	-164.2(3)	O10	C33	C34	C35	-47.6(6)
C02	C03	O09	C20	-24.0(3)	O10	C33	C34	C39	134.1(4)
C04	C03	O09	C20	97.7(3)	C39	C34	C35	C36	0.5(5)
C05	C04	O10	C33	112.9(4)	C33	C34	C35	C36	-177.9(4)
C03	C04	O10	C33	-122.9(4)	C34	C35	C36	C37	-0.4(6)
C04	C05	O11	C26	130.6(4)	C35	C36	C37	C38	-0.6(6)
C06	C05	O11	C26	-110.1(4)	C36	C37	C38	C39	1.5(7)
C01	C06	O12	C40	124.8(4)	C35	C34	C39	C38	0.4(6)
C05	C06	O12	C40	-112.9(4)	C33	C34	C39	C38	178.8(4)
C01	O07	C13	C14	-158.1(3)	C37	C38	C39	C34	-1.4(6)
O07	C13	C14	C19	52.6(5)	C06	O12	C40	C41	-165.8(4)
O07	C13	C14	C15	-129.2(4)	O12	C40	C41	C42	115.6(6)
C19	C14	C15	C16	2.8(6)	O12	C40	C41	C46	-72.2(6)
C13	C14	C15	C16	-175.6(4)	C46	C41	C42	C43	0.6(8)
C14	C15	C16	C17	0.5(7)	C40	C41	C42	C43	173.1(6)
C15	C16	C17	C18	-3.5(8)	C41	C42	C43	C44	0.3(11)
C16	C17	C18	C19	3.3(8)	C42	C43	C44	C45	-0.4(11)
C15	C14	C19	C18	-3.1(6)	C43	C44	C45	C46	-0.5(9)
C13	C14	C19	C18	175.2(4)	C42	C41	C46	C45	-1.5(7)
C17	C18	C19	C14	0.2(7)	C40	C41	C46	C45	-173.9(5)
C02	O08	C20	O09	25.7(3)	C44	C45	C46	C41	1.5(8)